

NASA CR-66632  
Aerotherm Report No. 68-29  
Aerotherm Copy No. \_\_\_\_\_

**FINAL REPORT**

**THERMOCHEMICAL ABLATION OF ROCKET  
NOZZLE INSERT MATERIALS**

by

Kimble J. Clark  
Roald A. Rindal  
Lance M. Inouye  
Robert M. Kendall

prepared for

NATIONAL AERONAUTICS AND SPACE ADMINISTRATION

February 15, 1968

Contract NAS 1-7366

Technical Management  
NASA Langley Research Center  
Hampton, Virginia  
Richard F. Mulliken



N 69-19832  
(ACCESSION NUMBER)  
131  
(PAGES)  
NASA-CR-66632 17  
(CODE)  
(CATEGORY)  
PAGELIMIT PORN 600



**AEROTHERM CORPORATION**

460 California Avenue, Palo Alto, California 94306 • Teletype (TWX): 415-492-9243

Distribution of this report is provided in the interest of information and is the responsibility of the author.  
Distribution outside the corporation or organization that prepared it.

## **ABSTRACT**

The resistance of potential rocket nozzle throat insert materials to chemical corrosion and melting is considered theoretically for several rocket propellant environments. Surface temperature and recession rate are evaluated for each of twelve materials in each of six propellant environments. The propellants considered include 2 liquids, 2 solids, and 2 hybrids. Potential throat insert materials include carbides, oxides, borides, nitrides, and pure elements. The assumptions embodied in the analysis are identified and the analysis technique is outlined. Superior performing insert materials with respect to corrosion resistance are identified and recommendations for future effort are given.

## TABLE OF CONTENTS

	Page
<b>ABSTRACT</b>	ii
<b>LIST OF FIGURES</b>	iv
<b>LIST OF TABLES</b>	iv
<b>LIST OF SYMBOLS</b>	v
<b>1. OBJECTIVE, SUMMARY, AND INTRODUCTION</b>	1
<b>2. ANALYSIS</b>	7
2.1 Propellant Compositions	8
2.2 Insulation Material Compositions	9
2.3 Thermochemical Data	9
2.4 Boundary Layer Edge State	10
2.5 Surface Mass Balance	11
2.6 Ablating Surface Thermodynamic State	12
2.7 Surface Energy Balance	14
<b>3. RESULTS</b>	20
3.1 Surface Ablation Characteristics	21
3.2 Energy Balance Solutions	23
3.3 Relative Material Performance	23
<b>4. CONCLUSIONS</b>	29
<b>5. RECOMMENDATIONS</b>	30
5.1 Validity and Applicability of Assumptions	30
5.2 Other Material Degradation Mechanisms	31
5.3 Additional Thermochemical Ablation Considerations	32
<b>REFERENCES</b>	33
<b>APPENDIX A - Thermochemical Data</b>	
<b>APPENDIX B - Aerotherm Chemical Equilibrium Computer Program</b>	
<b>APPENDIX C - Steady State Ablation Energy Balance</b>	

## **LIST OF FIGURES**

- 1-6 Surface Ablation Characteristics for 72 Material-Propellant Combinations**
- 7-12 Surface Energy Balance Solutions for 72 Material-Propellant Combinations**

## **LIST OF TABLES**

- I Propellant Thermodynamic and Chemical Data**
- II Insulation Material Thermodynamic and Chemical Data**
- III Chamber and Throat Conditions**
- IV Boundary Layer Edge Gas Elemental Composition and Enthalpy at Nozzle Throat**
- V Steady State Ablation Results**
  - (a) Propellant No. 1 - OF<sub>2</sub> Diborane
  - (b) Propellant No. 2 - FLOX Methane
  - (c) Propellant No. 3 - Aluminized Solid
  - (d) Propellant No. 4 - Beryllium Solid
  - (e) Propellant No. 5 - N<sub>2</sub>O<sub>4</sub> - Aluminum Hybrid
  - (f) Propellant No. 6 - OF<sub>2</sub> - Lithium Hybrid

### LIST OF SYMBOLS

$\dot{B}$	defined as $((\rho v)_w + \dot{\dot{m}}_e)/\rho_e u_e C_M$
$B'$	defined as $(\rho v)_w/\rho_e u_e C_M$
$\dot{B}_e$	defined as $\dot{\dot{m}}_e/\rho_e u_e C_M$
$C_p$	specific heat
$F$	geometry radiation view factor
$F^o$	free energy
$h_{298}^{3000}$	defined as $\int_{298}^{3000} C_p(T) dT$
$\Delta h_{298}^o$	heat of formation at 298°K
$\dot{h}_i^w$	heat of formation of species $i$ at wall temperature
$(h_w)$ edge gas	enthalpy of edge gas at wall temperature
$h$	enthalpy
$H_r$	recovery enthalpy
$K$	mass fraction
$Le$	Lewis number
$\dot{m}$	mass flux
$Pr$	Prandtl number
$q_{rad}$	radiation energy flux to wall
$Sc$	Schmidt number
$\dot{s}$	surface recession rate
$s_{3000,1}$	entropy at 3000°K and 1 atm
$T$	temperature
$\tilde{z}_i^*$	driving potential for mass transfer (Ref. 1)

## LIST OF SYMBOLS (concluded)

### GREEK

$\alpha$	absorptivity
$\beta_1, \beta_2, \beta_3$	curve-fit constants for $C_p$
$\epsilon$	emissivity
$\rho$	density
$\rho_e u_e C_H$	heat-transfer coefficient
$\rho_e u_e C_M$	mass-transfer coefficient
$(\rho v)_w$	transpiration mass flux normal to the wall
$\sigma$	Stefan-Boltzmann constant

### SUBSCRIPTS

c	denotes char
e.g.	denotes edge gas
k	pertains to chemical element k
l	denotes surface run-off material
M	denotes melt temperature
p	denotes particles
w	denotes wall
*	denotes throat

### SUPERSCRIPT

*	denotes condensed species when applied to chemical symbol, e.g., C* represents condensed phase carbon rather than its vapor
---	---

## **SECTION 1**

### **OBJECTIVE, SUMMARY, AND INTRODUCTION**

#### **OBJECTIVE**

The objective of this investigation has been to identify on a theoretical basis those materials which may be expected to suffer minimal surface recession due to thermochemical mechanisms under the environments imposed on rocket nozzle throats by various propellant combinations.

#### SUMMARY

A theoretical investigation has been conducted to identify rocket-nozzle-throat insert materials which will experience minimum chemical corrosion in various rocket-combustion-product environments. Theoretical calculations for the rates of chemical attack and melting are presented for a matrix of 12 insert materials subjected to environments characteristic of 6 rocket propellants. Throat insert materials considered include carbides of tantalum, hafnium, titanium, and zirconium; oxides of beryllium, zirconium, and hafnium; zirconium nitride; and the elements tungsten, carbon, and tantalum. The propellants considered include 2 liquids,  $\text{OF}_2\text{-B}_2\text{H}_6$  and Flox- $\text{CH}_4$ ; 2 solids, aluminized and beryllized; and 2 hybrids,  $\text{N}_2\text{O}_4$  - aluminized fuel and  $\text{OF}_2$  - lithium + lithium hydride fuel. All predictions for the rates of chemical attack and melting of insert materials considered a combustion chamber pressure of 300 psia and a 2.5-inch throat diameter.

The predictions resulted from an analysis which includes consideration of the following phenomena.

- 1) A realistic treatment of boundary layer transport phenomena accounting, in an approximate manner, for energy and mass transfer events associated with unequal diffusion coefficients for all boundary layer species.
- 2) All possible chemical reactions are considered at the ablating surface between the insert material and boundary layer gases.
- 3) A realistic model for removing chemically stable condensed phase species from the surface when they are at their melt temperature.
- 4) The surface energy balance includes consideration of radiation from the stream and from the wall, and energy transfer associated with all chemical reactions and mass transfer both in the boundary layer and at the surface.

The calculations were performed imposing the following restrictions upon the various phenomena.

- 1) Reaction rates between all species at the surface occur fast enough such that chemical equilibrium is achieved.
- 2) Any chemically stable, condensed phase species which forms at the surface will adhere to the surface unless it is above its melt temperature or the melt temperature of the insert material.
- 3) Steady state ablation is achieved and the insert material is presumed to be thermally semi-infinite.

Throat insert material surface temperature and recession rate are presented for all 72 material-propellant combinations. Considering linear surface recession rate, the following materials appear most promising from a thermochemical point of view in each environment.

OF <sub>2</sub> -B <sub>2</sub> H <sub>6</sub>	hafnium carbide and tantalum carbide + 11% carbon hypereutectic
Flox-Methane	tungsten and carbon
Aluminum-Solid	hafnium carbide, hafnium dioxide and tungsten
Beryllium-Solid	tungsten, tantalum carbide, and tantalum carbide hypereutectic
Aluminum-Hybrid	tungsten, tantalum carbide, and tantalum carbide hypereutectic
Lithium-Hybrid	the carbides of tantalum and hafnium are followed closely by carbon (or graphite), however the carbides operate at, or dangerously near, their melt temperatures, so it is expected that carbon would be best in actual practice.

## INTRODUCTION

An essential consideration in the design of advanced rocket propulsion systems is the selection of materials which will provide adequate thermal protection for the various rocket nozzle components. Because it is important from an operational point-of-view to minimize surface recession in the throat region of the nozzle, it is desirable that careful consideration be given to the selection of materials for fabricating rocket nozzle throat inserts. The efforts reported herein are directed toward identifying materials which have superior resistance to chemical corrosion in various rocket propellant environments. These efforts were conducted between June 1967 and February 1968 under contract to the NASA Langley Research Center (Contract Number NAS1-7366).

The performance of a rocket nozzle throat insert material may generally be considered to depend upon its susceptibility to chemical corrosion, melting, or thermal stress failure. Each of these factors must be considered in selecting the most promising candidate material for a particular rocket exhaust product environment. Because of ill defined high temperature material properties and a lack of totally adequate theoretical techniques it is not possible, from theoretical considerations alone, to precisely specify the optimum material composition, geometric configuration, thickness distribution, and bonding technique for a specific application. Selection of the most promising throat insert design results from theoretical considerations of a preliminary nature which enable a substantial reduction in the number of potential material candidates for a given application. The list of materials remaining after this preliminary "weeding out" process may then be further scrutinized with more sophisticated theoretical considerations, subscale experiments, and finally, by full-scale design verification tests. This report

presents the results of a preliminary theoretical "weeding out" process which is directed toward selecting throat insert materials that appear superior from chemical corrosion considerations for propulsion systems operating on a number of propellants of current and future interest. Results of theoretical screening calculations are presented for a matrix of six propellants and twelve materials for a total of 72 material-propellant combinations. The results are based upon consideration of material degradation associated with thermochemical ablation and melting phenomena. No consideration has been given to structural integrity, cost, or weight. It is believed that the results of this study will provide useful guidelines for future research directed toward selecting optimum insulation materials for a variety of propulsion environments.

All calculations were performed for boundary conditions corresponding to a chamber pressure of 300 psia and a 2.5-inch throat diameter. The propellants and insulation materials considered in the analysis are summarized here.

Propellants

Liquids	{	OF <sub>2</sub> - B <sub>2</sub> H <sub>6</sub>
		FLOX - CH <sub>4</sub>
Solids	{	NH <sub>4</sub> ClO <sub>4</sub> - (Al + rubber)
		NH <sub>4</sub> ClO <sub>4</sub> - (Be + rubber)
Hybrids	{	N <sub>2</sub> O <sub>4</sub> - (Al + rubber)
		OF <sub>2</sub> - (Li + LiH + rubber)

Materials

Elements	{ W C Ta
Carbides	{ TaC TaC + 11% C Hypereutectic HfC TiC ZrC
Oxides	{ BeO ZrO <sub>2</sub> HfO <sub>2</sub>
Nitride	ZrN

Calculations have been performed to evaluate the ablation rate and surface temperature of each of the above materials when subjected to conditions at the throat of rocket engines operating on each of the above propellants. The calculations include realistic treatments of (1) heat and mass transfer processes in the multicomponent, chemically reacting boundary layer, (2) chemical corrosion of the material by propellant products, (3) formation of any chemically stable condensed phase product at the surface resulting from reactions between the material and the environment, and (4) the removal of melting materials from the surface. Results of the calculations include specification of the steady state material surface temperature and recession rate for each propellant system.

The analysis techniques employed for the study are described first, in Section 2, and are followed, in Section 3 by a presentation and discussion of the material performance results. Conclusions are given in Section 4 and are followed in Section 5, by recommendations for future work.

## SECTION 2

### ANALYSIS

Evaluation of the chemical compatibility of the 72 material-propellant combinations requires that detailed consideration be given to heat and mass transfer processes and chemical reactions at the material surface. The analysis reported herein is based upon the approximate film-coefficient approach for characterizing the multicomponent, chemically reacting boundary layer introduced in Reference 1. The present investigation may be considered to represent a significant generalization and extension of an earlier investigation of the chemical compatibility of materials and propellants reported in Reference 2. The present investigation is more extensive in that solid-and hybrid-rocket propellants are considered in addition to liquid propellants; and the investigation is more general in that multicomponent diffusion processes are considered in the approximate boundary layer treatment and the removal of liquid material from the surface is accounted for. The results reported in Reference 2 considered liquid layer removal only when the liquid layer was of the same composition as the basic throat insert material. For example, removal of liquid  $HfO_2$  from the surface of an  $HfO_2$  material was considered, but not the removal of liquid  $HfO_2$  from an HfC material. It is important to consider the latter case since the high melt temperature HfC may oxidize to form the lower melt temperature oxide ( $HfO_2$ ) at the surface and, as a result, the oxide may be removed from the surface to expose more HfC which will in turn be oxidized.

Evaluation of the materials resistance to chemical corrosion requires specification of the following.

- (1) The chemical composition of the propellants.
- (2) The chemical composition of the materials.

- (3) Fundamental thermodynamic data for all molecular species that may result from chemical reactions between the propellants and the materials.
- (4) The thermodynamic state of propellant combustion products at the boundary layer edge.
- (5) A means for evaluating the rate of transfer of chemical species to and from the ablating surface accounting for boundary layer transport processes and removal of liquid material from the ablating surface.
- (6) A means for evaluating the thermodynamic state of gases and condensed phase material at the ablating surface.
- (7) A means for performing a surface energy balance in order to evaluate surface temperature and recession rate.

Each of the above considerations is given attention in the remainder of this section. Primary attention is given to a general description of the basic treatments, and, in most cases, detailed aspects of the various developments are relegated to a series of appendices at the end of the text.

## 2.1 Propellant Compositions

Detailed information relating to the chemical composition and chamber enthalpy of each of the six propellant systems is presented in Table I. The list contains 2 liquid, 2 solid, and 2 hybrid propellants. In addition to the enthalpy and molecular and elemental composition given for all propellants, the oxidizer-to-fuel mass ratio (O/F) is given for the liquid and hybrid systems. The reported enthalpy is consistent with the tabulated propellant compositions and storage temperatures. The initial temperature for all solid propellant grains is taken as room temperature ( $298^{\circ}\text{K}$ ). All of the quantities listed in Table I are required and will be

employed subsequently for establishing the boundary-layer-edge thermodynamic state.

### 2.2 Insulation Material Compositions

The present study is directed toward identifying nozzle throat insert materials which are chemically compatible with different propellant systems. A desire to identify materials which would result in minimum surface recession dictates the choice of high melt temperature, high density materials, rather than reinforced organic composites which would typically be employed in nozzle inlet and expansion cones. The materials selected for the present investigation are listed in Table II along with their elemental composition, heat of formation, and density. The elemental composition is necessary for evaluating the surface chemical state, and the heat of formation will be employed for performing the surface energy balance.

### 2.3 Thermochemical Data

Evaluation of the boundary layer edge state and calculation of the chemical composition and thermodynamic state of products at the ablating surface requires specification of certain fundamental thermodynamic functions for each molecular species to be considered. Since it is not possible, *a-priori*, to specify which of many possible molecules are going to exist to a significant extent, it is most expeditious to consider all possible molecular arrangements between the chemical elements present in the propellant and insulation material. Basic information requiring specification for each species is the heat of formation and entropy at a base temperature, and the specific heat over the temperature range of interest. For condensed phase species, the melt temperature is also required. A significant part of the present investigation was devoted to acquiring and, preparing in the appropriate format, thermochemical data for the many molecular species possible with the material propellant combinations to be

considered. A detailed description of the required data, the references consulted, and a tabulation of the data employed for the present investigation is given in Appendix A.

#### 2.4 Boundary Layer Edge State

The thermodynamic state of the boundary layer edge products is an important boundary condition for evaluating boundary layer energy and mass transfer processes. Boundary layer edge conditions at the throat insert are evaluated by performing a chemical equilibrium, isentropic flow expansion from chamber conditions to the sonic throat ( $M=1$ ) condition. All calculations are performed for a nominal chamber pressure of 300 psia utilizing the propellant chemistry information in Table I and the thermodynamic data for molecular species presented in Appendix A. The chamber condition and isentropic expansion calculations were performed with the Aerotherm ACE (Aerotherm Chemical Equilibrium) program. A brief description of the ACE program is given in Appendix B. Details of the generalized mathematical treatment are presented in Reference 3, and Reference 4 presents a description of how results from the ACE program are employed to perform a surface energy balance.

Results of the isentropic flow calculations are presented in Table III which displays the chamber temperature and the static temperature and pressure at the throat for each of the six propellant systems. Also shown in the Table is a list of the most significant boundary layer edge products, and the mass fraction and composition of particulate material at the boundary layer edge for the propellants containing aluminum or beryllium. Consideration of the momentum of the BeO and  $Al_2O_3$  particles and the curvature of nozzle throats leads to the conclusion that significant impingement of particles on the throat insert surface would not be expected (Ref. 5). Subsequent consideration

of boundary layer mass transfer processes will be limited to considering only the gas phase, and, as such, it is appropriate to evaluate the gas phase elemental composition and enthalpy to represent the boundary layer edge condition at the nozzle throat. Table IV contains boundary layer edge gas elemental composition and enthalpy for the six propellants. This table differs from the propellant compositions in Table I in that the mass fractions for Al, Be, and O have been reduced by the amounts of these elements present in the particles as shown in Table III. The total enthalpy shown in Table IV is the total enthalpy (thermal + chemical + kinetic) of the boundary layer edge gas alone, and does not include any energy associated with particles.

The boundary layer edge gas elemental composition presented in Table IV will be utilized to represent an important boundary condition for the surface mass and energy balance considerations discussed subsequently.

## 2.5 Surface Mass Balance

The rate at which chemical elements and/or mass are transported to and from the surface of the throat insert material is evaluated by the film coefficient approach for the chemically reacting, multicomponent boundary layer presented in Reference 1.

$$\dot{m}\tilde{k}_{k_M} = \rho_e U_e C_M \left( \tilde{z}_{k_w}^* - \tilde{z}_{k_e}^* \right) + (\rho v)_w \tilde{k}_{k_w} + \dot{m}_g \tilde{k}_{k_g} \quad (1)$$

The term on the left represents the mass rate at which element k is supplied to the surface resulting from ablation of the insert material. The first term on the right represents the net mass transfer of element k from the surface due to boundary

layer gas diffusional and convection events. The second term on the right is the flux due to mass addition to the boundary layer at the surface and the last term represents the rate at which condensed phase (i.e. liquid or solid) material is swept from the surface. Summation of Equation (1) over all "k" elements yields the overall mass balance.

$$\dot{m} = (\rho v)_w + \dot{m}_\ell \quad (2)$$

Normalizing Equation (2) by the boundary layer mass transfer coefficient  $(\rho_e U_e C_M)$  obtains:

$$\tilde{B} = B' + B_\ell \quad (3)$$

In Equation (3), the quantities represent normalized total ablation rate, chemical ablation rate, and mechanical ablation rate, respectively.

Evaluation of the quantities  $\tilde{Z}_{kw}^*$ ,  $\tilde{k}_{kw}$ , and  $\tilde{k}_{kl}$  requires specification of the chemical composition of both gas and condensed phase material at the surface. The method for evaluating the chemical composition at the ablating surface is discussed next.

## 2.6 Ablating Surface Thermodynamic State

The molecular composition of gases adjacent to the ablating surface represents an important boundary condition for evaluating heat and mass transfer processes through the boundary layer. The dependence of boundary layer mass transfer processes upon the wall gas composition is illustrated above, in Equation 1. The dependence of boundary layer energy transfer rates upon wall

gas composition is discussed in the next section (2.7). Another important aspect of chemical composition at the ablating surface is associated with chemical reactions which may occur between the gases and the throat insert material. This consideration establishes the chemical compatibility of an insert material with a given propellant environment. Consideration of these reactions dictates, for example, whether the surface may be attacked chemically to form gaseous products which may diffuse away from the surface, or whether a chemically stable film may be formed which protects the material from further chemical attack. In some instances, the surface energy balance will dictate a surface temperature above the melt temperature of the protective film, and in such instance, it is most realistic to allow the liquid to be removed from the surface thereby revealing more insert material for further chemical attack.

In order to systematically account for the many possible reactions that may occur for the 72 material-propellant combinations being considered in the present study the following assumptions are imposed relative to the composition of condensed phase material at the ablating surface.

- (1) Chemical equilibrium will be achieved between all gas and condensed phase material at the ablating surface. That is, the rate at which various molecular products may be formed is limited only by the rate at which the reactants are supplied.
- (2) Chemically stable condensed phase material will be permitted to exist at the surface provided the surface temperature is below its melt temperature and the melt temperature of the insert material.

The first assumption is believed quite appropriate for the high-temperature, high-pressure environments being considered and its meaning is reasonably straight-forward to understand.

The meaning of the second assumption is best illustrated by considering an example. As will be discussed subsequently, in Section 3, chemical equilibrium sometimes dictates the formation of tungsten carbide on the surface of a tungsten throat insert. Note that the melt temperature of tungsten carbide is significantly higher than the melt temperature of tungsten. If the surface energy balance results in a predicted surface temperature which is less than the melt temperature of tungsten, the carbide will adhere to the surface and provide a protective barrier for the tungsten substrate. If, however, the predicted surface temperature is above the melt temperature of tungsten, the tungsten carbide will be removed mechanically since it would not be expected to stick to the liquid substrate.

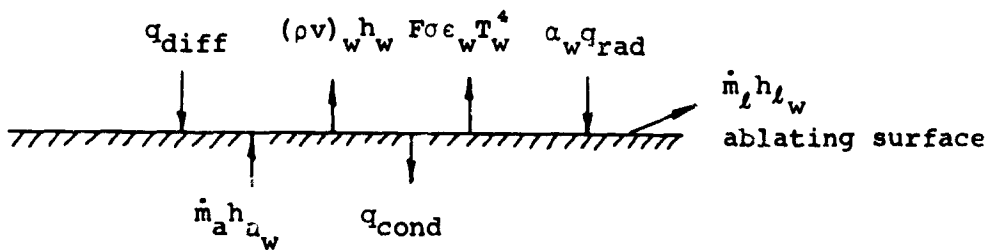
Solution of the chemical equilibrium relations within the constraints of the conservation equations for chemical elements (Equation 1) is accomplished with the ACE program described in Appendix B. The mechanics of obtaining solutions consists of specifying the boundary-layer-edge state, the insert material composition, the pressure, thermodynamic data for all species (Appendix A), and an array of normalized ablation rates ( $\dot{B}$ ). As discussed in Reference 1, with this information, and within the constraints of chemical equilibrium, it is possible to calculate the surface temperature and other terms pertaining to the chemical composition for each specified value of the ablation rate parameter  $\dot{B}$ . The actual ablation rate and surface temperature is then determined by performing a surface energy balance.

## 2.7 Surface Energy Balance

Evaluation of the surface temperature and recession rate is accomplished by performing an energy balance at the heated surface of the nozzle throat insert material. Performing the surface energy balance requires specification of the magnitudes of energy transfer at the surface associated with the following events.

1. Transfer of energy to the surface from the boundary layer as a result of thermal energy transfer and as a result of chemical reactions in the boundary layer and at the ablating surface  $q_{\text{diff}}$ .
2. Transfer of energy from the surface due to blowing or suction at the surface,  $(\rho v)_w h_w$ .
3. Transfer of energy from the surface as a result of liquid layer run-off,  $\dot{m}_l h_{lw}$ .
4. Transfer of radiation energy to and from the surface,  $\alpha_w q_{\text{rad}}$  and  $F\sigma\epsilon_w T_w^4$ , respectively.
5. Transfer of energy to the surface from below the surface in the form of high temperature insert material as it is overtaken by the receding surface,  $\dot{m}_a h_{aw}$ .
6. Conduction of energy from the surface into the insert material by virtue of a temperature gradient,  $q_{\text{cond}}$ .

Each of these terms are depicted in the sketch below.

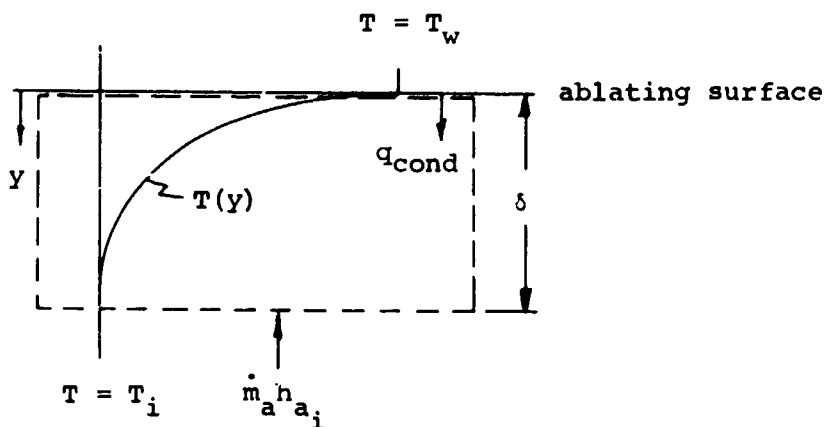


Performing a surface energy balance obtains

$$q_{\text{diff}} - (\rho v)_w h_w + \dot{m}_a h_{aw} - \dot{m}_l h_{lw} + \alpha_w q_{\text{rad}} - F\sigma\epsilon_w T_w^4 - q_{\text{cond}} = 0 \quad (4)$$

Upon specification of a heat transfer coefficient, evaluation of all terms in Equation (4) is reasonably straightforward except the conduction term,  $q_{\text{cond}}$ . Evaluation of the conduction term requires specification of a particular throat insert geometry in

addition to temperature dependent material thermal properties. These properties are often difficult to come by and it would be unfortunate to restrict the result of the present investigation to a particular throat insert geometry. A desire to retain greater generality in the present results prompted consideration of a simplified, but realistic, approximation for representing the conduction term. The assumption of steady state ablation of the insert material is believed appropriate for the high energy flux environments being considered, and has been adopted in the present investigation. The essence of the approximation is illustrated in the following sketch.



A control volume of thickness,  $\delta$ , extends from the ablating surface ( $y=0$ ) to a point in the material where the insert material temperature,  $T(y)$ , is equal to its initial value ( $T_i$  = room temp.). The steady state analysis is based on the assumption that the temperature distribution is invariant with time,  $T(y) \neq f(\text{time})$ . Since the control volume energy content is dependent only upon the temperature distribution, it may be stated that the rate of change of energy content within the control volume is zero. An energy balance on the control volume then obtains:

$$q_{\text{cond}} = \dot{m}_a (h_{aw} - h_{ai}) \quad (5)$$

Substitution into Equation (4) results in a surface energy balance equation which is independent of material thermal properties and insert geometry.

$$q_{\text{diff}} - (cv)_w h_w + \dot{m}_a h_{ai} - \dot{m}_l h_{lw} + \alpha_w q_{\text{rad}} - F \sigma \epsilon_w T_w^4 = 0 \quad (6)$$

The terms in Equation (6) and their evaluation are given detailed attention in Appendix C where it is shown that the surface energy balance may be written in terms of quantities readily available from the output of the ACE computer program. The ACE program was employed to obtain combined solutions of the species conservation equations and chemical equilibrium relations as discussed above, in Sections 2.5 and 2.6. In appendix C, the surface energy balance (Eq.6) is developed in the following form.

$$\begin{aligned} & \frac{C_H}{C_M} (H_r - H_w)_{\substack{\text{edge} \\ \text{gas}}} + \sum_i \left( \tilde{z}_{i,e}^* - \tilde{z}_{i,w}^* \right) \Delta h_i^T - B' h_w - B_l h_{lw} \\ & + \dot{B} h_{ai} + \frac{1}{\rho_e U_e C_M} (\alpha_w q_{\text{rad}} - \alpha_p \sigma \epsilon_w T_w^4) = 0 \end{aligned} \quad (7)$$

For a given material-propellant combination, all terms in Equation 7 are available from the ACE program output as a function of the total ablation rate parameter,  $\dot{B}$ , with the following exceptions: the ratio of heat-to-mass transfer coefficients,  $\frac{C_H}{C_M}$ , the heat

transfer coefficient,  $\rho_e U_e C_H$ , and the radiation terms. The surface energy balance equation is solved by evaluating each term as a function of  $\dot{B}$  until Equation 7 is satisfied. The means employed for evaluating each of these terms is described in Appendix C, but it is appropriate to briefly review the assumptions employed in their evaluation at this point.

The ratio of mass-to-heat-transfer coefficient is given by the Chilton-Colburn Analogy.

$$\frac{C_M}{C_H} = L e^{2/3}$$

The heat transfer coefficient is selected to have a nominal value corresponding to a 2.5-inch-diameter throat with a chamber pressure of 300 psia

$$\rho_e U_e C_{H_0} = 0.5 \text{ lb/ft}^2 \text{- sec}$$

Radiation from the particle laden stream is evaluated by assuming the nozzle throat "sees" only itself, and by assuming radiation from the particle cloud is represented by the stream static temperature, and an effective cloud emmisivity,  $\epsilon_p = \alpha_p$ . The resulting radiation fluxes for the three propellant environments containing particles are.

Propellant	$q_{rad}$ (Btu/ $\text{ft}^2$ -sec)
Aluminum Solid	345
Beryllium Solid	495
Aluminum Hybrid	684

For the other three propellant environments considered ( 2 liquids, and the lithium hybrid) no particles are present in the flow, so for these propellants the net radiation flux is zero. It is interesting to note, that for no net radiation interchange the surface energy balance (Eq.7) may be solved independent of the heat transfer coefficient,  $\rho_e U_e C_{H_0}$ .

$$\frac{C_H}{C_M} (H_r - H_w)_{\text{edge}} + \sum_{\text{gas}} \left( \tilde{z}_{i_e}^* - \tilde{z}_{i_w}^* \right) \Delta h_i^T - B' h_w - B_\ell h_{\ell w} + \dot{B} h_{ai} = 0$$

(8)

This is an interesting result, because it means that the surface energy balance solutions for the environments without particles are valid independent of the throat insert diameter.

Solution of the surface energy balance equations (Eqs. 7 and 8 for the environments with and without particles respectively) represents the culmination of the investigation. The results of this investigation, including the calculated steady state surface temperature and recession rate for each of the 72 material-propellant combinations is presented in the next section.

SECTION 3  
RESULTS

The previous section and appendices A through C describe a specific approach for evaluating the corrosion resistance of nozzle throat insert materials in rocket exhaust product environments. This section presents the results of an investigation utilizing these techniques for analyzing a matrix of twelve materials and six propellant environments. The results are presented in the form of the steady state ablation rate and surface temperature for each of the 72 material-propellant combinations.

Tables V(a) through V(f) present a summary of the performance of each insert material in each of the environments. Table V(a) is for the  $\text{OF}_2\text{-B}_2\text{H}_6$  environment, V(b) through V(f) correspond respectively to Flox-methane, aluminum-solid, beryllium-solid, aluminum-hybrid, and  $\text{OF}_2$ -lithium hybrid. Each table presents the following information for all 12 materials.

- (1) Insert material composition
- (2) Insert material density
- (3) Insert material melt temperature
- (4) Steady state surface temperature,  $T_w$
- (5) Normalized total mass loss rate,  $\dot{B}$
- (6) Linear surface recession rate,  $\dot{s}$
- (7) Chemical composition of chemically stable condensed phase material on the surface (surface species)
- (8) The primary mode of surface recession, chemical or melt

Approximately half way through performing the ablation calculations, a modification was made to the ACE program which resulted in printing out the relative rates of material removed in the liquid and gas phase,  $B_L$  and  $B'$  respectively. For the material-

propellant combinations where this information was readily available on the program output, the values of  $B'$  and  $B_{\ell}$  are shown in addition to  $B$ . It is emphasized that both chemical and mechanical (liquid removal) ablation are considered for all solutions, but their relative rates are shown for only about half the solutions.

In addition to the steady state ablation rate and surface temperature results shown in Table V, a significant part of the results from the investigation are shown in Figures 1 through 12. Figures 1 through 6 present the normalized ablation rate parameter,  $B$ , as a function of temperature for all 12 materials in each of the 6 environments. Figures 7 through 12 present solutions to the surface energy balance for all materials in each of the 6 environments. Because the results presented in Figures 1 through 12 are intermediate to the final answers given in Table V, it is appropriate that they be discussed first.

### 3.1 Surface Ablation Characteristics

Figures 1 through 6 present the normalized ablation rate parameter,  $B$ , for all 72 material-propellant combinations. Each of these figures has 12 parts (a through l), one part for each of the 12 materials. The surface ablation characteristics shown in the figures are machine plots and represent combined solutions of the boundary layer species conservation equations and the chemical equilibrium relations at the ablating surface. The surface ablation characteristics illustrate how fast the material will be consumed at a given surface temperature as a combined result of all possible chemical reactions and removal of liquid material from the surface.

Evaluation of the surface temperature and recession rate in a given environment required solving the surface energy balance which is discussed in the next section. The results presented in Figures 1 through 6 give some information relative to the primary ablation mechanisms. For example, Figure 1(a) indicates

that tungsten is not ablated to any significant extent in the  $\text{OF}_2-\text{B}_2\text{H}_6$  environment until it reaches its melt temperature ( $6570^\circ\text{R}$ ), at which point the ablation rate increases with no increase in surface temperature. This characteristic is a result of the fact that tungsten is not chemically attacked in the  $\text{OF}_2-\text{B}_2\text{H}_6$  environment for temperatures at or below its melt temperature. As a result, the only mechanism for tungsten ablation in this environment is melting.\* The rate of melting is established from performing an energy balance. It is interesting to contrast tungsten ablation in the  $\text{OF}_2-\text{B}_2\text{H}_6$  environment (Fig. 1a) with its ablation characteristics in the aluminized solid propellant environment (Figure 3a) (note the scale change on  $\dot{B}$ ). Although the chemical ablation rate in this environment is also small for temperatures less than the melt temperature ( $\dot{B} = 0.05$  at  $T = T_{\text{melt}}$ ) it is noted that the temperature is first constant at  $4172^\circ\text{R}$  (the melt temperature of  $\text{Al}_2\text{O}_3$ ) and then monotonically increases to the tungsten melt temperature. The region of constant temperature of  $4172^\circ\text{R}$  is represented by the precipitation of  $\text{Al}_2\text{O}_3$  upon the surface and its subsequent removal as a liquid. This region is accompanied by oxidation of the tungsten until a value of  $\dot{B} = 0.007$  is reached, at which point, higher tungsten ablation rates demand a higher surface temperature in order for the material to be consumed chemically. Finally, at  $\dot{B} = 0.05$ , the tungsten melt temperature is reached and further surface recession must result from removal of tungsten liquid. The characteristic of several horizontal lines (constant temperature regions) shown in Figure 3(a) is representative of many of the material-propellant combinations. In these cases the constant temperature region represents the existence of a chemically stable liquid layer which is being mechanically removed from the surface.

\* Excluding thermal shock effects

### 3.2 ENERGY BALANCE SOLUTIONS

The steady state energy balance equation was presented above, in Section 2.7 (Eq. (7)) and details pertaining to its solution for each material-propellant environment are described in Appendix C. Solution of the energy balance equation is accomplished with a computer program (ESUM) which takes the output of the ACE program, evaluates each term in the energy balance equation (Eq. (7)), computes the sum, and plots it as a function of the normalized ablation rate parameter,  $\dot{B}$ . Examination of the energy balance Equation (7) reveals that when the sum is zero, the energy balance is satisfied. The sum of the terms in the energy balance equation (Energy Imbalance) are machine plotted as a function of  $\dot{B}$  for each material-propellant combination and are shown in Figures 7 through 12. Each figure has 12 parts (a through l) which correspond to the 12 materials.

These figures reveal the value of  $\dot{B}$  which satisfies the energy balance (Energy Imbalance = 0) and also illustrate the magnitude of the energy imbalance for higher and lower values of the ablation rate. A positive energy imbalance corresponds to more energy being added to the material than it can reject through the ablation process. During an actual rocket firing the ablation rate will increase with time and the extra energy will cause the surface temperature and ablation rate to increase until the steady state value is achieved.

### 3.3 RELATIVE MATERIAL PERFORMANCE

The results presented in Tables V(a) through V(f) for each of the propellant environments illustrate the relative susceptibility to chemical erosion and/or melting of a number of materials. As indicated above, in Section 2.7, the energy balance solutions for the environments without particles are valid independent of heat transfer coefficient. Thus, the solutions for the normalized ablation rate,  $\dot{B}$ , are valid for the  $\text{OF}_2\text{-B}_2\text{H}_6$ ,

Flox-methane, and  $\text{OF}_2$ -lithium hybrid environments independent of nozzle throat diameter. For the environments containing particles, the reported  $\dot{B}$  depends on throat diameter because of the dependence of the radiation term on throat diameter. In addition to the normalized ablation rate parameter,  $\dot{B}$ , Table V includes a tabulation of the linear recession rate,  $\dot{s}$ , for a heat transfer coefficient corresponding to a throat diameter of 2.5 inches. The linear recession rate is related to  $\dot{B}$  through Equation (C-8) (Appendix C). Some of the better performing materials in each propellant environment are discussed in the following paragraphs. Because primary emphasis is given to materials suitable for nozzle insert application, the relative performance of materials is based upon minimum linear recession rate,  $\dot{s}$ , rather than minimum mass loss rate,  $\dot{B}$ .

$\text{OF}_2\text{-B}_2\text{H}_6$  - As indicated in Table V(a), the high temperature carbides perform best in this environment, however some of the metals have a greater affinity for boron than others which results in conversion of the metal carbide to a metal boride. The metal boride has a low melt temperature and is removed mechanically (e.g.,  $\text{ZrB}_2$ ). Other carbides have lower melt temperatures (e.g.,  $\text{TiC}^*$ ) and are removed as liquid without appreciable chemical attack. The two materials which are superior from a thermochemical point of view are hafnium carbide ( $\text{HfC}^*$ ) and the tantalum carbide-carbon hypereutectic ( $\text{TaC}^* + 11\% \text{C}^*$ ). A particularly interesting result shown in Table V(a) is the fact that the mixture of  $\text{TaC}^*$  and  $\text{C}^*$  performs substantially better than either  $\text{TaC}^*$  or  $\text{C}^*$ . It would be interesting to evaluate the performance of various  $\text{TaC}^* - \text{C}^*$  mixtures in order to establish the composition which yields minimum recession rate. Comparison of the results shown in Table V(a) with results reported earlier, in Reference 2, reveals some significant discrepancies in the predicted recession rate,  $\dot{B}$ , for roughly equivalent environments ( $\text{O/F} = 3.0$  vs 3.5 here). Consideration of the source of the discrepancy leads to the conclusion that it is a direct result

of the unequal diffusion coefficient effect for this environment. Unequal diffusion coefficient effects were not considered in the results presented in Reference 2. This effect causes hydrogen atoms to diffuse through the boundary layer to combine on the surface much faster than previously considered. The higher energy release to the surface associated with higher hydrogen atom recombination produces a substantial increase in the surface temperature, which results in a higher ablation rate.

Flox-Methane - Table V(b) indicates that tungsten is the best material in this environment. Most all the materials considered perform well in this environment. Because its low total temperature results in low surface temperatures, no melting is predicted to occur and all recession results purely from thermochemical events. Some difficulty was encountered in obtaining energy balance solutions for the materials containing tantalum because there are two values of surface temperature which satisfy the species conservation and chemical equilibrium relations for a given ablation rate. One range of solutions occurs for surface temperatures in the vicinity of  $6000^{\circ}\text{R}$  where a  $\text{TaC}^*$  surface is predicted to exist. Another battery of solutions exists for surface temperatures in the vicinity of  $2500^{\circ}\text{R}$  where a carbon surface is predicted to exist. Energy balances are not obtained for either of these solutions because in one case the surface temperature is far too high, and in the other, it is far too low. It is clear that an energy balance will be obtained for some intermediate temperature levels, but it is not clear what the recession rate should be because there are two chemical recession rates for each surface temperature value. The results presented in Table V(b) are based upon extrapolating the high recession rate curve to a solution of the energy balance equation. As such, the recession rates shown for the materials containing tantalum are maximum values, and the actual rates may be substantially less.

Aluminized-Solid - The results shown in Table V(c) indicate that tungsten, hafnium carbide, and hafnium dioxide suffer very little surface recession in this environment. It is noted that the chemical recession rate parameter ( $B'$ ) is negative for some materials in this environment. This is a result of condensation of  $Al_2O_3^*$  liquid at the surface and its subsequent removal in the liquid phase. This condensation may actually be occurring on many materials but for most of them chemical attack is producing gas phase products which are leaving the surface at a greater mass rate than aluminum and oxygen bearing vapors are reaching the surface. As a result, the chemical attack rate,  $B'$ , is positive for most of the materials.

Beryllium-Solid - Results for this environment shown in Table V(d) indicate that tungsten is the superior insert material, followed closely by second and third place tantalum carbide and tantalum carbide hypereutectic, respectively. It is interesting to note that all three tantalum containing materials react to form a chemically stable tantalum nitride surface. The calculations assume that chemically stable condensed phase compounds will stick to the surface provided they do not melt at the surface temperature of the insert material. Referring to Table V(d), it is noted that the surface temperature for tantalum is at its melt temperature, and, as a result, it would be unrealistic to allow the nitride to stick to the liquid substrate. For this reason tantalum is predicted to have a high recession rate resulting from liquid layer removal. Because the predicted surface temperatures for tantalum carbide and tantalum carbide hypereutectic are below their melt temperatures, however, the tantalum nitride is presumed to adhere to the surface and provide a protective film for these materials.

$N_2O_4$ -Aluminum Hybrid - As evidenced by comparing Tables V(d) and V(e), the relative performance of materials in this environment is about the same as in the beryllium-solid propellant environment. Tungsten is best and is followed by tantalum carbide

and its hypereutectic. Significantly higher surface temperatures are predicted for this environment, however, and as a result, the predicted temperature for the tungsten insert is dangerously close to its melt temperature.

OF<sub>2</sub>-Lithium Hybrid - This environment produces such high surface temperature that all but two materials are predicted to melt. One of these, tantalum carbide, gets within 150°R of its melt temperature ( $T_{melt} = 7690^{\circ}\text{R}$ ), and the other, carbon, is predicted to operate at 6800°R. From a thermochemical, and melting point of view, the best materials, in order of performance, are: tantalum carbide hypereutectic, tantalum carbide, halfnium carbide, and carbon. It is most likely that in practice carbon (or graphite) would end up the best because of the extremely high temperatures (and corresponding low strength) achieved by the other materials.

These results are believed realistic within the restrictions imposed on the analysis, and the restrictions are believed appropriate for calculations of a preliminary screening nature. Specifically, the chemical equilibrium assumption is believed quite good, and the film coefficient approach to boundary layer transport phenomena is believed quite realistic. The potentially most severe restrictions are: (1) the assumption that chemically stable films will adhere to the surface, and (2) that steady state ablation is achieved. Evaluation of errors associated with the second assumption is straightforward since analytical modeling of transient heat conduction is well in hand. It would seem reasonable to expect that the steady state assumption is appropriate for firing times much greater than 10 seconds. For shorter firing times the results reported in Table V are probably pessimistic. It is difficult to assess probable errors associated with the first assumption (that films stick) and no attempt is made to verify its applicability here. It is recognized that in actual practice, certain mechanisms not considered in this analysis may dominate, and preclude successful utilization of materials which appear superior from a thermochemical point of view. Such mechanisms as insert ejection resulting from low high-temperature

strength, or thermal shock have not been considered. The analysis was performed because of the established importance of thermochemical erosion and the reported results are believed quite realistic from a thermochemical erosion point of view.

SECTION 4

CONCLUSIONS

The conclusions which may be reached from this investigation are summarized quantitatively in Tables V(a) through V(f) which display the surface recession rate and surface temperature for all materials considered in each of the six environments. Considering minimum surface recession rate to be the primary indicator of superior nozzle throat insert performance, the following list summarizes the best materials in each environment.

OF <sub>2</sub> - B <sub>2</sub> H <sub>6</sub>	hafnium carbide and tantalum carbide + 11% carbon hypereutectic
Flox-Methane	tungsten and carbon
Aluminum-Solid	hafnium carbide, hafnium dioxide and tungsten
Beryllium-Solid	tungsten, tantalum carbide, and tantalum carbide hypereutectic
Aluminum-Hybrid	Tungsten, tantalum carbide, and tantalum carbide hypereutectic
Lithium-Hybrid	the carbides of tantalum and hafnium are followed closely by carbon (or graphite), however, the carbides operate at, or dangerously near, their melt temperatures, so it is expected that carbon would be best in actual practice.

It is emphasized that the above material ratings relate only to material performance from a chemical corrosion and melting point-of-view. No consideration has been given to weight, cost, or structural integrity. The above material ratings may be considered in both an encouraging and a discouraging light. They are discouraging in that no really new, superior materials have been identified. On the other hand, it is encouraging that a purely theoretical approach, free from any empiricism, has yielded results which tend to confirm the findings of years of experimental effort; that the best throat insert materials may be selected from tungsten, carbon (or graphite), and the high temperature carbides.

SECTION 5  
RECOMMENDATIONS

It is recommended that the more promising materials be investigated further to establish, (1) the validity and applicability of certain assumptions embodied in the thermochemical ablation calculations, and (2) to investigate the magnitude of material degradation mechanisms not considered in the present investigation. The assumptions warranting further investigation, and other mechanisms which should be considered are identified, and a specific course of action for their investigation is presented here.

5.1 VALIDITY AND APPLICABILITY OF ASSUMPTIONS

The two potentially most severe restrictions embodied in the thermochemical ablation calculations are (1) the assumption that chemically stable films which are formed on the surface will adhere to it, and (2) that steady state ablation is achieved. Evaluation of the applicability of the second assumption may be accomplished in a straightforward manner with currently available transient heat conduction codes. It is recommended that transient heat conduction solutions be performed for a range of chamber pressures and throat diameters of interest to establish approximate firing times for which the steady state assumption is appropriate. In the event the steady state assumption is unrealistic for some conditions of interest, suitable approximations may be introduced to account for transient effects (see e.g., Figures 11 and 12 of Reference 2).

Examination of the validity of the first assumption, that chemically stable films adhere to the surface, may best be accomplished experimentally. It is recommended that a series of experiments be conducted which consist of exposing a small, flat sample of insert material to a high temperature, high shear environment containing the primary gas phase species which react

with the insert to produce the chemically stable film. Post test chemical and photomicrographic analysis of the surface will reveal the presence or absence of the protective film. These experiments should be conducted in an arc plasma facility (see e.g., Ref. 12) in order that the surface temperature may be accurately measured and controlled over the entire range of interest.

### 5.2 OTHER MATERIAL DEGRADATION MECHANISMS

In addition to thermochemical attack the insert material may perform poorly as a result of thermal shock or low strength at high temperature. The ability to prejudge the importance of thermal shock effects is directly related to how well the material properties are known. When fairly accurate measurements or estimates of thermal diffusivity, elastic modulus, and thermal expansion coefficient are available, it is possible with existing computer codes (see e.g., Ref. 12) to make a realistic assessment of potential thermal shock problems for a given material-environment combination. For those promising insert materials where realistic property estimates may be made, thermal stress calculations should be made corresponding to temperature distributions early in time where thermal gradients are large.

Unfortunately, realistic estimates of material properties are often difficult to come by, and in these cases, it is necessary to resort to some form of experimentation. Perhaps the most efficient means of establishing a material's susceptibility to thermal shock is to expose small samples to an environment which will produce temperature levels and gradients encompassing the range of interest. This may be readily accomplished with the same arc-plasma technique as recommended above for investigating the ability of films to adhere to the surface. It is therefore recommended that experiments be conducted on small samples in an arc-plasma environment to acquire data on thermal shock

resistance of insert materials. These experiments should be accompanied by the means for accurately monitoring and controlling the 2 primary independent variables, temperature level and temperature gradient.

It is also recommended that stress analyses be conducted in the high temperature (late time) regime for interesting materials. These analyses should include consideration of nonlinear dependence of material mechanical properties on temperature, and the analyses should include temperature and pressure distributions representative of realistic boundary conditions with a realistic insert geometry. The analysis techniques employed in the present investigation may be employed for evaluating realistic boundary conditions appropriate for such calculations.

### 5.3 ADDITIONAL THERMOCHEMICAL ABLATION CONSIDERATIONS

The results of the present investigation revealed some interesting results relative to the thermochemical ablation of tantalum carbide-carbon mixtures. It was found that a certain mixture results in less ablation than experienced with either the parent material or the dilutant. It is recommended that additional computations be performed to investigate the thermochemical ablation performance of other percentage mixtures. It is anticipated that mixtures different from that considered herein will result in lower recession rates. It is also recommended that details of the results reported herein be given careful scrutiny in order to identify any particular advantageous or detrimental chemical reactions which may suggest material modifications, or other materials which are particularly suited to environments of current interest.

REFERENCES

1. Kendall, R. M., Rindal, R. A., and Bartlett, E. P.: A Multi-component Boundary Layer Chemically Coupled to an Ablating Surface. AIAA Jour., Vol. 5, No. 6, June 1967.
2. Rindal, R. A., Flood, D. T., and Kendall, R. M.: Analytical and Experimental Study of Ablation Material for Rocket-Engine Application. NASA Contract NAS7-218, NASA CR-54757, May 1966.
3. Kendall, R. M.: A General Approach to the Thermochemical Solution of Mixed Equilibrium-Nonequilibrium, Homogeneous or Heterogeneous Systems, Part V of Final Report, Contract NAS9-4599, Aerotherm Report 66-7, Part V, March 14, 1967.
4. Moyer, C. B. and Rindal, R. A.: Finite Difference Solution for the In-Depth Response of Charring Materials Considering Surface Chemical and Energy Balances. Part II of Final Report, Contract NAS9-4599, Aerotherm Report 66-7, Part II, March 14, 1967.
5. Bailey, W. S., Nilson, E. N., Serra, R. A., and Zupnik, T. F.: Gas Particle Flow in an Axisymmetric Nozzle. ARS Jour. Vol. 31, No. 6, June 1961.
6. JANAF Thermochemical Tables. The Dow Chemical Co., Midland, Michigan.
7. Perry, Robert H., Chilton, Cecil H., and Kirkpatrick, Sidney, D.: Chemical Engineer's Handbook, Fourth Edition, McGraw-Hill Book Company, New York, 1963.
8. Hodgman, Charles D.: Handbook of Chemistry and Physics, Thirty-Fourth Edition. Chemical Rubber Publishing Co., Cleveland, Ohio, 1952.
9. Armstrong, D.L.: Liquid Propellants for Rockets. Presented in the Chemistry of Propellants, edited by S.S. Penner and J. Ducarne, AGARD Combustion and Propulsion Panel, Pergamon Press, 1960.
10. Schmidt, Harold W. and Harper, Jack T.: Handling and Use of Fluorine and Fluorine-Oxygen Mixtures in Rocket Systems. NASA SP-3037, Lewis Research Center, Cleveland, Ohio, 1967.
11. Private Communication with John Feenster, United Technology Center.
12. Schaefer, J. W., Dahm, T. J., Rodriguez, D. R., Wool, M. R., and Clark, K. J.: Studies in Support of the NASA Large Solid Booster Program. First and Second Quarterly Progress Reports, Contract NAS7-534, Aerotherm Project 7012, July 20, 1967.

TABLE I  
PROPELLANT THERMODYNAMIC AND CHEMICAL DATA \*\*

Propellant	O/F	H	Li	Be	B	C	N	O	F	Al	C1	* Propellant Injection or Chamber Enthalpy cal./gm
OF <sub>2</sub> + B <sub>2</sub> H <sub>6</sub> , Liquid Fuel storage temp = 128°K Oxidizer storage temp = 180°K	3.5	.0483			.1737				.2305	.5475		-83.7
FLOX + CH <sub>4</sub> , Liquid 54.3% F <sub>2</sub> in FLOX Fuel storage temp = 111.4°K Oxidizer storage temp = 87.4°K	2.185	.0785				.2350			.3135	.3730		-478.4
NH <sub>4</sub> ClO <sub>4</sub> +(Al+rubber binder), Solid Binder composition: C <sub>7.134</sub> H <sub>10.714</sub> T <sub>0.0775</sub> O <sub>0.1517</sub>	--	.03975				.12320	.08590	.39050		.15050	.20900	-475.3
NH <sub>4</sub> ClO <sub>4</sub> +(Be+rubber binder), Solid Binder composition: C <sub>7.134</sub> H <sub>10.714</sub> T <sub>0.0775</sub> O <sub>0.1517</sub>	--	.0404			.1200				.08825	.40644		-440.14
N <sub>2</sub> O <sub>4</sub> + (Al + rubber binder), C <sub>4</sub> H <sub>6</sub> Hybrid Binder composition:	1.60	.0235				.1880	.1872	.4283		.1730		-2.25
OF <sub>2</sub> + (Li+LiH+rubber binder), Hybrid Binder Composition: C <sub>4</sub> H <sub>6</sub>	3.20	.0201	.0804			.1371			.2288	.5336		-165.2 Liquid OF <sub>2</sub> @128°K

\* Relative to JANAF thermal and chemical base states (Ref. 6)

\*\*Basic data obtained from References 7-11.

TABLE II  
INSULATION MATERIAL THERMODYNAMIC AND CHEMICAL DATA

Material	Elemental Mass Fractions, gm element/gm material							Heat of Formation*, cal/gm	Density gm/cc
	W	C	Ta	Hf	Ti	Zr	Be		
W	1.000							0	19.28
C		1.000						0	2.26
Ta			1.000					0	16.60
TaC	0.0624	0.9376						-179.0	14.65
TaC + 11% C	0.1655	0.8345						-160.0	8.48
HfC	0.0631	0.9359						-236.0	12.70
TiC	0.2007		0.7993					-731.0	4.92
ZrC	0.1163			0.8837				-436.0	6.74
BeO					0.3602	0.6398		-5,720.0	3.06
ZrO <sub>2</sub>						0.2595		-2,120.0	5.73
HfO <sub>2</sub>						0.1...		-1,262.0	9.68
ZrN					0.8669		0.1331	-828.0	7.09

\*Relative to JANAF thermal and chemical base state (Ref. 6).

TABLE III  
CHAMBER AND THROAT CONDITIONS\*

Propellant	$T_C$ (°R)	$T_R^*$ (°R)	$P^*$ (atm)	Significant Molecular Species at Throat	$K_i$ Condensed Phase Mass Fraction
#1 $\text{OF}_2 + \text{B}_2\text{H}_6$	7,668	7,256	11.75	$\text{FH}, \text{H}_2, \text{BF}, \text{HO}, \text{H}_2\text{O},$ $\text{BF}_2\text{O}, \text{BO}, \text{BHO}_2, \text{BO}_2, \text{F},$ $\text{BF}_2, \text{BHO}, \text{O}$	0
#2 $\text{FLOX} + \text{CH}_4$	4,840	4,266	11.20	$\text{FH}, \text{CO}, \text{H}_2$	0
#3 $\text{NH}_4\text{ClO}_4 + (\text{Al}$ + rubber binder)	5,784	5,434	11.75	$\text{H}_2\text{O}, \text{CO}, \text{ClH}, \text{H}_2, \text{H}, \text{N}_2, \text{CO}_2,$ $\text{Al}_2\text{O}_3^*, (\text{Cl}, \text{AlCl}_2, \text{AlCl},$ $\text{HO}, \text{O}, \text{AlHO}_2, \text{NO})$	$K_{\text{Al}_2\text{O}_3^*} = 0.2535$
#4 $\text{NH}_4\text{ClO}_4 + (\text{Be}$ + rubber binder)	6,174	5,874	11.85	$\text{H}_2, \text{CO}, \text{ClH}, \text{Cl}, \text{H}, \text{H}_2\text{O},$ $\text{BeCl}, \text{N}_2, \text{BeO}^*$	$K_{\text{BeO}^*} = 0.2340$
#5 $\text{N}_2\text{O}_4 + (\text{Al}$ + rubber binder)	6,711	6,393	11.85	$\text{CO}, \text{H}_2, \text{N}_2, \text{H}, \text{N}_2\text{O}, \text{Al}, \text{AlO},$ $\text{O}, \text{Al}_2\text{O}, \text{AlHO}_2, \text{CO}_2, \text{HO},$ $\text{Al}_2\text{O}_3^*$	$K_{\text{Al}_2\text{O}_3^*} = 0.2750$
#6 $\text{OF}_2 + (\text{Li} + \text{LiH}$ + rubber binder)	7,987	7,513	11.65	$\text{CO}, \text{Fd}, \text{FLi}, \text{F}, \text{H}, \text{HO}, \text{O},$ $\text{H}_2, \text{Li}$	0

\* Based on 360 psia (20.43 atm) chamber pressure

TABLE IV  
BOUNDARY LAYER EDGE GAS ELEMENTAL COMPOSITION AND ENTHALPY OF NOZZLE THROAT

Propellant	Enthalpy* cal/gr	Elemental Mass Fraction* gr element gr edge gas								
		H	Li	Be	B	C	N	O	F	
#1 $\text{OF}_2 - \text{B}_2\text{H}_6$	-83.6	0.0483			0.1737			0.2305	0.5475	
#2 $\text{FLOX} - \text{CH}_4$	-477.0	0.0785			0.2350			0.3135	0.3730	
#3 $\text{NH}_4\text{ClO}_4 - (\text{Al} + \text{Binder})$	+288.0	0.0533			0.1653	0.1152	0.3639			0.2804
#4 $\text{NH}_4\text{ClO}_4 - (\text{Be} + \text{Binder})$	+476.0	0.0528	0.0468		0.1580	0.1153	0.3352			0.2919
#5 $\text{N}_2\text{O}_4 - (\text{Al} + \text{Binder})$	+952.0	0.0324			0.2593	0.2582	0.4122			0.0379
#6 $\text{OF}_2 - (\text{Li} + \text{LiH} + \text{Binder})$	-165.0	0.0201	0.0804		0.1371		0.2288	0.5336		

\*The above values for enthalpy and elemental composition pertain only to the gas phase products of the nozzle throat. Particulate materials are not considered. The enthalpy is the total enthalpy of the gases (thermal + chemical + kinetic).

TABLE V

STEADY STATE ABLATION RESULTS  
(a) Propellant No. 1 - OF<sub>2</sub> Diborane

Material	Density	Melt Temp OR	Surface Temp OR	$\dot{B}$	B'	$B_d$	$\dot{S}^*$ mils/sec	Surface Species	Primary Erosion Node
W*	19.28	6570.0	6570.0	12.493			11.07	W*	Melt
C*	2.26	> 8000	6233.0	0.397	0.0		10.78	C*	Chemical
Ta*	16.60	5886.0	5886.0	19.81			17.2	Ta*	Melt
TaC*	14.65	7691.4	6300.0	5.07			11.5	TaC <sub>2</sub> *	Chemical + Melt
TaC+11% C	8.48	7691.4	6791.7	1.1033			6.68	TaC*	Chemical
HfC*	12.70	7488.0	6506.0	2.09			6.93	F <sub>2</sub> Hf* or HfC*	Chemical + Melt
TiC*	4.92	6318.0	6318.0	1.038			10.92	TiC*	Melt
ZrC*	6.74	6777.0	6594.1	1.234			13.05	B <sub>2</sub> Zr* or ZrC*	Chemical + Melt
BeO*	3.06	5076.0	5076.0	2.53			31.4	BeO*	Melt
ZrO <sub>2</sub> *	5.73	5310.0	5310.0	8.12			31.05	ZrO <sub>2</sub> *	Melt
HfO <sub>2</sub> *	9.68	5706.0	5706.0	10.04			20.34	HfO <sub>2</sub> *	Melt
ZrN*	7.09	5805.0	5805.0	5.615			61.96	ZrN*	Melt

\* Based on a heat transfer coefficient,  $\rho_e U_e C_{H_2O} = 0.5 \text{ lb}/\text{ft}^2\text{-sec}$

TABLE V (continued)

## (b) Propellant No. 2 - FLOX Methane

Material	Density	Melt Temp °R	Surface Temp °R	$\dot{B}$	B'	$B_2$	$\dot{S}^*$ mils/sec	Surface Species	Primary Erosion Mode
W*	19.28	6570.0	4388.0	0.0	0.0	0.0	0.0	CW2* or C*	Chemical
C*	2.26	> 8000	4674.0	0.0139	0.0	0.0	0.437	C*	Chemical
Ta*	16.60	5886.0	4700.0   Estimate	< 0.7			< 3.0	TaC* or C*	Chemical
TaC*	14.65	7691.4	4699.0   Extrapolation	0.565	0.565	0.0	2.59	TaC* or C*	Chemical
TaC*+11% <i>C</i>	8.48	7691.4	4397.0   Extrapolation	0.135	0.135	0.0	1.54	TaC* or C*	Chemical
HfC*	12.70	7488.0	4871.0	0.379			1.84	C*	Chemical
TiC*	4.92	6318.0	4607.0	0.0567			0.806	C*	Chemical
ZrC*	6.74	6777.0	4676.0	0.09997			1.02	C*	Chemical
BeO*	3.06	5076.0	4370.0	0.126			2.81	BeO*	Chemical
ZrO <sub>2</sub> *	5.73	5310.0	4660.0	0.111			1.32	ZrO <sub>2</sub> *	Chemical
HfO <sub>2</sub> *	9.68	5706.0	4209.0	0.300	0.279	0.021	2.00	HfO <sub>2</sub> *	Chemical
ZrN*	7.09	5805.0	4744.0	0.451	0.340	0.111	4.04	ZrO <sub>2</sub> *	Chemical

\* Based on a heat transfer coefficient,  $\rho_{\text{e}} U_{\text{e}} C_{\text{H}_2\text{O}} = 0.5 \text{ lb/ft}^2\text{-sec}$

(c) Propellant No. 3 - Aluminized Solid

Material	Density	Melt Temp °R	Surface Temp °R	B'	B'	B <sub>d</sub>	$\dot{S}^*$ mils/sec	Surface Species	Primary Erosion Mode
W*	19.28	6570.0	5557.0	0.021	+0.021	0.0	0.080	W*	Chemical
C*	2.26	> 8000	5042.0	0.151	0.151	0.0	4.66	C*	Chemical
Ta*	16.60	5886.0	5595.0	0.520	-0.058	0.578	2.36	TaN*	Chemical + Melt
TaC*	14.65	7691.4	5457.0	0.3744	-0.0299	0.4043	1.898	TaN*	Chemical + Melt
TaC*+11%G	8.48	7691.4	5533.0	0.270	+0.056	0.214	2.21	TaN*	Chemical + Melt
HfC*	12.70	7488.0	5568.0	0.00109	+0.00105	0.00004	0.005	H'-O <sub>2</sub> *	Chemical
TiC*	4.92	6318.0	5230.0	0.3123	+^ 127	0.185	4.47	TiN*	Chemical + Melt
ZrC*	6.74	6777.0	5421.0	0.545	+0.245	0.300	5.46	ZrO <sub>2</sub> * or ZrN*	Chemical + Melt
P <sub>2</sub> O <sub>5</sub> *	3.06	5076.0	5076.0	0.411	+0.001	0.410	9.99	BeO*	Melt
ZrO <sub>2</sub> *	5.73	5310.0	5310.0	0.7645	+0.00	0.7645	9.88	ZrO <sub>2</sub> *	Melt
HfO <sub>2</sub> *	9.68	5706.0	5565.0	0.0012	+0.00116	0.00004	0.009	HfO <sub>2</sub> *	Chemical
ZrN*	7.09	5865.0	5435.0	0.7755	+0.1601	0.6154	7.605	ZrO <sub>2</sub> * or ZrN*	Chemical + Melt

\* Based on a heat transfer coefficient,  $\sigma_{ee} C_{H_2O} = 0.5 \text{ lb}/\text{ft}^2 \cdot \text{sec}$

TABLE V (continued)  
(d) Propellant No. 4 - Beryllium Solid

Material	Density	Melt Temp °R	Surface Temp °O	B'	B	$\dot{S}^*$ mils/sec	Surface Species	Primary Erosion Mode
W*	19.28	6570.0	5980.0	0.00166	0.0	0.006	W*	Chemical
C*	2.26	> 8000	5540.	0.1643	0.0	4.84	C*	Chemical
Ta*	16.60	5886.0	5886.0	0.913	0.450	3.863	TaN*	Melt
TaC†	14.65	7691.4	5813.0	0.130	+0.130	0.0	0.594	Chemical
TaC*+11% C	8.48	7691.4	5806.0	0.0892	+0.0875	0.0016	TaN*	Chemical
HfC*	12.70	7488.0	5767.0	0.7933	+0.253	0.50	0.752	Chemical + Melt
TiC*	4.92	6318.0	5763.0	0.2502	+0.201	0.0490	3.49	HfC*
ZrC*	6.74	6777.0	5820.0	0.475	+0.324	0.151	3.35	TiN*
BeO*	3.06	5076.0	5076.0	1.067	-0.002	1.069	25.0	ZrN*
ZrO <sub>2</sub> *	5.73	5310.0	5310.0	2.68	-0.02	2.70	33.5	BeO*
HfO <sub>2</sub> *	9.68	5706.0	5706.0	1.714	0.0	1.714	12.6	Melt
ZrN*	7.09	5805.0	5799.0	0.697	+0.282	0.415	6.31	ZrO <sub>2</sub> *
								Chemical + Melt

\* Based on a heat transfer coefficient,  $\rho_e U e_{H_2} = 0.5 \text{ lb}/\text{ft}^2\text{-sec}$

TABLE V (continued)  
(e) Propellant No. 5 -  $N_2O_4$  - Aluminum Hybrid

Material	Density	Melt Temp °R	Surface Temp °R	$\dot{B}$	$B'$	$B_\ell$	$\dot{S}^*$ mils/sec	Surface Species	Primary Erosion Mode
W*	19.28	6570.0	6488.0	0.00532	+0.00532	0.0	0.02	W*	Chemical
C*	2.26	> 8000	6008.0	0.200	+0.200	0.0	6.27	C*	Chemical
Ta*	16.60	5886.0	5886.0	14.77	+0.2	14.97	71.5	TaN*	Melt
TaC*	14.65	7691.4	6377.0	0.222	$\pm 0.147$	0.0745	1.07	Ta <sub>2</sub> C*	Chemical + Melt
TaC*+11% <i>C</i>	8.48	7691.4	6392.0	C.1398	+0.1347	0.0051	1.19	Ta <sub>2</sub> C* or TaN*	Chemical
HfC*	12.70	7488.0	6444.0	0.546	-0.008	0.554	3.29	HfN*	Chemical + Melt
TiC*	4.92	6318.0	6138.0	0.546	+0.066	0.480	8.24	TiC*	Melt
ZrC*	6.74	6777.0	6341.0	0.373	-0.004	0.377	4.24	ZrC* or ZrN*	Chemical + Melt
BeO*	3.06	5076.0	5076.0	1.523	-0.03	1.553	38.5	BeO*	Melt
ZrO <sub>2</sub> *	5.73	5310.0	5310.0	4.40	-0.04	4.44	42.5	ZrO <sub>2</sub> *	Melt
HfO <sub>2</sub> *	9.68	5706.0	5706.0	4.65	-0.03	4.68	37.1	HfO <sub>2</sub> *	Melt
ZrN*	7.09	5805.0	5805.0	2.91	-0.03	2.94	31.7	ZrN*	Melt

\* Based on a heat transfer coefficient,  $\rho_{eeH_O}^{U}$  = 0.5 lb/ft<sup>2</sup> -sec

TABLE V (continued)  
(f) Propellant No. 6 - OF<sub>2</sub> - Lithium Hybrid

Material	Density	Melt Temp °R	Surface Temp °R	B̄	B'	B <sub>2</sub>	$\dot{S}^*$ mils/sec	Surface Species	Primary Erosion Mode
W*	19.28	6570.0	6570.0	8.36			11.7	W*	Melt
C*	2.26	> 8000	6798.0	0.195	+0.195	0.0	7.04	C*	Chemical
Ta*	16.60	5886.0	5886.0	10.946	+0.314	10.632	52.8	Ta*	Melt
TaC*	14.65	7691.4	7543.0	0.996			4.49	TaC*	Chemical
TaC*+11% C	8.48	7691.4	7691.4	0.368			3.37	TaC*	Chemical + Melt
HfC*	12.70	7488.0	7014.0	1.40	+1.40	0.0	6.65	HfC*	Chemical
TiC*	4.92	6318.0	6318.0	0.586			8.76	C*	Chemical + Melt
ZrC*	6.74	6777.0	6614.0	0.941	-0.191	1.132	13.54	ZrC* or C*	Chemical + Melt
BeO*	3.06	5076.0	5076.0	1.385			26.0	BeO*	Melt
ZrO <sub>2</sub> *	5.73	5310.0	5310.0	2.53			29.3	ZrO <sub>2</sub> *	Melt
HfO <sub>2</sub> *	9.68	5706.0	5706.0	5.70			19.7	HfO <sub>2</sub> *	Melt
ZrN*	7.09	5805.0	5805.0	2.295	-0.27	2.322	32.2	ZrN*	Melt

\* Based on a heat transfer coefficient,  $\rho_e U_e C_{H_2O} = 0.5 \text{ lb/ft}^2\text{-sec}$

Figure 1(c)

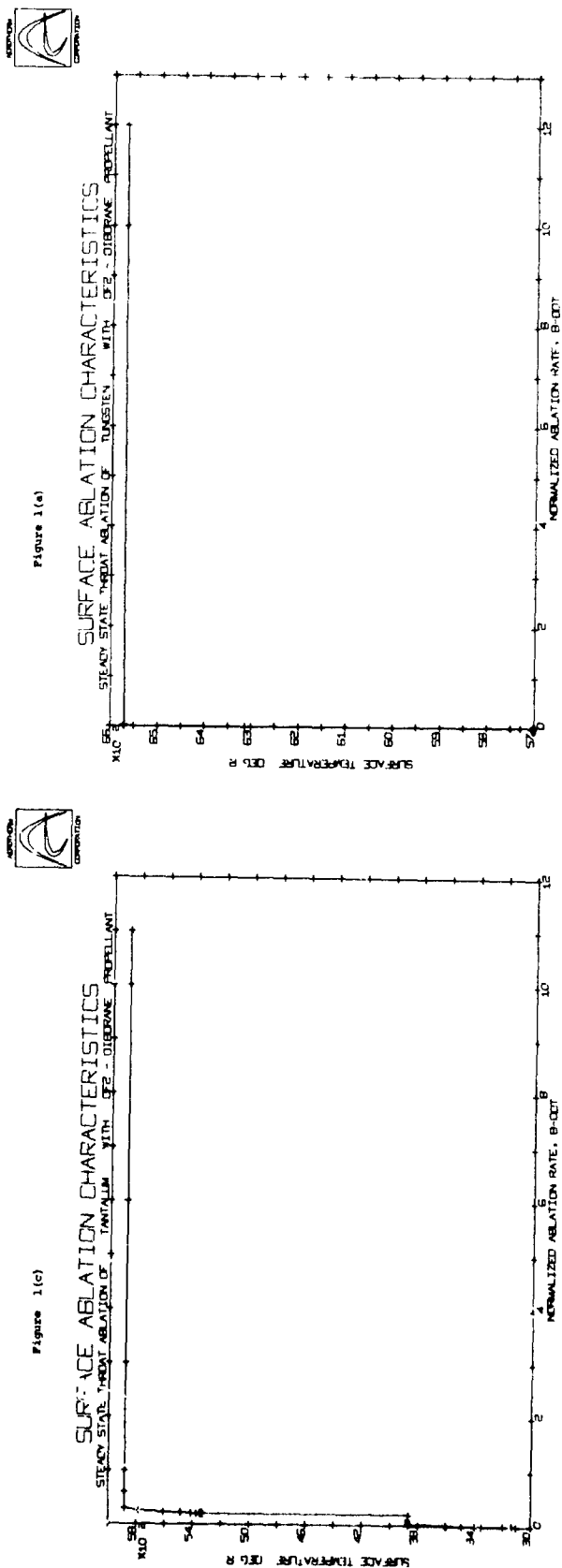


Figure 1(d)

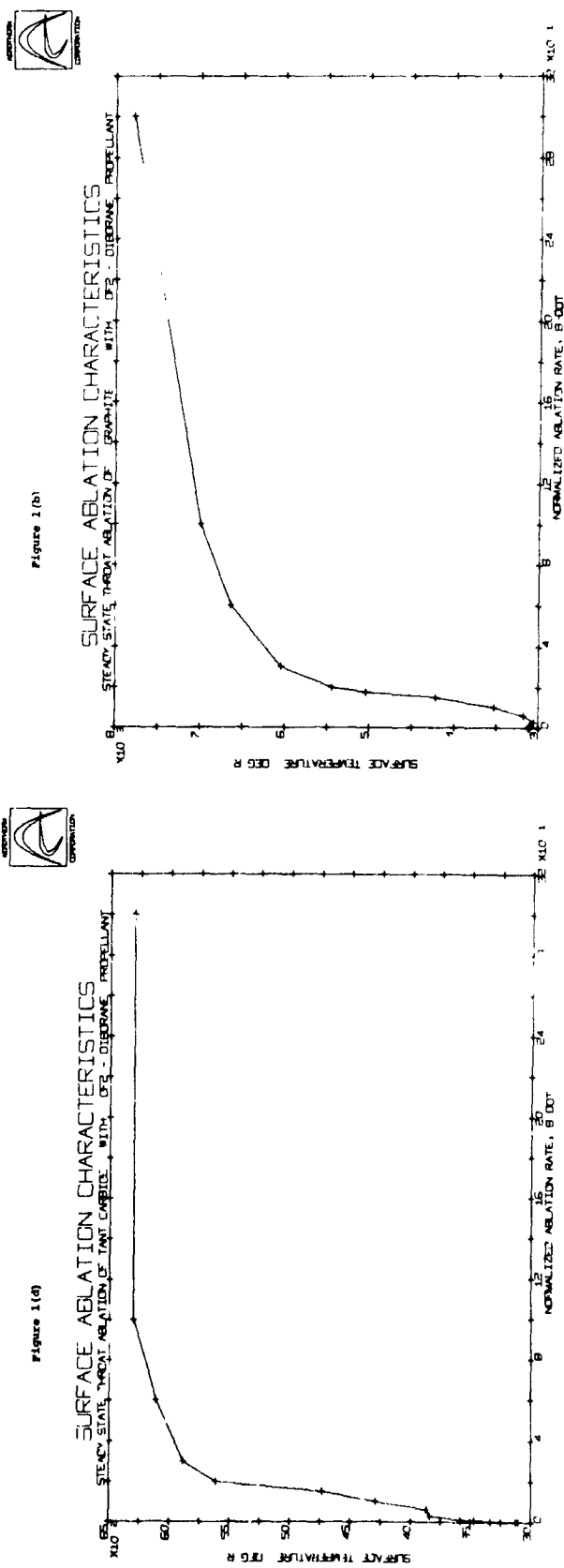


Figure 1(a)

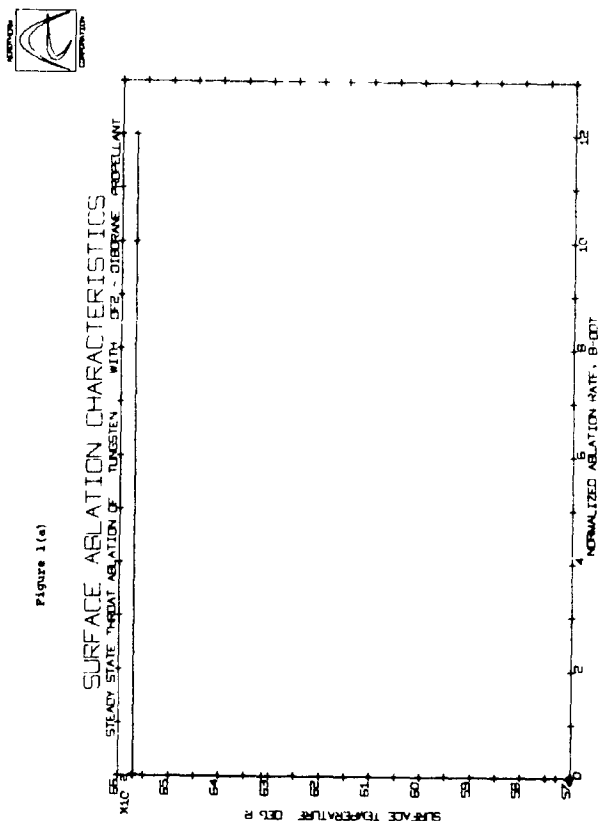


Figure 1(b)

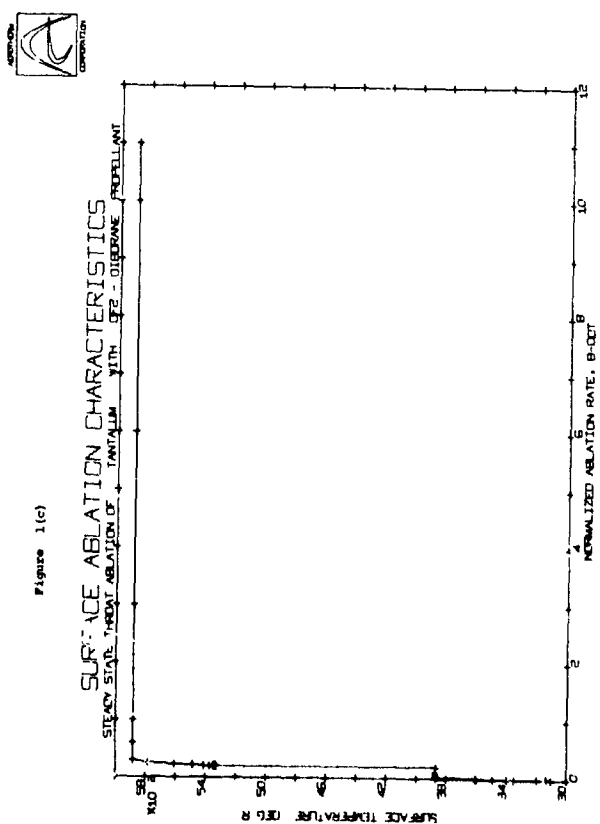


Figure 1(e)

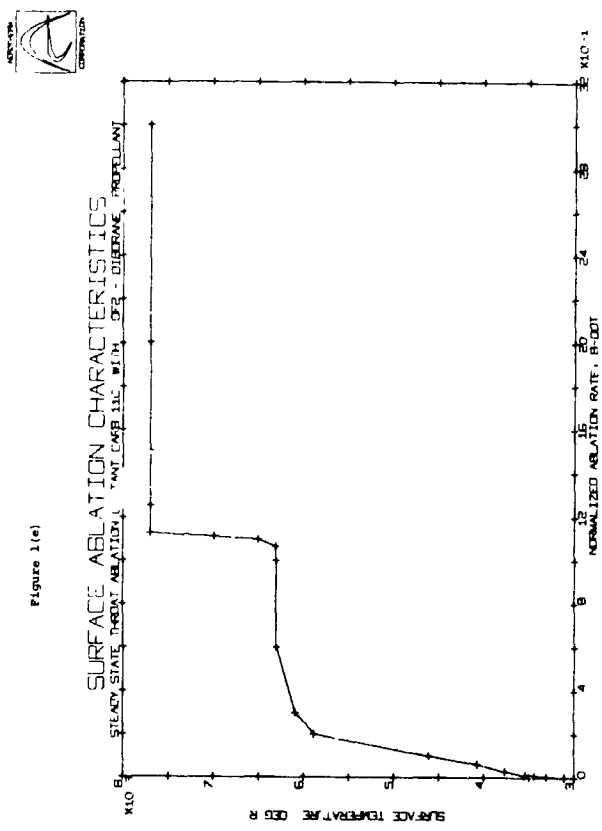


Figure 1(f)

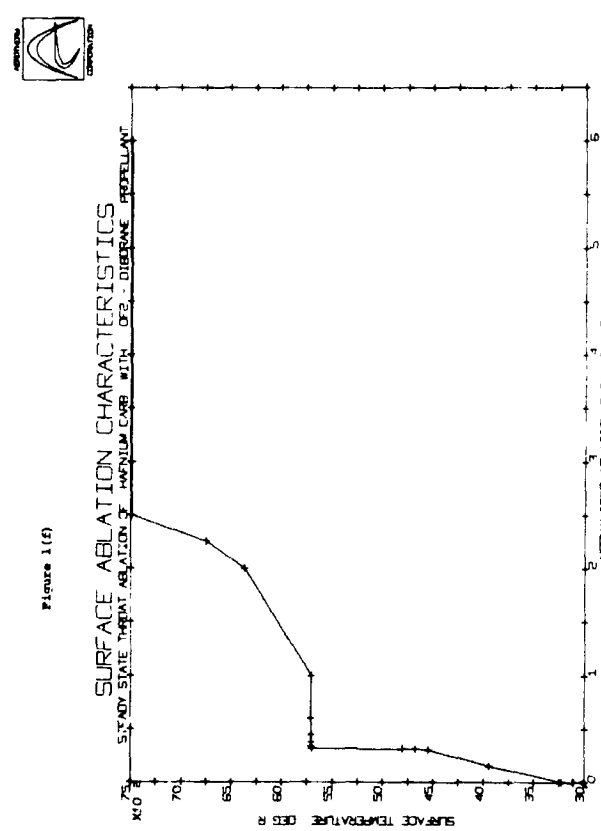


Figure 1(g)

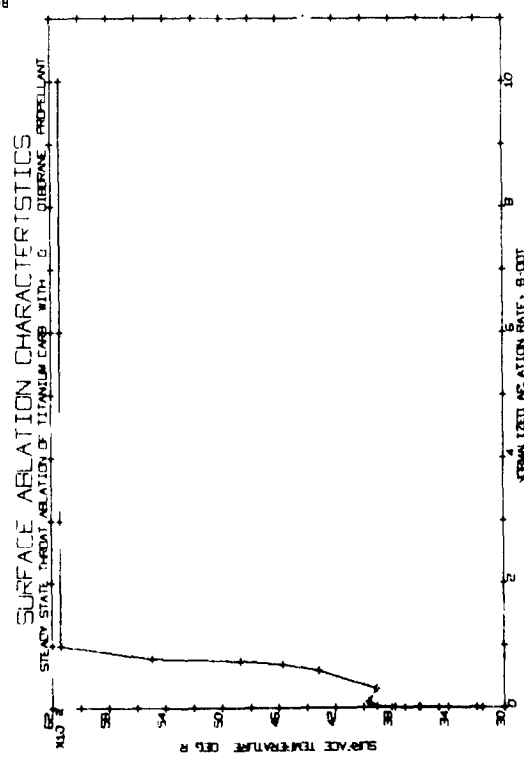


Figure 1(h)

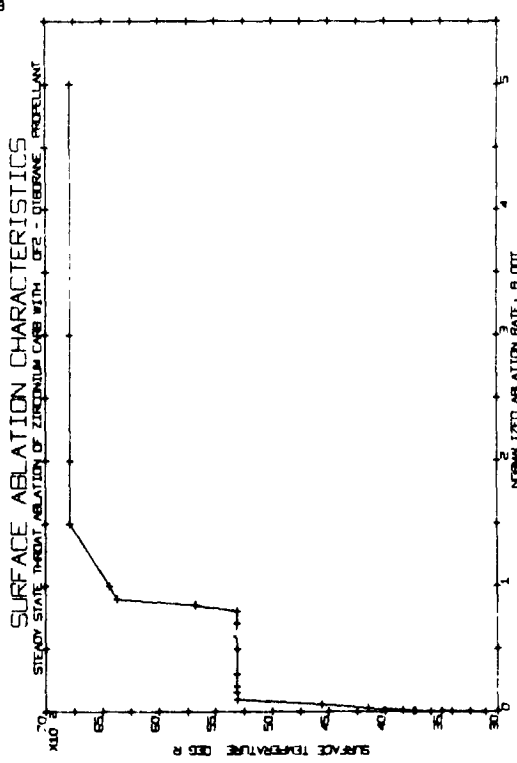


Figure 1(1)

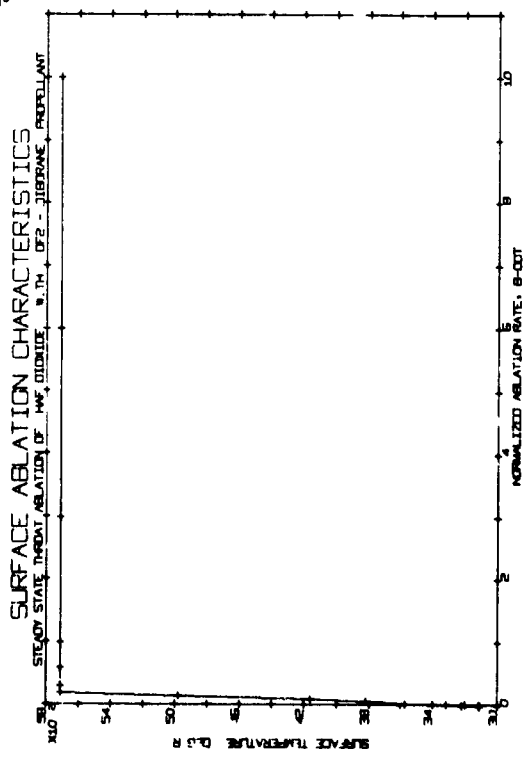


Figure 1(1)

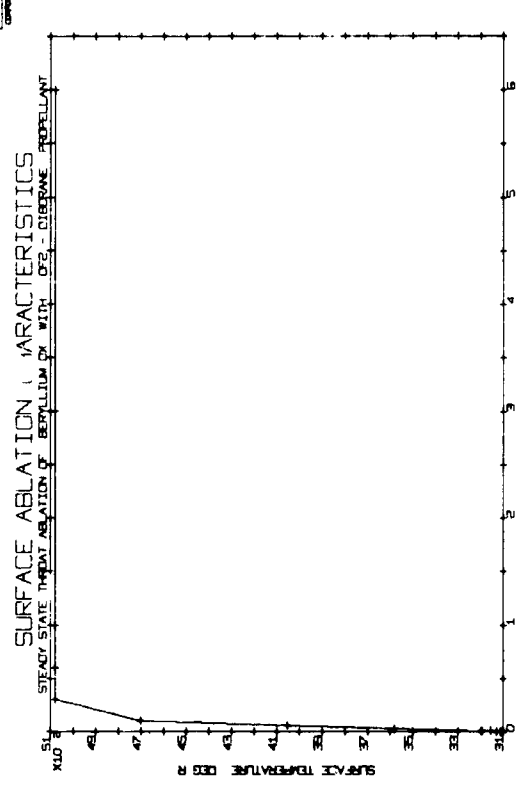


Figure 1(1)

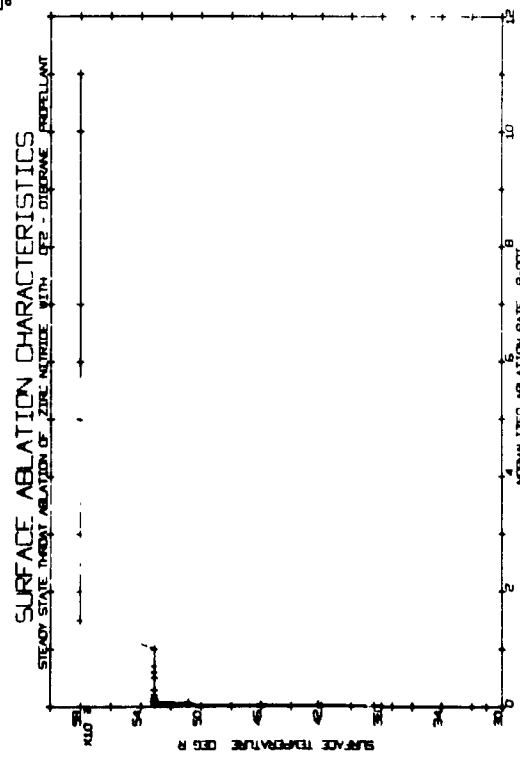


Figure 1(1)

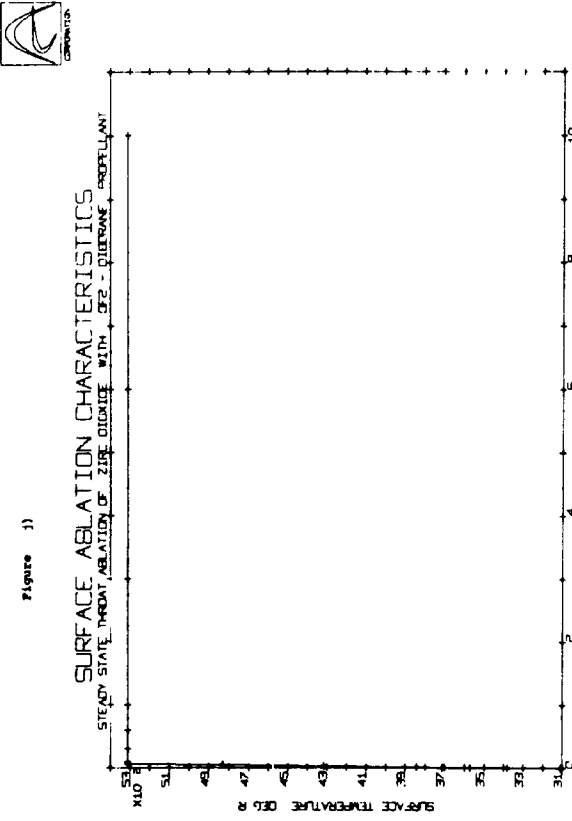


Figure 2 (c)

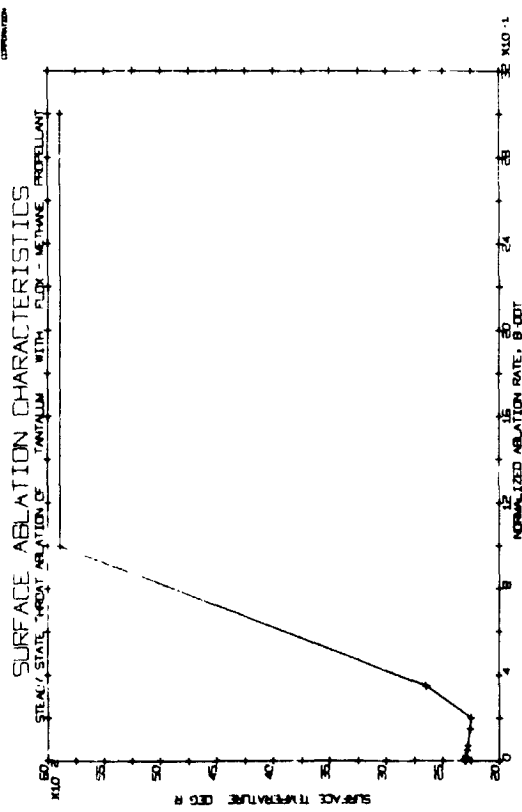


Figure 2 (a)

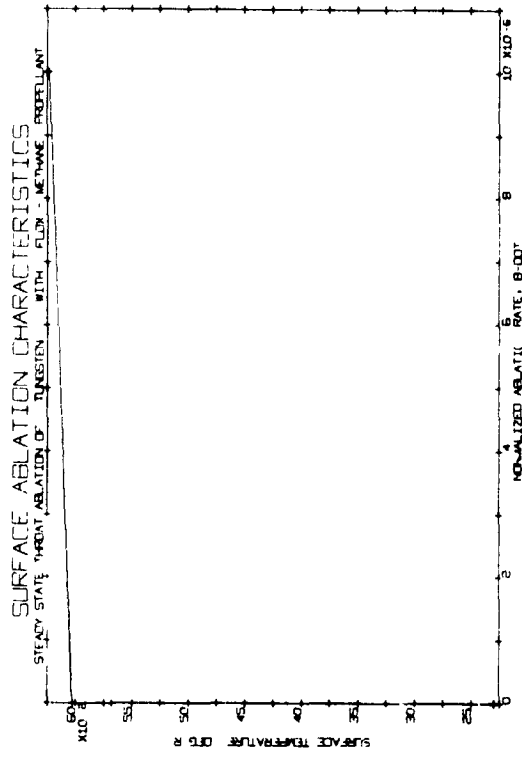


Figure 2(d)

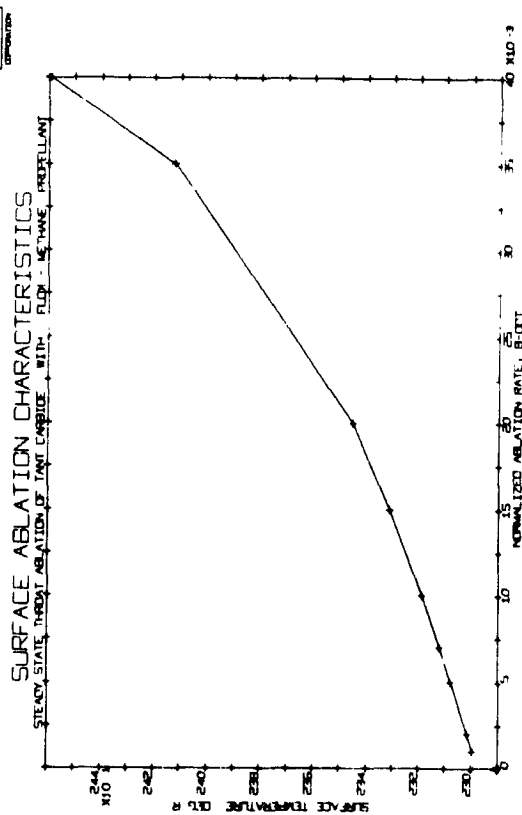


Figure 2(b)

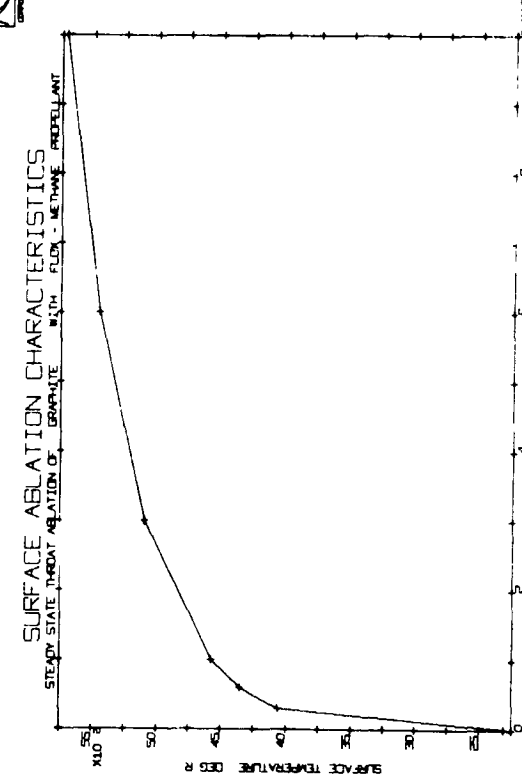


Figure 2(e)

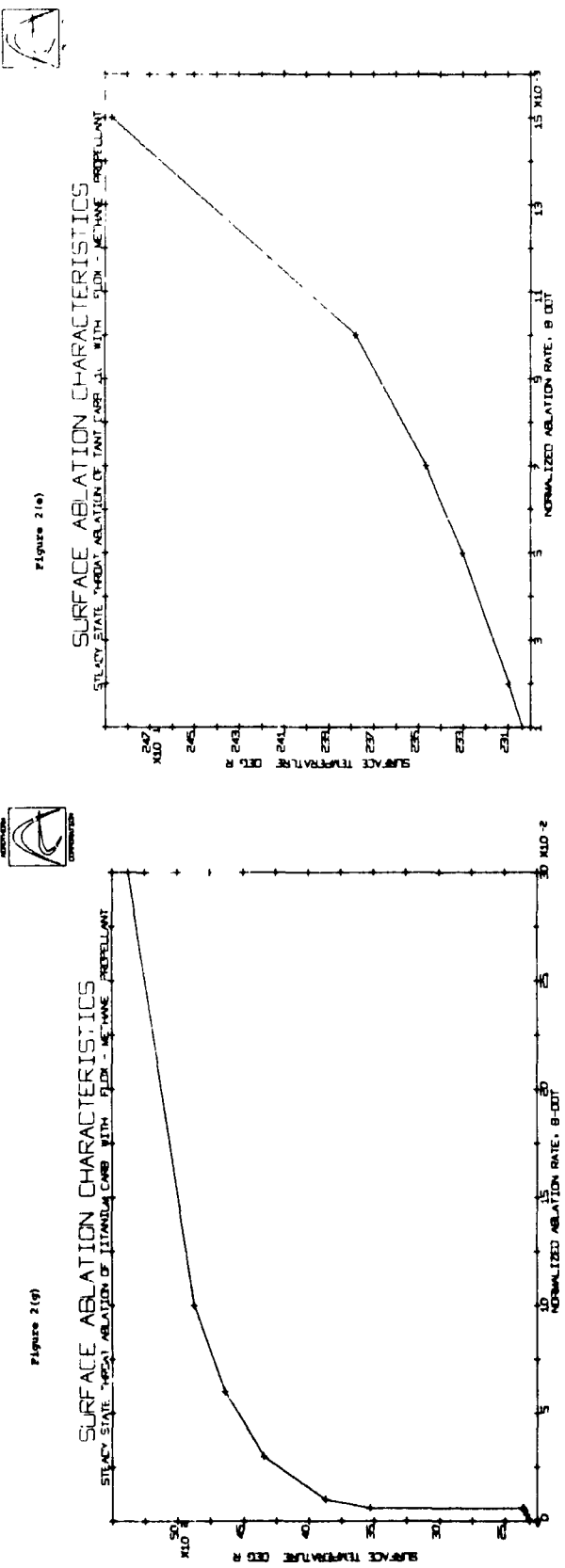
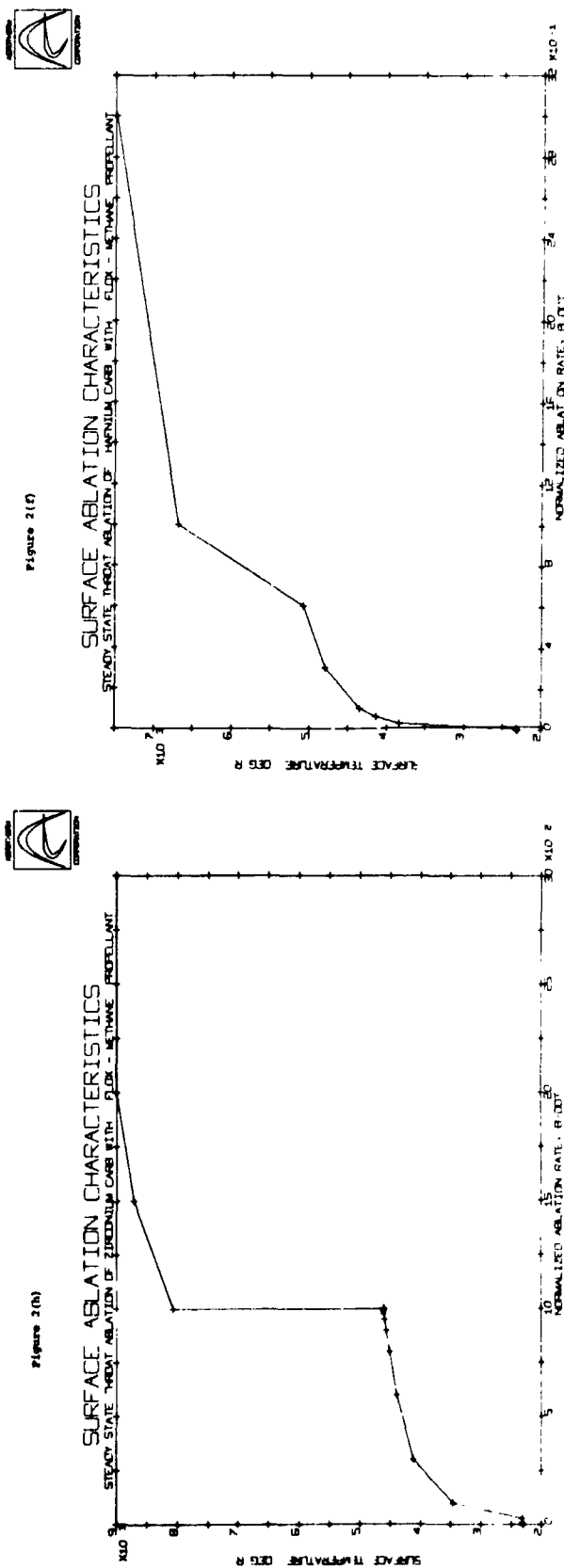
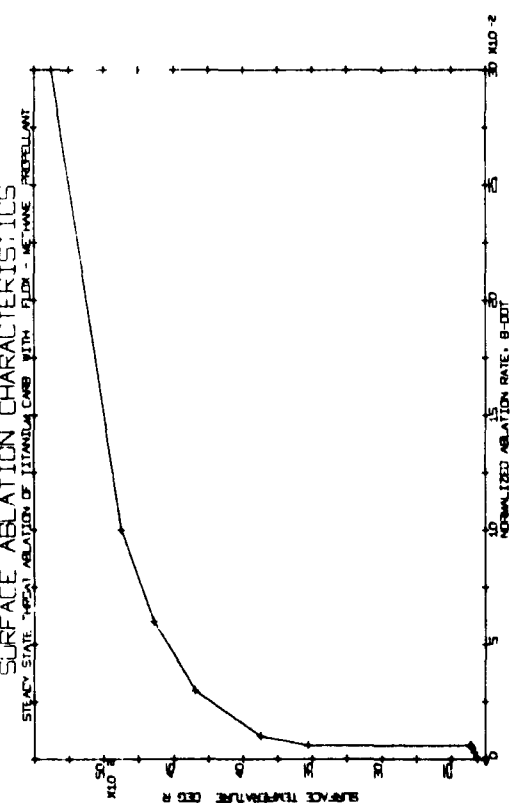


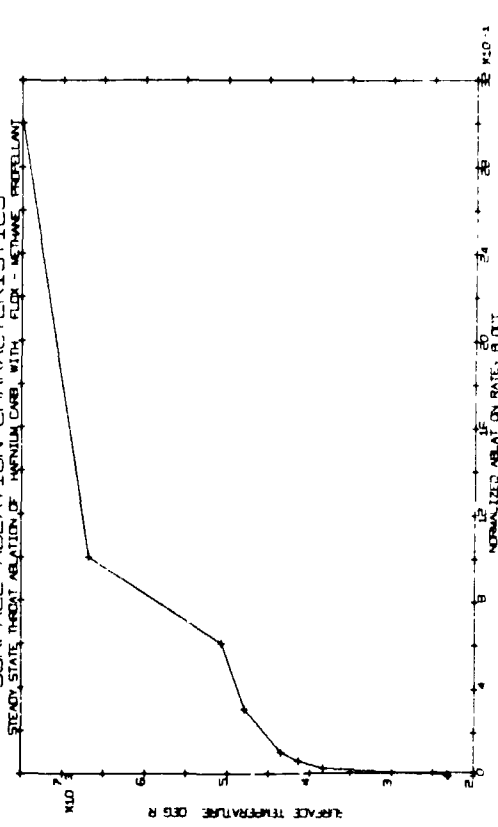
Figure 2(f)



SURFACE ABLATION CHARACTERISTICS  
STEADY STATE HEAT ABALION OF TANT C-100 WITH FLUORINE PROPELLANT



SURFACE ABLATION CHARACTERISTICS  
STEADY STATE HEAT ABALION OF HYPALUM C-100 WITH FLUORINE PROPELLANT



SURFACE ABLATION CHARACTERISTICS  
STEADY STATE HEAT ABALION OF TANT C-100 WITH FLUORINE PROPELLANT

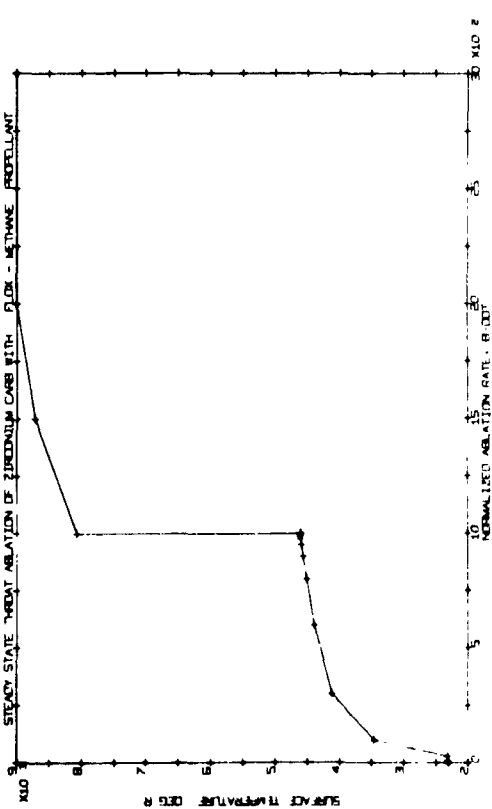




Figure 2(5)

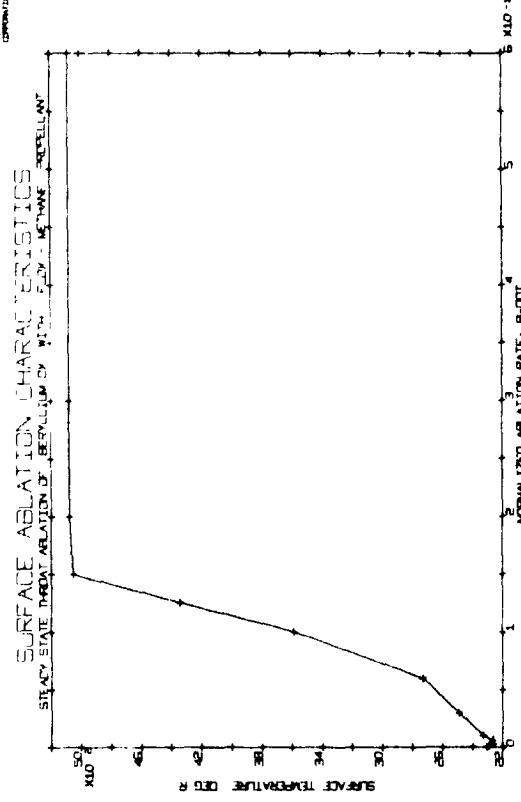


Figure 2(6)

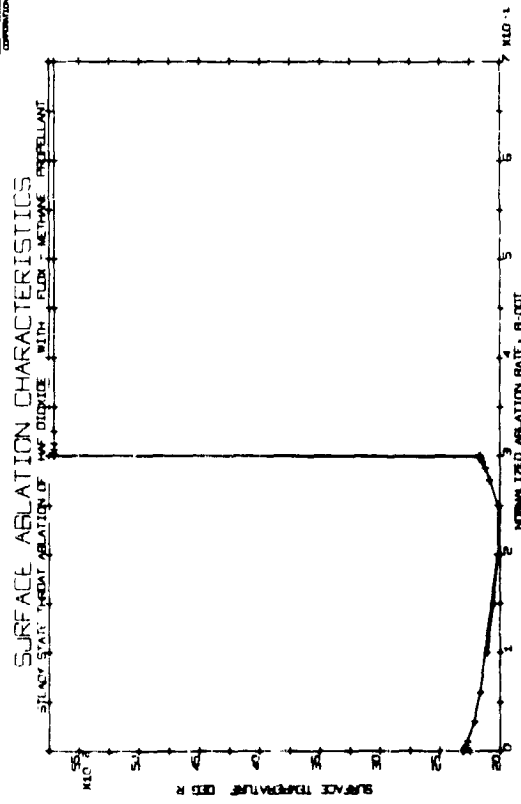


Figure 2(1)

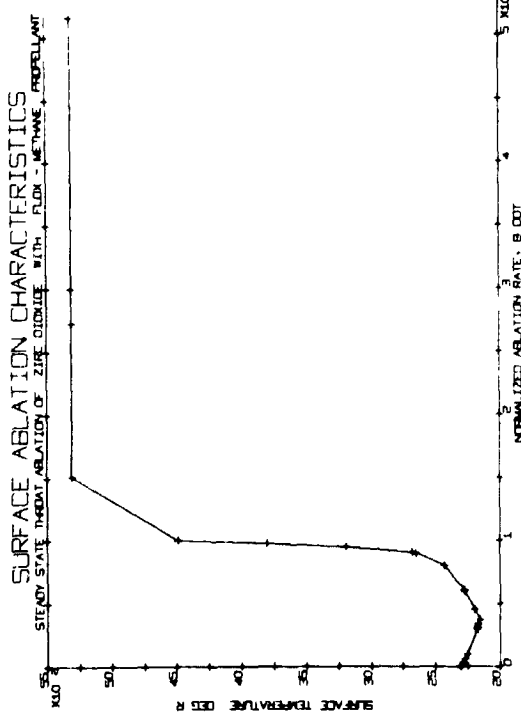


Figure 2(1)

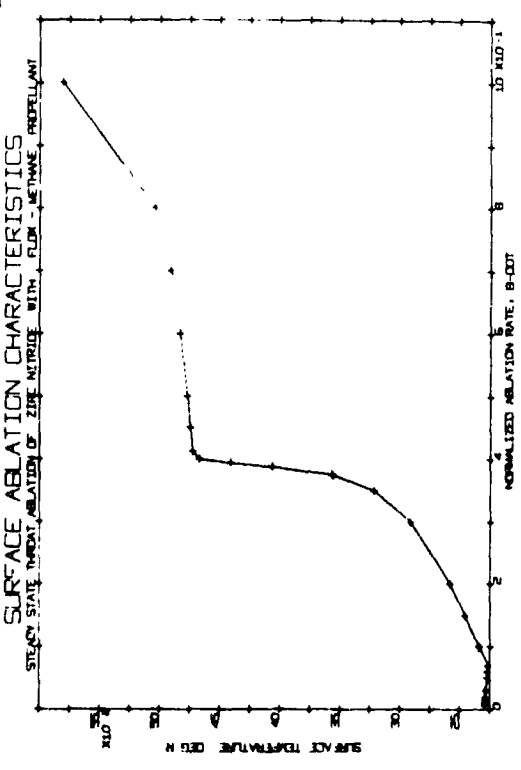




Figure 3(a)

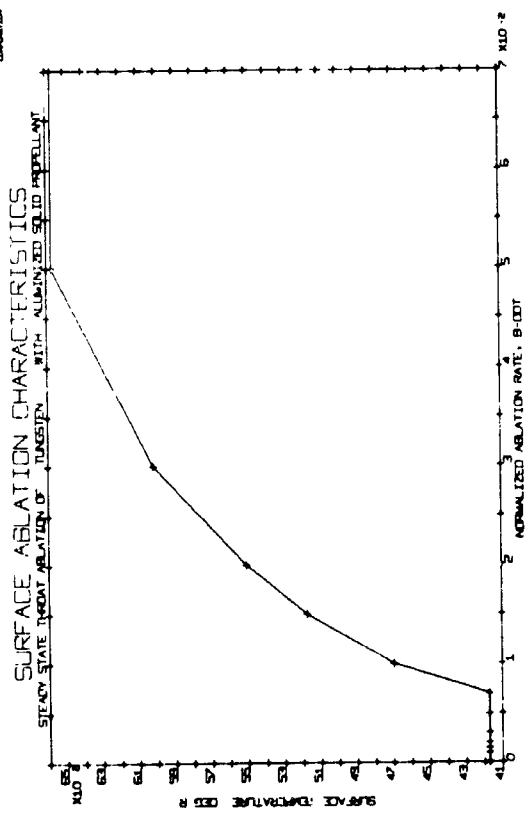


Figure 3(b)

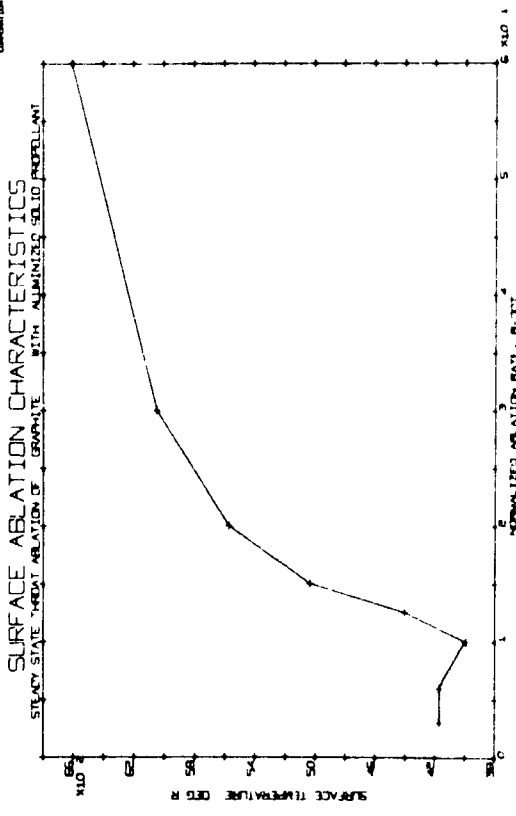


Figure 3(c)

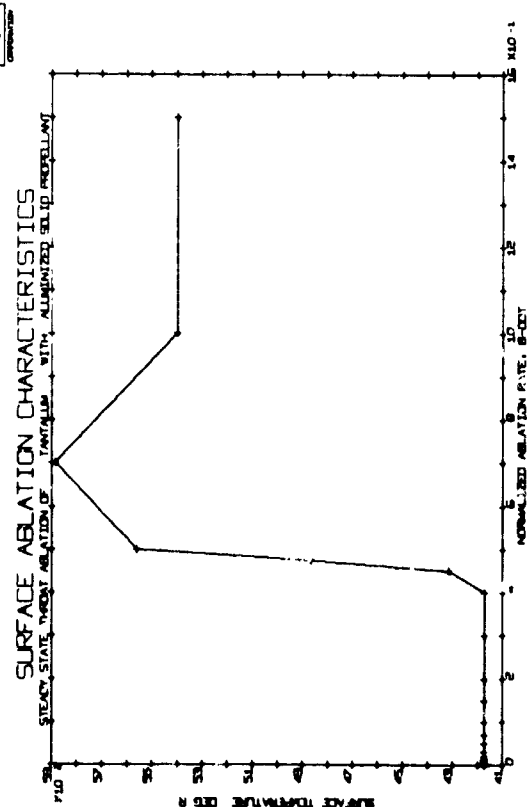


Figure 3(d)

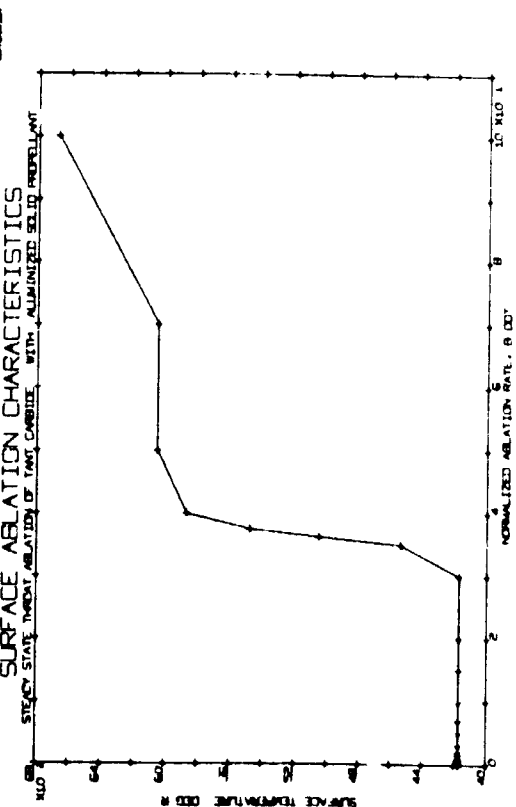


Figure 3-19

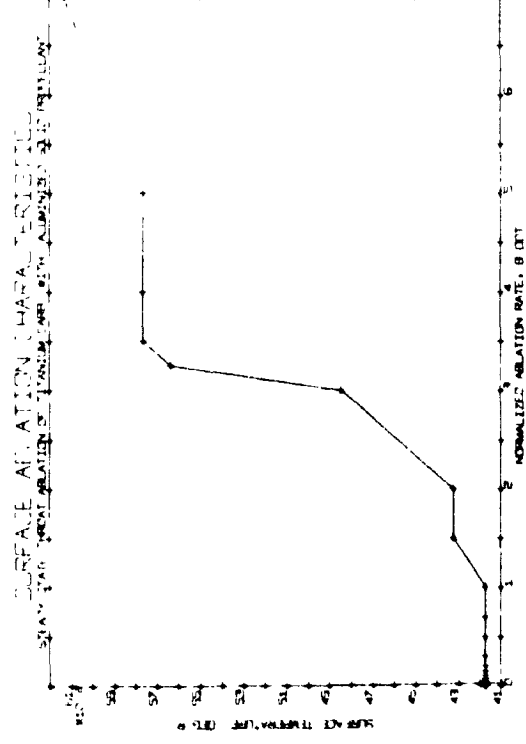


Figure 3-19

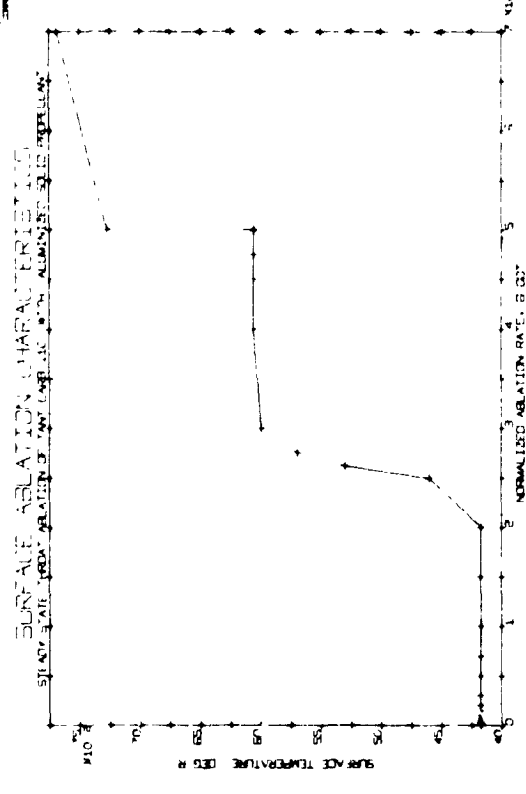


Figure 3-20

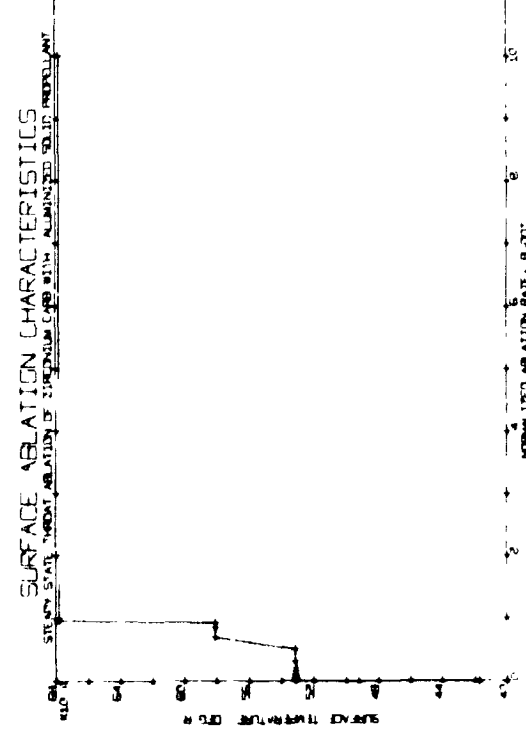


Figure 3-20

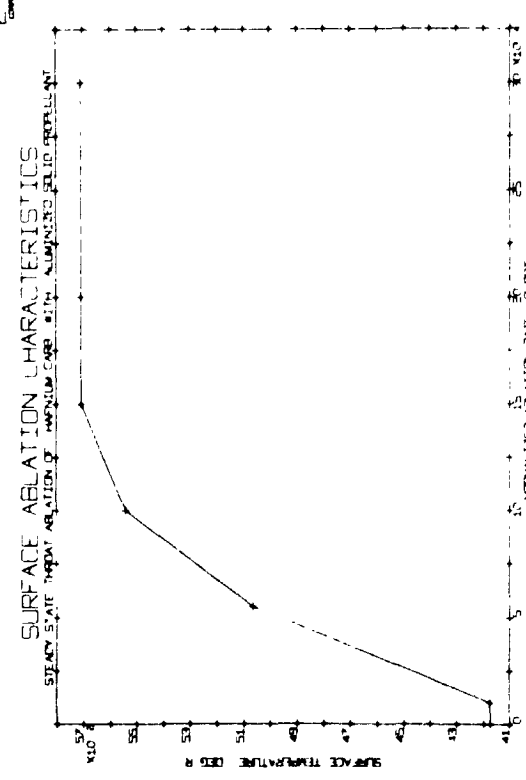


Figure 3(1)

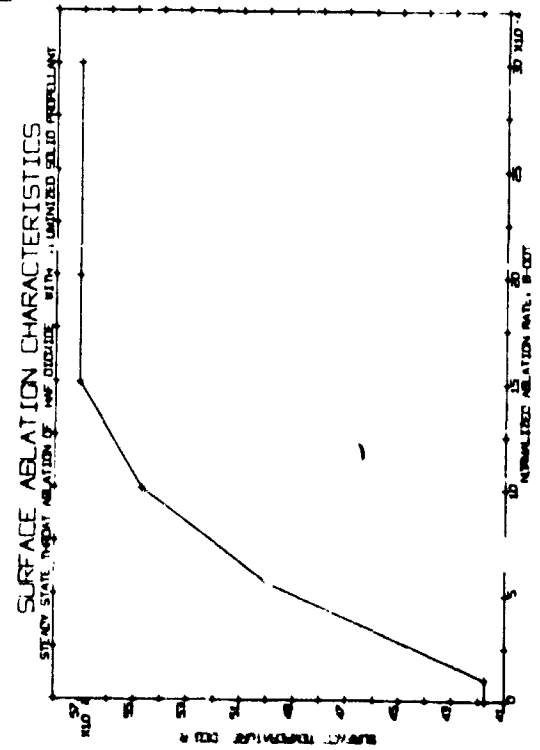


Figure 3(1)

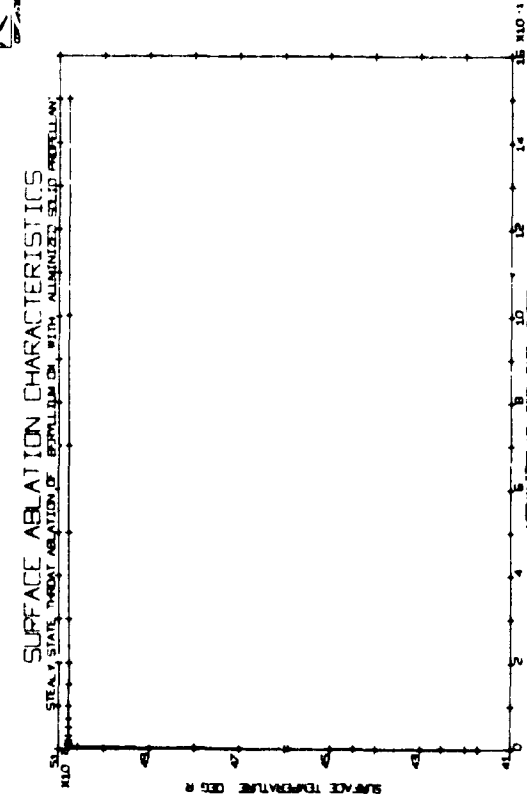


Figure 3(1)

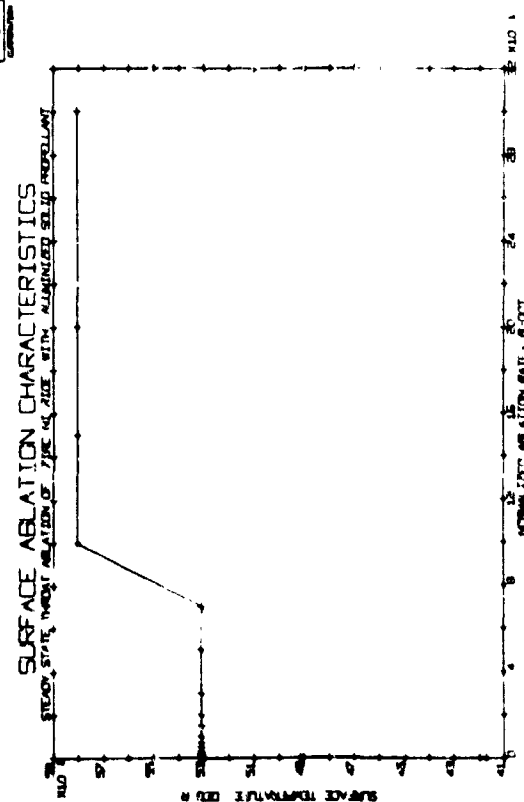


Figure 3(1)

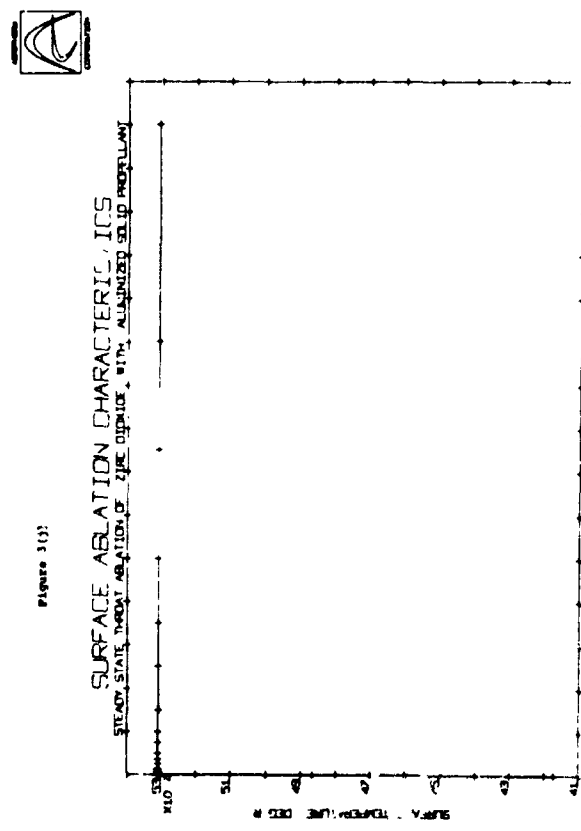


Figure 4(a)

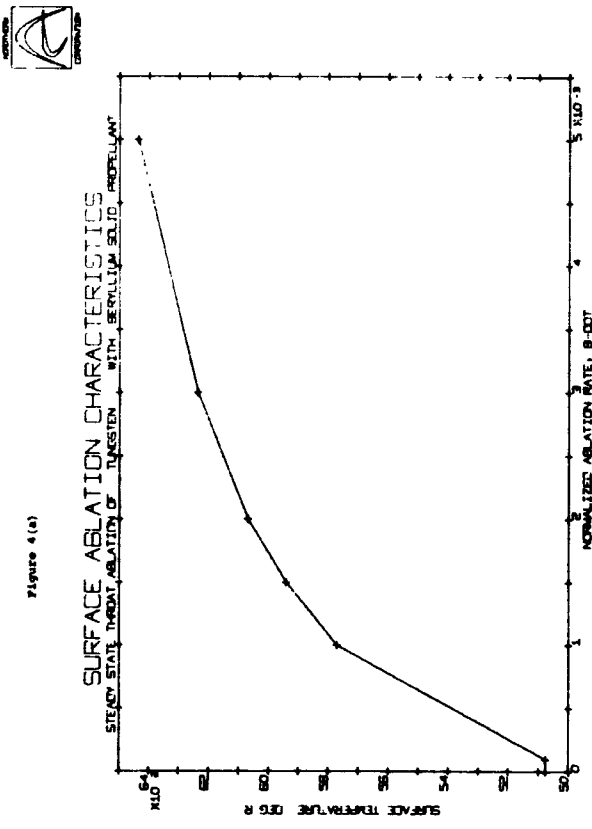


Figure 4(b)

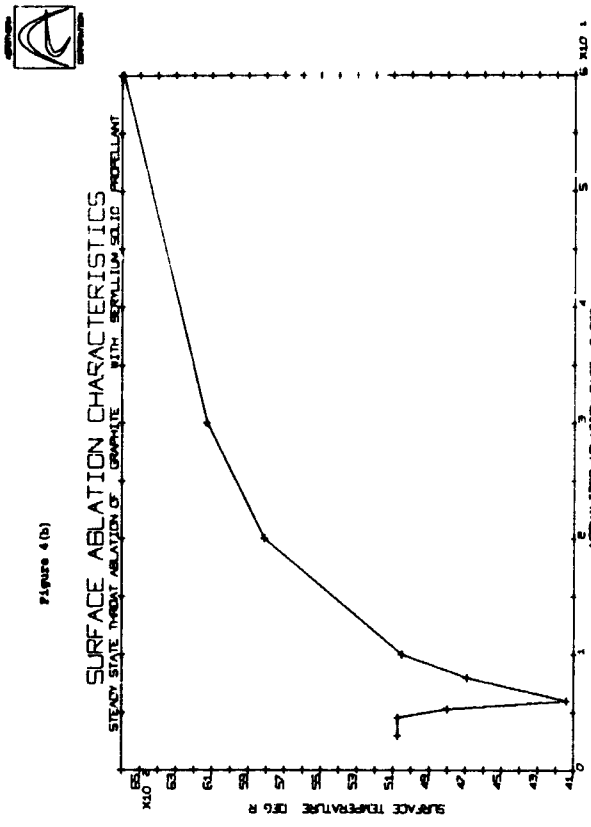


Figure 4(c)

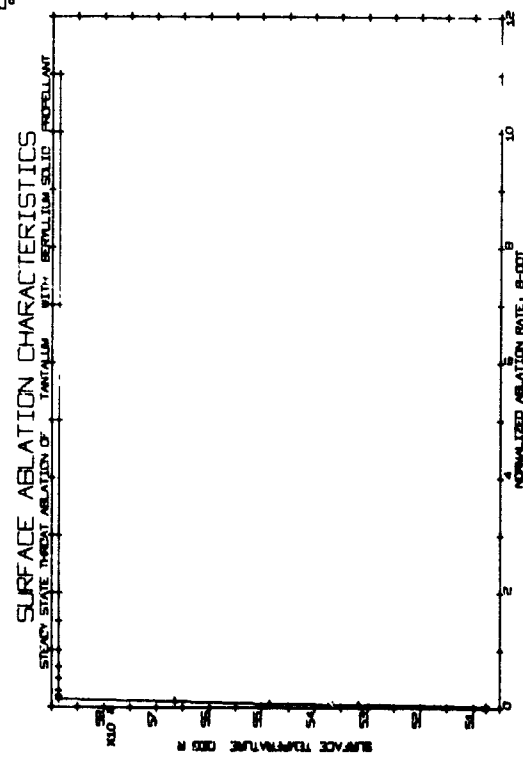


Figure 4(d)

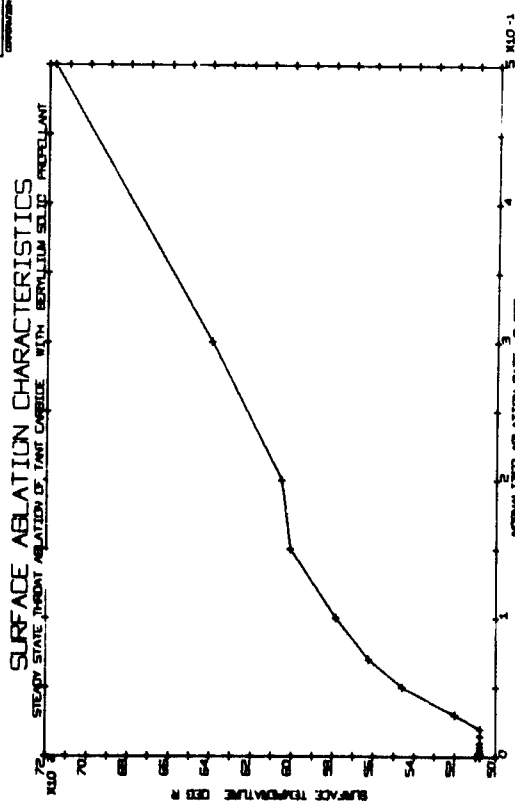


Figure 4(e)

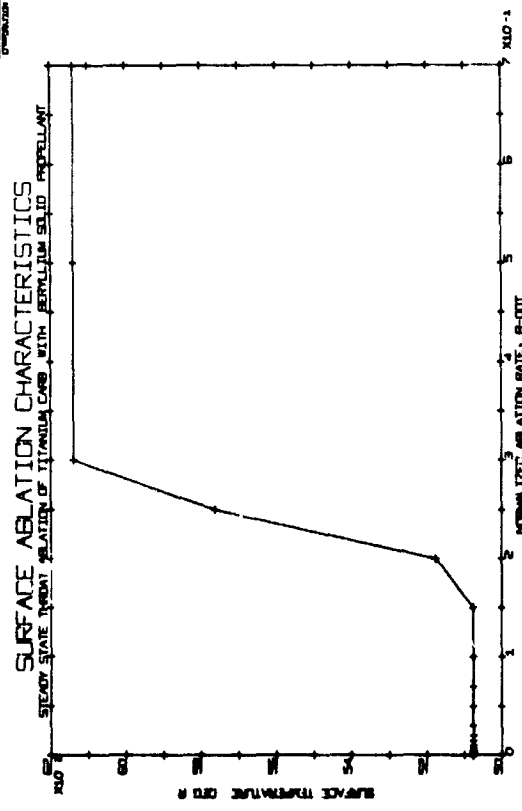


Figure 4(f)

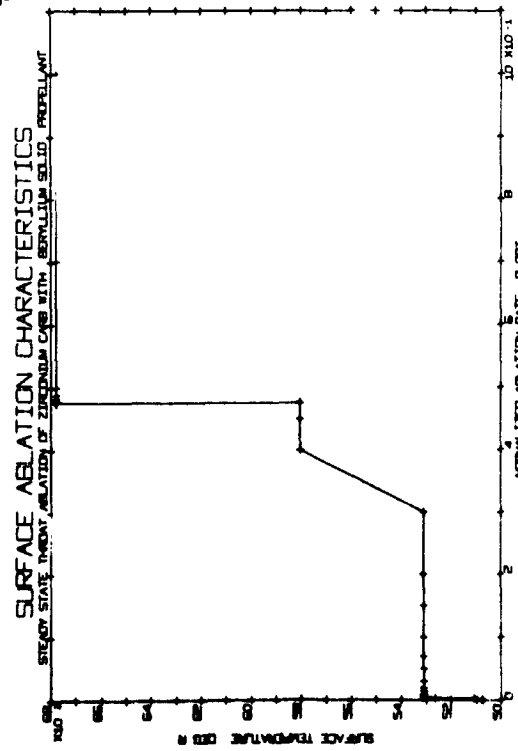


Figure 4(g)

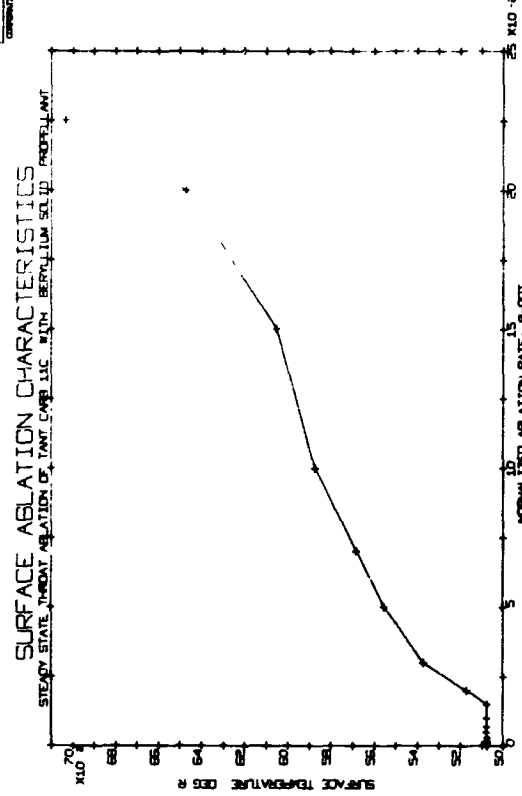


Figure 4(h)

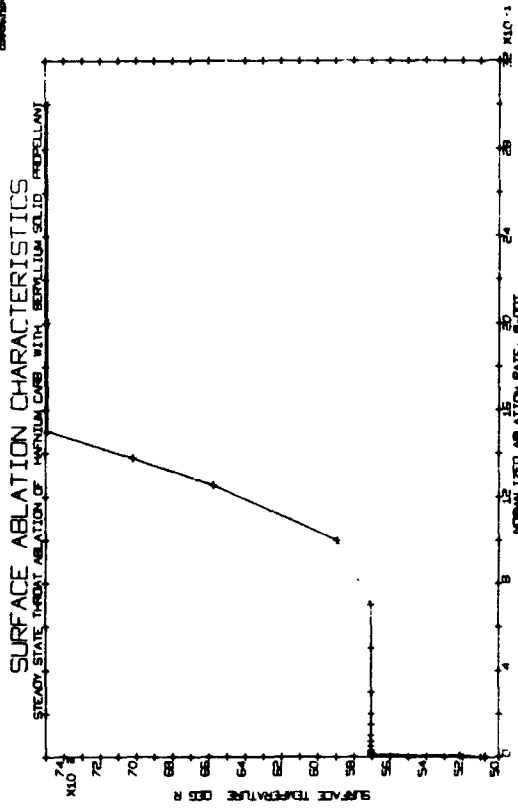


Figure 4 (k)

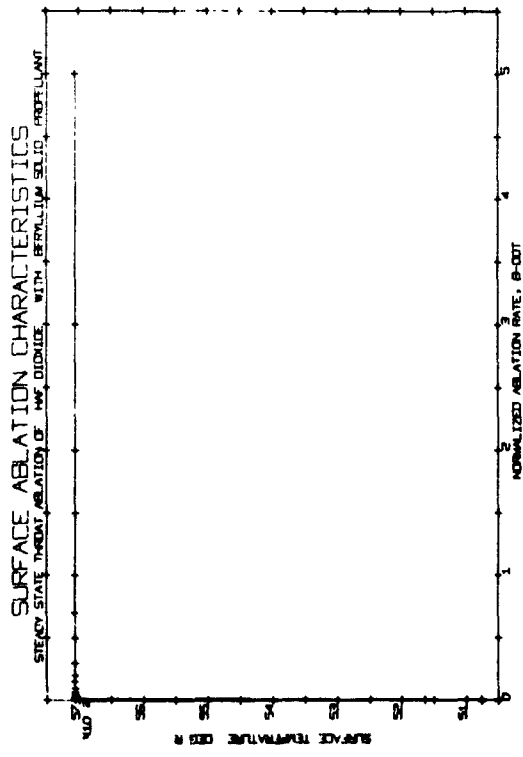


Figure 4 (l)

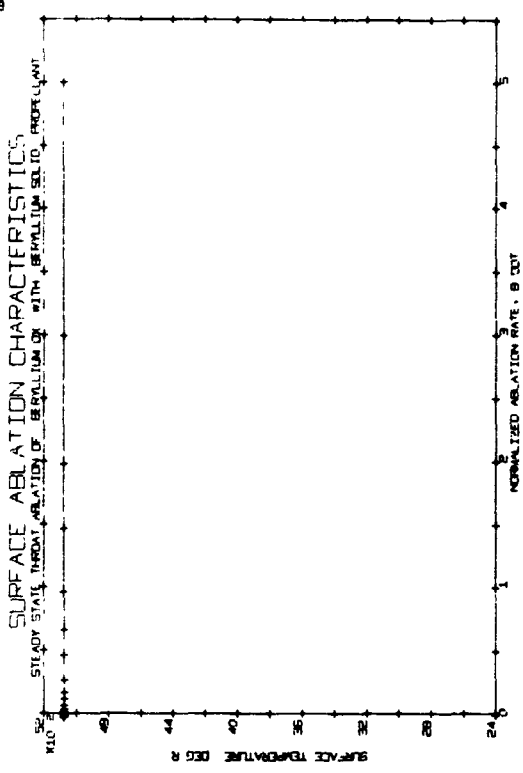


Figure 4 (l)

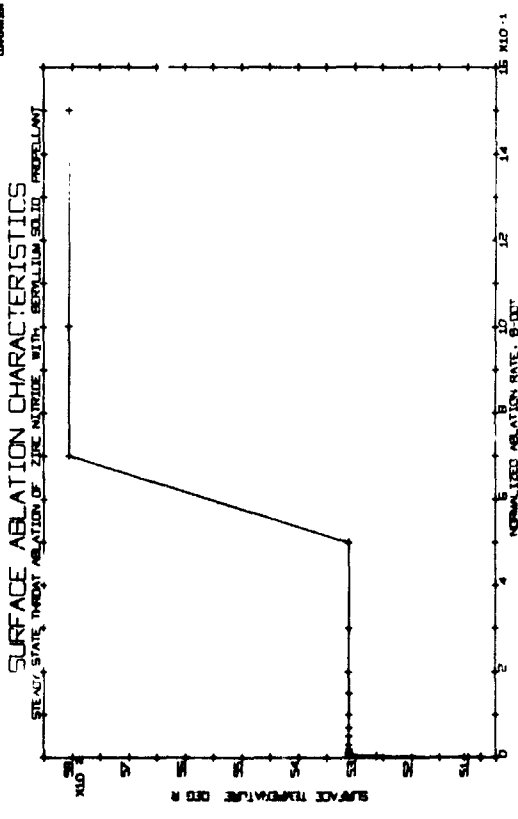


Figure 4 (l)

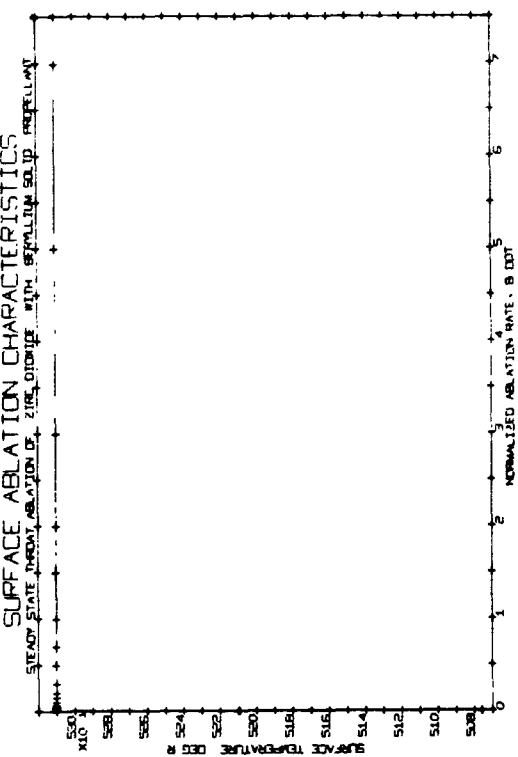




Figure 5(a)

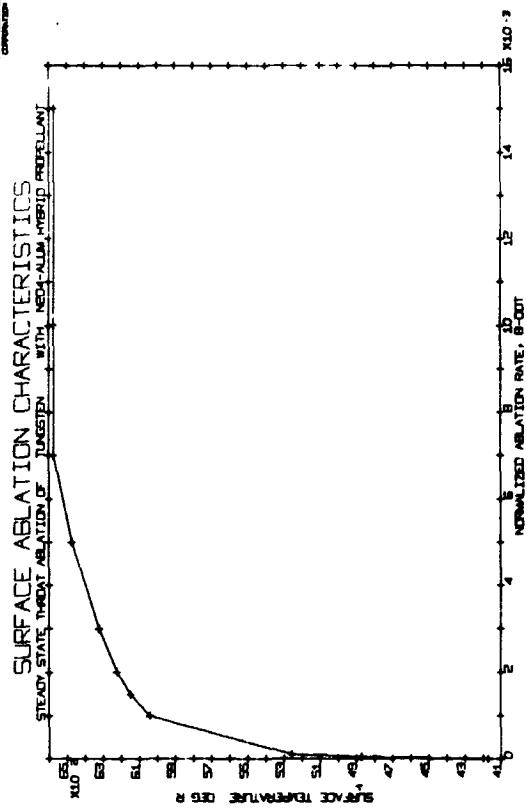


Figure 5(b)

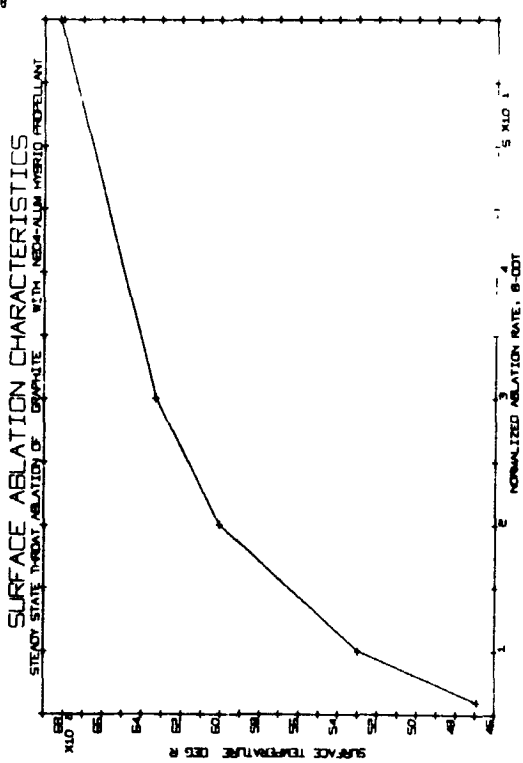


Figure 5(c)

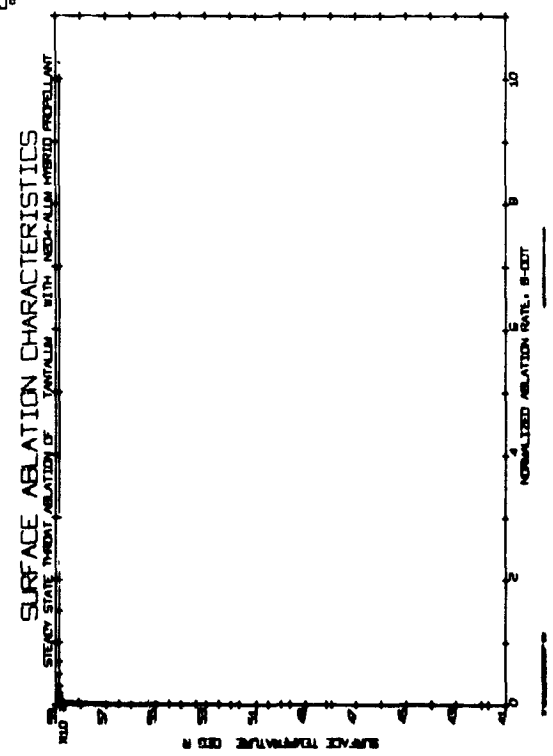


Figure 5(d)

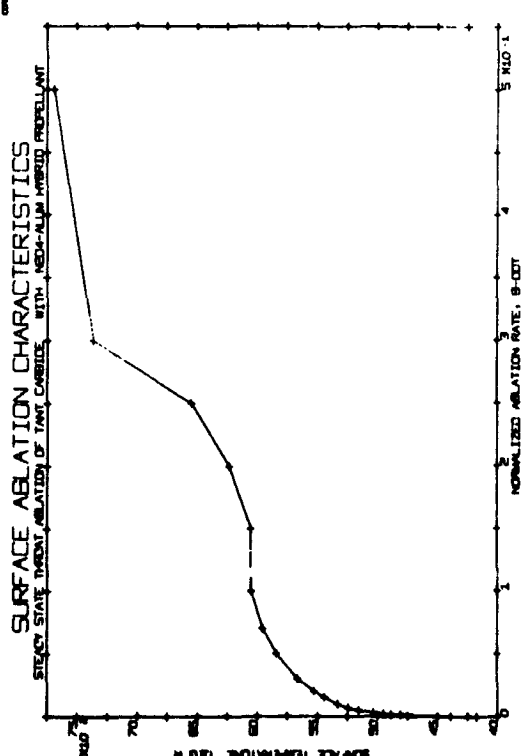


Figure 5(e)

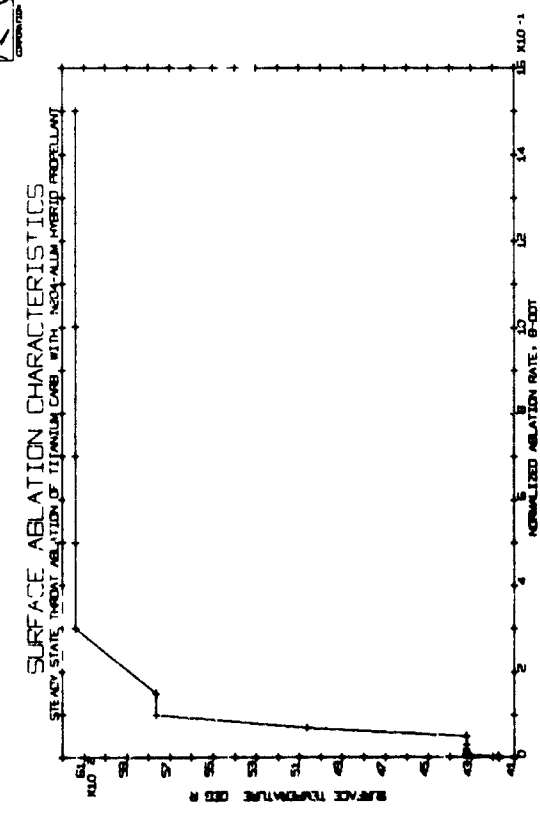


Figure 5(f)

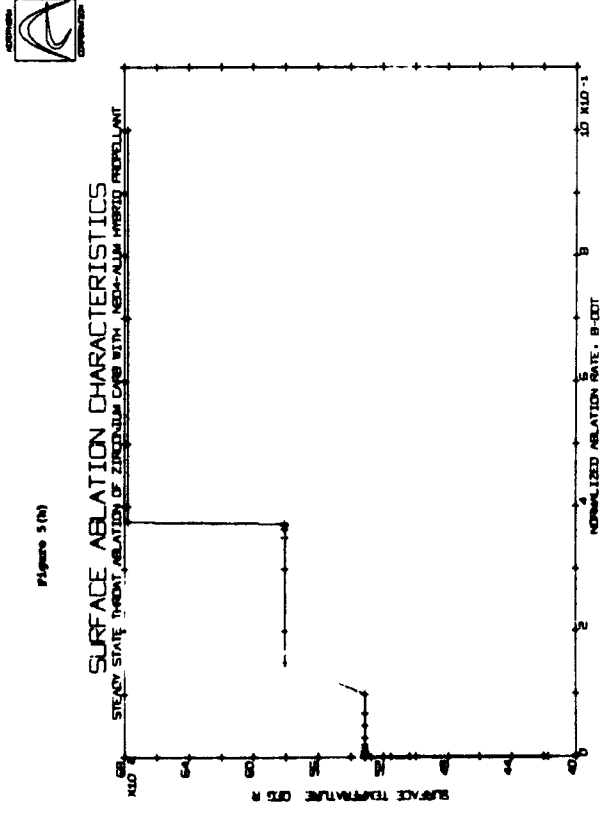


Figure 5(g)

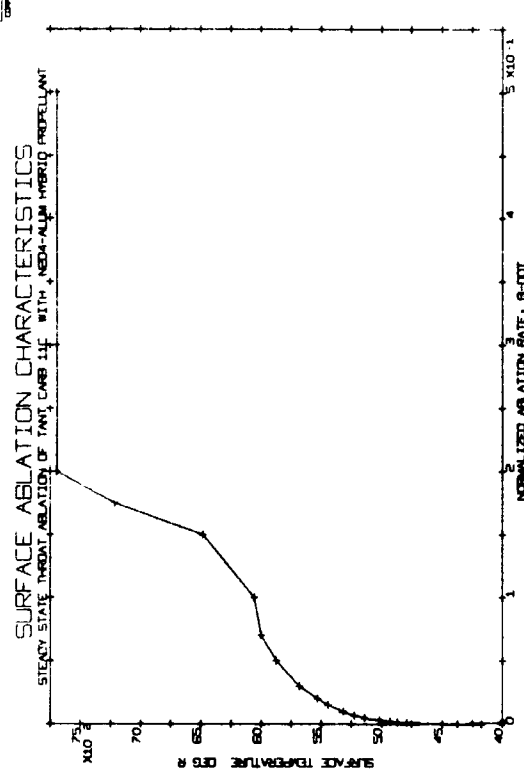


Figure 5(h)

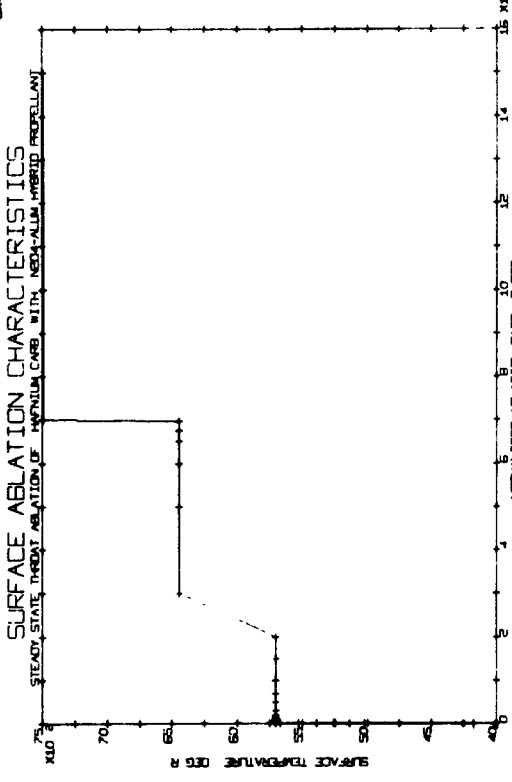


Figure 5(i)

Figure 5(1)

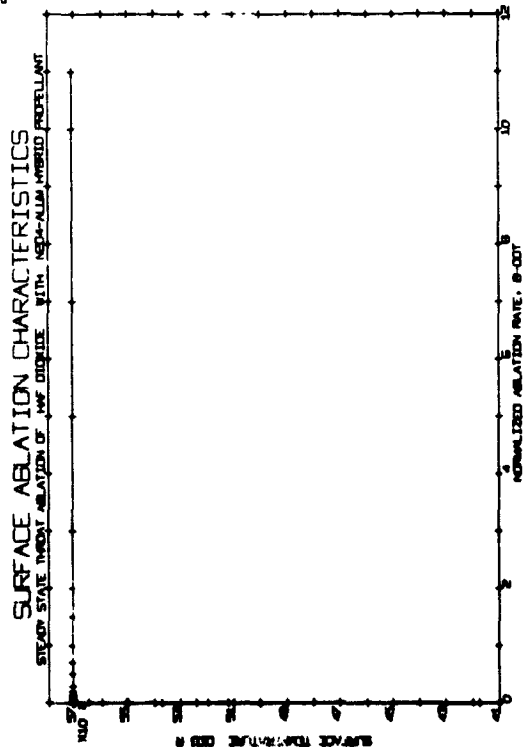


Figure 5(1)

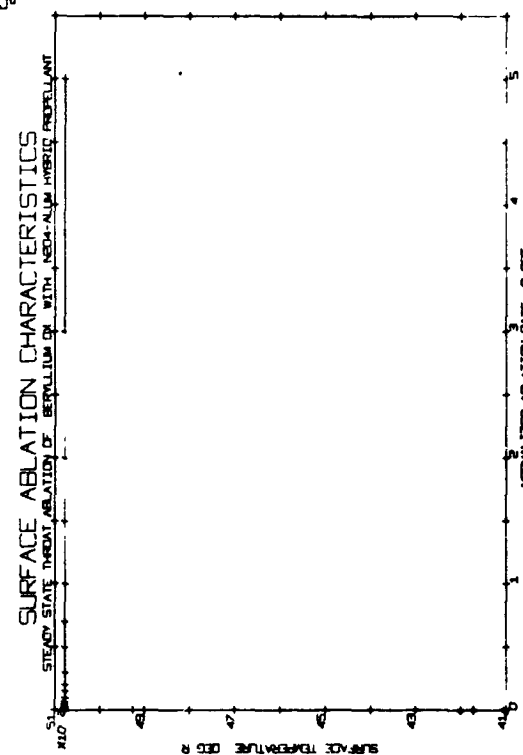


Figure 5(2)

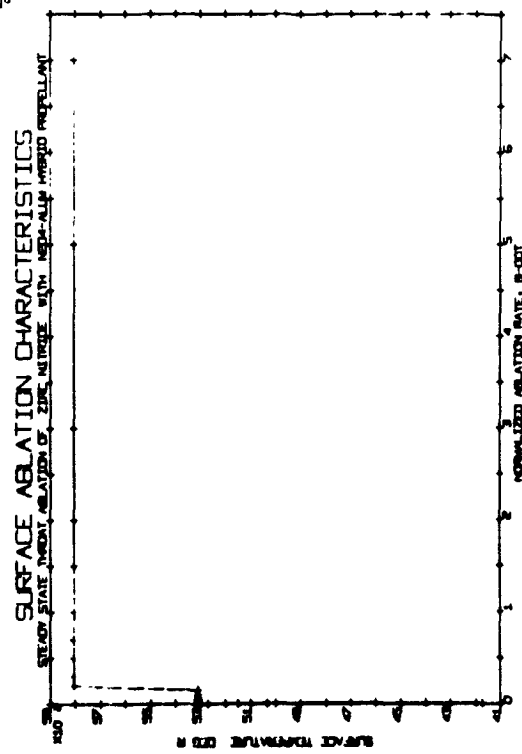


Figure 5(2)

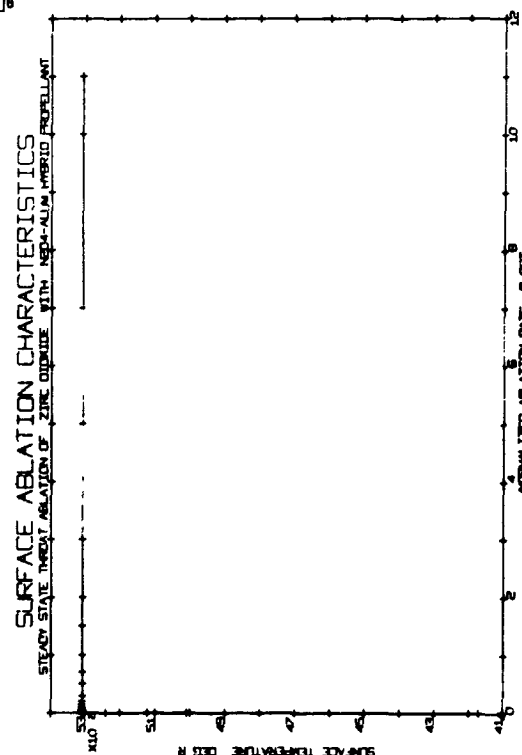


Figure 6(a)

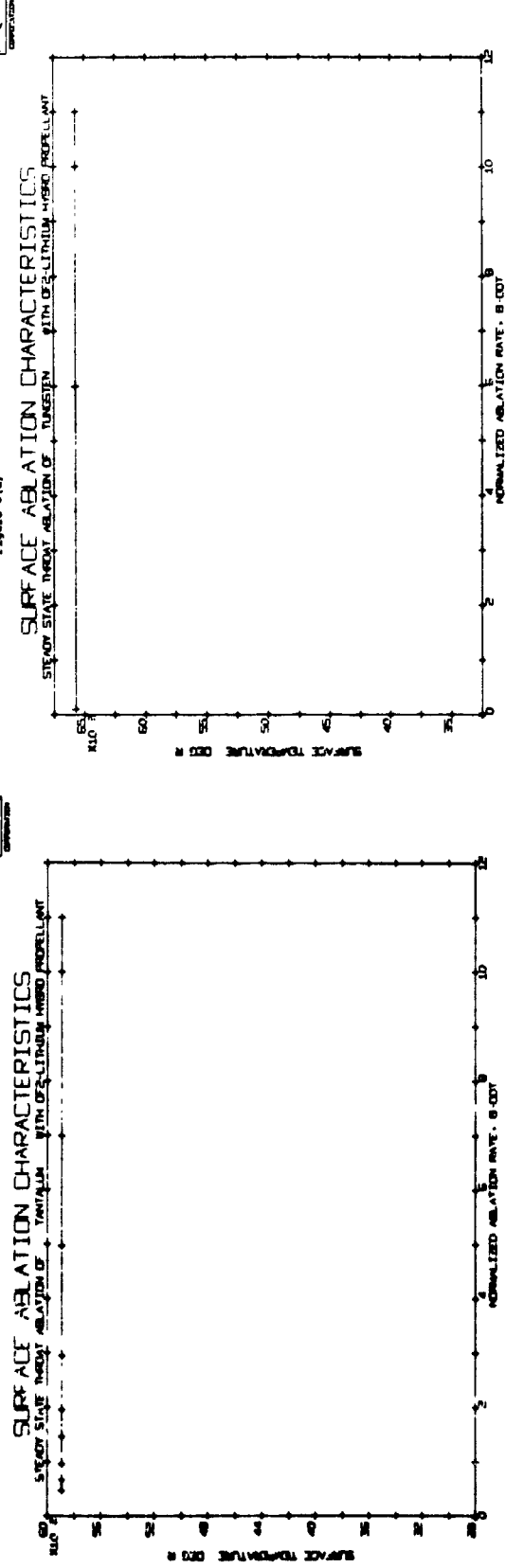
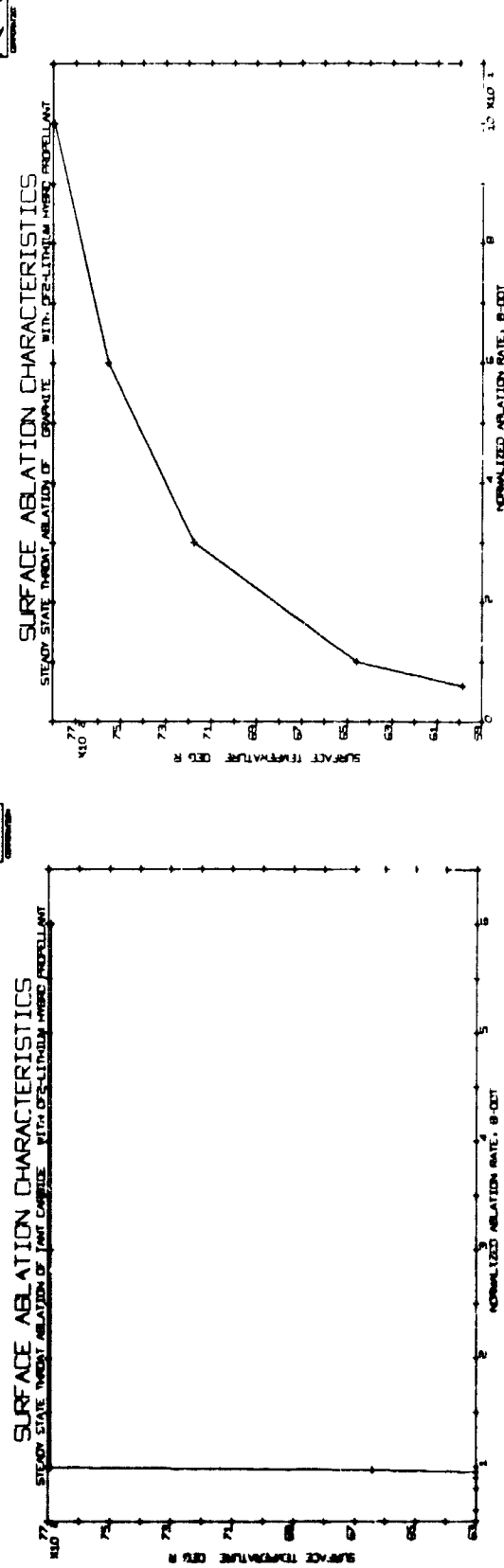


Figure 6(b)



AIAA

Figure 6(a)

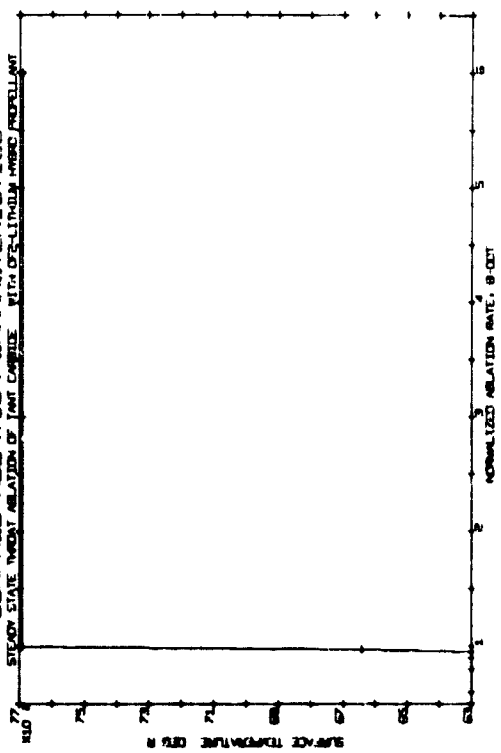
AIAA



Figure 6(b)



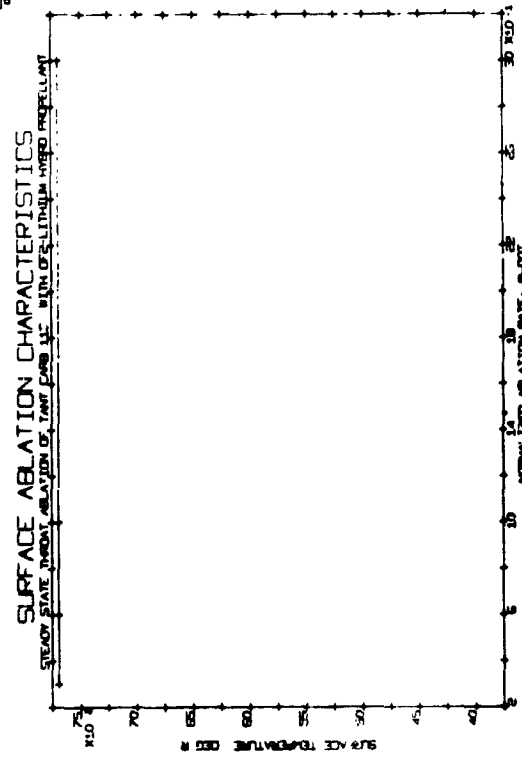
Figure 6(c)



AIAA

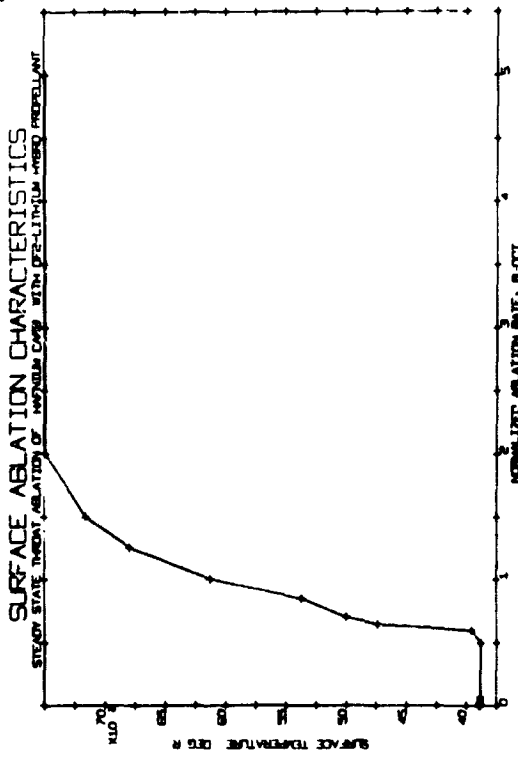
A

Figure 6(a)



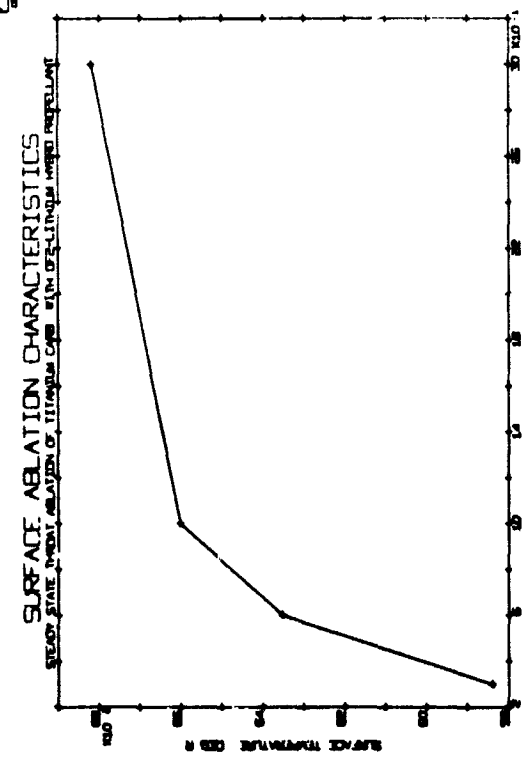
A

Figure 6(b)



A

Figure 6(c)



A

Figure 6(d)

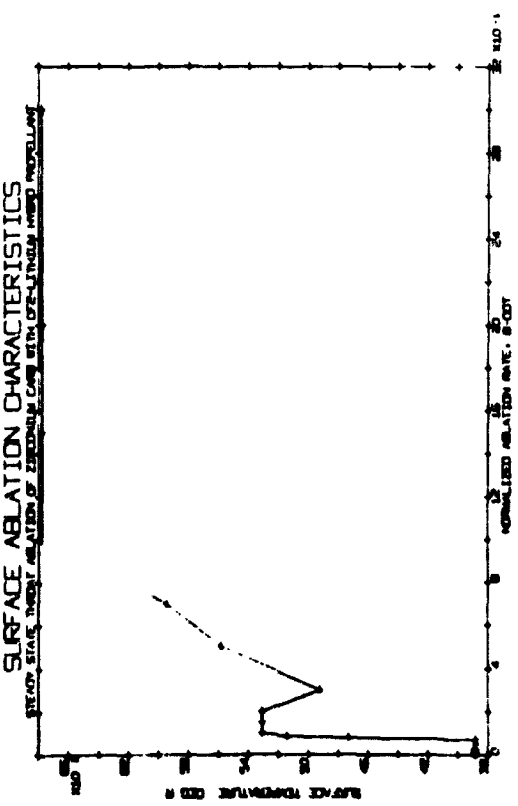


Figure 6(a)

Figure 6(i)

### SURFACE ABLATION CHARACTERISTICS

STEADY STATE ABLATION OF ZINC ALUMINATE WITH DZ-LITIGNE LIQUID PROPELLANT

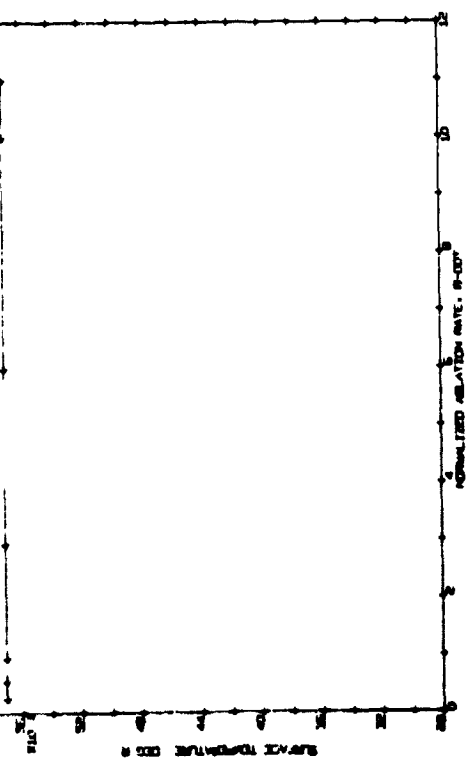


Figure 6(b)

Figure 6(ii)

### SURFACE ABLATION CHARACTERISTICS

STEADY STATE ABLATION OF ZINC ALUMINATE WITH DZ-LITIGNE LIQUID PROPELLANT

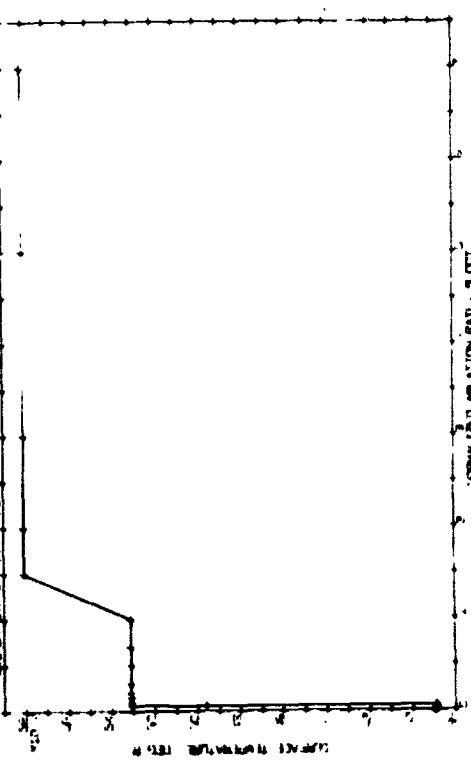
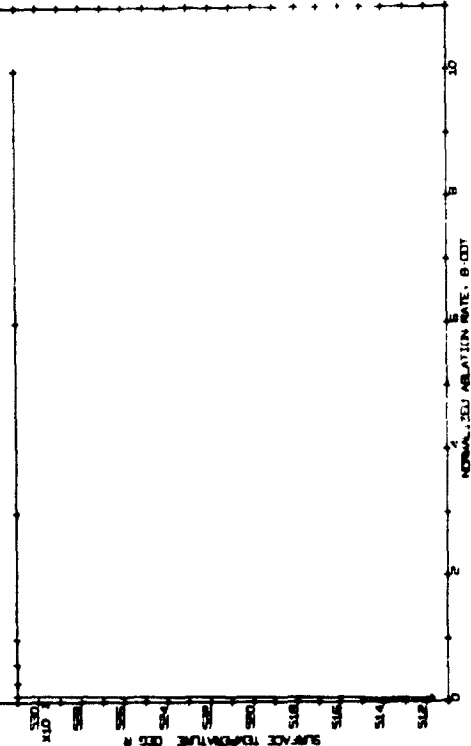


Figure 6(iii)

Figure 6(i)

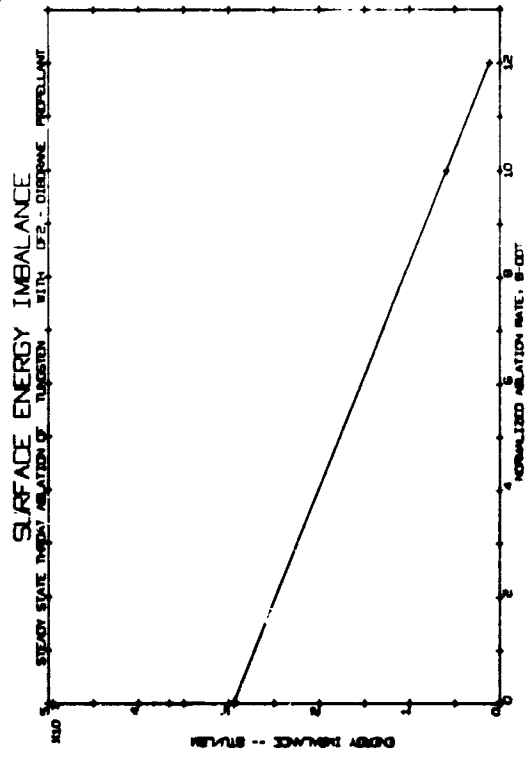
### SURFACE ABLATION CHARACTERISTICS

STEADY STATE ABLATION OF ZINC ALUMINATE WITH DZ-LITIGNE LIQUID PROPELLANT



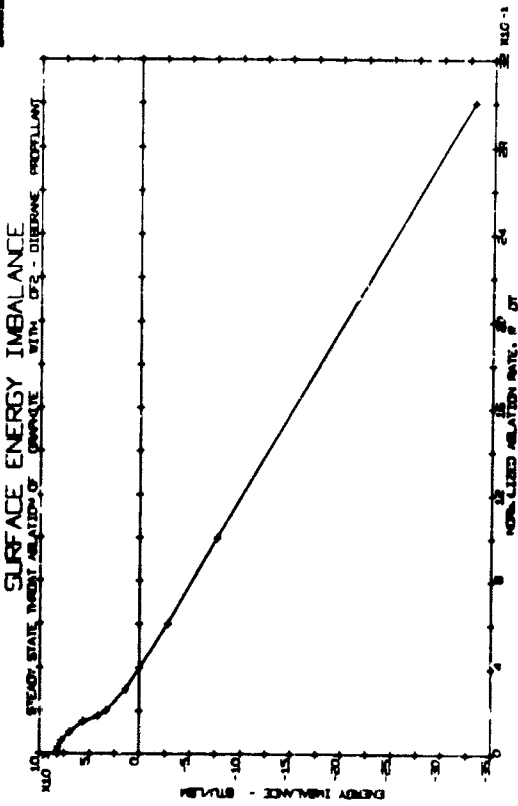
(A)

Figure 7(a)



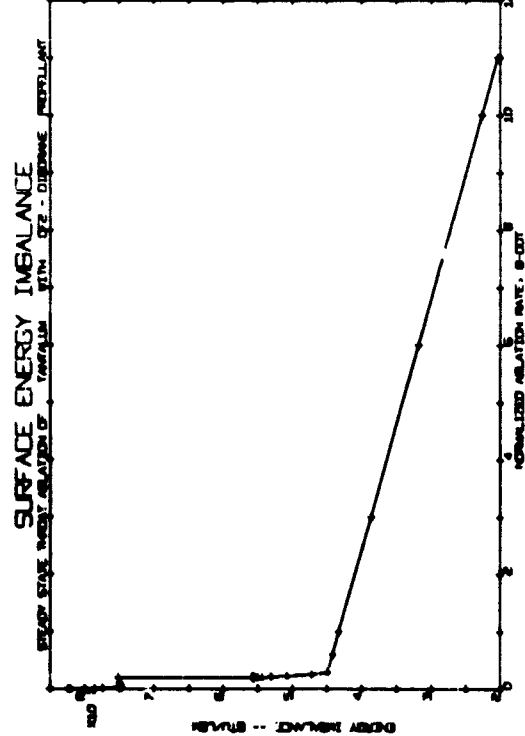
(A)

Figure 7(b)



(A)

Figure 7(c)



(A)

Figure 7(d)

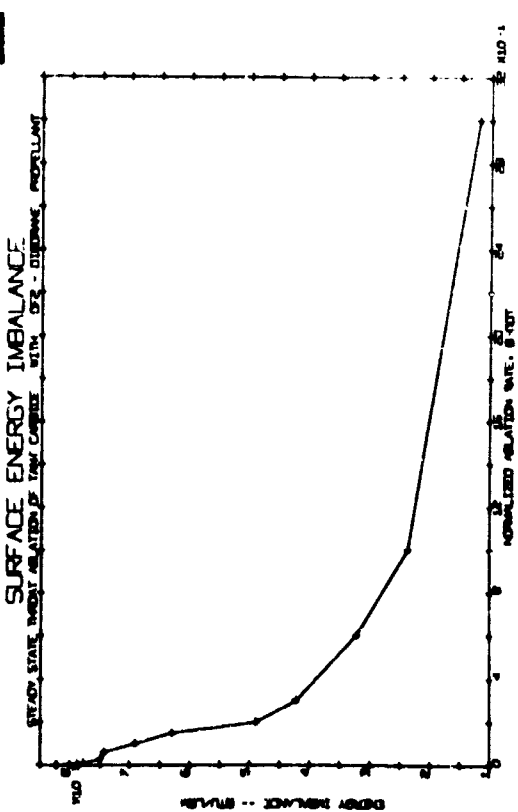


Figure 7(a)

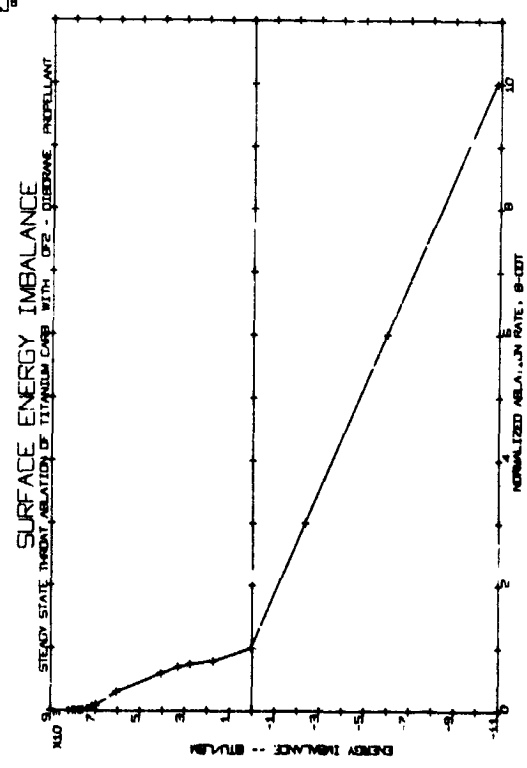


Figure 7(b)

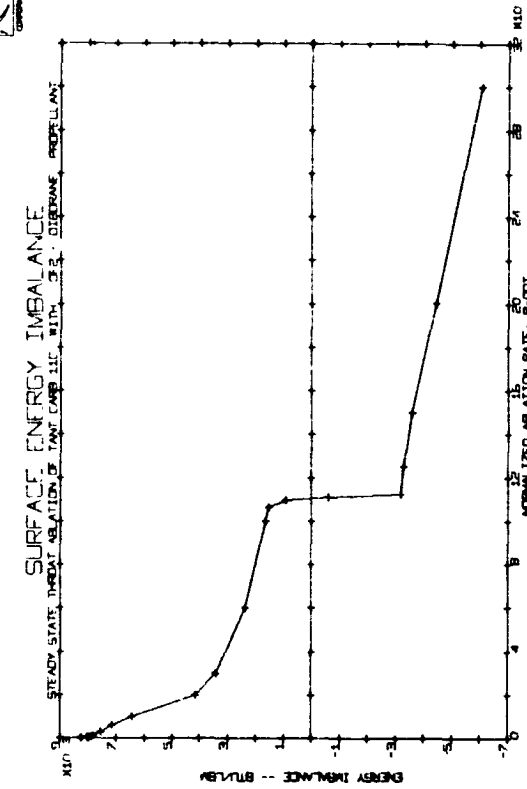


Figure 7(c)

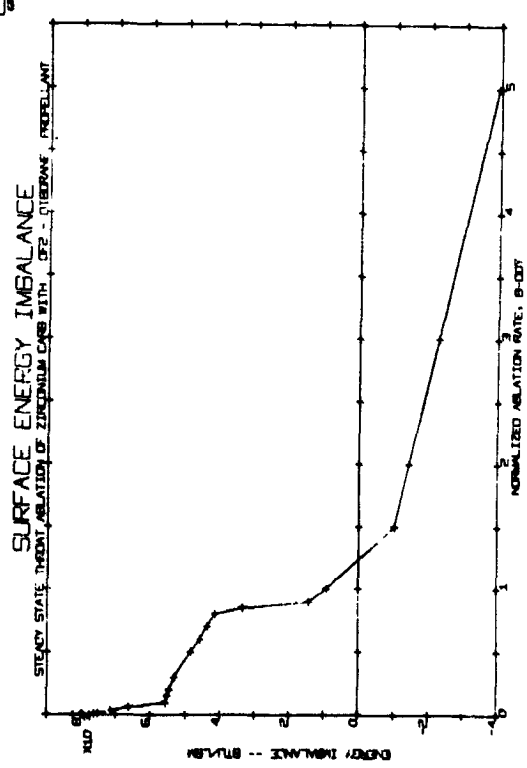
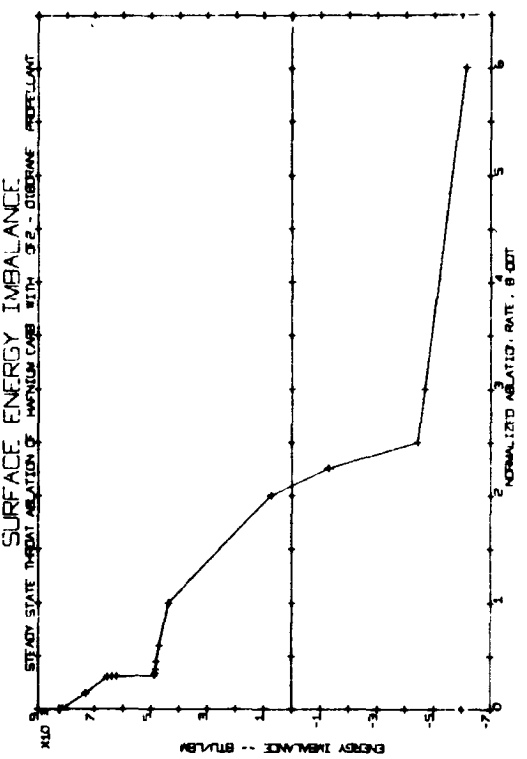


Figure 7(d)



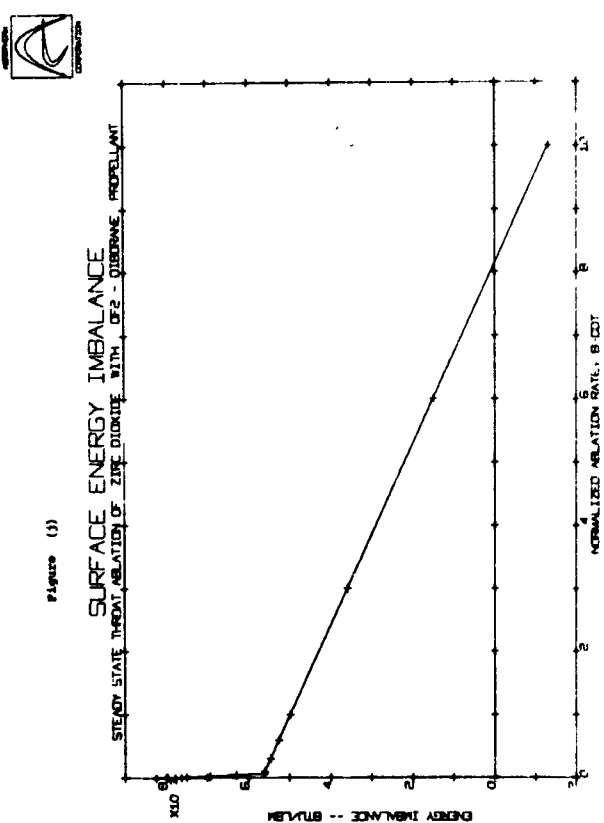
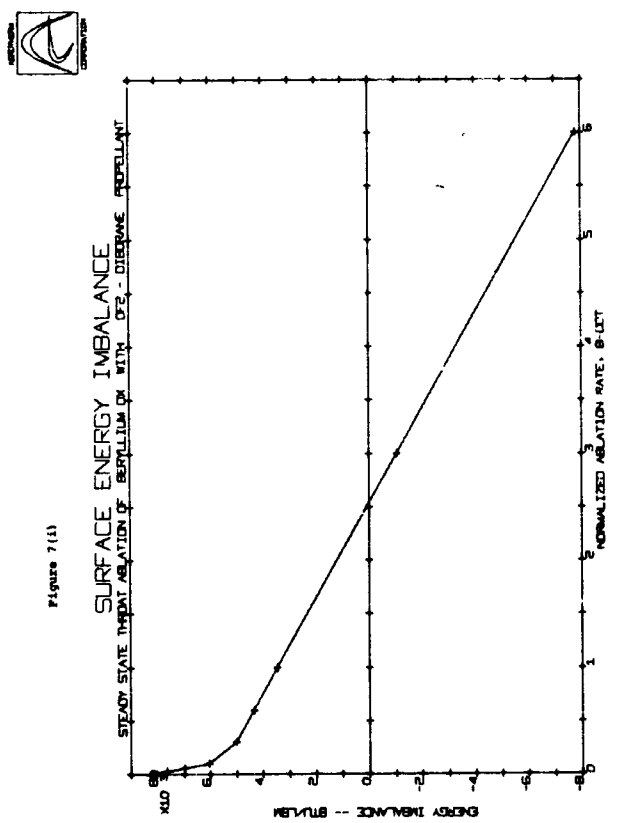
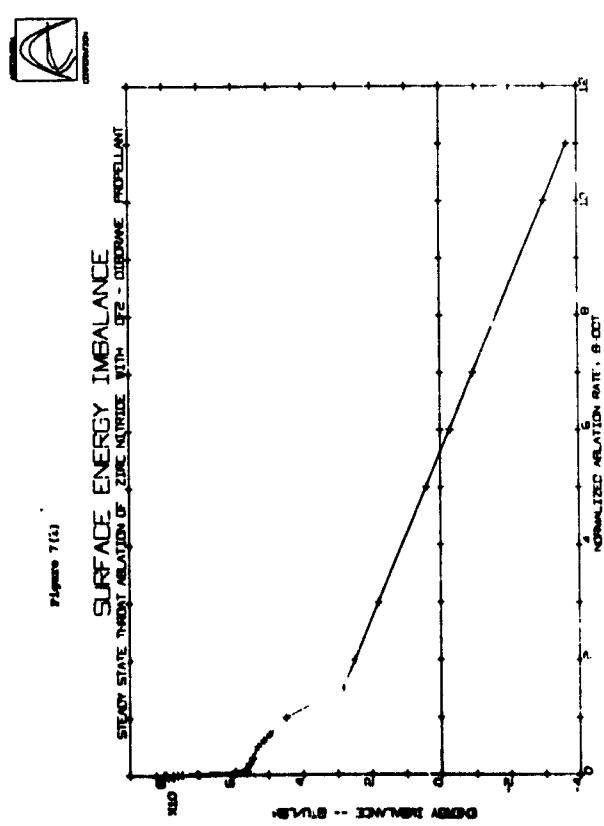
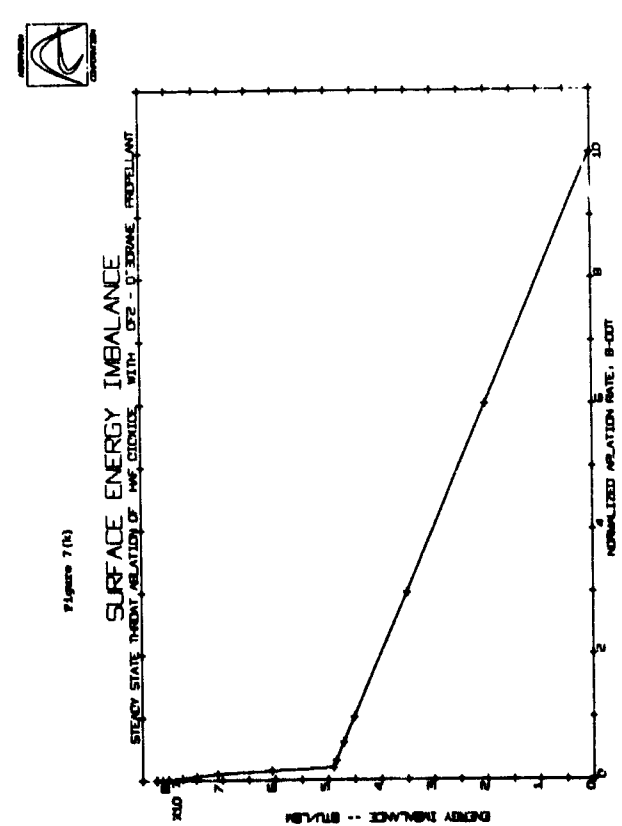


Figure 8(a)

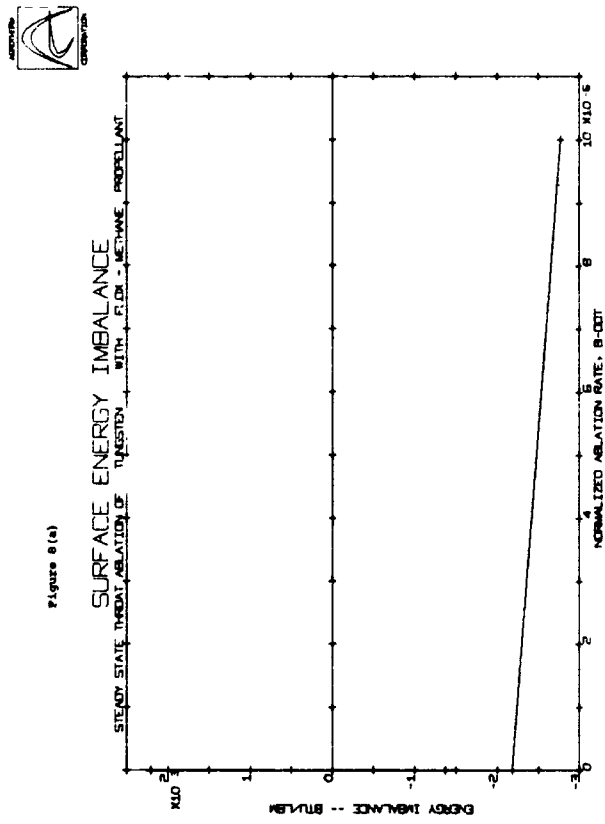


Figure 8(b)

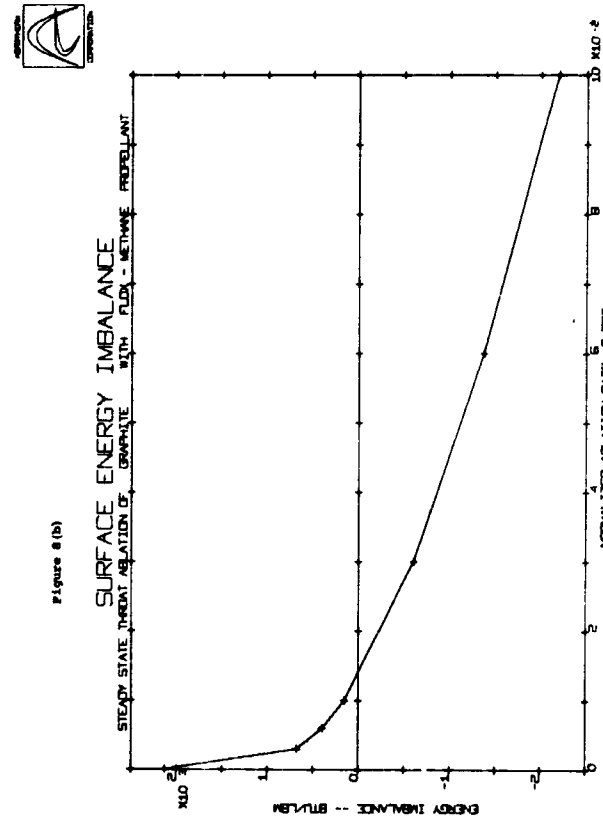


Figure 8(c)

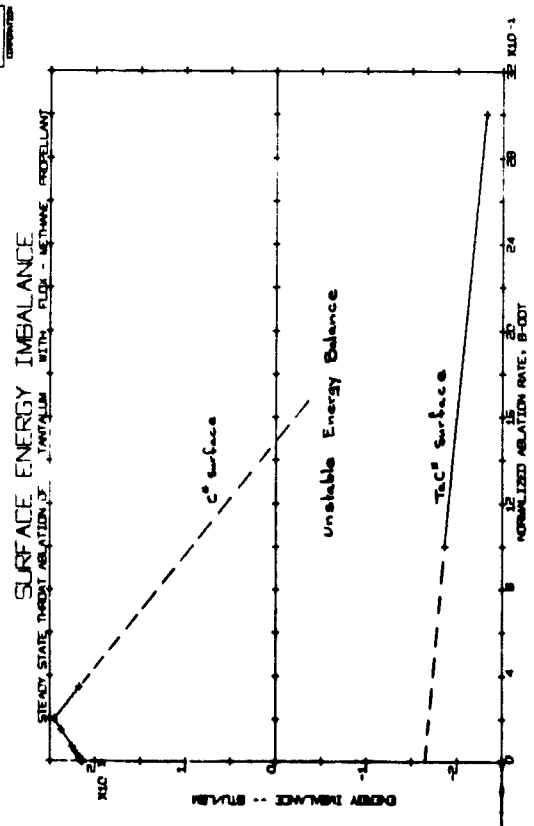


Figure 8(d)

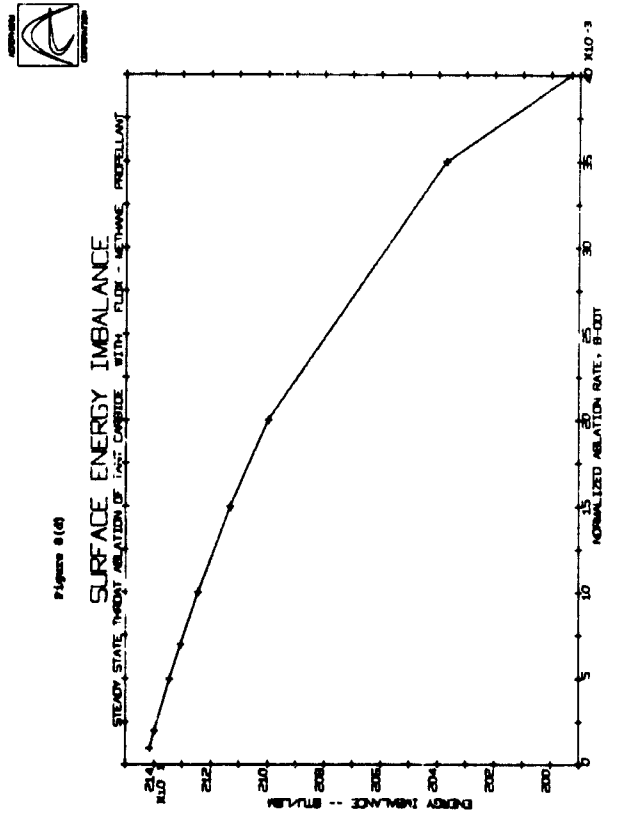




Figure 8(a)

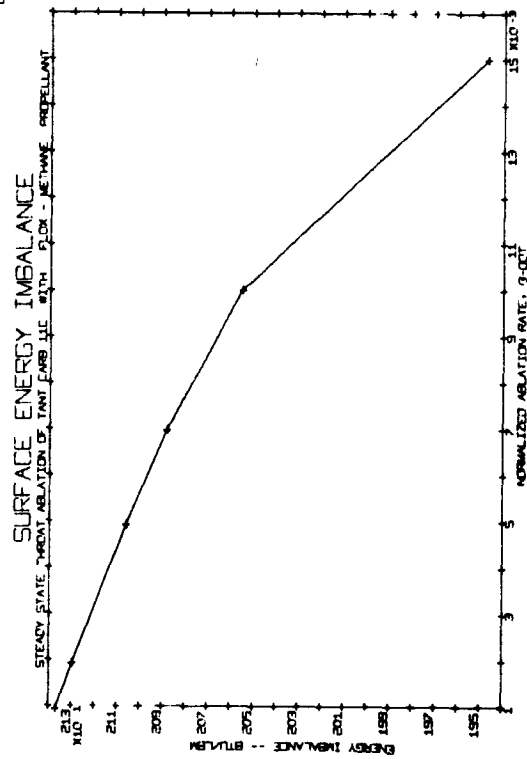


Figure 8(b)

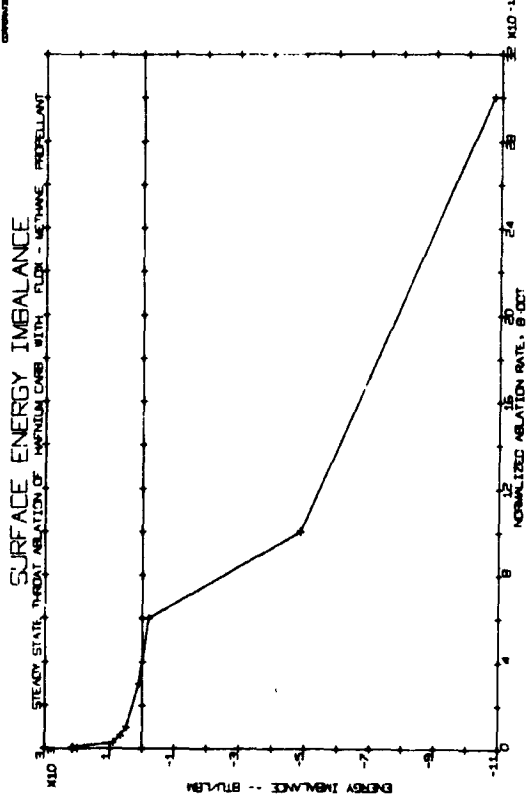


Figure 8(c)

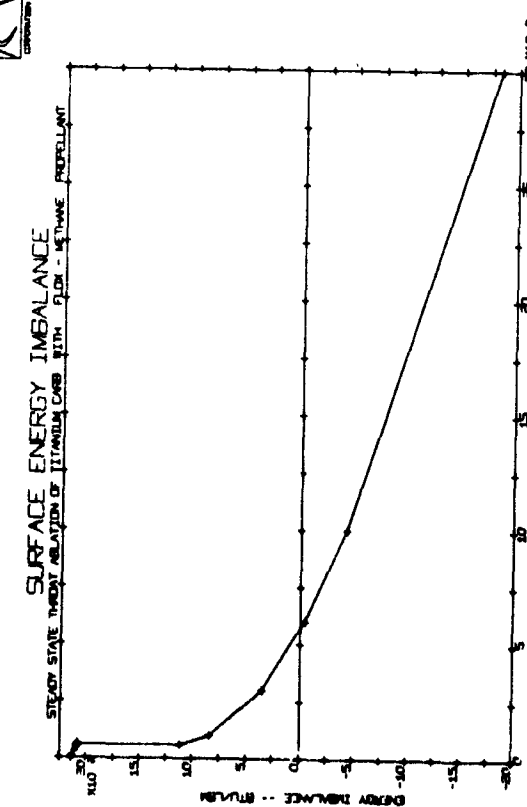


Figure 8(d)

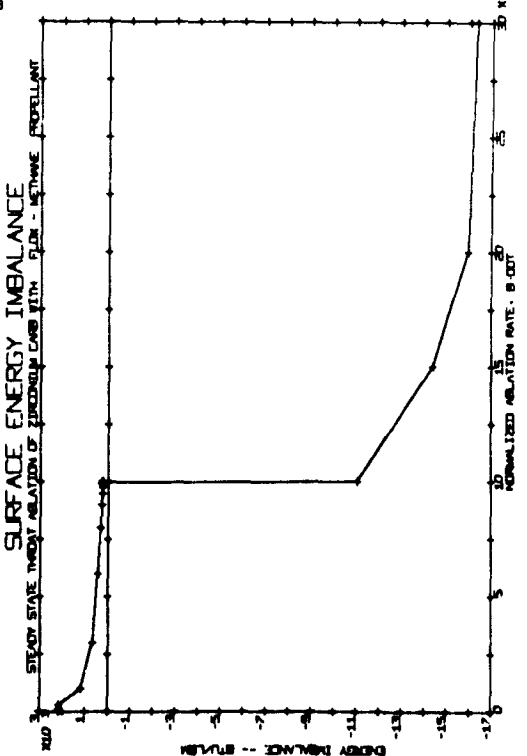


Figure 8(1)

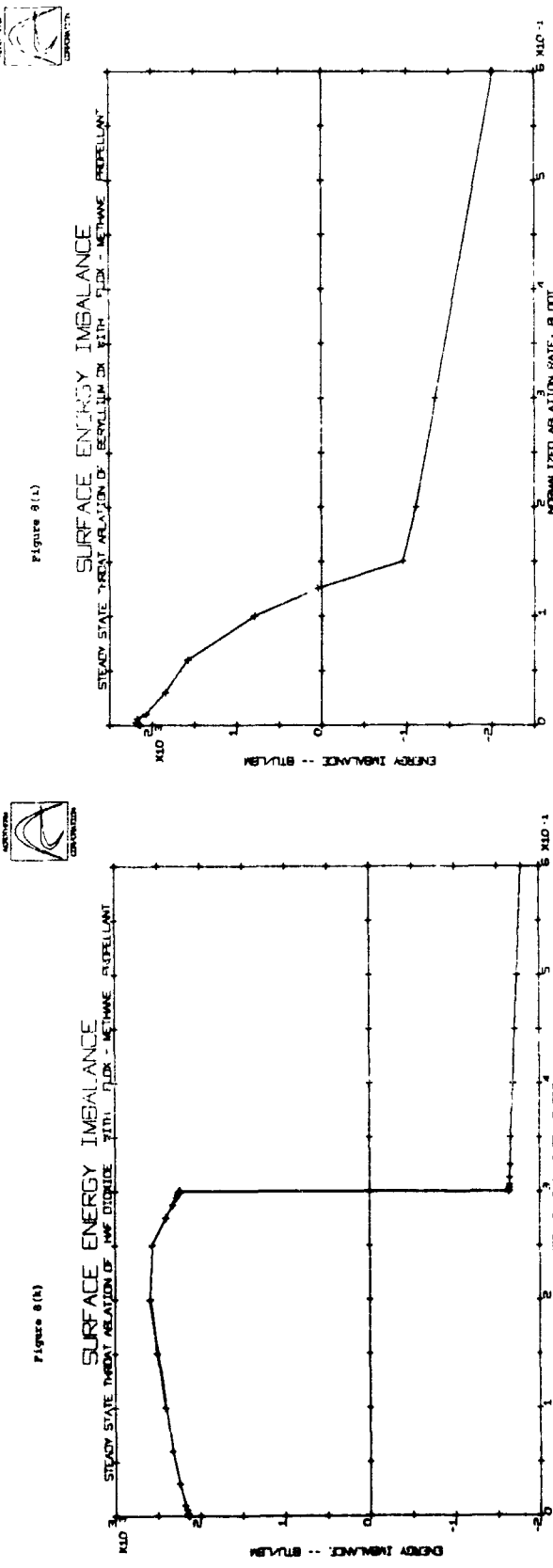


Figure 8(1)

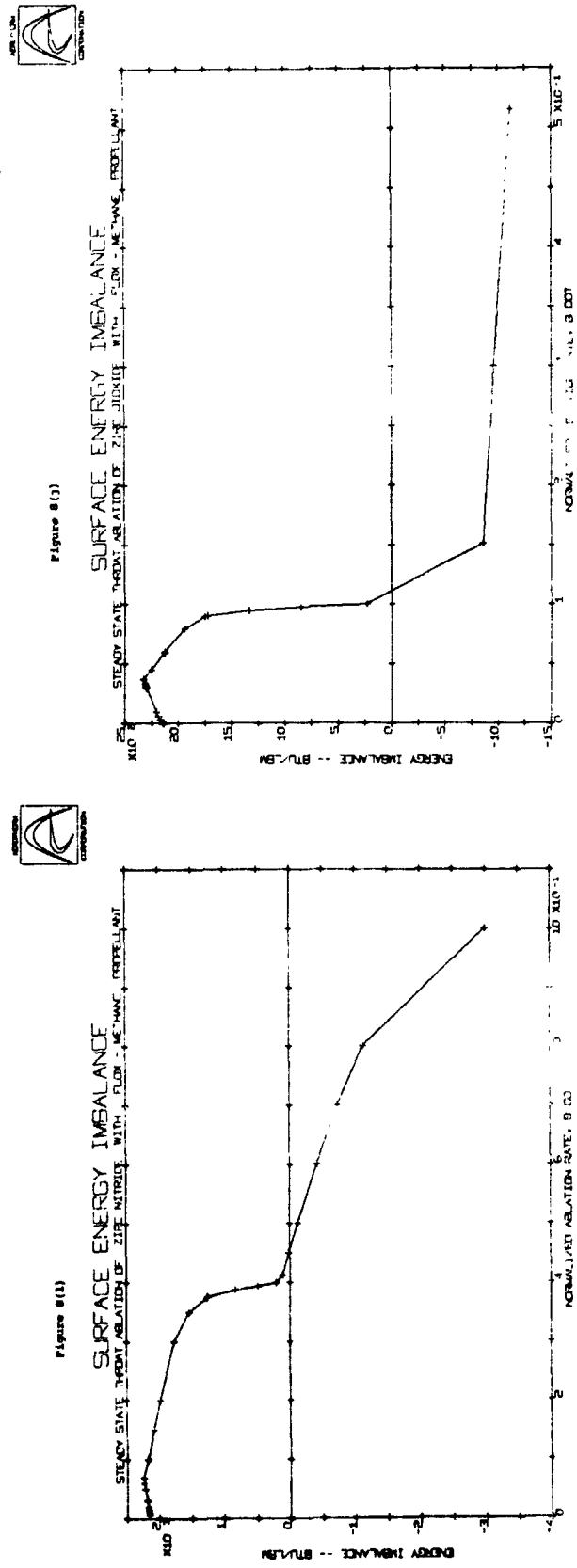


Figure 8(1)

Figure 9(a)

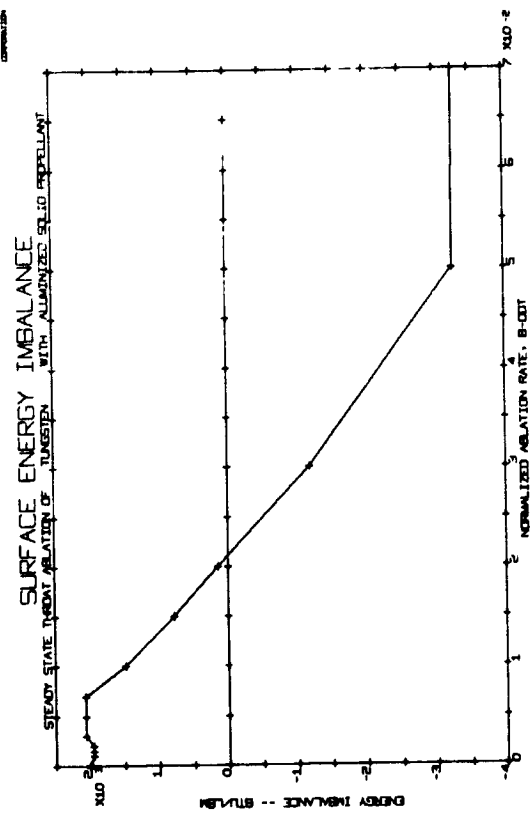


Figure 9(b)

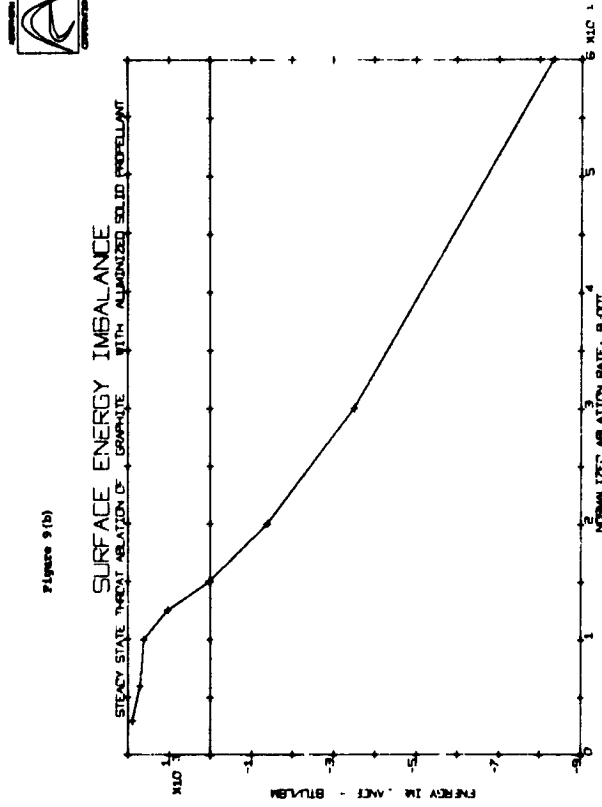


Figure 9(c)

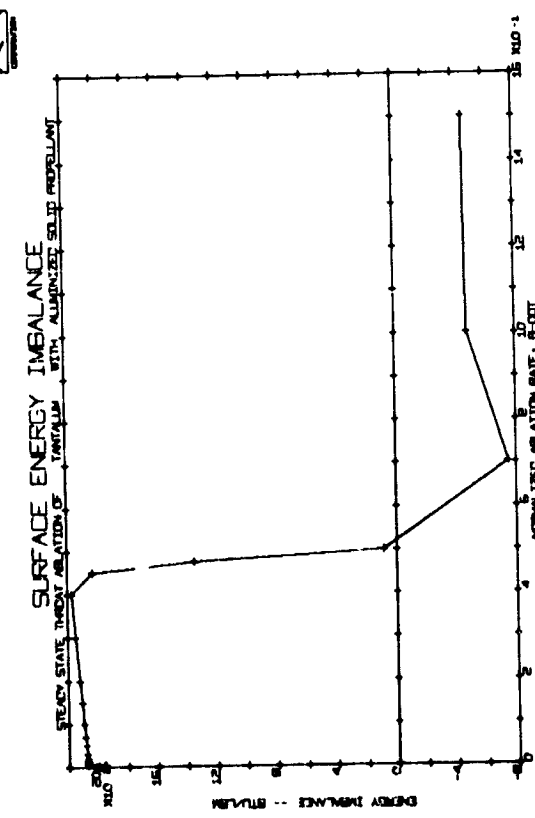


Figure 9(d)

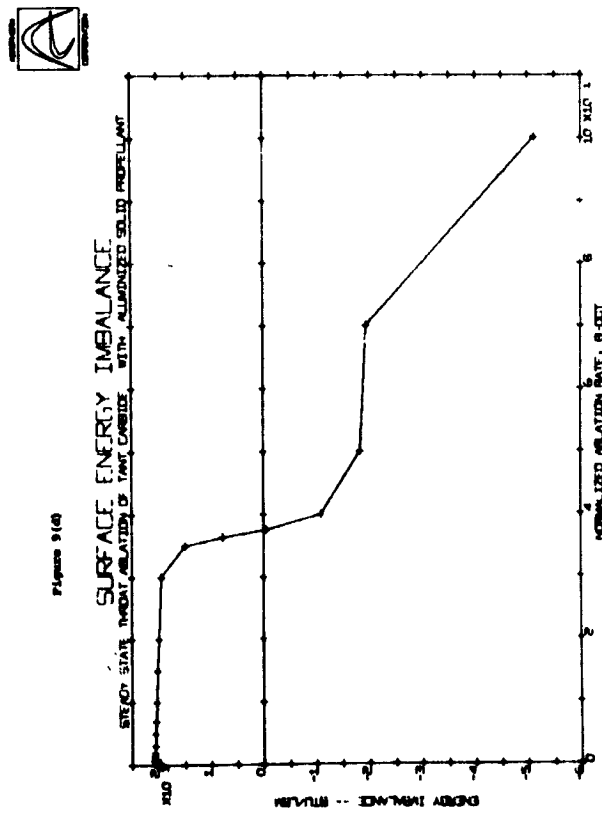


Figure 9(e)

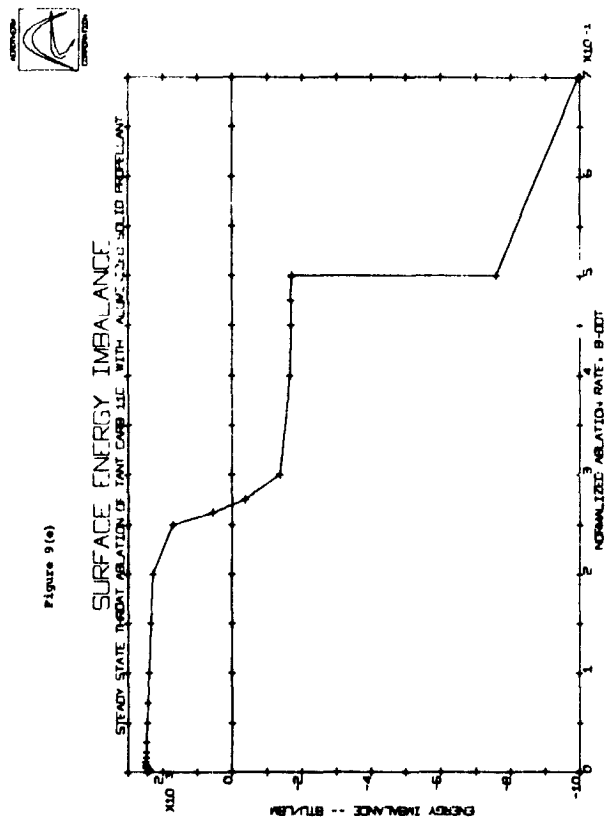


Figure 9(f)

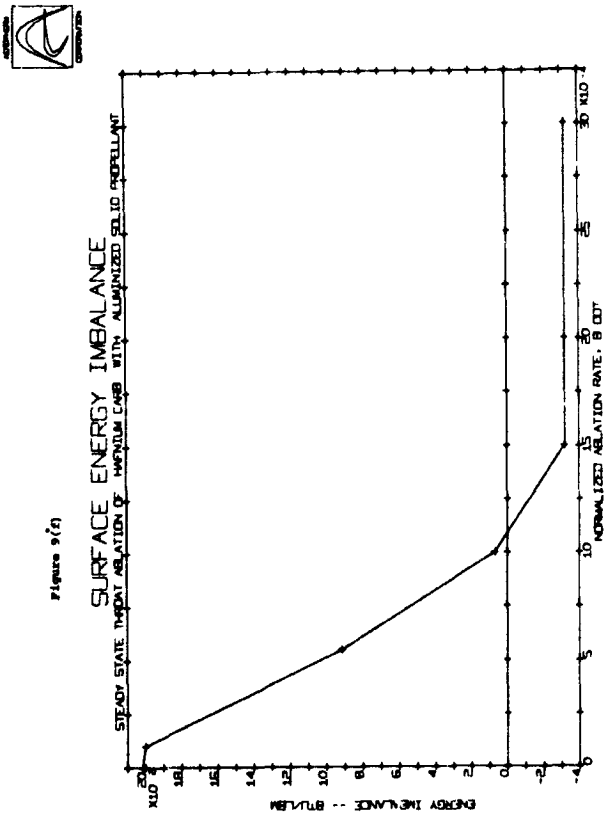


Figure 9(g)

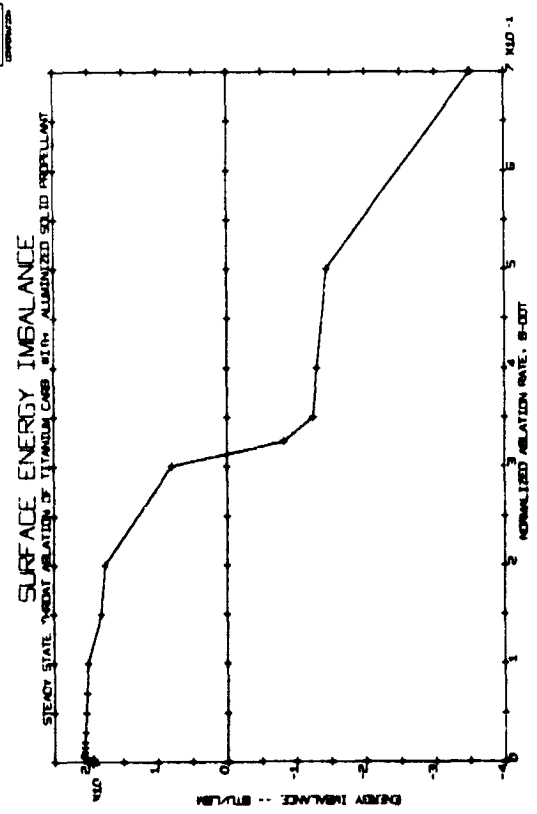


Figure 9(h)

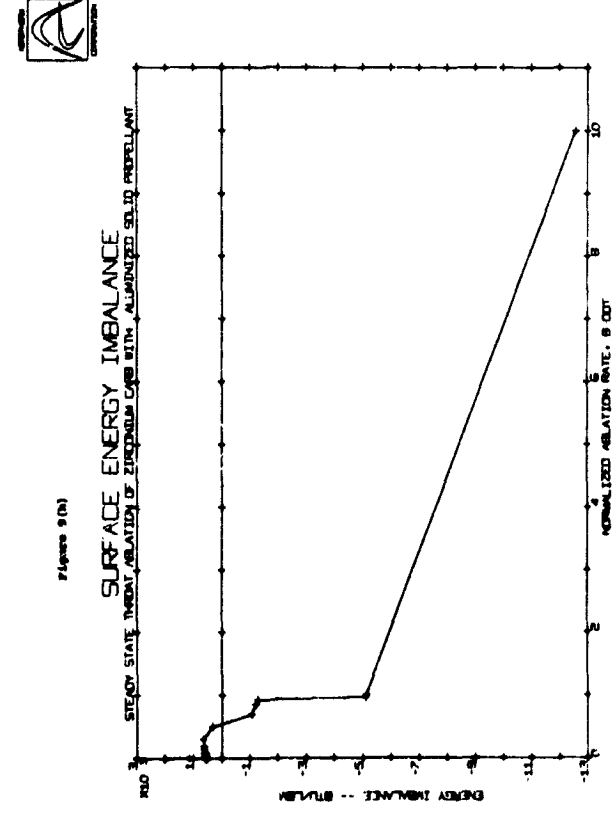


Figure 9(1)

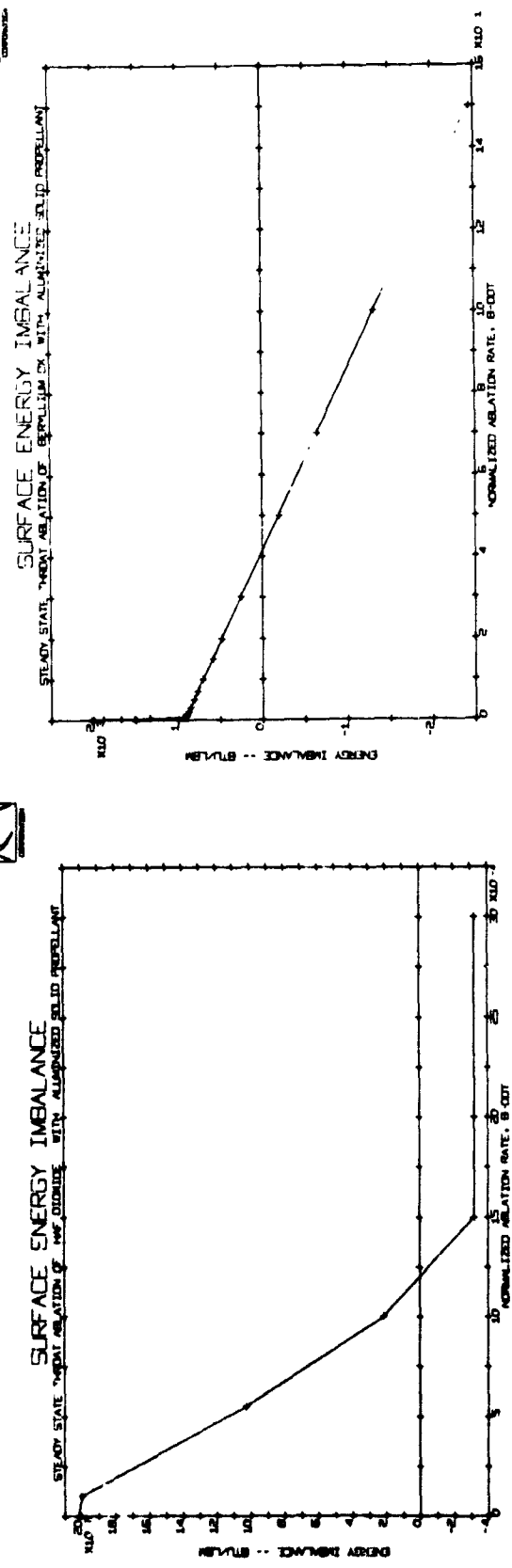


Figure 9(2)

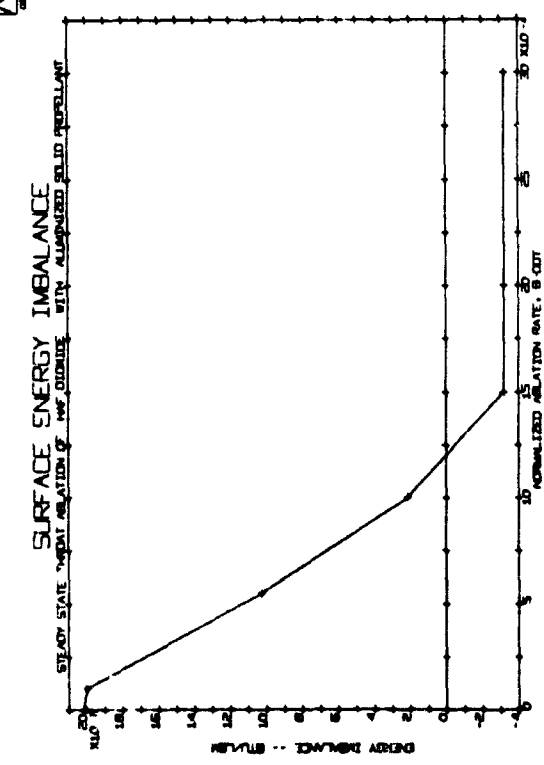


Figure 9(3)

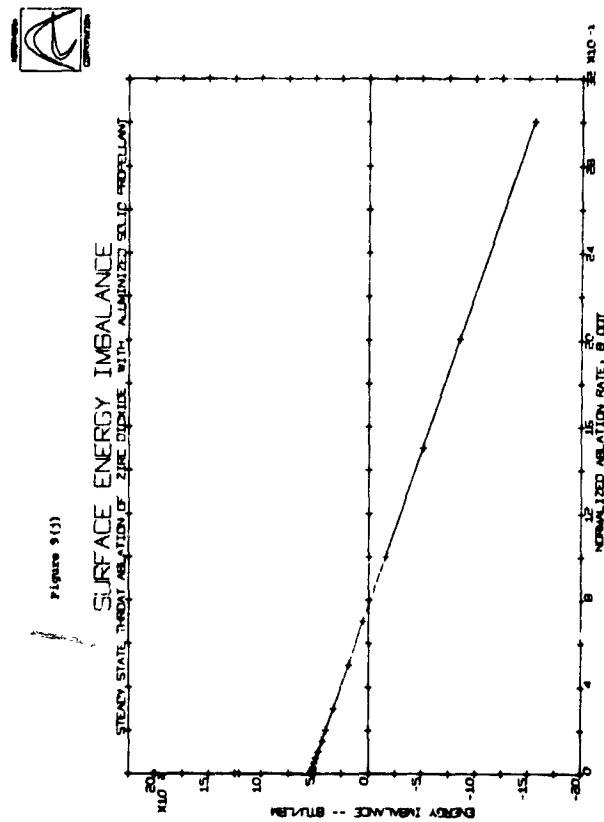


Figure 9(4)

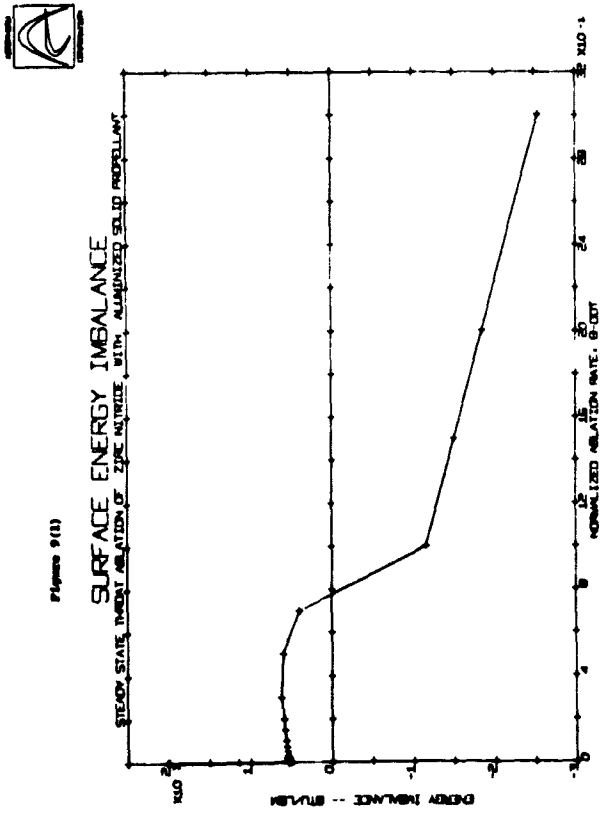


Figure 9(5)

Figure 10(c)

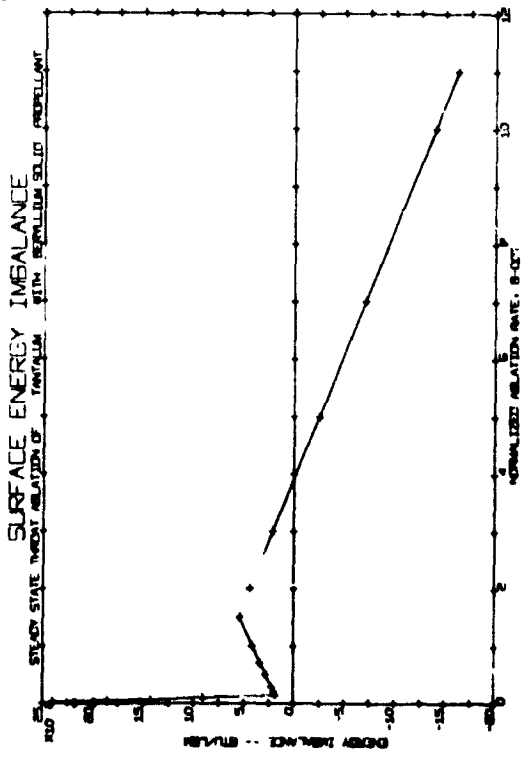


Figure 10(d)

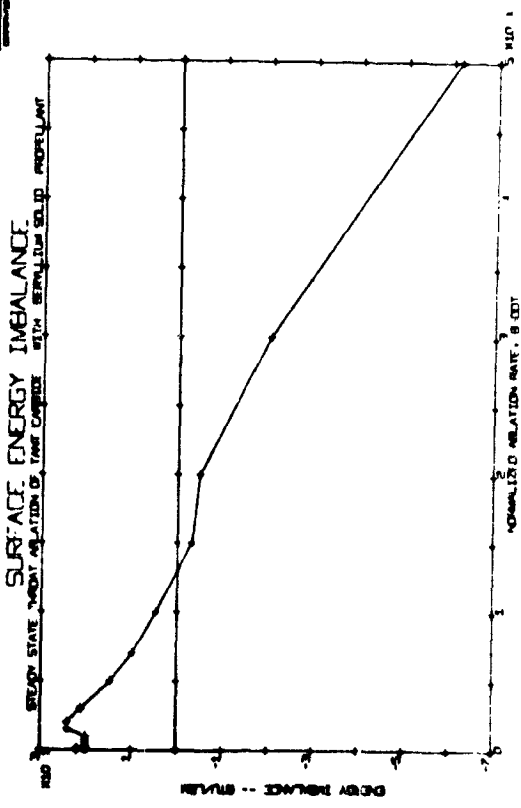


Figure 10(a)

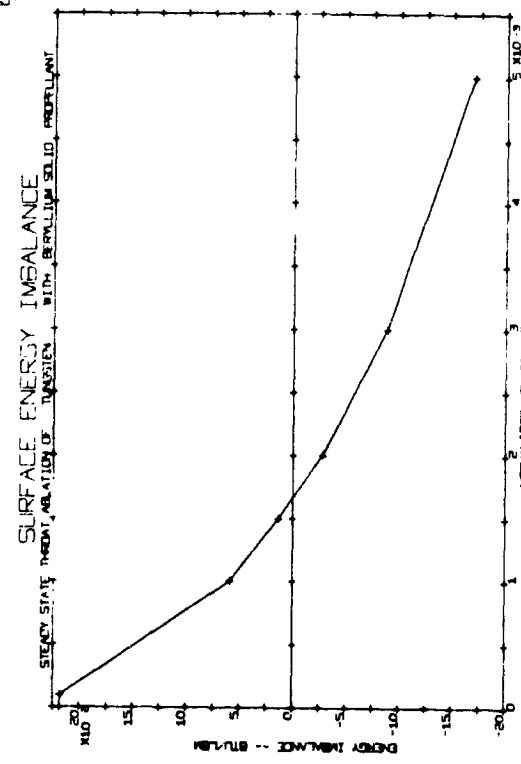


Figure 10(b)

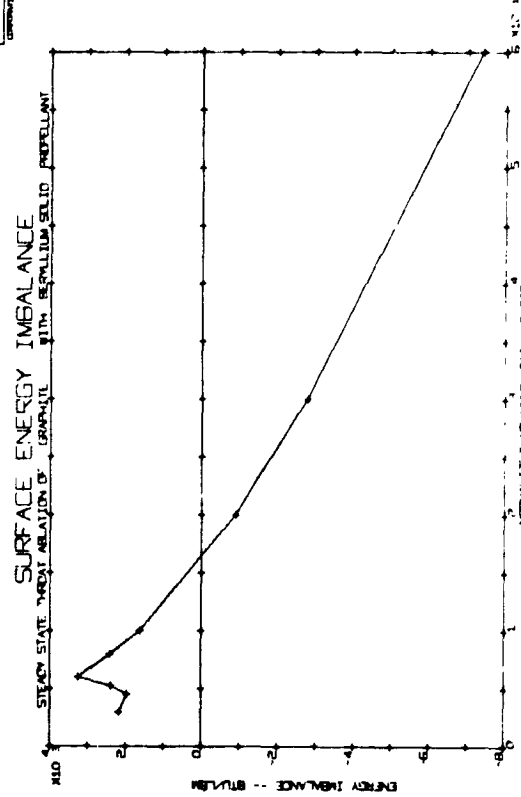




Figure 10(e)

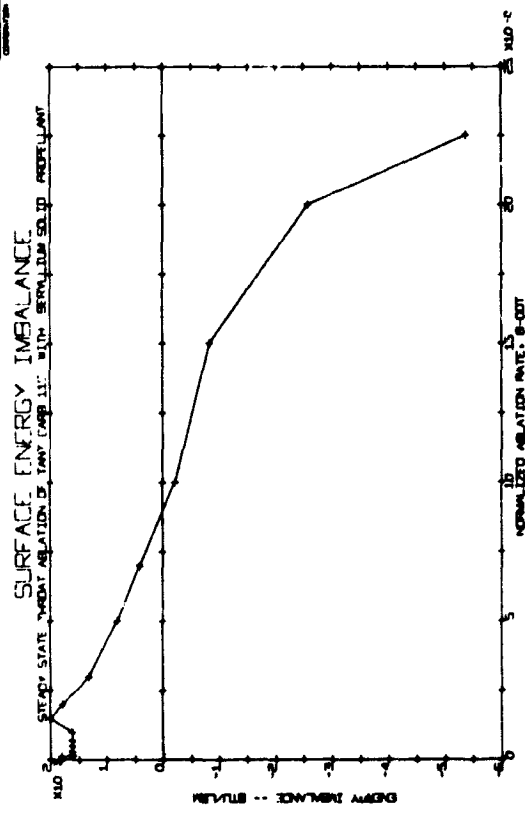


Figure 10(f)

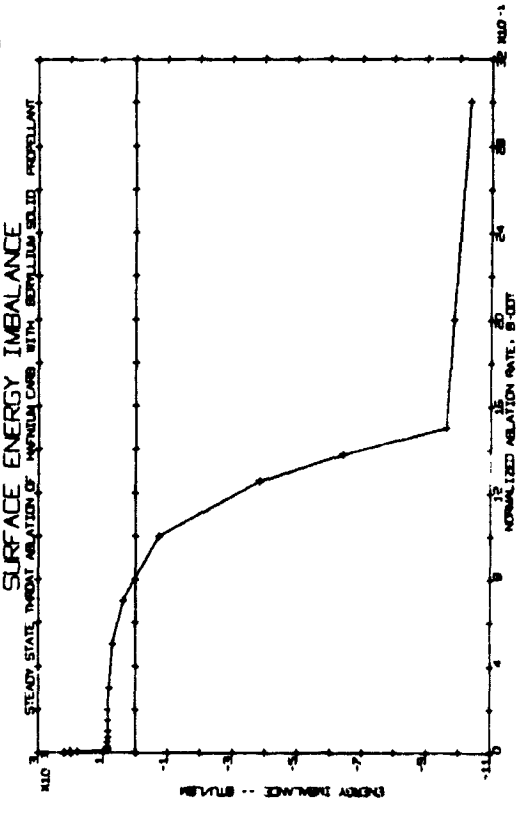


Figure 10(g)

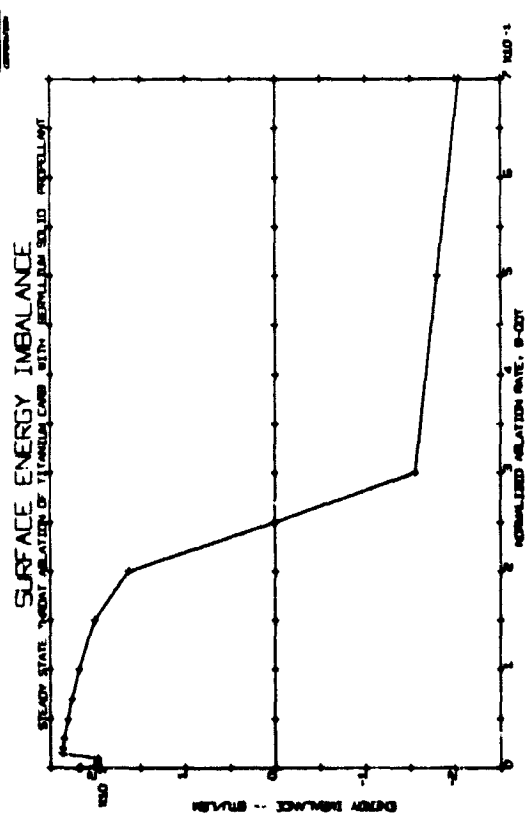
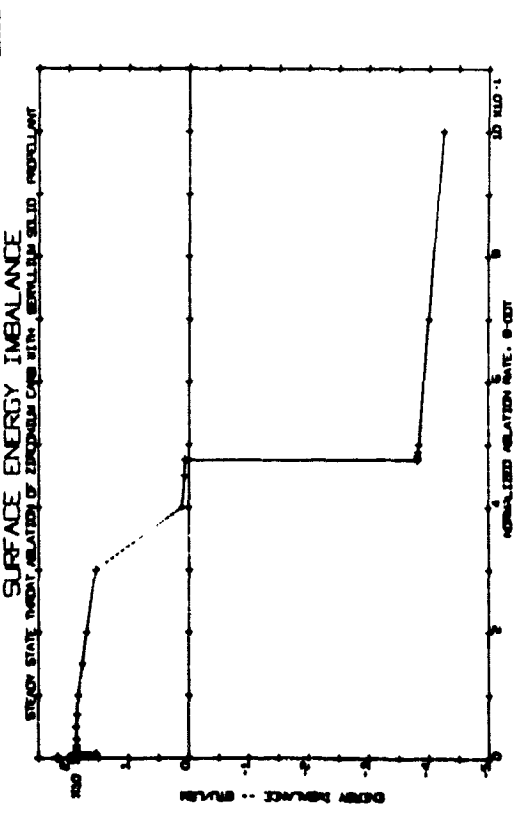
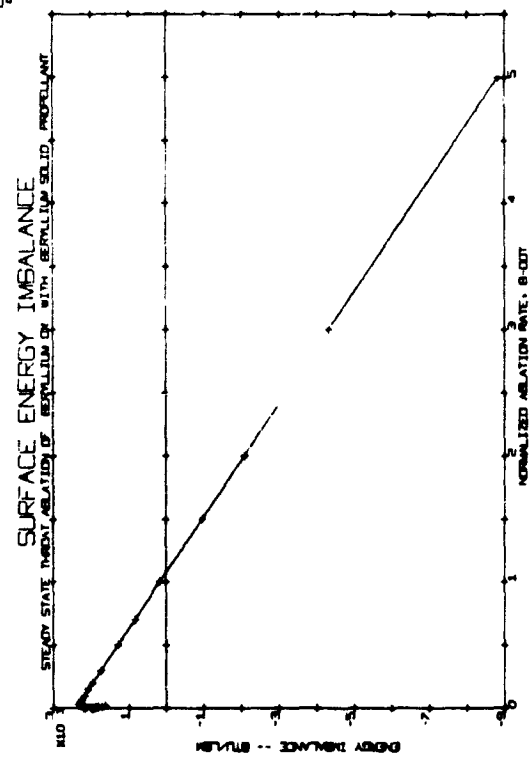


Figure 10(h)



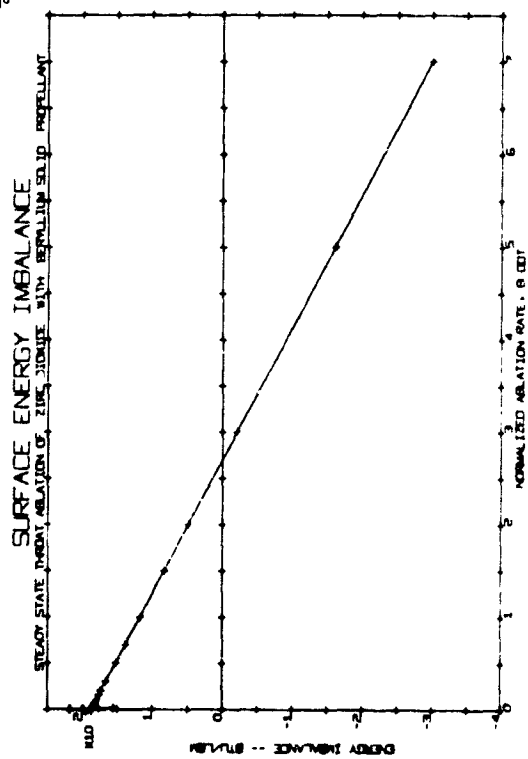
A

Figure 10(1)



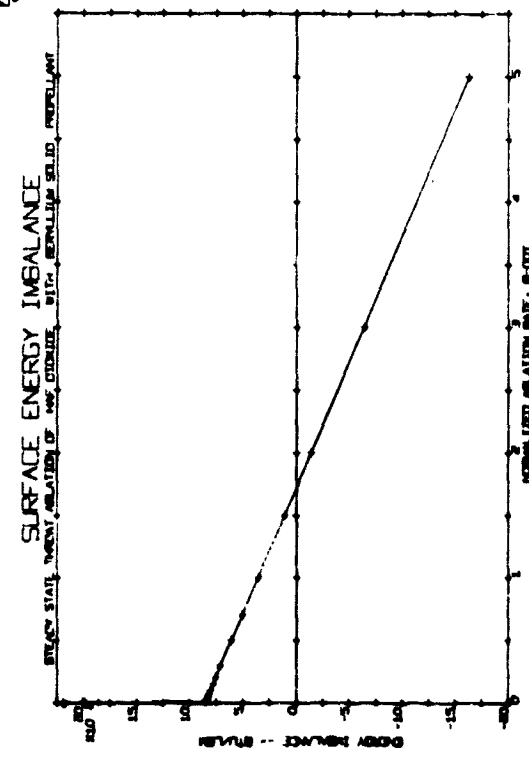
A

Figure 10(1)



A

Figure 10(1)



A

Figure 10(1)

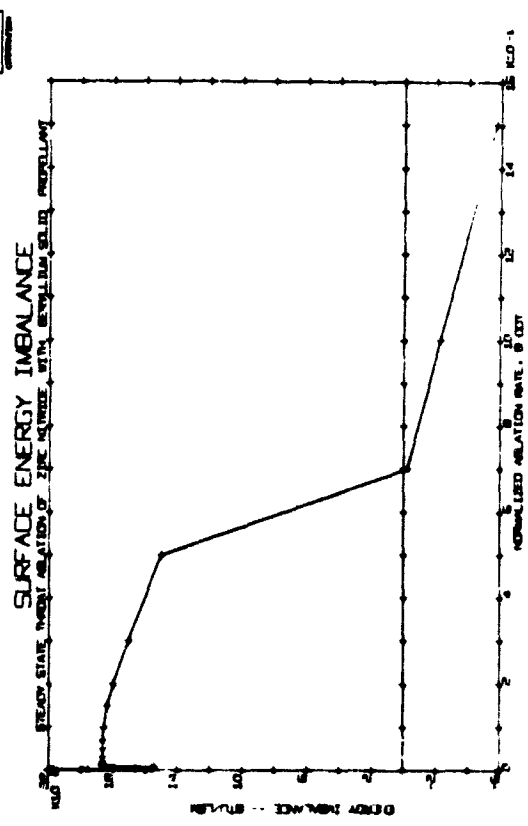




Figure 11(a)

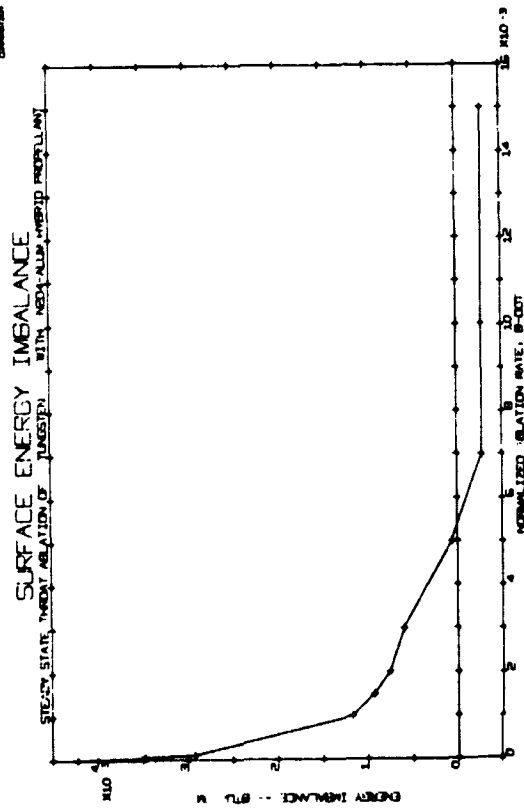


Figure 11(b)

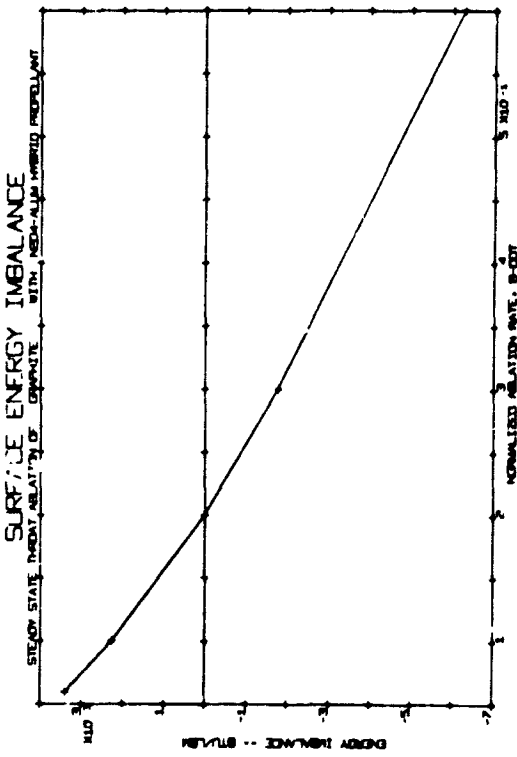


Figure 11(c)

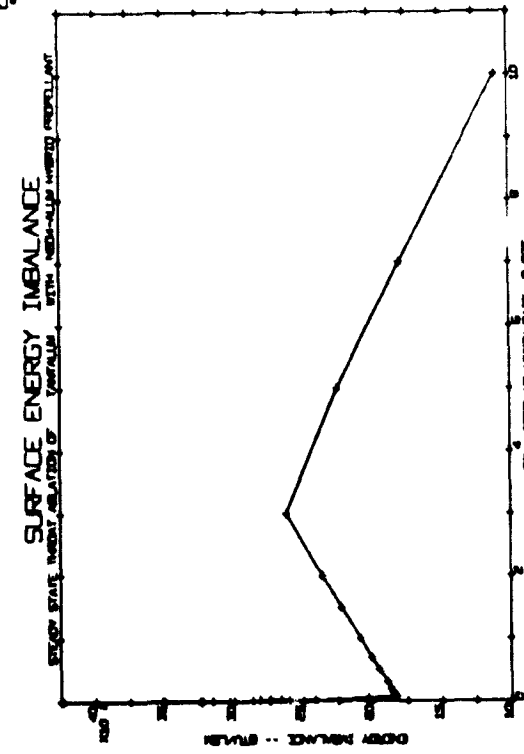


Figure 11(d)

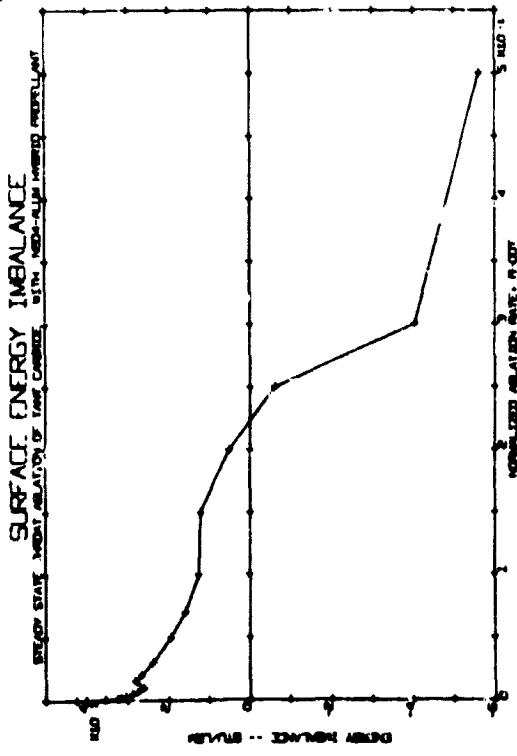


Figure 11(g)

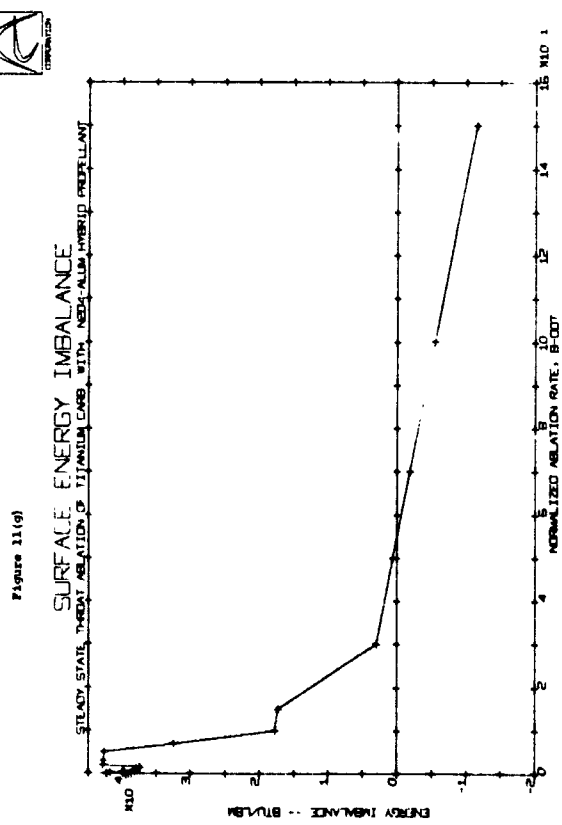


Figure 11(e)

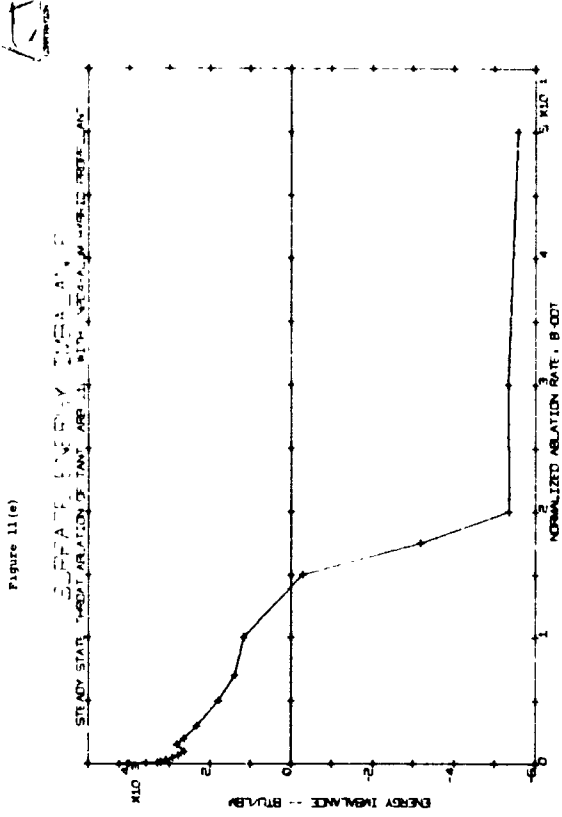


Figure 11(h)

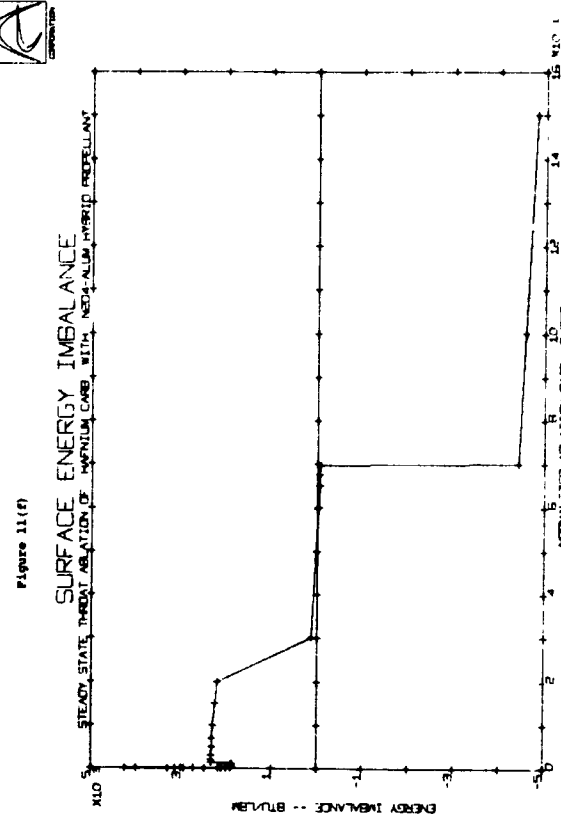
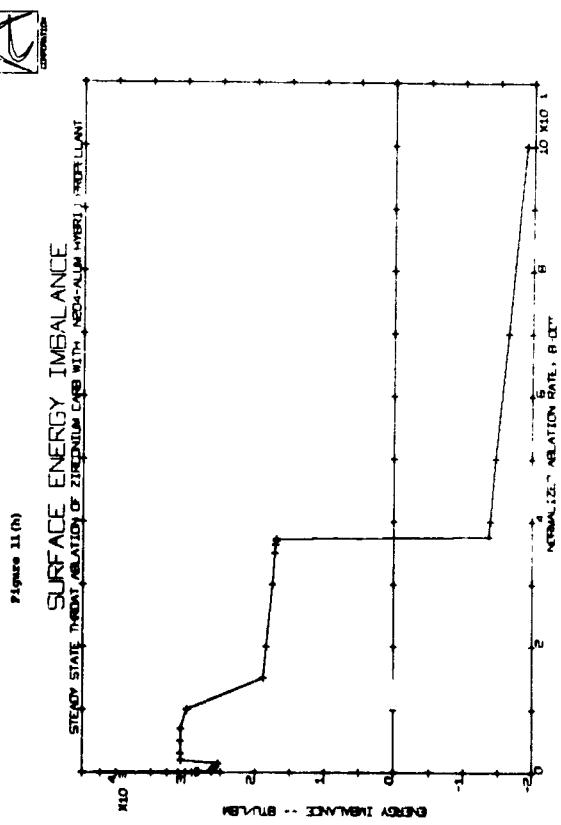


Figure 11(1)

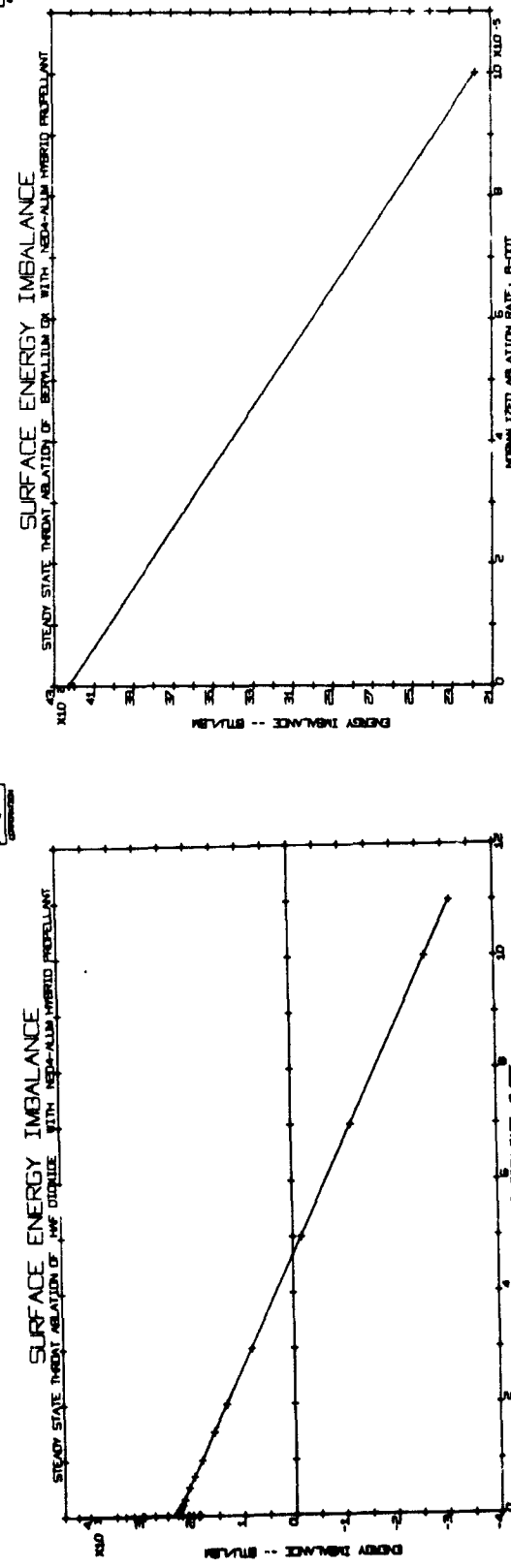


Figure 11(2)

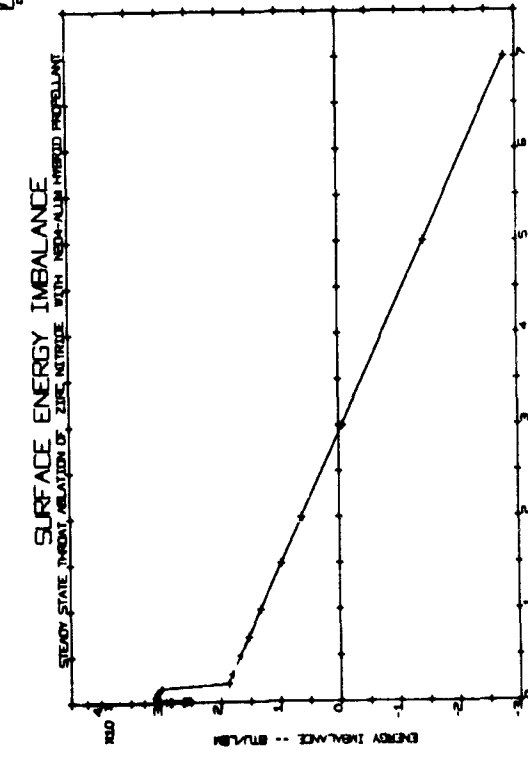


Figure 11(3)

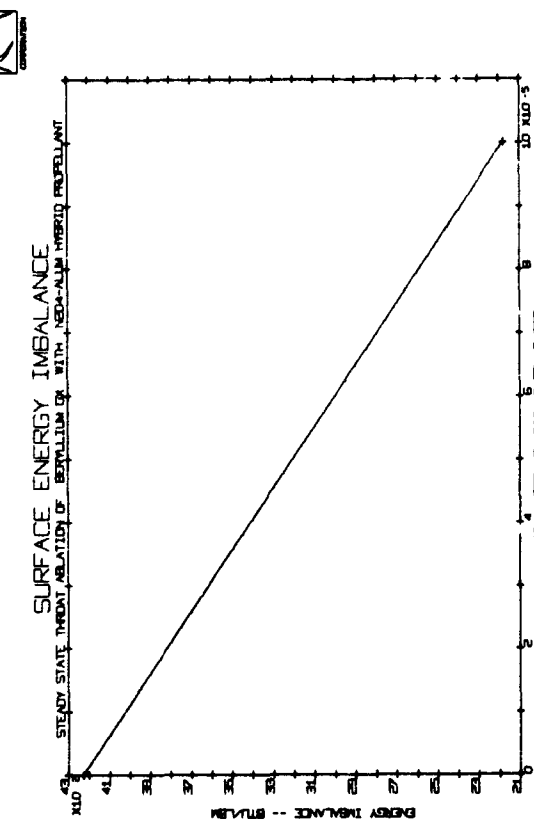


Figure 11(4)

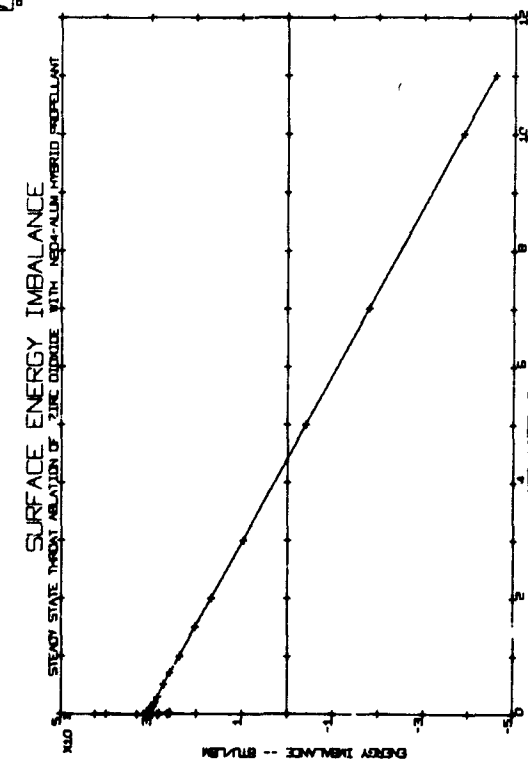


Figure 12(c)

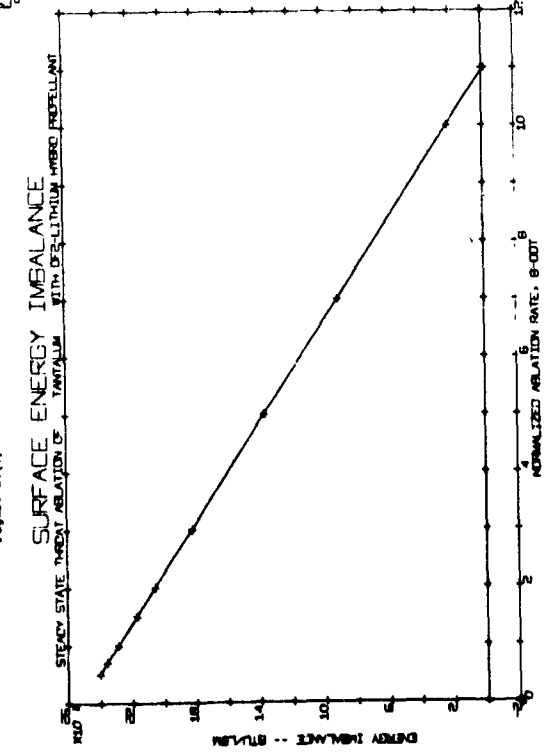


Figure 12(a)

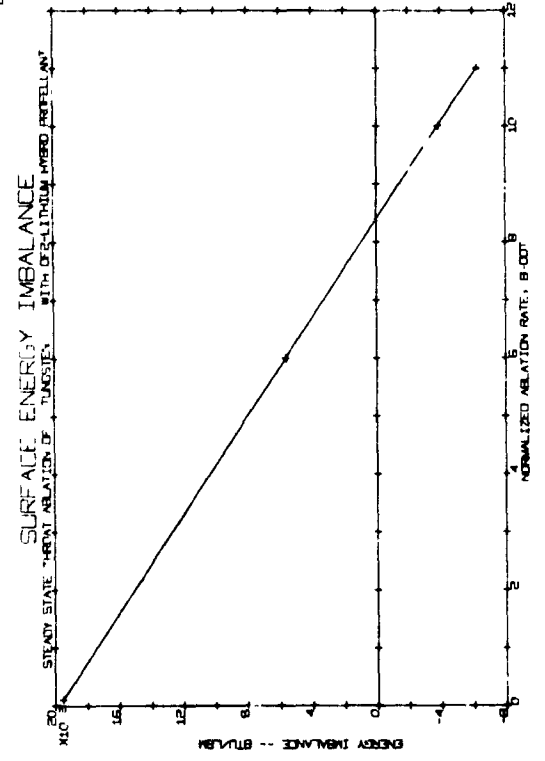


Figure 12(d)

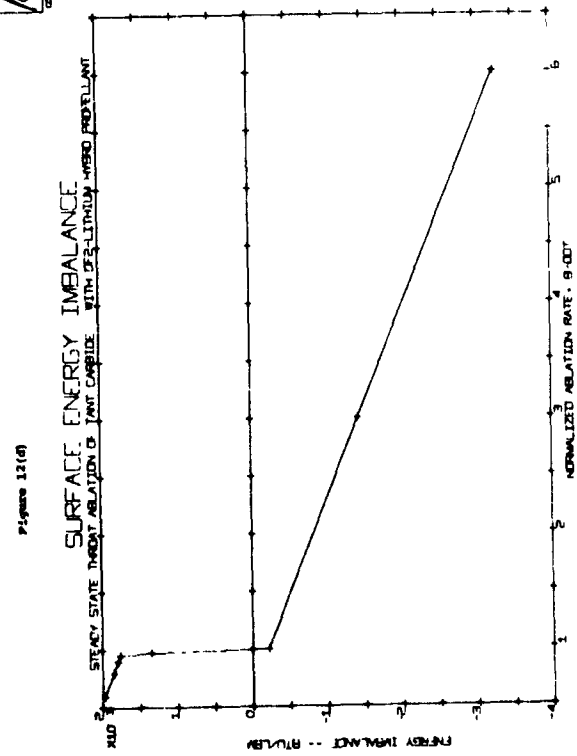


Figure 12(b)

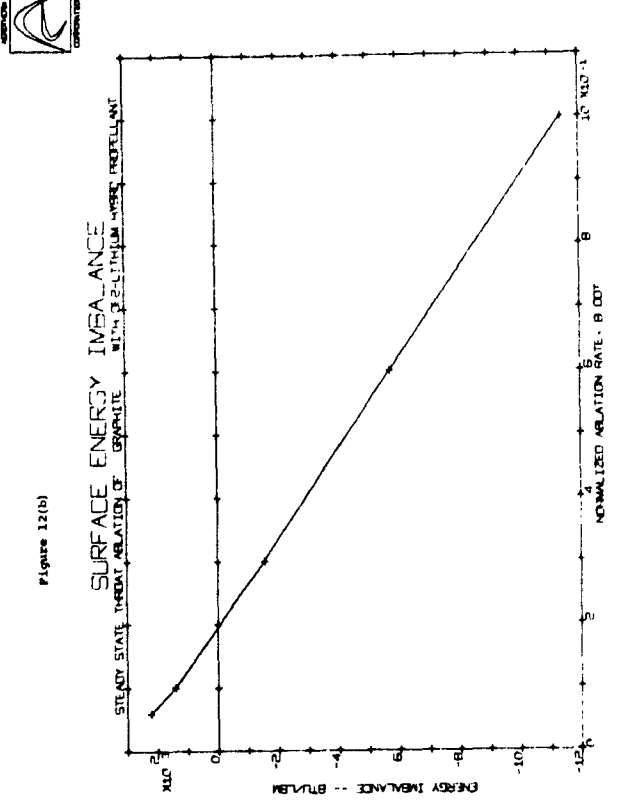


Figure 12(e)

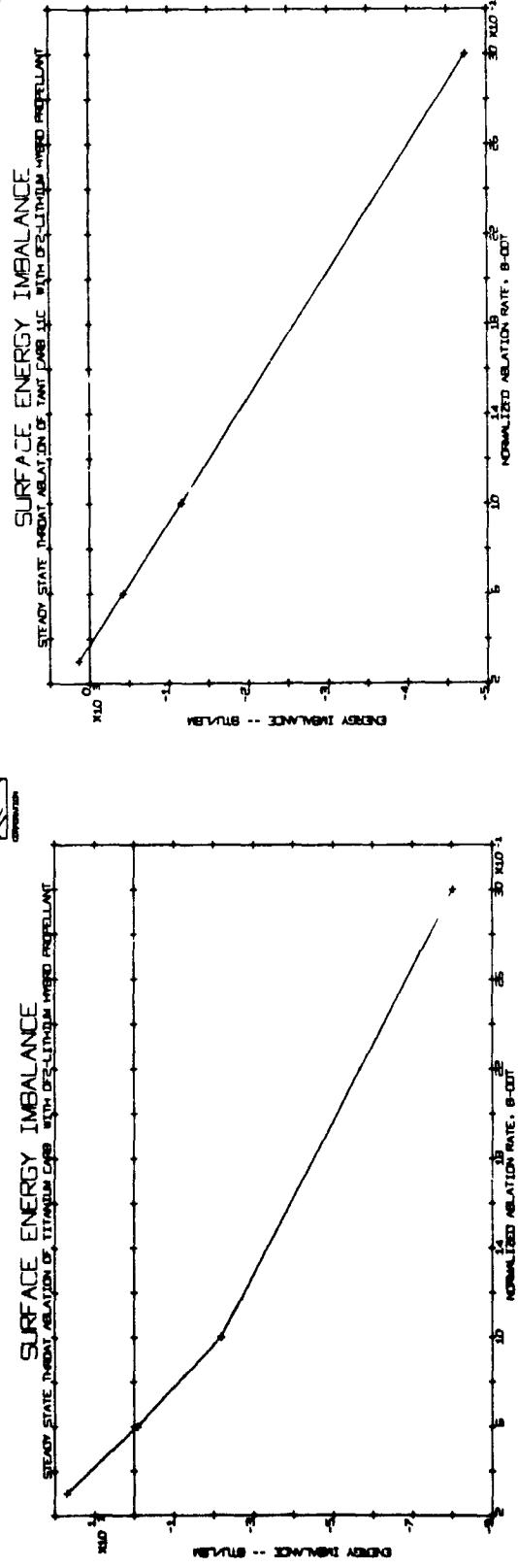


Figure 12(f)

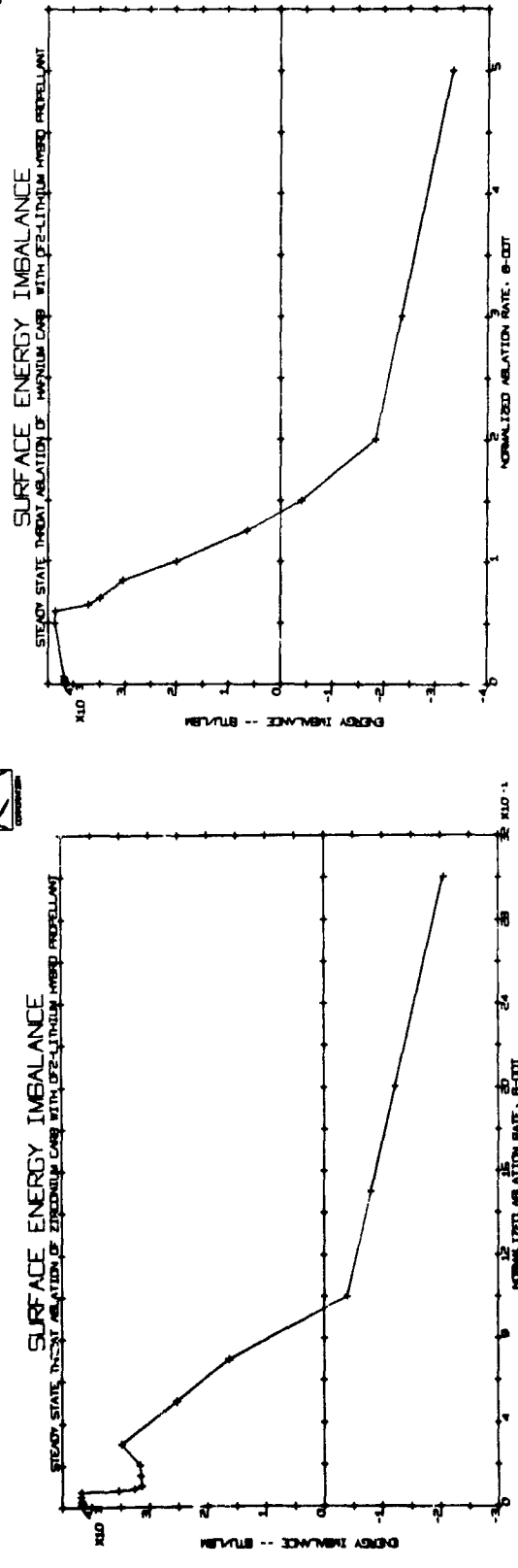


Figure 12(g)

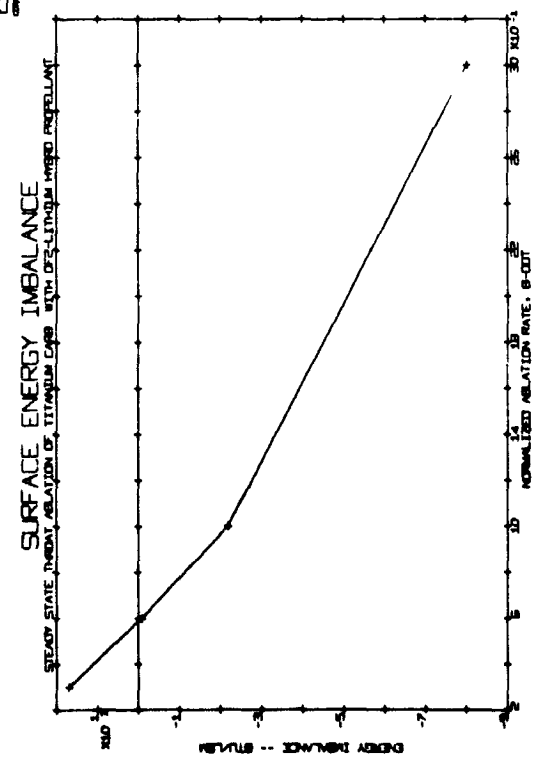


Figure 12(h)

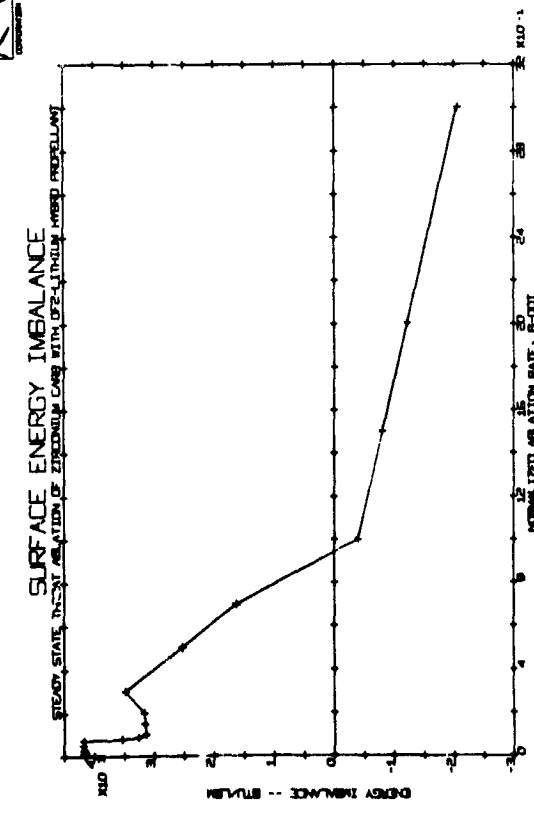


Figure 12(1)

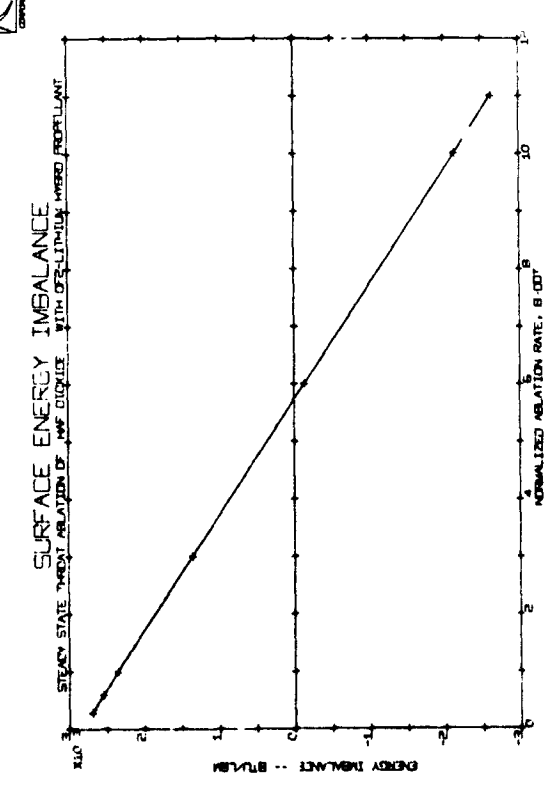


Figure 12(1)

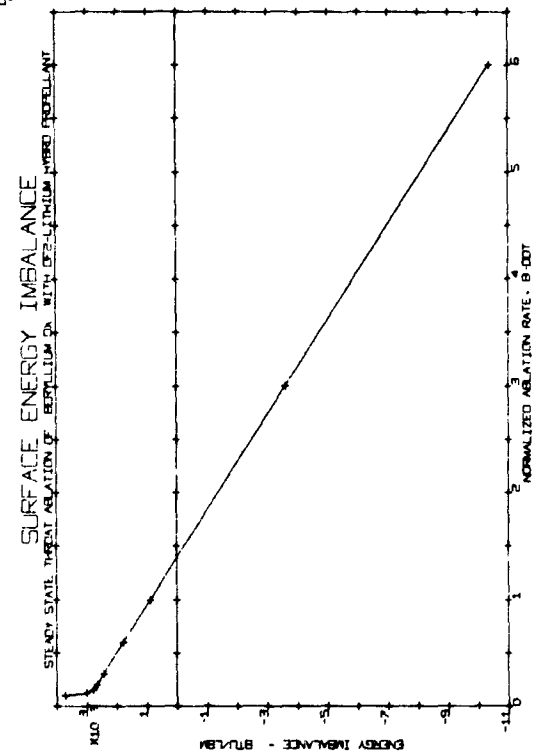


Figure 12(1)

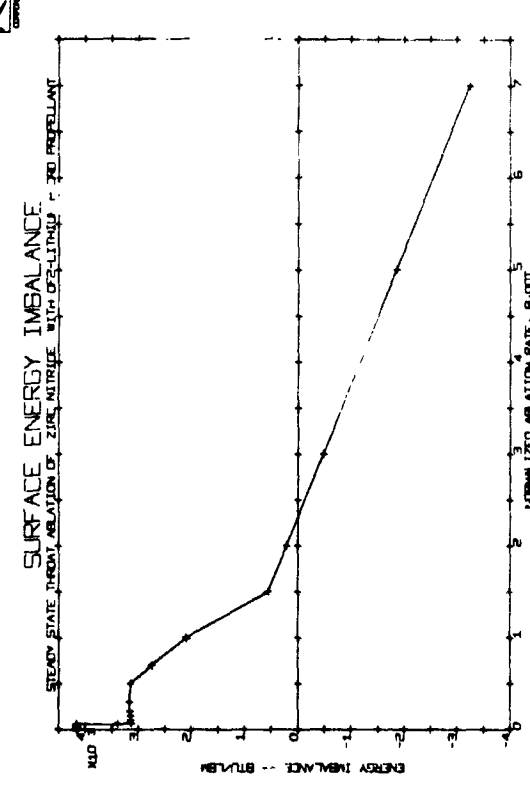
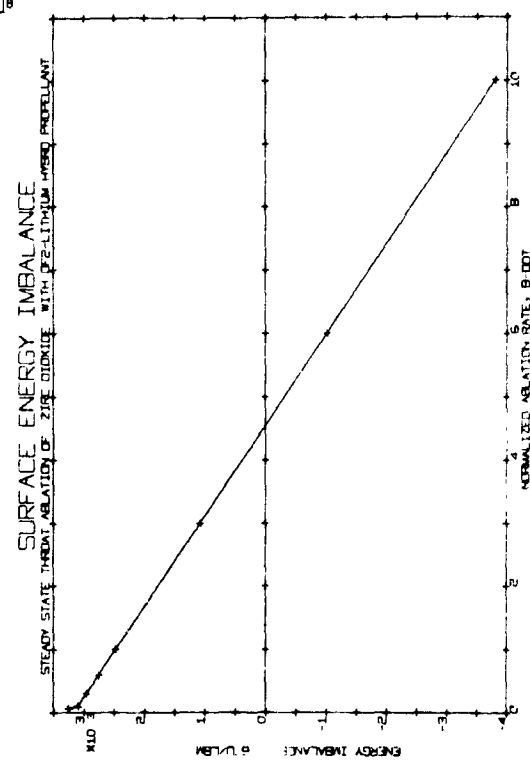


Figure 12(1)



**APPENDIX A**  
**THERMOCHEMICAL DATA**

## APPENDIX A

### THERMOCHEMICAL DATA

Thermochemical data for a large number of molecular species are required for performing chemical equilibrium calculations for the 72 material-propellant combinations considered in the present investigation. This appendix describes the procedure by which thermodynamic data was selected from the literature and complied in the appropriate format.

#### SECTION A.1

##### SELECTION OF APPROPRIATE MOLECULAR SPECIES FOR WHICH THERMODYNAMIC DATA WAS COMPILED

For each particular propellant-material combination a chemical system must be defined which contains all molecular species suspected to appear in significant quantity. The selection of such eligible species depends upon the chemical elements present in a given propellant-material system.

Past studies at Aerotherm in the field of ablation have resulted in the accumulation of thermodynamic data containing the elements Al, B, Be, Ca, C, Cl, F, Hf, H, Mg, N, O, Si, Ti, W, and Zr. However, an examination of the propellants and materials for the present investigation reveals that thermodynamic data for systems containing only the above elements are insufficient. Specifically, for the present study the data library was enlarged to also consider systems with the elements Ta and Li in combination with many of the above elements.

The following simple approach was taken in selecting molecular species for which thermodynamic data was obtained. References A-1, A-2, A-3, and A-4 were consulted and thermodynamic data for any species which (1) was included in these sources, and (2) was also a likely-present species for any one of the seventy-two propellant-material combinations, was then incorporated into the thermodynamic data collection (if not already present). The

result was the addition of 141 species into the existing Aerotherm molecular species thermodynamic data library.

The complete library of thermochemical data employed in the present study is illustrated in Table A-1.

#### SECTION A.2

##### SOURCES IN THE LITERATURE FOR THERMODYNAMIC DATA

As mentioned above, the JANAF tables and the publications by Aeronutronic, Schick, and Duff and Baur (Refs. A-1 through A-4) were consulted for thermodynamic data.

The data in these sources is arranged in tabular form with specific heat, heat of formation, sensible enthalpy, free energy function, and entropy as a function of temperature for each molecular species. All the sources are consistent in that they use the same physical units and the same thermodynamic and chemical base states. In each source the base states are taken as the elements in their normal state at 298°K and 1 atm pressure, i.e., the heat of formation for any molecular or atomic species existing in its natural state at these conditions is defined as zero.

#### SECTION A.3

##### COMPILED AND ARRANGEMENT OF THE THERMODYNAMIC DATA IN THE APPROPRIATE FORMAT FOR THE ACE PROGRAM

The specific thermodynamic information received by the ACE (Aerotherm Chemical Equilibrium) program for each molecular species, and the thermodynamic data format is identical to that of Reference A-5. This is the case because the ACE program, is in fact, a very extensive rewrite of the program of Reference A-5. The thermodynamic data format has been preserved and includes the following information.

- (1) Heat of formation at 298°K,  $\Delta h_{298}^{\circ}$
- (2) Sensible enthalpy increase from 298°K to 3000°K,  

$$h_{298}^{3000} = \int_{298}^{3000} C_p(T) dT$$
- (3) The three constants in the specific heat equation

$$C_p(T) = \beta_1 + \beta_2 T + \beta_3 T^{-2} \quad (A-1)$$

- (4) Entropy at 1 atmosphere and 3000 K,  $S_{3000,1}$
- (5) For the melting-solid condensed phase species,  
 a fail temperature,  $T_M$

The fail temperature of item (5) is taken as the melt temperature.

For the purpose of input to the ACE program, all the thermodynamic data is contained on punched cards, with three cards required for each molecular species. Table A-1 is a computer listing of these punched cards. A computer program developed at Aerotherm, TCDATA, was used to: (1) least-squares curve-fit the tabulated  $C_p(T)$  data, and (2) punch out the quantities  $\Delta h_{298}^{\circ}$ ,  $\beta_1$ ,  $\beta_2$ ,  $\beta_3$ ,  $S_{3000,1}$ , and  $T_M$  on cards. Reference A-6 describes the TCDATA computer program.

Input for the TCDATA program is the thermodynamic data taken directly from the references. The  $C_p(T)$  function is curve fitted over two temperature ranges:

- (1) 500-3000°K and 3000-5000°K for gas phase and solid condensed phase species
- (2) 5000- $T_M$ °K and  $T_M$ -5000°K for melting-solid condensed phase species, where  $T_M$  is the melt temperature.

For each curve fit both the input values of  $C_p(T)$  and the calculated values from Equation (A-1) are pointed out. In addition, the free-energy function,  $(F^{\circ} - \Delta h_{298}^{\circ})/Z$ , is calculated from the following equation, which is derived utilizing Equation (A-1) and the basic thermodynamic relations:

A-4

$$\begin{aligned}
 -S_1 \left[ \ln \frac{3000}{T} + \left( 1 - \frac{3000}{T} \right) \right] + S_2 T \left\{ \left( 1 - \frac{3000}{T} \right) - \frac{1}{2} \left[ 1 - \left( \frac{3000}{T} \right)^2 \right] \right\} \\
 + S_3 \left( \frac{1}{T^2} \right) \left\{ 1 - \frac{T}{3000} - \frac{1}{2} \left[ 1 - \left( \frac{T}{3000} \right)^2 \right] \right\} = \left( \frac{h_{298}^{3000} - \Delta h_{298}^o}{T} \right) \\
 - S_{3000,1} - \left( \frac{F - \Delta h_{298}^o}{T} \right) \quad (A-2)
 \end{aligned}$$

From a comparison of the specific heat and free energy function computed from Equations (A-1) and (A-2) with the corresponding input values from the references an indication of the accuracy of the  $C_p(T)$  curve-fit is obtained, and errors in the input quantities  $\Delta h_{298}^o$ ,  $h_{298}^{3000}$ , and  $S_{3000,1}$ , are readily detected and corrected. Table A-2 illustrates the listed output of the TCDATA program for representative gas phase, and melting-solid condensed phase species.

In summary, Table A-1 contains the complete thermodynamic data library used in the present study, with information for 141 of the molecular species being generated during the presented investigation. The following comments are pertinent to Table A-1.

- (1) the thermodynamic information for each molecular species is contained on three cards (or lines).
- (2) The first card contains the code designation of the species (example:  $\text{Al}_2\text{O}_3$  has 2 Al atoms (atomic number 13) and 3 O atoms (atomic number 8) hence the code designation 003008002013 on the left hand side of card one), the source of the data, and the chemical name of the species.
- (3) The second and third cards contain the quantities  $\Delta h_{298}^o$ ,  $h_{298}^{3000}$ ,  $S_1$ ,  $S_2$ ,  $S_3$ , and  $S_{3000,1}$  for a lower and an upper temperature range.

- (4) If the species is a melting-solid condensed phase, the temperature dividing the two temperature ranges is the melt temperature (or fail temperature)
- (5) The species phase index P is 1 for gas phase, 2 for solid phase, and 3 for liquid phase.
- (6) The decimal point on each number is assumed to be to the left of the left-most digit, and the power-of-ten is the signed one-digit number to the right of each 6-place base number.

#### REFERENCES - APPENDIX A

- A-1 JANAF Thermochemical Tables. The Dow Chemical Co., Midland, Michigan.
- A-2 Peters, D. L., et.al.: Chemical Corrosion of Rocket Liner Materials and Propellant Performance Studies. Final Technical Report. Aeronutronic Division of Ford Motor Co., Publication No. U-2384, Dec. 15, 1963.
- A-3 Schick, Harold L.: Thermodynamics of Certain Refractory Compounds, Volumes I and II. Academic Press, New York, 1966.
- A-4 Duff, R.E. and Baur, S.H.: Equilibrium Composition of the C/H System at Elevated Temperatures. J. Chem. Phys., Vol. 36, P. 1754, April 1962.
- A-5 Browne, H.N., Williams, M.M., and Cruise, D.R.: The theoretical Computation of Equilibrium Compositions, Thermodynamic Properties, and Performance Characteristics of Propellant Systems. U.S. Naval Ordnance Test Station, NAVWEPS Rept. 7043, June, 1960.
- A-6 User's Manual: Computer Program for Curve-Fitting Thermochemical Data and Preparing Data Cards for Input to ACE or EST, Aerotherm Corporation, September, 1966.

TABLE A-1 - THERMOCHEMICAL DATA

$\Delta h_{298}^{\circ}$	$\int_{298}^{3000} C_p dT$	$\beta_1$	$\beta_2$	$\beta_3$	$S_{3000,1}$	T	T	Phase	Species
cal/mole	cal/mole	cal/mole	cal/mole	cal/mole	cal/mole	°K	°K		
		$^{\circ}\text{K}$	$^{\circ}\text{K}^2$	$^{\circ}\text{K}^{-1}$					
1 13 0 0 0 0 0 0 0 0	OJANAF 03/61								AL
78000065 13461065 49290561 113634-4 70696765 50844062	500.	3000.	1	O·AL					
78000065 13461065 39567461 204094-3 36177767 50844062	3000.	5000.	1	O·AL					
1 6 1 13 0 0 0 0 0 0	OJANAF 12/60								ALC
20995866 24044065 89690961-757687-5-75253265 74665062	500.	3000.	1	O·ALC					
20995866 24044065 96160961-128042-3-26456767 74665062	3000.	5000.	1	O·ALC					
1 13 1 17 0 0 0 0 0 0	OJANAF 06/61								ALCL
11620065 24469065 8953C561 115091-3-92925165 75038062	500.	3000.	1	O·ALCL					
11620065 24469065 95108961 835189-5-22315667 75038062	3000.	5000.	1	O·ALCL					
1 8 1 13 1 17 0 0 0 0	OJANAF 12/60								ALCLO
55000065 39199065 14887962 3287-5-39253566 92044062	500.	3000.	1	O·ALCLO					
55000065 39199065 15861362-1-6492-3-4034967 92044062	3000.	5000.	1	O·ALCLO					
1 13 2 17 0 0 0 0 0 0	OJANAF 06/61								ALCL2
78000065 37117065 13889662 586012-5-13732966 10081363	500.	3000.	1	O·ALCL2					
78000065 37117065 13649362 486738-4 86968466 10081363	3000.	5000.	1	O·ALCL2					
1 13 3 17 0 0 0 0 0 0	OJANAF 06/61								ALCL3
14042366 52816065 19948562-209903-4-44644266 11958463	500.	3000.	1	O·ALCL3					
14042366 52816065 20448462-109302-3-25606267 11958463	3000.	5000.	1	O·ALCL3					
1 8 1 9 1 13 0 0 0 0	OJANAF 03/64					111			ALFO
14020066 38690065 14880062 650586-5-58992966 87698062	1000.	3000.	1	O·ALFO	1				
14020066 38690065 14894562 160258-5-58833466 87698062	3000.	5000.	1	O·ALFO	1				
1 1 1 13 0 0 0 0 0 0	OJANAF 06/63								ALH
62000065 23387065 88538761 181289-3-70865866 63829062	500.	3000.	1	O·ALH					
62000065 23387065 95119561 483217-4-30412867 63829062	3000.	5000.	1	O·ALH					
1 1 1 8 1 13 0 0 0 0	OJANAF 12/60								ALHO
34470064 36734065 14807362 231376-4-15546267 80355062	500.	3000.	1	O·ALHO					
34470064 36734065 14399162 973440-4 11574766 80355062	3000.	5000.	1	O·ALHO					
1 1 2 8 1 13 0 0 0 0	OJANAF 12/60								ALHO2
10900066 48050065 19145162 162758-3-25325767 98976062	500.	3000.	1	O·ALHO2					
10900066 48050065 20874362-198656-3-83376467 98976062	3000.	5000.	1	O·ALHO2					
1 7 1 13 0 0 0 0 0 0	OJANAF 12/60								ALN
10450066 24067065 89246061 115329-3-21237066 74297062	500.	3000.	1	O·ALN					
10450066 24067065 86167761 172650-3 10104567 74297062	3000.	5000.	1	O·ALN					
1 8 1 13 0 0 0 0 0 0	OJANAF 03/62								ALO
21398065 23805065 89558761 772498-4-32962566 71859062	500.	3000.	1	O·ALO					
21398065 23805065 91640861 387904-4-11651167 71859062	3000.	5000.	1	O·ALO					
2 13 6 17 0 0 0 0 0 0	OJANAF 03/64					111			AL2CL6
10920066 11629066 43707062 353763-5-64481266 21144663	1000.	3000.	1	O·AL2CL6	1				
10920066 11629066 43710162 159950-5-62028766 21144663	3000.	5000.	1	O·AL2CL6	1				
1 8 2 13 0 0 0 0 0 0	OJANAF 09/61								AL2O
31440065 35970065 13889162 485413-5-66326566 91200062	500.	3000.	1	O·AL2O					
31440065 35970065 14465662-108570-3-27892057 91200062	3000.	5000.	1	O·AL2O					
2 8 2 13 0 0 0 0 0 0	OJANAF 12/61								AL2O2
95397065 50497065 19859362 224091-5-13414467 10566563	500.	3000.	1	O·AL2O2					
95397065 50497065-18546862 738440-2 14499569 10566563	3000.	5000.	1	O·AL2O2					
1 4 0 0 0 0 0 0 0 0	OJANAF 09/61								BE
78255065 13438065 46469561 112298-3 33437466 44021062	500.	3000.	1	O·BE					
78255065 13438065 105297-3 109147-2 14771468 4021062	3000.	5000.	1	O·BE					
1 4 1 17 0 0 0 0 0 0	OJANAF 03/64					111			BECL
30000064 23983065 89341161 908676-4-22243566 71909062	1000.	3000.	1	O·BECL	1				
30000064 23983065 89469161 882523-4-26706956 71909062	3000.	5000.	1	O·BECL	1				
1 4 2 17 0 0 0 0 0 0	OJANAF 09/61								BECL2
57911965 38920965 14699662 608946-4-42594966 89904962	500.	3000.	1	O·BECL2					

TABLE A-1 (continued)

7911965	38820965	14900762	485558-6-60489366	89904962	3000.	5000.1	0.BECL2
1	4	1	9 0 0 0 0 0 0 0	OJA,AF	03/63		BtF
49678065	23468065	88869961	919571-4-42176666	68402062	500.	3000.1	0.BEF
49678065	23468065	84293461	174020-3 14813767	68402062	3000.	5000.1	0.BEF
1	4	2	9 0 0 0 0 0 0 0	OJA,AF	12/63		BtF2
19130066	37416065	14790562	289774-4-11567267	82283062	500.	3000.1	0.BLF2
19130066	37416065	13815462	209528-3 27448167	82283062	3000.	5000.1	0.BEF2
1	3	1	4 3 9 0 0 0 0 0	OJANAF	12/62		BEF3LI
21200066	64920965	25003962	245923-3-13832767	11553563	500.	3000.1	0.BEF3LI
21200066	64920965	25820862	207241-5-21513467	11553563	3000.	5000.1	0.BEF3LI
1	1	1	4 0 0 0 0 0 0 0	OJA,AF	3/63		BtH
76768065	22936065	87722461	184173-3-92490866	60772062	500.	3000.1	0.BEH
76768065	22936065	88473961	160554-3-96355666	60772062	3000.	5000.1	0.BEH
1	1	1	4 1 8 0 0 0 0 0	OJA,AF	09/63		BtHU
25000065	32173065	12985462	208547-3-23949467	78513062	500.	3000.1	0.BEH.
25000065	32173065	13903362-916197-5-47778467	78513062	3000.	5000.1	0.BEH.	
2	1	1	4 0 0 0 0 0 0 0	OJA,AF	12/60		BtH2
30000065	34578065	14580762	757364-4-27716267	67653062	500.	3000.1	0.BEH2
30000065	34578065	15355662-872682-4-53447067	67653062	3000.	5000.1	0.BEH2	
2	1	1	4 2 8 0 0 0 0 0	OJA,AF	09/63		BEH2u2
15850066	59395065	24452462	313890-3-47355067	10366763	500.	3000.1	0.BEH2u2
15850066	59395065	25282962	957844-4-63211667	10366763	3000.	5000.1	0.BEH2u2
1	4	1	7 0 0 0 0 0 0 0	OJA,AF	06/63		BE..
10199966	23659965	87183561	168927-3-25321766	69292962	500.	3000.1	0.BE ..
10199966	23659965	89412661	102713-3-47170466	69292962	3000.	5000.1	0.BE ..
1	4	1	8 0 0 0 0 0 0 0	OJA,AF	09/63		BEU
31000065	23184065	98545061	909641-4-55257066	66142062	500.	3000.1	0.BE ..
31000065	23184065	89416761	685229-4-73120466	66142062	3000.	5000.1	0.BE ..
2	4	4	17 0 0 0 0 0 0 0	OJANAF	12/60		BE2CL4
17899966	84452965	31682662	340183-4-45656966	16202763	500.	3000.1	0.BE2CL4
17899966	84452965	31787662	141294-5-52119766	16202763	3000.	5000.1	0.BE2CL4
2	4	1	8 0 0 0 0 0 0 0	OJA,AF	09/63		BE2U
15000065	37534965	14188262	210823-3-68158366	82927962	500.	3000.1	0.BE2
15000065	37534965	14904062-185011-6-14266867	82927962	3000.	5000.1	0.BE2 ..	
2	4	2	8 0 0 0 0 0 0 0	OJA,AF	09/63		BE2J2
98000065	49836065	19785462	208746-4-16301167	98856062	500.	3000.1	0.BE2 ..
98000065	49836065	19288362	113721-3 33709666	98856062	3000.	5000.1	0.BE2 ..
3	4	3	8 0 0 0 0 0 0 0	OJA,AF	09/63		BE3U3
25200066	76880065	31614962	406679-4-41304867	12470263	500.	3000.1	0.BE3U3
25200066	76880065	32026862-453443-4-55155567	12470263	3000.	5000.1	0.BE3 ..	
4	4	4	8 0 0 0 0 0 0 0	OJA,AF	09/63		BE4U4
38000066	10785666	43611262	233046-4-43931467	15656263	500.	3000.1	0.BE4 ..
38000066	10785666	43940962-408308-4-56294167	15656263	3000.	5000.1	0.BE4 ..	
5	4	5	8 0 0 0 0 0 0 0	OJA,AF	09/63		Bt5U5
50500066	13716966	55387462	617881-4-54257167	18429963	500.	3000.1	0.Bt5 ..
50500066	13716966	55519762	226391-4-55592767	18429963	3000.	5000.1	0.BE5 ..
6	4	6	8 0 0 0 0 0 0 0	OJA,AF	09/63		BE6U6
63600066	16637366	67240562	798827-4-65803867	21157263	500.	3000.1	0.BE6 ..
63600066	16637366	66523962	197656-3-33114567	21157263	3000.	5000.1	0.BE6 ..
1	5	0	0 0 0 0 0 0 0 0	OJA,AF	12/60		B
13261866	13424065	50602461-307108-4-98564165	48121062	500.	3000.1	0.B	
13261866	13424065	50745861-121838-4-72635366	48121062	3000.	5000.1	0.B	
1	5	2	9 1 17 0 0 0 0 0	OJANAF	12/63		BCLF2
21160066	50383065	19831162	886329-5-14740367	10626763	500.	3000.1	0.BCLF2
21160066	50383065	19558062	581861-4-34753466	10626763	3000.	5000.1	0.BCLF2
1	5	1	9 2 17 0 0 0 0 0	OJANAF	12/63		BCLF2

TABLE A-1 (continued)

15400066	51119065	19846062	578157-5-11017867	11042363	500.	3000.1	0.BCL2F
15400066	51119065	19805762	126436-4-92435066	11042363	3000.	5000.1	0.BCL2F
1 5 1	9 0 0	0 0 0	0 0 0 0 0	OJA,AF	12/60		BF
45469065	23289065	88779561	901824-4-52610966	66936062	500.	3000.1	0.BF
45469065	23289065	81685961	210898-3-27933467	66936062	3000.	5000.1	0.BF
1 5 1	8 1 9	0 0 0	0 0 0 0 0	OJA,AF	12/63		BF
14400066	37466065	14801762	227294-4-13405267	84390062	500.	3000.1	0.BF
14400066	37466065	15787062	169659-3-50134567	84390062	3000.	5000.1	0.BF
1 5 2	9 0 0	0 0 0	0 0 0 0 0	OJA,AF	12/62		BF
13000066	35249065	13798162	306556-4-97951566	87486062	500.	3000.1	0.BF
13000066	35249065	14864762	178860-3-50725567	87486062	3000.	5000.1	0.BF
1 1 1	5 2 9	0 0 0	0 0 0 0 0	OJA,AF	12/65		BF
17539966	47279965	17517662	676573-3-12632567	94916962	500.	3000.1	0.BF
17539966	47279965	19823162	682930-5-39299767	94916962	3000.	5000.1	0.BF
1 5 1	8 2 9	0 0 0	0 0 0 0 0	OJA,AF	12/65		BF
24999966	49731965	19010662	255063-3-10608967	10327163	500.	3000.1	0.BF
24999966	49731965	19867362	528861-6-18983867	10327163	3000.	5000.1	0.BF
1 5 3	9 0 0	0 0 0	0 0 0 0 0	OJA,AF	12/63		BF
27010066	49694065	19764362	260131-4-17492567	10031763	500.	3000.1	0.BF
27010066	49694065	19010062	163117-3-13377567	10031763	3000.	5000.1	0.BF
1 1 1	5 0 0	0 0 0	0 0 0 0 0	OJA,AF	03/63		BH
10563066	22637065	87172361	193099-3-11388067	59324062	500.	3000.1	0.BH
10563066	22637065	96234461	127652-4-44256867	59324062	3000.	5000.1	0.BH
1 1 1	5 1 8	0 0 0	0 0 0 0 0	OJA,AF	12/60		BH
47127065	35603065	14297462	167620-3-20113667	76473062	500.	3000.1	0.BH
47127065	35603065	11239262	644865-3-13496768	76473062	3000.	5000.1	0.BH
1 1 1	5 2 8	0 0 0	0 0 0 0 0	OJA,AF	06/63		BH
13410066	45664065	18228062	425108-3-30104467	92490062	500.	3000.1	0.BH
13410066	45664065	16874662	521159-3-69979867	92490062	3000.	5000.1	0.BH
2 1 1	5 0 0	0 0 0	0 0 0 0 0	OJA,AF	12/60		BH
66000065	32748065	13181962	199298-3-21134667	72822062	500.	3000.1	0.BH
66000065	32748065	13341162	907704-4-58006966	72822062	3000.	5000.1	0.BH
2 1 1	5 2 8	0 0 0	0 0 0 0 0	OJA,AF	12/60		BH
45000065	59706065	24630762	263481-3-47631967	10907463	500.	3000.1	0.BH
45000065	59706065	24601562	206036-3-24430667	10907463	3000.	5000.1	0.BH
3 1 1	5 0 0	0 0 0	0 0 0 0 0	OJA,AF	12/60		BH
18000065	42459065	17900762	501613-3-49570967	76379062	500.	3000.1	0.BH
18000065	42459065	18689062	214061-3-46413167	76379062	3000.	5000.1	0.BH
3 1 1	5 3 8	0 0 0	0 0 0 0 0	OJA,AF	03/61		BH
23860066	86073065	35684662	478490-3-72041967	13180863	500.	3000.1	0.BH
23860066	86073065	37752962	-105305-4-12723768	13180863	3000.	5000.1	0.BH
1 5 1	7 0 0	0 0 0	0 0 0 0 0	OJA,AF	09/63		B.
15200066	24462065	88011061	108795-3-11244666	69936062	500.	3000.1	0.B.
15200066	24462065	88075061	998189-4 72366865	69936062	3000.	5000.1	0.BN
1 5 1	8 0 0	0 0 0	0 0 0 0 0	OJA,AF	06/62		BU
57440064	22645065	86219761	136981-3-63170466	67024062	500.	3000.1	0.BU
57440064	22645065	80348661	210252-3-26465367	67024062	3000.	5000.1	0.BU
1 5 2	8 0 0	0 0 0	0 0 0 0 0	OJA,AF	06/63		B
72600065	37930065	14855262	119400-4-99943566	85636062	500.	3000.1	0.B
72600065	37930065	11826862	637770-3-93585967	85636062	3000.	5000.1	0.B
2 5 0	0 0 0	0 0 0	0 0 0 0 0	OJA,AF	12/60		B
19930066	23809065	89101761	112093-3-321956	67851062	500.	3000.1	0.B
19930066	23809065	72442561	412560-3-68791867	67851062	3000.	5000.1	0.B
1 4 2	5 4 8	0 0 0	0 0 0 0 0	OJA,AF	12/62		B2BEU4
31960066	90251065	37311562	103876-3-54373267	14295663	500.	3000.1	0.B2BEU4
31960066	90251065	36468762	244001-3-16353467	14295663	3000.	5000.1	0.B2BEU4

TABLE A-1 (continued)

2	5	4	9	0	0	0	0	0	0	0	0	0	0	0	0	0	OJANAF	12/64	B2F4
34219966	77100965	29445462	401125-3-16275467	13749063	500.	3000.1	0	0	0	0	0	0	0	0	0	0	OJANAF	12/64	0.B2F4
34219966	77100965	30793562	121509-5-29627467	13749063	3000.	5000.1	0	0	0	0	0	0	0	0	0	0	OJANAF	03/66	0.B2F4
4	1	2	5	4	8	0	0	0	0	0	0	0	0	0	0	0	OJANAF	03/66	B2H4U4
30699966	12574066	45088762	266027-2-33260567	17964363	500.	3000.1	0	0	0	0	0	0	0	0	0	0	OJANAF	03/66	0.B2H4U4
30699966	12574066	54311962	450391-4-15723568	17964363	3000.	5000.1	0	0	0	0	0	0	0	0	0	0	OJANAF	03/66	0.B2H4U4
6	1	2	5	0	0	0	0	0	0	0	0	0	0	0	0	0	OJANAF	12/64	B2H6
97999964	95764965	34157362	274368-2-38016667	12553963	500.	3000.1	0	0	0	0	0	0	0	0	0	0	OJANAF	12/64	0.B2H6
97999964	95764965	43528662	258895-4-14763068	12553963	3000.	5000.1	0	0	0	0	0	0	0	0	0	0	OJANAF	03/66	0.B2H6
7	5	2	8	0	0	0	0	0	0	0	0	0	0	0	0	0	OJANAF	03/61	B2U2
11160066	51550065	20788562	370455-5-25133167	98397062	500.	3000.1	0	0	0	0	0	0	0	0	0	0	OJANAF	03/61	0.B2U2
11160066	51550065	19664162	203148-3-28490867	98397062	3000.	5000.1	0	0	0	0	0	0	0	0	0	0	OJANAF	03/61	0.B2U2
2	5	3	8	0	0	0	0	0	0	0	0	0	0	0	0	0	OJANAF	03/61	B2U3
21010065	61507065	25777762-153675-4-42751467	11171063	500.	3000.1	0	0	0	0	0	0	0	0	0	0	OJANAF	03/61	0.B2U3	
21010066	61507065	23928662	345774-3-32940267	11171063	3000.	5000.1	0	0	0	0	0	0	0	0	0	0	OJANAF	03/61	0.B2U3
2	1	3	5	3	8	1	9	0	0	0	0	0	0	0	0	0	OJANAF	12/65	B3FH2U3
38199966	11819966	44494262	150977-2-35241367	16600763	500.	3000.1	0	0	0	0	0	0	0	0	0	0	OJANAF	12/65	0.B3FH2U3
38199966	11819966	49606562	101166-4-90440667	16600763	3000.	5000.1	0	0	0	0	0	0	0	0	0	0	OJANAF	12/65	0.B3FH2U3
1	1	3	5	3	8	2	9	0	0	0	0	0	0	0	0	0	OJANAF	12/65	B3F2H03
47499966	12073366	46025062	107470-2-33048567	17250263	500.	3000.1	0	0	0	0	0	0	0	0	0	0	OJANAF	12/65	0.B3F2H03
47499966	12073366	49641062	544339-5-69782667	17250263	3000.	5000.1	0	0	0	0	0	0	0	0	0	0	OJANAF	03/65	0.B3F2H03
3	5	3	8	3	9	0	0	0	0	0	0	0	0	0	0	0	OJANAF	03/65	B3F3U3
56530066	12323466	47239562	722094-3-29233467	17908563	500.	3000.1	0	0	0	0	0	0	0	0	0	0	OJANAF	03/65	0.B3F3U3
56530066	12323466	49656162	357165-5-52729567	17908563	3000.	5000.1	0	0	0	0	0	0	0	0	0	0	OJANAF	03/65	0.B3F3U3
3	1	3	5	3	8	0	0	0	0	0	0	0	0	0	0	0	OJANAF	03/65	B3H3U3
29100066	11549666	42777162	198595-2-36811467	15736563	500.	3000.1	0	0	0	0	0	0	0	0	0	0	OJANAF	03/65	0.B3H3U3
29100066	11549666	49556362	166186-4-11521668	15736563	3000.	5000.1	0	0	0	0	0	0	0	0	0	0	OJANAF	03/65	0.B3H3U3
3	1	3	5	6	8	0	0	0	0	0	0	0	0	0	0	0	OJANAF	12/64	B3H3U6
54299966	16088966	59469462	222751-2-38164267	20830963	500.	3000.1	0	0	0	0	0	0	0	0	0	0	OJANAF	12/64	0.B3H3U6
54299966	16088966	67236562	437510-4-14758168	20830963	3000.	5000.1	0	0	0	0	0	0	0	0	0	0	OJANAF	12/64	0.B3H3U6
6	1	3	5	3	7	0	0	0	0	0	0	0	0	0	0	0	OJANAF	03/65	B3H6U3
12189966	15018066	53739762	387996-2-51894467	18038363	500.	3000.1	0	0	0	0	0	0	0	0	0	0	OJANAF	03/65	0.B3H6U3
12189966	15018066	67133162	581970-4-22542968	18038363	3000.	5000.1	0	0	0	0	0	0	0	0	0	0	OJANAF	03/65	0.B3H6U3
1	6	0	0	0	0	0	0	0	0	0	0	0	0	0	0	0	OJANAF	03/61	C
17088666	13550065	444433&1	228125-3-40983066	49287062	500.	3000.1	0	0	0	0	0	0	0	0	0	0	OJANAF	03/61	0.C
17088666	13550065	412212&1	261908-3-26288667	49287062	3000.	5000.1	0	0	0	0	0	0	0	0	0	0	OJANAF	03/61	0.C
1	5	1	6	0	0	0	0	0	0	0	0	0	0	0	0	0	OJANAF	06/63	CB
19800066	23387065	887101&1	987600-4-46166666	68965062	500.	3000.1	0	0	0	0	0	0	0	0	0	0	OJANAF	06/63	0.CB
19800066	23387065	864500&1	1347F0-3-599853&6	68965062	3000.	5000.1	0	0	0	0	0	0	0	0	0	0	OJANAF	06/63	0.CB
1	6	1	17	0	0	0	0	0	0	0	0	0	0	0	0	0	OJANAF	12/60	CCL
13200066	23785065	890513&1	416720-4-15433366	736510&2	500.	3000.1	0	0	0	0	0	0	0	0	0	0	OJANAF	12/60	0.CCL
13200066	23785065	857088&1	993826-4-129567&7	736510&2	3000.	5000.1	0	0	0	0	0	0	0	0	0	0	OJANAF	12/60	0.CCL
1	6	3	9	1	17	0	0	0	0	0	0	0	0	0	0	0	OJANAF	03/64	111
16600066	65432065	25705362	334186-4-17244467	12068063	1000.	3000.1	0	0	0	0	0	0	0	0	0	0	OJANAF	03/64	0.CCLF3
16600066	65432065	258243&2	146187-5-19327567	12068063	3000.	5000.1	0	0	0	0	0	0	0	0	0	0	OJANAF	03/64	0.CCLF3
1	6	1	7	1	17	0	0	0	0	0	0	0	0	0	0	0	OJANAF	12/60	CCLN
32200065	37509065	415997&3-109631-0-65141969	86893062	500.	3000.1	0	0	0	0	0	0	0	0	0	0	0	OJANAF	12/60	0.CCLN
32200065	37509065	13474462	286947-3-348958&7	86893062	3000.	5000.1	0	0	0	0	0	0	0	0	0	0	OJANAF	12/60	0.CCLN
1	6	1	8	1	17	0	0	0	0	0	0	0	0	0	0	0	OJANAF	03/65	CCLO
15000065	35511965	13126962	228137-3-40866366	92661962	500.	3000.1	0	0	0	0	0	0	0	0	0	0	OJANAF	03/65	0.CCLO
15000065	35511965	13900362	148315-5-12488967	92661962	3000.	5000.1	0	0	0	0	0	0	0	0	0	0	OJANAF	03/65	0.CCLO
1	6	2	17	3	0	0	0	0	0	0	0	0	0	0	0	0	OJANAF	03/65	CCL2
75000055	36300965	13733562	526254-4-38161766	93648962	500.	3000.1	0	0	0	0	0	0	0	0	0	0	OJANAF	03/64	0.CCL2
75000065	36300965	13911462-748804-7-56029866	93648962	3000.	5000.1	0	0	0	0	0	0	0	0	0	0	OJANAF	03/64	0.CCL2	
1	6	2	9	2	17	0	0	0	0	0	0	0	0	0	0	0	OJANAF	03/64	111
11500066	66224065	25747762	222257-4-13902667	12562963	1000.	3000.1	0	0	0	0	0	0	0	0	0	0	OJANAF	03/64	0.CCL2F2

TABLE A-1 (continued)

11500066	66224065	25828862	844195-6-15424567	12562963	3000.	5000.1	0.CCL2F2	1	
1 6 1	8 2 17	0 0 0	0 0 0	0 0 0	OJANAF	12/60	CCL2		
52600065	50595065	19734862	333599-4-13314167	10889963	500.	3000.1	0.CCL2		
52600065	50595065	18974562	170558-3	18068367	10889963	3000.	5000.1	0.CCL2	
1 6 3	17 0 0	0 0 0	0 0 0	0 0 0	OJANAF	03/65	CCL3		
34999965	51660965	19596762	821072-4-60355666	11324263	500.	3000.1	0.CCL3		
34999965	51660965	19862562	165563-5-82364666	11324263	3000.	5000.1	0.CCL3		
1 6 1	9 3 17	0 0 0	0 0 0	0 0 0	OJANAF	03/64	111	CCL3F	
68000065	66993065	25781162	137845-4-10662867	12891163	1000.	3000.1	0.CCL3F	1	
68000065	66993065	25833362	838371-7-11661067	12891163	3000.	5000.1	0.CCL3F	1	
1 6 4	17 0 0	0 0 0	0 0 0	0 0 0	OJANAF	12/60	CCL4		
25940065	67654065	25827762	144070-5-82897766	12998363	500.	3000.1	0.CCL4		
25940065	67654065	25302362	998371-4	12433967	12998363	3000.	5000.1	0.CCL4	
1 6 1	9 0 0	0 0 0	0 0 0	0 0 0	OJANAF	03/61	CF		
74400065	23463065	86982961	942918-4-46950366	70128062	500.	3000.1	0.CF		
74400065	23463065	81097461	241697-3	26474567	70128062	3000.	5000.1	0.CF	
1 6 1	7 1 9	0 0 0	0 0 0	0 0 0	OJANAF	06/61	CFN		
30000064	37014065	14675662	528937-4-15692467	83695062	500.	3000.1	0.CFN		
30000064	37014065	15682162	-153382-3-50579467	83695062	3000.	5000.1	0.CFN		
1 6 1	8 1 9	0 0 0	0 0 0	0 0 0	OJANAF	12/65	CFO		
40999965	34797065	13007162	264190-3-61832566	87319962	500.	3000.1	0.CFU		
40999965	34797065	13956262	-131517-4-19423467	87319962	3000.	5000.1	0.CFU		
1 6 2	9 0 0	0 0 0	0 0 0	0 0 0	OJANAF	12/63	CF2		
30000065	34974065	13855262	128704-4-11869667	87632062	500.	3000.1	0.CF2		
30000065	34974065	14254262	-646408-4-26853867	87632062	3000.	5000.1	0.CF2		
1 6 1	8 2 9	0 0 0	0 0 0	0 0 0	OJANAF	12/63	CF2		
15250066	49056065	19696762	418619-4-20635867	10060763	500.	3000.1	0.CF2		
15250066	49056065	19529162	621854-4-11047767	10060763	3000.	5000.1	0.CF2		
1 6 3	9 0 0	0 0 0	0 0 0	0 0 0	OJANAF	12/63	CF3		
11650066	49860065	19786562	200977-4-16638467	10216163	500.	3000.1	0.CF3		
11650066	49860065	19657562	404917-4-10531067	10216163	3000.	5000.1	0.CF3		
1 6 4	9 0 0	0 0 0	0 0 0	0 0 0	OJANAF	12/63	CF4		
22700066	64542065	24363762	395728-3	72301065	11362763	500.	3000.1	0.CF4	
22700066	64542065	26543062	-135803-3-51896667	11362763	3000.	5000.1	0.CF4		
1 1 1	6 0 0	0 0 0	0 0 0	0 0 0	OJANAF	03/61	CH		
14200666	22130065	82607961	302211-3-10018467	61612062	500.	3000.1	0.CH		
14200666	22130065	70709161	463281-3	55286067	61612062	3000.	5000.1	0.CH	
1 1 1	6 3 17	0 0 0	0 0 0	0 0 0	OJANAF	12/60	CHCL3		
25000065	63476065	25277962	125963-3-28782467	12124563	500.	3000.1	0.CHCL3		
25000065	63476065	25785062	237794-5-41056167	12124563	3000.	5000.1	0.CHCL3		
1 1 1	6 1 8	1 9 0	0 0 0	0 0 0	OJANAF	06/61	CHFO		
90000065	46239965	16782162	878833-3-12835267	94441962	500.	3000.1	0.CHF0		
90000065	46239965	19800862	951575-5-49809067	94441962	3000.	5000.1	0.CHF0		
1 1 1	6 3 9	0 0 0	0 0 0	0 0 0	OJANAF	12/63	CHF3		
16510066	61103065	25211362	141526-3-40040567	10908263	500.	3000.1	0.CHF3		
16510066	61103065	25928462	-224709-4-60301967	10908263	3000.	5000.1	0.CHF3		
1 1 1	6 1 7	0 0 0	0 0 0	0 0 0	OJANAF	03/61	CHN		
31200065	35593065	13702362	552243-3-22895567	75862062	500.	3000.1	0.CHN		
31200065	35593065	17889562	-295052-3-18367168	75862062	3000.	5000.1	0.CHN		
1 1 1	6 1 7	1 8 0	0 0 0	0 0 0	OJANAF	12/60	CHS		
27900065	46193065	17970162	469024-3-20090467	92899062	500.	3000.1	0.CHM		
27900065	46193065	21016762	-229915-3-10556668	92899062	3000.	5000.1	0.CHM		
1 1 1	6 1 8	0 0 0	0 0 0	0 0 0	OJANAF	03/61	CHU		
29000064	32367065	12803362	300638-3-20172167	78983062	500.	3000.1	0.CHU		
29000064	32367065	10302862	633312-3	12161568	78983062	3000.	5000.1	0.CHU	
2 1 1	6 0 0	0 0 0	0 0 0	0 0 0	OJANAF	12/62	CH2		

TABLE A-1 (continued)

95000065	32996065	13289462	413822-3-290273&7	68494062	500.	3000.1	0.CH2
95000065	32996065	14072862	132150-3-239493&7	68494062	3000.	5000.1	0.CH2
2 1 1	6 2 17	0 0 0	0 0 0	OJANAF	12/60		CH2CL2
22400065	59579065	247355&2	249585-3-481774&7	11026963	500.	3000.1	0.CH2CL2
22400065	59579065	258799&2-161283-4	794316&7	11026963	3000.	5000.1	0.CH2CL2
2 1 1	6 2 9	0 0 0	0 0 0	OJANAF	12/63		CH2F2
10720066	57924065	246913&2	260835-3-564164&7	10222863	500.	3000.1	0.CH2F2
10720066	57924065	256947&2	195707-4-815777&7	10222863	3000.	5000.1	0.CH2F2
2 1 1	6 1 8	0 0 0	0 0 0	OJANAF	03/61		CH2O
27700065	43791065	184022&2	379921-3-431982&7	848880&2	500.	3000.1	0.CH2O
27700065	43791065	189628&2	161963-3-372770&7	848880&2	3000.	5000.1	0.CH2O
3 1 1	6 0 0	0 0 0	0 0 0	OJANAF	12/62		CH3
31940065	43419065	182763&2	401025-3-461203&7	786040&2	500.	3000.1	0.CH3
31940065	43419065	204899&2-10	8028-3-114692&8	786040&2	3000.	5000.1	0.CH3
3 1 1	6 1 17	0 0 0	0 0 0	OJANAF	12/60		CH3CL
20634065	56030065	241353&2	388635-3-654504&7	972200&2	500.	3000.1	0.CH3CL
20634065	56030065	256598&2	197863-4-103065&8	972200&2	3000.	5000.1	0.CH3CL
3 1 1	6 1 9	0 0 0	0 0 0	OJANAF	12/63		CH3F
56000065	55223065	241434&2	386480-3-701904&7	935320&2	500.	3000.1	0.CH3F
56000065	55223065	257207&2	985709-5-110460&8	935320&2	3000.	5000.1	0.CH3F
4 1 1	6 0 0	0 0 0	0 0 0	OJANAF	03/61		CH4
17995065	53079065	230948&2	677896-3-755061&7	825970&2	500.	3000.1	0.CH4
17995065	53079065	236053&2	374323-3-368234&7	825970&2	3000.	5000.1	0.CH4
1 6 1	7 0 0	0 0 0	0 0 0	OJANAF	12/62		CN
10900066	23249065	655906&1	115326-2 479517&6	669760&2	500.	3000.1	0.CN
10900066	23249065	988013&1	313855-3-649453&7	669760&2	3000.	5000.1	0.CN
1 5 1	8 0 0	0 0 0	0 0 0	OJANAF	03/61		CO
26417065	22357065	865040&1	117021-3-898211&6	653700&2	500.	3000.1	0.CO
26417065	22357065	115496&2-424139-3	131563&8	653700&2	3000.	5000.1	0.CO
1 6 2	9 0 0	0 0 0	0 0 0	OJANAF	03/61		C02
94054065	36535065	144559&2	210386-3-182392&7	798480&2	500.	3000.1	0.C02
94054065	36535065	156451&2-381561-4-	602768&7	798480&2	3000.	5000.1	0.C02
2 6 0	0 0 0	0 0 0	0 0 0	OJANAF	9/61		C2
19899966	24699065	77661261	696081-3 185649&6	685519&2	500.	3000.1	0.C2
19899966	24699065	104162&2	566841-4-640205&7	685519&2	3000.	5000.1	0.C2
1 4 2	6 0 0	0 0 0	0 0 0	OJANAF	12/63		C2BE
13500066	36774065	17404262-702548-3	572915&7	816180&2	500.	3000.1	0.C2BE
13500066	36774065	136768&2	233788-3 253563&7	816180&2	3000.	5000.1	0.C2BE
2 6 2	9 0 0	0 0 0	0 0 0	OJANAF	12/60		C2F2
51300065	52669065	206993&2	383288-4-175788&7	102918&3	500.	3000.1	0.C2F2
51300065	52669065	212155&2-681801-4-	352776&7	102918&3	3000.	5000.1	0.C2F2
2 6 4	9 0 0	0 0 0	0 0 0	OJANAF	06/63		C2F4
15170066	79312065	316735&2	255243-4-306132&7	134856&3	500.	3000.1	0.C2F4
15170066	79312065	305382&2	247246-3 116982&7	134856&3	3000.	5000.1	0.C2F4
2 6 6	9 0 0	0 0 0	0 0 0	OJANAF	09/65		C2F6
31679966	10811566	417073&2	306660-3-219022&7	165819&3	500.	3000.1	0.C2F6
31679966	10811566	429440&2-413096-4-	392508&7	165819&3	3000.	5000.1	0.C2F5
1 1 2	6 0 0	0 0 0	0 0 0	ODUFF BAUER	6/61		C2H
11739566	34962065	134210&2	469100-3-187509&7	781140&2	500.	3000.1	0.C2H
11739566	34962065	148516&2	109402-3-503862&7	781140&2	3000.	5000.1	0.C2H
2 1 2	6 0 0	0 0 0	0 0 0	OJANAF	03/61		C2H2
54190065	48257065	189960&2	769044-3-409039&7	849690&2	500.	3000.1	0.C2H2
54190065	48257065	203952&2	389062-3-645297&7	849690&2	3000.	5000.1	0.C2H2
3 1 2	6 0 0	0 0 0	0 0 0	ODUFF BAUER	6/61		C2H3
65925065	56243065	230065&2	691322-3-499095&7	965150&2	500.	3000.1	0.C2H3
65925065	56243065	239033&2	331771-3-335425&7	965150&2	3000.	5000.1	0.C2H3

TABLE A-1 (continued)

4	1	2	6	0	0	0	0	0	0	0	0	0	0	0	0	0	0	OJANAF	12/60	C2H4
124960&5	676830&5	294887&2	526568-3-865313&7	101790&3	500.	3000.	1	0	0	0	0	0	0	0	0	0	0	O.C2H4	O.C2H4	
124960&5	676830&5	313872&2	616238-4-131858&8	101790&3	3000.	5000.	1	0	0	0	0	0	0	0	0	0	0	O.C2H4	O.C2H4	
4	1	2	6	1	8	0	0	0	0	0	0	0	0	0	0	0	0	OJANAF	12/60	C2H40
121900&5	813210&5	353747&2	546144-3-964936&7	117211&3	500.	3000.	1	0	0	0	0	0	0	0	0	0	0	O.C2H40	O.C2H40	
121900&5	813210&5	373112&2	690621-4-141968&8	117211&3	3000.	5000.	1	0	0	0	0	0	0	0	0	0	0	O.C2H40	O.C2H40	
6	1	2	6	0	0	0	0	0	0	0	0	0	0	0	0	0	0	ODUFF BAUER	6/61	C2H6
203200&5	892710&5	484236&2-169721-2-193680&8	119447&3	500.	3000.	1	0	0	0	0	0	0	0	0	0	0	0	O.C2H6	O.C2H6	
203200&5	892710&5	393119&2	764877-3-383891&7	119447&3	3000.	5000.	1	0	0	0	0	0	0	0	0	0	0	O.C2H6	O.C2H6	
2	6	2	7	0	0	0	0	0	0	0	0	0	0	0	0	0	0	OJANAF	3/61	C2N2
738699&5	511070&5	188740&2	559856-3-896873&6	985479&2	500.	3000.	1	0	0	0	0	0	0	0	0	0	0	O.C2N2	O.C2N2	
738699&5	511070&5	208204&2	630229-5-346865&7	985479&2	3000.	5000.	1	0	0	0	0	0	0	0	0	0	0	O.C2N2	O.C2N2	
3	6	0	0	0	0	0	0	0	0	0	0	0	0	0	0	0	0	OJANAF	12/60	C3
189670&6	366220&5	146441&2	622536-4-168227&7	798410&2	500.	3000.	1	0	0	0	0	0	0	0	0	0	0	O.C3	O.C3	
189670&6	366220&5	144782&2	792232-4-646877&6	798410&2	3000.	5000.	1	0	0	0	0	0	0	0	0	0	0	O.C3	O.C3	
1	1	3	6	0	0	0	0	0	0	0	0	0	0	0	0	0	0	ODUFF RAUER	6/61	C3H
127703&6	489620&5	194464&2	508379-3-311933&7	928820&2	500.	3000.	1	0	0	0	0	0	0	0	0	0	0	O.C3H	O.C3H	
127703&6	489620&5	199582&2	245687-3-632514&6	928820&2	3000.	5000.	1	0	0	0	0	0	0	0	0	0	0	O.C3H	O.C3H	
2	1	3	6	0	0	0	0	0	0	0	0	0	0	0	0	0	0	ODUFF BAUER	6/61	C3H2
106522&6	635170&5	247444&2	992918-3-437596&7	1046666&3	500.	3000.	1	0	0	0	0	0	0	0	0	0	0	O.C3H2	O.C3H2	
106522&6	635170&5	266623&2	364767-3-467730&7	1046666&3	3000.	5000.	1	0	0	0	0	0	0	0	0	0	0	O.C3H2	O.C3H2	
3	1	3	6	0	0	0	0	0	0	0	0	0	0	0	0	0	0	ODUFF BAUER	6/61	C3H3
764850&5	709520&5	286929&2	766031-3-548098&7	113604&3	500.	3000.	1	0	0	0	0	0	0	0	0	0	0	O.C3H3	O.C3H3	
764850&5	709520&5	291672&2	456238-3-138601&7	113604&3	3000.	5000.	1	0	0	0	0	0	0	0	0	0	0	O.C3H3	O.C3H3	
4	1	3	6	0	0	0	0	0	0	0	0	0	0	0	0	0	0	ODUFF BAUER	6/61	C3H4
442940&5	822470&5	372219&2-528861-4-101994&8	120293&3	500.	3000.	1	0	0	0	0	0	0	0	0	0	0	0	O.C3H4A	O.C3H4A	
442940&5	822470&5	344271&2	578173-3-208515&7	120293&3	3000.	5000.	1	0	0	0	0	0	0	0	0	0	0	O.C3H4A	O.C3H4A	
5	1	3	6	0	0	0	0	0	0	0	0	0	0	0	0	0	0	ODUFF BAUER	6/61	C3H5
324310&5	946210&5	397325&2	958555-3-904683&7	141759&3	500.	3000.	1	0	0	0	0	0	0	0	0	0	0	O.C3H5	O.C3H5	
324310&5	946210&5	395073&2	733720-3-949766&6	141759&3	3000.	5000.	1	0	0	0	0	0	0	0	0	0	0	O.C3H5	O.C3H5	
3	6	2	8	0	0	0	0	0	0	0	0	0	0	0	0	0	0	OJANAF	12/60	C3O2
830000&4	652120&5	263775&2	103904-3-350368&7	112723&3	500.	3000.	1	0	0	0	0	0	0	0	0	0	0	O.C3O2	O.C3O2	
830000&4	652120&5	263543&2	882201-4-287091&7	112723&3	3000.	5000.	1	0	0	0	0	0	0	0	0	0	0	O.C3O2	O.C3O2	
1	17	0	0	0	0	0	0	0	0	0	0	0	0	0	0	0	0	OJANAF	03/61	CL
289220&5	140280&5	508338&1-272037-4	290013&6	516230&1	500.	3000.	1	0	0	0	0	0	0	0	0	0	0	O.CL	O.CL	
289220&5	140280&5	539251&1-770696-4-114573&7	516230&2	3000.	5000.	1	0	0	0	0	0	0	0	0	0	0	0	O.CL	O.CL	
1	1	1	17	0	0	0	0	0	0	0	0	0	0	0	0	0	0	OJANAF	03/61	CLH
219700&5	218640&5	839693&1	214828-3-125475&7	623640&2	500.	3000.	1	0	0	0	0	0	0	0	0	0	0	O.CLH	O.CLH	
219700&5	218640&5	837177&1	193261-3-44600266	623640&2	3000.	5000.	1	0	0	0	0	0	0	0	0	0	0	O.CLH	O.CLH	
1	1	1	8	1	17	0	0	0	0	0	0	0	0	0	0	0	0	OJANAF	12/60	CLHO
220000&5	329450&5	130281&2	197747-3-200191&7	828260&2	500.	3000.	1	0	0	0	0	0	0	0	0	0	0	O.CLHO	O.CLHO	
220000&5	329450&5	143860&2-989737-4-621082&7	828260&2	3000.	5000.	1	0	0	0	0	0	0	0	0	0	0	0	O.CLHO	O.CLHO	
1	7	1	8	1	17	0	0	0	0	0	0	0	0	0	0	0	0	OJANAF	12/60	CLNO
126200&5	371090&5	138156&2	387830-3-101834&7	925450&2	500.	3000.	1	0	0	0	0	0	0	0	0	0	0	O.CLNO	O.CLNO	
126200&5	371090&5	146390&2	226016-3-405949&7	925450&2	3000.	5000.	1	0	0	0	0	0	0	0	0	0	0	O.CLNO	O.CLNO	
1	7	2	8	1	17	0	0	0	0	0	0	0	0	0	0	0	0	OJANAF	12/60	CLNO2
631000&4	499320&5	197869&2	190793-4-171145&7	105068&3	500.	3000.	1	0	0	0	0	0	0	0	0	0	0	O.CLNO2	O.CLNO2	
631000&4	499320&5	197732&2	214466-4-165191&7	105068&3	3000.	5000.	1	0	0	0	0	0	0	0	0	0	0	O.CLNO2	O.CLNO2	
1	8	1	17	0	0	0	0	0	0	0	0	0	0	0	0	0	0	OJANAF	12/60	CLO
241920&5	240570&5	889291&1	123702-3-171206&6	740940&2	500.	3000.	1	0	0	0	0	0	0	0	0	0	0	O.CLO	O.CLO	
241920&5	240570&5	810727&1	268314-3-299502&7	740940&2	3000.	5000.	1	0	0	0	0	0	0	0	0	0	0	O.CLO	O.CLO	
1	8	1	17	1	73	0	0	0	0	0	0	0	0	0	0	0	0	CAERONUT	12/63	CLOTA
269000&5	394449&5	148013&2	307113-4-247585&6	996810&2	500.	3000.	1	0	0	0	0	0	0	0	0	0	0	O.CLOTA	O.CLOTA	
269000&5	394449&5	149009&2	429203-6-326265&6	996810&2	3000.	5000.	1	0	0	0	0	0	0	0	0	0	0	O.CLOTA	O.CLOTA	
1	8	1	17	1	22	0	0	0	0	0	0	0	0	0	0	0	OJANAF	09/63	CLOTI	
583999&5	393229&5	148081&2	287419-4-291237&6	957819&2	500.	3000.	1	0	0	0	0	0	0	0	0	0	0	O.CLOTI	O.CLOTI	

TABLE A-1 (continued)

58399965	39322965	149075&2-497840-6-396537&6	957819&2	3000.	5000.1	0.CLO2T
2 8 1 17 0 0 0	0 0 0 0 0 0	OJANAF 12/60				CLO2
25000065	36578065	13849162 190480-3-689759&6	911340&2	500.	3000.1	0.CLO2
25000065	36578065	13178862 311873-3 206608&7	911340&2	3000.	5000.1	0.CLO2
2 8 1 17 1 73 0	0 0 0 0 0 0	0AERONUT 12/63				CLO2TA
11790066	51008965	19006462 131954-3-308599&6	112019&3	500.	3000.1	0.CLO2TA
11790066	51008965	19004862 132242-3-302450&6	112019&3	3000.	5000.1	0.CLO2TA
1 17 1 73 0 0 0	0 0 0 0 0 0	0AERONUT 12/63				CLTA
10999966	24049965	89406161 481168-6-365113&5	807199&2	500.	3000.1	0.CLTA
10999966	24049965	89406861 373406-6-342073&5	807199&2	3000.	5000.1	0.CLTA
1 17 1 22 0 0 0	0 0 0 0 0 0	OJANAF 03/64		111		CLTI
11120065	24969065	89434061 213417-3-509498&5	803570&2	1000.	3000.1	0.CLTI 1
11120066	24969065	89431261 213789-3-584666&5	803570&2	3000.	5000.1	0.CLTI 1
1 17 1 40 0 0 0	0 0 0 0 0 0	OJANAF 09/64				CLZR
13820066	24847965	89395961 182985-3-409359&5	823209&2	500.	3000.1	0.CLZR
13820066	24847965	89487161 181211-3-751669&5	823209&2	3000.	5000.1	0.CLZR
2 17 0 0 0 0 0	0 0 0 0 0 0	OJANAF 03/61				CL2
000000-0	24429065	85223461 273227-3 287718&6	737600&2	500.	3000.1	0.CL2
000000-0	24429065	10032962-141907-4-554731&7	737600&2	3000.	5000.1	0.CL2
1 8 2 17 0 0 0	0 0 0 0 0 0	OJANAF 12/60				CL20
18100365	36360065	13865062 123715-4-433229&6	937110&2	500.	3000.1	0.CL20
18100365	36360065	13757462 285555-4 982909&5	937110&2	3000.	5000.1	0.CL20
1 8 2 17 1 73 0	0 0 0 0 0 0	0AERONUT 12/63				CL20TA
10380066	47891965	17640062 182442-3-192326&6	114148&3	500.	3000.1	0.CL20TA
10380066	47891965	17639462 182657-3-193076&6	114148&3	3000.	5000.1	0.CL20TA
1 8 2 17 1 22 0	0 0 0 0 0 0	OJANAF 09/63				CL20TI
13040066	52740965	19789162 249143-4-295992&6	120934&3	500.	3000.1	0.CL20TI
13040066	52740965	19867262 941633-6-351944&6	120934&3	3000.	5000.1	0.CL20TI
2 8 2 17 1 74 0	0 0 0 0 0 0	OJANAF 09/62				CL202W
17669966	66621965	25305362 156514-3-899219&6	129988&3	500.	3000.1	0.CL202W
17669966	66621965	25825362 144163-5-139247&7	129988&3	3000.	5000.1	0.CL202W
2 17 1 73 0 0 0	0 0 0 0 0 0	0AERONUT 12/63				CL2TA
33000065	40020965	14898362 186835-5-807838&5	104064&3	500.	3000.1	0.CL2TA
33000065	40020965	14898962 885973-6-598835&5	104064&3	3000.	5000.1	0.CL2TA
2 17 1 22 0 0 0	0 0 0 0 0 0	OJANAF 03/64		111		CL2TI
72300065	39929065	14904562-165309-6-117562&6	101672&3	1000.	3000.1	0.CL2TI 1
72300065	39929065	14909462-837104-6-143133&6	101672&3	3000.	5000.1	0.CL2TI 1
2 17 1 74 0 0 0	0 0 0 0 0 0	OJANAF 09/62				CL2W
41999965	37377965	13906862 121848-5-679906&5	106269&3	500.	3000.1	0.CL2W
41999965	37377965	13906462 699149-6-494906&5	106269&3	3000.	5000.1	0.CL2W
2 17 1 40 0 0 0	0 0 0 0 0 0	OJANAF 06/62				CL2ZR
78000065	37413065	13908462 616176-6-565136&5	105306&3	500.	3000.1	0.CL2ZR
78000065	37413065	13916062-927493-6-836992&5	105306&3	3000.	5000.1	0.CL2ZR
1 8 3 17 1 73 0	0 0 0 0 0 0	0AERONUT 12/63				CL30TA
18720066	60274965	22740362 955899-4-604370&6	136504&3	500.	3000.1	0.CL30TA
18720066	60274965	22299962 220000-3 290216&1	136504&3	3000.	5000.1	0.CL30TA
3 17 1 73 0 0 0	0 0 0 0 0 0	0AERONUT 12/63				CL3TA
43999965	53321965	19865462 199767-5-121173&6	123674&3	500.	3000.1	0.CL3TA
43999965	53321965	19873462-228699-6-133198&6	123674&3	3000.	5000.1	0.CL3TA
3 17 1 22 0 0 0	0 0 0 0 0 0	OJANAF 03/64		111		CL3TI
12930066	52761065	19867862 118482-5-327898&6	120469&3	1000.	3000.1	0.CL3TI 1
12930066	52761065	19870362 381686-6-328488&6	120469&3	3000.	5000.1	0.CL3TI 1
3 17 1 40 0 0 0	0 0 0 0 0 0	OJANAF 06/64				CL3ZR
14400066	53227965	19862162 323901-5-152085&6	125542&3	500.	3000.1	0.CL3ZR
14400066	53227965	19871662 145442-6-153972&6	125542&3	3000.	5000.1	0.CL3ZR
1 8 4 17 1 74 0	0 0 0 0 0 0	OJANAF 09/62				CL40W

TABLE A-1 (continued)

15919986	82825985	31401982	116882-3-91400386	15351883	500.	3000.1	O.CL4OW
15919986	82825985	31785982	166981-5-12592887	15351883	3000.	5000.1	O.CL4OW
4 17 1	74 0	C 0	0 0 0 0 0 0	OJANAF 09/62		CL4W	
81999985	68376085	25775482	175999-4-46080386	13943783	500.	3000.1	O.CL4W
81999985	68376085	25829382	900417-6-49552086	13943783	3000.	5000.1	O.CL4W
4 17 1	73 0	0 0 0 0 0 0	OAERONUT 12/63		CL4TA		
13599986	69103985	25799882	118271-6-19996386	15045283	500.	3000.1	O.CL4TA
13599986	69103985	25796882	470731-6-18268286	15045283	3000.	5000.1	O.CL4TA
4 17 1	22 0	0 0 0 0 0 0	OJANAF 03/64	111	CL4TI		
18241086	68866085	25830182	104658-5-32701186	14216183	1000.	3000.1	O.CL4TI 1
18241086	68866085	25833082	192447-6-32959786	14216183	3000.	5000.1	O.CL4TI 1
4 17 1	40 0	0 0 0 0 0 0	OJANAF 12/63		CL4ZR		
20703086	69130085	25875082-109792-4-30730086	14670683	500.	3000.1	O.CL4ZR	
20703086	69130085	25676282	298633-4 37977886	14670683	3000.	5000.1	O.CL4ZR
5 17 1	73 0	0 0 0 0 0 0	CAFRONU 12/63		CL5TA		
18299986	84260985	31599782	116090-6-36994586	17089683	500.	3000.1	O.CL5TA
18299986	84260985	31603982-684834-6-38614986	17089683	3000.	5000.1	O.CL5TA	
5 17 1	74 0	0 0 0 0 0 0	OJANAF 12/62		CL5W		
11849986	84898985	31680182	572370-4-35833886	17470583	500.	3000.1	O.CL5W
11849986	84898985	31859682-311503-6-42035886	17470583	3000.	5000.1	O.CL5W	
6 17 1	74 0	0 0 0 0 0 0	OJANAF 12/62		CL6W		
14200086	10082686	37726882	945283-5-38858886	18334183	500.	3000.1	O.CL6W
14200086	10082686	37759682-311649-6-42035286	18334183	3000.	5000.1	O.CL6W	
1 9 0	0 0 0 0 0 0	OJANAF 06/61		F			
18860085	13683085	48903081	256070-4 21541386	49791082	500.	3000.1	O.F
18860085	13683085	58397181-157585-3-36587687	49791082	3000.	5000.1	O.F	
1 1 1	9 0 0 0 0 0	OJANAF 12/63		FH			
64800085	21054085	77554681	348201-3-12246087	58697082	500.	3000.1	O.FH
64800085	21054085	88898181	799284-4-41903887	58697082	3000.	5000.1	O.FH
1 1 1	8 1 9 0 0 0 0 0 0	OJANAF 12/60		FHO			
26100085	32668085	12735682	288514-3-18050187	79942082	500.	3000.1	O.FHO
26100085	32668085	15410082-262264-3-11881488	79942082	3000.	5000.1	O.FHO	
1 3 1	9 0 0 0 0 0 0 0 0	OJANAF 12/63		FLI			
79499985	24120985	88469581	165100-3-19130786	67782982	500.	3000.1	O.FLI
79499985	24120985	89364781	137543-3-25295886	67782982	3000.	5000.1	O.FLI
1 3 1	8 1 9 0 0 0 0 0 0	OJANAF 09/65		FLIC			
21999985	36131985	13731382	534540-4-43833086	88447082	500.	3000.1	O.FLIC
21999985	36131985	13917482-114126-5-63910786	88447082	3000.	5000.1	O.FLIO	
1 7 1	9 0 0 0 0 0 0 0 0	OJANAF 12/60		FN			
58600085	23438085	90009881-168131-4-40090886	68351082	500.	3000.1	O.FN	
58600085	23438085	82258481	144314-3 22248687	68351082	3000.	5000.1	O.FN
1 7 1	8 1 9 0 0 0 0 0 0	OJANAF 06/61		FNO			
15700085	35180085	13756382	383019-4-10555787	87811082	500.	3000.1	O.FNO
15700085	35180085	12974282	179442-3 21727687	87811082	3000.	5000.1	O.FNO
1 7 2	8 1 9 0 0 0 0 0 0	OJANAF 12/62		FNO2			
19000085	49474085	19706582	401052-4-18351087	10153283	500.	3000.1	O.FNO2
19000085	49474085	18912382	183090-3 14525987	10153283	3000.	5000.1	O.FNO2
1 8 1	9 0 0 0 0 0 0 0 0	OJANAF 12/60		FO			
32400085	23438085	88084981	432306-4-15731586	70193082	500.	3000.1	O.FO
32400085	23438085	76312981	227095-3 58512287	70193082	3000.	5000.1	O.FO
1 8 1	9 1 73 0 0 0 0 0 0	CAERONUT 12/63		FOTA			
76300085	39246085	14789482	340405-4-31102586	96065982	500.	3000.1	O.FOTA
76300085	39246085	14912682-147296-5-46131286	96065982	3000.	5000.1	O.FOTA	
1 8 1	9 1 22 0 0 0 0 0 0	OJANAF 09/63		FOTI			
10349986	39011985	14771982	396376-4-38603186	92153982	500.	3000.1	O.FOTI
10349986	39011985	14899782	713489-6-48512986	92153982	3000.	5000.1	O.FOTI

TABLE A-1 (continued)

TABLE A-1 (continued)

TABLE A-1 (continued)

21300066	69183965	25818262	469797-5-20098266	1-955062	500.	3000.1	0.HAFCL4
21300066	69183965	25829462	657340-6-19308066	14955063	3000.	5000.1	0.HAFCL4
1 9 1	72 0 0	0 0 0 0 0 0 0	0 OAERONUT	U-2045	3/63		HAFF
21000065	23804065	89907161-135220-4-20834966	79328062	500.	3000.1	0.HAFF	
21000065	23804065	99181861-187198-3-38662867	79328062	3000.	5000.1	0.HAFF	
2 9 1	72 0 0	0 0 0 0 0 0 0	0 OAERONUT	U-2045	3/63		HAFF2
14300066	39528065	14882862	588453-5-24769466	98363062	500.	3000.1	0.HAFF2
14300066	39528065	14254352	123301-3 22389767	98363062	3000.	5000.1	0.HAFF2
3 9 1	72 0 0	0 0 0 0 0 0 0	0 OAERONUT	U-2045	3/63		HAFF3
28000066	52559065	19861162	297024-5-41435066	12091463	500.	3000.1	0.HAFF3
28000066	52559065	18635462	235933-3 43266867	12091463	3000.	5000.1	0.HAFF3
4 9 1	72 0 0	0 0 0 0 0 0 0	0 OAERONUT	U-2045	3/63		HAFF4
41000066	68342065	25924162-252420-4-68815066	13881063	500.	3000.1	0.HAFF4	
41000066	68342065	25888182-917862-5-79763166	13881063	3000.	5000.1	0.HAFF4	
1 9 1	17 1 72	0 0 0 0 0 0 0	0 OAERONUT	12/63			HAFCL0
59999965	39453965	14821362	211401-4-24972166	10124163	500.	3000.1	0.HAFCL0
59999965	39453965	14975662-110914-4-76865366	10124163	3000.	5000.1	0.HAFCL0	
1 9 2	17 1 72	0 0 0 0 0 0 0	0 OAERONUT	12/63			HAFCL20
14899966	52660965	19775762	286141-4-31177766	12342363	500.	3000.1	0.HAFCL20
14899966	52680965	19873262-172343-6-41182766	12342363	3000.	5000.1	0.HAFCL20	
1 9 1	9 1 72	0 0 0 0 0 0 0	0 OAERONUT	U-2045	3/63		HAFOF
10900066	39225065	14893062	288115-5-40196066	98403052	500.	3000.1	0.HAFOF
10900066	39228065	14406262	959603-4 14658967	98403052	3000.	5000.1	0.HAFOF
1 9 2	9 1 72	0 0 0 0 0 0 0	0 OAERONUT	U-2045	3/63		HAFOF2
24800066	52184065	19905762-950324-5-64131666	11753863	500.	3000.1	0.HAFOF2	
24800066	52194065	20406867-998477-4-27114667	11753863	3000.	5000.1	0.HAFOF2	
1 9 1	72 0 0	0 0 0 0 0 0 0	0 OAERONUT	U-2045	3/63		HAFO
30000065	23531065	89877861-129961-4-33114166	75955062	500.	3000.1	0.HAFO	
30000065	23531065	10342262-267763-3-56428767	75955062	3000.	5000.1	0.HAFO	
2 8 1	72 0 0	0 0 0 0 0 0 0	0 OAERONUT	U-2045	3/63		HAFO2
85000065	38882065	14918462-435346-5-59714666	92540062	500.	3000.1	0.HAFO2	
85000065	38882065	15588362-132986-3-31528267	92540062	3000.	5000.1	0.HAFO2	
1 1 0	0 0 0	0 0 0 0 0 0 0	0 OJANAF	12/60			H
52102065	13423065	48022361	555469-4 17309566	38862062	500.	3000.1	0.H
52102065	13423065	30875261	315025-3 92974467	38862062	3000.	5000.1	0.H
1 1 1	3 0 0	0 0 0 0 0 0 0	0 OJANAF	12/60			HLI
32099965	23913965	85837061	317570-3-28279866	60252062	500.	3000.1	0.HLI
32099965	23913965	89353481	212672-3-61529066	60252062	3000.	5000.1	0.HLI
1 1 1	3 1 8	0 0 0 0 0 0 0	0 OJANAF	03/66			HLIO
58799965	12547065	11352462	689304-3-53452166	77787962	500.	3000.1	0.HLIC
58799965	12547065	13772662	184203-4-42018567	77787962	3000.	5000.1	0.HLIC
1 1 1	7 0 0	0 0 0 0 0 0 0	0 OJANAF	12/60			MN
79200065	21766065	82313361	281555-3-12689667	60929062	500.	3000.1	0.MN
79200065	21766065	76545761	359853-3 16077867	60929062	3000.	5000.1	0.MN
1 1 1	7 1 8	0 0 0 0 0 0 0	0 OJANAF	12/60			MNC
23800065	32755065	13382062	122061-3-23240367	78385062	500.	3000.1	0.MNO
23800065	32755065	14152362-470424-4-46913567	78385062	3000.	5000.1	0.MNO	
1 1 1	7 2 8	0 0 0 0 0 0 0	0 OJANAF	06/63			MNO2
14340065	46880065	19027862	189744-3-30875267	96231062	500.	3000.1	0.MNO2
14340065	46880065	21028462-229017-3-97861867	96231062	3000.	5000.1	0.MNO2	
1 1 1	7 3 8	0 0 0 0 0 0 0	0 OJANAF	06/63			MNO3
32100065	60912065	25354862	608154-4-45053267	11085163	500.	3000.1	0.MNO3
32100065	60912065	26628362-145785-3-10265668	11085163	3000.	5000.1	0.MNO3	
1 1 1	8 0 0	0 0 0 0 0 0 0	0 OJANAF	12/60			HO
93300064	21404065	77319361	394386-3-97356166	61382062	500.	3000.1	0.HO
93300064	21404065	96514451-443528-4-69611567	61382062	3000.	5000.1	0.HO	

TABLE A-1 (continued)

1	1	2	8	0	0	0	0	0	0	0	0	0	0	0	0	0	0	OJANAF	03/64	111	H02	
50000064	32534065	12716162	292770-3-17227967	79979062	1000.	3000.	1	0	0	0	0	0	0	0	0	0	0	O.H02	1			
50000064	32534065	13802862	147088-4-39955167	79979062	3000.	5000.	1	0	0	0	0	0	0	0	0	0	0	O.H02	1			
1	1	1	40	0	0	0	0	0	0	0	0	0	0	0	0	0	0	OJANAF	06/63		HZR	
12339966	23644965	85864461	254949-3-28166266	70906062	500.	3000.	1	0	0	0	0	0	0	0	0	0	0	O.HZR				
12339966	23644965	89378461	150671-3-62871266	70906062	3000.	5000.	1	0	0	0	0	0	0	0	0	0	0	O.HZR				
2	1	0	0	0	0	0	0	0	0	0	0	0	0	0	0	0	0	OJANAF	03/61		H2	
000000-0	21210065	71196361	621950-3-71269466	48465062	500.	3000.	1	0	0	0	0	0	0	0	0	0	0	O.H2				
000000-0	21210065	68179461	589854-3-26510667	48465062	3000.	5000.	1	0	0	0	0	0	0	0	0	0	0	O.H2				
2	1	2	3	2	8	0	0	0	0	0	0	0	0	0	0	0	0	OJANAF	12/60		H2L1202	
16939966	72584965	26164362	152064-2-19733167	11527363	500.	3000.	1	0	0	0	0	0	0	0	0	0	0	O.H2L1202				
16939966	72584965	31500862	392659-4-10004568	11527363	3000.	5000.	1	0	0	0	0	0	0	0	0	0	0	O.H2L1202				
2	1	1	7	0	0	0	0	0	0	0	0	0	0	0	0	0	0	OJANAF	12/65		H2N	
40099965	30579965	97586261	114401-2-51897066	70158062	500.	3000.	1	0	0	0	0	0	0	0	0	0	0	O.H2N				
40099965	30579965	13741962	229493-4-61002467	70158062	3000.	5000.	1	0	0	0	0	0	0	0	0	0	0	O.H2N				
2	1	1	8	0	0	0	0	0	0	0	0	0	0	0	0	0	0	OJANAF	03/61		H2C	
57798065	30201065	11225462	811397-3-26080067	68421062	500.	3000.	1	0	0	0	0	0	0	0	0	0	0	O.H2O				
57798065	30201065	15727862	191548-3-17359968	68421062	3000.	5000.	1	0	0	0	0	0	0	0	0	0	0	O.H2O				
2	1	4	8	1	74	0	0	0	0	0	0	0	0	0	0	0	0	OJANAF	09/64		H20W	
21659066	94183965	34955662	805073-3-15465367	15978663	500.	3000.	1	0	0	0	0	0	0	0	0	0	0	O.H20W				
21659966	94183965	37709062	634563-5-47621567	15978663	3000.	5000.	1	0	0	0	0	0	0	0	0	0	0	O.H20W				
3	1	1	7	0	0	0	0	0	0	0	0	0	0	0	0	0	0	OJANAF	09/65		H3V	
10970065	41630965	12518662	219670-2-97853166	76908062	500.	3000.	1	0	0	0	0	0	0	0	0	0	0	O.H3N				
10970065	41630965	16632062	923148-3-36133767	76908062	3000.	5000.	1	0	0	0	0	0	0	0	0	0	0	O.H3N				
4	1	2	7	0	0	0	0	0	0	0	0	0	0	0	0	0	0	OJANAF	12/65		H4N2	
22789965	68535965	22985662	241933-2-19593167	10809963	500.	3000.	1	0	0	0	0	0	0	0	0	0	0	O.H4N2				
22789965	68535965	31431962	487945-4-13970568	10809963	3000.	5000.	1	0	0	0	0	0	0	0	0	0	0	O.H4N2				
1	3	0	0	0	0	0	0	0	0	0	0	0	0	0	0	0	0	OJANAF	06/62		LI	
38410065	13523965	47276361	158709-3-47137865	44651962	500.	3000.	1	0	0	0	0	0	0	0	0	0	0	O.LI				
38410065	13523965-809815-0	140477-2	16240368	44551962	3000.	5000.	1	0	0	0	0	0	0	0	0	0	0	O.LI				
1	3	1	7	0	0	0	0	0	0	0	0	0	0	0	0	0	0	OJANAF	12/60		LIN	
38999965	23166965	85092961	200208-3-29628566	69614962	500.	3000.	1	0	0	0	0	0	0	0	0	0	0	O.LIN				
38999965	23166965	89383261	744435-4-76190466	69614962	3000.	5000.	1	0	0	0	0	0	0	0	0	0	0	O.LIN				
1	3	1	8	0	0	0	0	0	0	0	0	0	0	0	0	0	0	OJANAF	03/64		LIO	
20099965	24307965	88963961	151565-3-14477166	70614962	500.	3000.	1	0	0	0	0	0	0	0	0	0	0	O.LIO				
20099765	24307965	89485661	136844-3-21689066	70614962	3000.	5000.	1	0	0	0	0	0	0	0	0	0	0	O.LIO				
2	3	0	0	0	0	0	0	0	0	0	0	0	0	0	0	0	0	OJANAF	03/64		LI2	
50400065	25480965	89395461	324634-3-40077355	68350062	500.	3000.	1	0	0	0	0	0	0	0	0	0	0	O.LI2				
50400065	25480965	89377261	324325-3-15283965	68350062	3000.	5000.	1	0	0	0	0	0	0	0	0	0	0	O.LI2				
2	3	1	8	0	0	0	0	0	0	0	0	0	0	0	0	0	0	OJANAF	03/64		LI20	
39900065	39011965	14731062	514971-4-37370666	87047962	500.	3000.	1	0	0	0	0	0	0	0	0	0	0	O.LI20				
39900065	39011965	14906362-2	213693-6-55540566	87047962	3000.	5000.	1	0	0	0	0	0	0	0	0	0	0	O.LI20				
2	3	2	8	0	0	0	0	0	0	0	0	0	0	0	0	0	0	OJANAF	03/64		LI202	
57999965	52942965	19849362	693308-5-24407566	10989063	500.	3000.	1	0	0	0	0	0	0	0	0	0	0	O.LI202				
57999965	52942965	19873162-130535-6	26823766	10989063	3000.	5000.	1	0	0	0	0	0	0	0	0	0	0	O.LI202				
1	7	0	0	0	0	0	0	0	0	0	0	0	0	0	0	0	0	OJANAF	03/61		N	
11296566	13437065	48694461	383516-4-95845065	48090062	500.	3000.	1	0	0	0	0	0	0	0	0	0	0	O.N				
11296566	13437065	42895761	240844-3-41727366	48090062	3000.	5000.	1	0	0	0	0	0	0	0	0	0	0	O.N				
1	7	1	8	0	0	0	0	0	0	0	0	0	0	0	0	0	0	OJANAF	06/63		NO	
21580065	22700065	87762361	899031-4-78965666	68849062	500.	3000.	1	0	0	0	0	0	0	0	0	0	0	O.NO				
21580065	22700065	91626061	657885-5-21251967	8849062	3000.	5000.	1	0	0	0	0	0	0	0	0	0	0	O.NO				
1	7	2	8	0	0	0	0	0	0	0	0	0	0	0	0	0	0	OJANAF	06/63		NO2	
80110064	34580065	13781962	315611-4-13376567	84889062	500.	3000.	1	0	0	0	0	0	0	0	0	0	0	O.NO2				
80110064	34580065	13015462	172586-3-17534067	84889062	3000.	5000.	1	0	0	0	0	0	0	0	0	0	0	O.NO2				
1	7	3	8	0	0	0	0	0	0	0	0	0	0	0	0	0	0	OJANAF	12/64		NO3	
17000065	49821965	19230162	191161-3-11212967	99897062	500.	3000.	1	0	0	0	0	0	0	0	0	0	0	O.NO3				

TABLE A-1 (continued)

17000065	498219&5	198709&2	577142-7-172913&7	998970&2	3000.	5000.1	0.N03
1 7 1 40	0 0 0 0	0 0 0 0	0 0 0 0	0JANAF	06/63		NZR
170499&6	239179&5	887078&1	944200-4-171363&6	756690&2	500.	3000.1	0.NZR
170499&6	239179&5	894116&1	730310-4-727280&6	756690&2	3000.	5000.1	0.NZR
2 7 0 0	0 0 0 0	0 0 0 0	0 0 0 0	0JANAF	03/61		N2
000000-0	221650&5	862699&1	116090-3-103715&7	637650&2	500.	3000.1	0.N2
000000-0	221650&5	984175&1-116232-3	612728&7	637650&2	3000.	5000.1	0.N2
2 7 1 8	0 0 0 0	0 0 0 0	0 0 0 0	0JANAF	12/60		N20
19500065	365450&5	144686&2	120489-3-153476&7	815900&2	500.	3000.1	0.N20
19500065	365450&5	123036&2	459018-3 942382&7	815900&2	3000.	5000.1	0.N20
2 7 3 8	0 0 0 0	0 0 0 0	0 0 0 0	0JANAF	12/64		N203
197999&5	617799&5	232121&2	477580-3-124103&7	1232176&3	500.	3000.1	0.N203
197999&5	617799&5	248304&2	102872-5-293892&7	1232176&3	3000.	5000.1	0.N203
2 7 4 8	0 0 0 0	0 0 0 0	0 0 0 0	0JANAF	9/64		N204
216999&4	785969&5	297734&2	594431-3-178833&7	134908&3	500.	3000.1	0.N204
216999&4	785969&5	317815&2	175630-5-385969&7	134908&3	3000.	5000.1	0.N204
2 7 5 8	0 0 0 0	0 0 0 0	0 0 0 0	0JANAF	12/64		N205
216999&4	915759&5	353051&2	147295-3-163350&7	1567196&3	500.	3000.1	0.N205
216999&4	915759&5	357365&2	624545-5-171267&7	1567196&3	3000.	5000.1	0.N205
1 8 0 0	0 0 0 0	0 0 0 0	0 0 0 0	0JANAF	06/62		0
595590&5	135220&5	497228&1	380768-5 154749&5	500960&2	500.	3000.1	0.0
595590&5	135220&5	657489&1-224268-3	891782&7	500960&2	3000.	5000.1	0.0
1 8 1 73	0 0 0 0	0 0 0 0	0 0 0 0	OSCHICK	12/63		OTA
519730&5	238109&5	880604&1	880117-4-144688&6	784739&2	500.	3000.1	0.OTA
519730&5	238109&5	788530&1	270582-3 321255&7	784739&2	3000.	5000.1	0.OTA
1 8 1 22	0 0 0 0	0 0 0 0	0 0 0 0	0JANAF	12/60		OTI
15100065	236840&5	894324&1	524336-4-319889&6	754390&2	500.	3000.1	0.OTI
15100065	236840&5	940250&1-354311-4	208089&7	754390&2	3000.	5000.1	0.OTI
1 8 1 74	0 0 0 0	0 0 0 0	0 0 0 0	0JANAF	3/63		OW
10500066	238640&5	900466&1	349295-4-310058&6	811400&2	500.	3000.1	0.OW
10500066	238640&5	997145&1-142914-3	420935&7	811400&2	3000.	5000.1	0.OW
1 8 1 40	0 0 0 0	0 0 0 0	0 0 0 0	0JANAF	06/61		OZR
21100065	215190&5	708186&1-324544-4	297703&6	741580&2	500.	3000.1	0.OZR
21100065	215190&5	696436&1-798961-6	538861&6	741580&2	3000.	5000.1	0.OZR
2 8 0 0	0 0 0 0	0 0 0 0	0 0 0 0	0JANAF	03/61		OZ
000000-0	234460&5	804370&1	510872-3-152718&6	679730&2	500.	3000.1	0.02
000000-0	234460&5	103071&2	290991-4-783079&7	679730&2	3000.	5000.1	0.02
2 8 1 73	0 0 0 0	0 0 0 0	0 0 0 0	OSCHICK	12/63		O2TA
467080&5	398859&5	140651&2	660868-3-429632&6	947319&2	500.	3000.1	0.02TA
467080&5	398859&5	177857&2-328414-3	720441&7	947319&2	3000.	5000.1	0.02TA
2 8 1 22	0 0 0 0	0 0 0 0	0 0 0 0	0JANAF	12/60		O2TI
79800065	385860&5	148550&2	129468-4-656075&6	880860&2	500.	3000.1	0.02TI
79800065	385860&5	138669&2	200463-3 317357&7	880860&2	3000.	5000.1	0.02TI
2 8 1 74	0 0 0 0	0 0 0 0	0 0 0 0	0JANAF	06/62		O2W
21000065	364020&5	138442&2	177526-4-364856&6	959960&2	500.	3000.1	0.02W
21000065	364020&5	130756&2	159997-3 271226&7	959960&2	3000.	5000.1	0.02W
2 8 1 40	0 0 0 0	0 0 0 0	0 0 0 0	0JANAF	06/61		O2ZR
82500065	387750&5	148912&2	309724-5-607547&6	903540&2	500.	3000.1	0.02ZR
82500065	387750&5	149990&2-192239-4	975347&6	903540&2	3000.	5000.1	0.02ZR
3 8 0 0	0 0 0 0	0 0 0 0	0 0 0 0	0JANAF	6/61		O3
34100065	360230&5	135311&2	238739-3-606511&6	960919&2	500.	3000.1	0.03
34100065	360230&5	139121&2	125613-3-980654&6	860919&2	3000.	5000.1	0.03
3 8 1 74	0 0 0 0	0 0 0 0	0 0 0 0	0JANAF	3/63		O3W
70000065	518660&5	1987236&2-425236-6	720531&6	111374&3	500.	3000.1	0.03W
70000065	518660&5	190447&2	158010-3 245041&7	111374&3	3000.	5000.1	0.03W
9 8 3 74	0 0 0 0	0 0 0 0	0 0 0 0	0JANAF	3/63		O9W3

TABLE A-1 (continued)

468510&6	178044&6	676402&2-219384-4-183063&7	278001&3	500.	3000.1	0.09W3	
468510&6	178044&6	672619&2	551037-4-506619&6	278001&3	3000.	5000.1	
12	8	4	74	0	0	OJANAF 3/63	
648740&6	2413/8&6	914477&2-117941-4-219886&7	360115&3	500.	3000.1	0.012W4	
648740&6	241378&6	914708&2-143699-4-233768&7	360115&3	3000.	5000.1	0.012W4	
1	73	0	0	0	0	OSCHICK 03/63	
186521&6	197669&5	633370&1	773443-3-396315&6	594170&2	500.	3000.1	
186521&6	197669&5	679089&1	599438-3	187114&6	594170&2	3000.	5000.1
1	22	0	0	0	0	OJANAF 12/60	
112490&6	156330&5	242864&1	157423-2	116689&7	558710&2	500.	3000.1
112490&6	156330&5	479336&1	106517-2-637108&2	558710&2	3000.	5000.1	
1	74	0	0	0	0	OJANAF 12/61	
201799&6	216540&5	512206&1	439362-3	683863&7	594080&2	500.	3000.1
201799&6	216540&5	108518&1	147027-2	153357&8	594080&2	3000.	5000.1
1	40	0	0	0	0	OJANAF 06/61	
145417&6	184270&5	606392&1	593613-3-861888&6	585830&2	500.	3000.1	
145417&6	184270&5	538554&1	770890-3	457018&6	585830&2	3000.	5000.1
4	6	0	0	0	0	OJANAF 12/60	
242321&6	511230&5	205903&2	623436-4-257703&7	986760&2	500.	3000.1	
242321&6	511230&5	210714&2-434895-4-404939&7	986760&2	3000.	5000.1		
1	1	4	6	0	0	OJUFF BAUER 6/61	
155196&6	645030&5	252172&2	574336-3-339547&7	113166&3	500.	3000.1	
155196&6	645030&5	249358&2	402513-3	377676&7	113166&3	3000.	5000.1
2	1	4	6	0	0	OJUFF BAUER 6/61	
111715&6	763230&5	298897&2	735927-3-430646&7	119311&3	500.	3000.1	
111715&6	763230&5	301707&2	456896-3	698124&6	119311&3	3000.	5000.1
3	1	4	6	0	0	OJUFF BAUER 6/61	
101975&6	851450&5	343217&2	855861-3-624935&7	1300726&3	500.	3000.1	
101975&6	851450&5	345194&2	564141-3-151557&6	1300726&3	3000.	5000.1	
4	1	4	6	0	0	OJUFF BAUER 6/61	
737050&5	971240&5	398132&2	961427-3-792442&7	139440&3	500.	3000.1	
737050&5	971240&5	395899&2	720956-3	577880&6	139440&3	3000.	5000.1
4	6	2	7	0	0	OJANAF 3/61	
127500&6	801239&5	297490&2	856052-3-152255&7	133063&3	500.	3000.1	
127500&6	801239&5	327212&2	952999-5-541654&7	133063&3	3000.	5000.1	
6	1	6	6	0	0	OJUFF BAUER 6/61	
197700&5	147317&6	626122&2	117808-2-139277&8	172317&3	500.	3000.1	
197700&5	147317&6	595572&2	140760-2	737034&7	172317&3	3000.	5000.1
1	13	0	0	0	0	OJANAF 03/61	
240000&4	189130&5	696390&1	125221-4	347759&5	251963&2	500.	3000.3
240000&4	189130&5	744466&1-758263-4-210774&7	251963&2	3000.	5000.3	10. AL*	
1	8	1	13	1	17	OJANAF 03/64	
189599&6	520567&5	190512&2	572817-3-702975&6	550490&2	500.	1500.2	
189599&6	514899&5	205116&2-165920-3-149571&7	548210&2	1500.	3000.2		
1	13	3	17	0	0	OJANAF 03/64	
168579&6	101100&6	185370&2	114499-1-169000-1	100183&3	300.	460.2	
160559&6	720036&5	274254&2-331897-3-164863&6	104630&3	460.	3000.3		
1	7	1	13	0	0	OJANAF 12/62	
760000&5	312665&5	122768&2-178828-4-673685&6	299013&2	500.	2790.2	100. ALN*	
760000&5	314405&5	408674&2-915846-4-230400&9	299601&2	2790.	5000.2	100. ALN*	
1	4	4	8	2	13	OJANAF 09/64	
544999&6	126706&6	349699&2	797503-2-109209&7	112014&3	500.	2000.2	
544999&6	126469&6	421930&2	570773-2-118459&8	111929&3	2000.	3000.2	
3	8	2	13	0	0	OJANAF 09/61	
400400&6	811817&5	319699&2	120451-4-217514&7	772577&2	500.	2318.2	
366770&6	759318&5	351153&2-192777-4-555942&6	893107&2	2318.	5000.3	100. AL203*	

TABLE A-1 (continued)

1	4	0	0	0	0	0	0	0	0	0	0	ANAF	09/61	BE*
000000-0	19302565	82812561-288958-5-173046&7	17059562	500.	1556.2	100.	BE*							
28810064	18270865	76954761-257476-5-213324&7	18426562	1556.	5000.3	100.	BE*							
1	4	2	17	0	0	0	0	0	0	0	0	OJANAF	06/65	BECL2*
11959966	62564565	16060562 445380-2-220604&6	65988362	300.	682.2	0.	BECL2*							
11739966	76315965	2901962 060 686422-2 804288&2	682.	2000.3	0.	BECL2*								
1	4	2	9	0	0	0	0	0	0	0	0	OJANAF	12/63	BEF2*
24195766	54621165	207446&2-139307-4 558937&6	583302&2	500.	2000.2	10.	BEF2*							
24195766	54861365	210844&2 256246-5-533447&6	584292&2	2000.	5000.2	10.	BEF2*							
1	4	1	8	0	0	0	0	0	0	0	0	OJANAF	09/63	BEO*
14310066	33703865	160771&2-434631-3-593740&7	291887&2	500.	2820.2	10.	BEO*							
12956266	35912265	153149&2 182960-3-190747&6	347723&2	2820.	5000.3	10.	BEO*							
1	4	4	8	1	74	0	0	0	0	0	0	OJANAF	06/63	BEO4W*
34289966	98283565	252843&2 695291-2-362685&6	102869&3	300.	1200.2	0.	BEO4W*							
34289966	93494765	325809&2 260825-2-336213&7	100859&3	1200.	2000.2	0.	BEO4W*							
2	4	1	6	0	0	0	0	0	0	0	0	OJANAF	03/62	BE2C*
22200065	51902865	229814&2-271974-5-635112&7	430672&2	500.	2401.2	100.	BE2C*							
65350064	52682665	195224&2 723914-5-483551&6	49990962	2401.	5000.3	100.	BE2C*							
3	4	2	7	0	0	0	0	0	0	0	0	OJANAF	03/63	BE3N2*
13780066	86364565	386258&2-227477-3-117238&8	776686&2	500.	2473.2	10.	BF3N2*							
11073566	91659865	288203&2-194536-3 779046&8	907280&2	2473.	5000.3	10.	BE3N2*							
1	1	1	5	2	8	0	0	0	0	0	0	OJANAF	12/64	BHO2*
19186966	84968365	943587&1 133656-1-323428&5	692658&2	300.	900.2	0.	BHO2*							
19186966	57318965	276870&2-207617-2-355870&7	568310&2	900.	1500.2	0.	BHO2*							
1	5	1	7	0	0	0	0	0	0	0	0	OJANAF	9/63	BN*
59510065	29189665	119161&2 239906-4-891069&6	257049&2	500.	2500.2	10.	BN*							
59510065	29073965	117157&2 257181-5-240029&6	256618&2	2500.	5000.2	10.	BN*							
1	5	1	22	0	0	0	0	0	0	0	0	OJANAF	06/65	BTI*
38299965	33268965	129194&2-176073-4-489089&6	352123&2	500.	2000.2	0.	BTI*							
38299965	33396965	121220&2 319999-3-403004-1	352605&2	2000.	4000.2	0.	BTI*							
1	5	1	74	0	0	0	0	0	0	0	0	CAERONUT	12/63	BW*
13499965	34417865	119128&2 672043-3-193521&6	354561&2	500.	3130.2	0.	BW*							
21499964	50062365	141139&2-189026-4-547590&6	404549&2	3130.	5000.3	0.	BW*							
4	1	2	5	4	8	0	0	0	0	0	0	OJANAF	03/66	B2H404*
33709966	19991166	287825&2 279798-1-837893&6	167294&3	300.	900.2	0.	B2H404*							
33709966	16434366	580007&2 572414-2-828021&7	151554&3	900.	1500.2	0.	B2H404*							
2	5	3	8	0	0	0	0	0	0	0	0	OJANAF	12/60	B203*
30097866	81153065	299659&2 700906-3-130981&7	828910&2	500.	3000.2	100.	B203*							
30097866	81153065	28886562 659184-3 884491&7	828910&2	3000.	5000.2	100.	B203*							
2	5	1	22	0	0	0	0	0	0	0	0	OJANAF	12/62	B2TI*
70000065	56096665	22647662 104772-2-711450&7	489143&2	500.	3193.2	100.	B2TI*							
60380065	58529265	26941562 126484-4 274920&6	526893&2	3193.	5000.3	100.	B2TI*							
2	5	1	73	0	0	0	0	0	0	0	0	OSCHICK	12/63	B2TA*
49999965	57336965	142119&2 449471-2-360061&6	535534&2	500.	3373.2	0.	B2TA*							
29999965	76776965	299999&2 148727-9 455735&1	593050&2	3373.	5000.3	0.	B2TA*							
2	5	1	40	0	0	0	0	0	0	0	0	OJANAF	03/63	B2Z*
71500065	52039865	218849&2 598057-3-804156&7	488198&2	500.	3323.2	1.	B2Z*							
60627065	54102465	250051&2 117452-4-472366&6	527046&2	3323.	5000.3	1.	B2Z*							
3	5	3	8	3	9	0	0	0	0	0	0	OJANAF	03/65	B3F303*
58649966	19079966	286473&2 258435-1-572281&6	18461563	300.	900.2	0.	B3F303*							
58649966	14274766	679396&2-414850-2-105348&8	163343&3	900.	1500.2	0.	B3F303*							
3	1	3	5	3	8	0	0	0	0	0	0	OJANAF	03/65	B3H303*
30169966	16724466	311184&2 194520-1-123978&7	157175&3	300.	1200.2	0.	B3H303*							
30169966	13971666	581678&2-647494-5-656656&7	145381&3	1200.	2000.2	0.	R3H303*							
1	6	0	0	0	0	0	0	0	0	0	0	OJANAF	03/61	C*
000000-0	14412065	58607561 953976-4-766621&6	121290&2	500.	3000.2	100.	C*							

TABLE A-1 (continued)

000000-0	14412065	485134&1	291605-3	30720267	12129062	3000.	5000.2	100.C*
4 5 1	6 0 0 0 0 0 0 0 0	OJANAF 12/65						CB4*
92999954	82959165	23056662	537468-2-10596167	68180162	500.	2743.2	0.CB4*	
18099965	79039065	32500062-160344-8-23791962	76763462	2743.	3500.3	0.CB4*		
1 6 1	73 0 0 0 0 0 0 0 0	OSCHICK 12/63						CTA*
34599965	39409065	10346762	271325-2-21034166	40158162	500.	4273.2	0.CTA*	
96000064	69752065	16000062-386322-9-18701162	47457362	4273.	5000.3	0.CTA*		
1 6 2	73 0 0 0 0 0 0 0 0	OSCHICK 12/63						CTA2*
47199955	57123265	15879662	333028-2-20495066	64018762	500.	2000.2	0.CTA2*	
47199965	57122765	15877462	333048-2-19776166	64018562	2000.	3500.2	0.CTA2*	
1 6 1	22 0 0 0 0 0 0 0 0	OJANAF 12/60						CTI*
43800065	34423065	13825862	127229-3-25026267	33290462	500.	3410.2	1.CTI*	
26866065	35183765	13176962-101042-4-24242367	38481862	3410.	5000.3	1.CTI*		
1 6 1	74 0 0 0 0 0 0 0 0	OSCHICK 06/63						CW*
83999964	41520665	12269662	206027-2-26795466	41902162	500.	1500.2	0.CW*	
83999964	41520365	12270462	205978-2-26796256	41901852	1500.	3000.2	0.CW*	
1 6 2	74 0 0 0 0 0 0 0 0	OSCHICK 06/63						CW2*
10999965	68513665	21460962	259918-2-34813666	74132362	500.	1500.2	0.CW2*	
10999965	68514765	21462062	259929-2-35100866	74132862	1500.	3000.2	0.CW2*	
1 6 1	40 0 0 0 0 0 0 0 0	OJANAF 03/62						CZR*
45000065	36010565	14908262	928757-4-32171567	37487762	500.	3765.2	100.CZR*	
24788065	36137765	15331762-712238-5-58771767	42878462	3765.	5000.3	100.CZR*		
2 3 1	6 3 8 0 0 0 0 0 0	OJANAF 03/66						CLI203*
29063966	20375466-13911061	449029-1	26636267	15165363	500.	993.2	0.CLI203*	
28163066	11471166	44319962	060 307862-1	12088563	993.	2000.3	0.CLI203*	
2 3 2	6 0 0 0 0 0 0 0 0	OJANAF 12/60						C2L12*
14199965	74449965	243628&2	241860-2-71307666	72819862	500.	1200.2	0.C2L12*	
14199965	74487465	24333762	244224-2-71200466	72836062	1200.	2000.2	0.C2L12*	
3 6 4	13 0 0 0 0 0 0 0 0	OJANAF 06/63						C3AL4*
48999965	11782466	41194362	249972-2-15950467	11487863	500.	1500.2	0.C3AL4*	
48999965	11664266	45435362	560830-3-45936767	11441063	1500.	3000.2	0.C3AL4*	
4 1 1	7 1 17 0 0 0 0 0 0	OJANAF 12/60						CLH4N*
75379965	87775965	23966762	525476-2-39231566	91048162	300.	1200.2	0.CLH4N*	
75379965	78968965	30000062-152997-9-247332-0	87232262	1200.	2000.2	0.CLH4N*		
4 1 1	7 4 8 1 17 0 0 0 0	OJANAF 12/62						CLH4N04*
70690065	27531466	14578762	523599-1	30244065	22415563	300.	900.2	0.CLH4N04*
70690065	23136466	62323262	200088-1-15058868	20522563	900.	1500.2	0.CLH4N04*	
2 8 2	17 1 74 0 0 0 0 0 0	OJANAF 12/62						CL202**
22999965	89457565	27418362	370121-2-37131766	11586463	500.	2000.2	0.CL202W*	
22999965	89492065	26794052	390918-2	46215966	11587763	2000.	3000.2	0.CL202W*
2 17 1	74 0 0 0 0 0 0 0 0	OJANAF 09/62						CL2W*
59999965	71429565	16841662	598042-2-26091466	84910062	500.	1200.2	0.CL2W*	
59999965	70892965	15128262	643102-2	14278267	84643662	1200.	2000.2	0.CL2W*
2 17 1	22 0 0 0 0 0 0 0 0	OJANAF 03/64						CL2TI*
12350066	63421165	16022162	451891-2-10773864	74497262	1000.	1500.2	10.CL2TI* 1	
12350066	63421165	16026562	451745-2-60451064	74497262	1500.	5000.2	10.CL2TI* 1	
2 17 1	40 0 0 0 0 0 0 0 0	OJANAF 06/62						CL2ZR*
13199966	65481965	17300062	419999-2-495100-1	78365962	500.	1000.2	0.CL2ZR*	
12799966	62143065	23000062	060-567740-1	82550062	1000.	3000.3	0.CL2ZR*	
3 17 1	73 0 0 0 0 0 0 0 0	OAEERONUT 12/63						CL3TA*
13050066	79005965	22999962	389998-2-16997166	99692352	500.	3000.2	0.CL3TA*	
13050066	79005965	22999162	390014-2-16739466	99692362	3000.	5000.2	0.CL3TA*	
3 17 1	22 0 0 0 0 0 0 0 0	OJANAF 03/64						CL3TI*
17240066	73154065	23358662	234506-2-19975166	93039162	1000.	1200.2	10.CL3TI* 1	
17240066	73403665	23017062	255718-2-74407865	93144562	1200.	5000.2	10.CL3TI* 1	
3 17 1	40 0 0 0 0 0 0 0 0	OJANAF 06/64						CL3ZR*

TABLE A-1 (continued)

205999&6	72024965	267063&2	293581-3-51644066	912102&2	500.	1200.2	0.CL3ZR*
205999&6	71434665	272430&2-107608-3-	596024&6	909566&2	1200.	2000.2	0.CL3ZR*
1 8 4	17 1 74	0 0 0	0 0 0	OJANAF	09/62		CL4OW*
177500&6	98471565	352914&2	929293-3-343552&6	13112963	500.	1200.2	0.CL4OW*
177500&6	98006665	362404&2	418369-3-827280&6	13093763	1200.	1500.2	0.CL4OW*
4 17 1	73 0 0	0 0 0	0 0 0	OAERONUT	12/63		CL4TA*
168799&6	85312965	318993&2	288162-6-289859&6	118034&3	500.	3000.2	0.CL4TA*
168799&6	85312965	31900162-828361-7-	287160&6	118034&3	3000.	5000.2	0.CL4TA*
4 17 1	74 0 0	0 0 0	0 0 0	OJANAF	09/62		CL4W*
120999&6	84019155	296394&2	101332-2-196512&6	119528&3	500.	1200.2	0.CL4W*
120999&6	83836765	299970&2	818320-3-374506&6	119453&3	1200.	1500.2	0.CL4W*
4 17 1	40 0 0	0 0 0	0 0 0	OJANAF	12/63		CL4ZR*
234700&6	75087365	219283&2-112411-3	155115&8	108878&3	500.	1500.2	10.CL4ZR*
234700&6	85521865	307042&2-120868-4	529248&7	113634&3	1500.	5000.2	10.CL4ZR*
5 17 1	74 0 0	0 0 0	0 0 0	OJANAF	12/62		CL5W*
136999&6	10265466	348099&2	204263-2-164312&6	155019&3	300.	503.2	0.CL5W*
132099&6	97806965	362000&2	060-141003-1	162827&3	503.	1500.3	0.CL5W*
6 17 1	74 0 0	0 0 0	0 0 0	OJANAF	12/62		CL6W*
163099&6	12267666	406378&2	225992-2-194696&6	166338&3	300.	557.2	0.CL6W*
157399&6	11457566	426000&2-183873-9-	575724-1	169291&3	557.	1500.3	0.CL6W*
1 3 1	9 0 0	0 0 0	0 0 0	OJANAF	12/63		FLI*
146499&6	46069565	10005962	434022-2-969818&5	427845&2	500.	1121.2	0.FLI*
140499&6	39862965	153400&2	060-303011-1	456860&2	1121.	3000.3	0.FLI*
2 9 1	72 C 0	0 0 0	0 0 0	OASSUMED SAME AS	F2ZR*		F2HAF*
220380&6	81055065	306608&2-210271-3-	798369&6	927673&2	500.	3000.3	100.F2HAF*
220380&6	81055065	266045&2	599714-3 154320&8	927673&2	3000.	5000.3	100.F2HAF*
2 9 1	40 0 0	0 0 0	0 0 0	OJANAF	06/61		F2ZR*
220380&6	81055065	306608&2-210271-3-	798369&6	927673&2	500.	3000.3	1.F2ZR*
220380&6	81055065	266045&2	599714-3 154320&8	927673&2	3000.	5000.3	1.F2ZR*
3 9 1	72 0 0	0 0 0	0 0 0	OASSUMED SAME AS	F3ZR*		F3HAF*
330000&6	97120665	429874&2	242608-4-136903&8	102064&3	500.	1601.2	100.F3HAF*
317884&6	86458165	319981&2	126208-5-241831&5	105028&3	1601.	5000.3	10.F3HAF*
3 9 1	22 0 0	0 0 0	0 0 0	OJANAF	06/64		F3TI*
337499&6	70376065	210999&2	300000-2 538249-2	813207&2	500.	1500.2	0.F3TI*
337499&6	70376065	210999&2	300000-2 898200-0	813207&2	1500.	2500.2	0.F3TI*
3 9 1	40 0 0	0 0 0	0 0 0	OJANAF	06/61		F3ZR*
330000&6	97120665	429874&2	242608-4-136903&8	102064&3	500.	1601.2	100.F3ZR*
317884&6	86458165	319981&2	126208-5-241831&5	105028&3	1601.	5000.3	100.F3ZR*
1 9 4	9 1 74	0 0 0	0 0 0	OJANAF	06/62		F4OW*
355999&6-11054866	668473&2-643885-1-	141487&7	848848&1	300.	383.2	0.F4OW*	
353999&6	97266965	360000&2	060-210350-2	123997&3	383.	2000.3	0.F4OW*
4 9 1	22 0 0	0 0 0	0 0 0	OJANAF	06/64		F4TI*
394189&6	82482065	294256&2	807356-3-204338&6	101008&3	300.	900.2	0.F4TI*
394189&6	840437&5	290416&2	141000-2-332655&6	101739&3	900.	1500.2	0.F4TI*
4 9 1	40 0 0	0 0 0	0 0 0	OJANAF	12/63		F4ZR*
45680066-67666166	-597645&3-992990-3	75874369-265363&3	500.	1200.2	10.F4ZR*		
45680066-75860265-134613&3	-213939-3	281649&9 236126&2	1200.	5000.2	10.F4ZR*		
6 9 1	74 0 0	0 0 0	0 0 0	OJANAF	12/63		F6W*
42700066-140109&7	-120974&4-196796-2150687610-	559815&3	500.	1200.2	10.F6W*		
42700066-275680&6-379896&3-119768-2	75862069-1386616&2	1200.	5000.2	10.F6W*			
6 9 1	74 0 0	0 0 0	0 0 0	OJANAF	12/63	111	F6W*
427000&6	113478&6	419996&2	223527-6 150363&3	157378&3	1000.	1200.3	10.F6W*
427000&6	113483&6	419852&2	738808-5 846970&4	157380&3	1200.	5000.3	10.F6W*
1 72 0	0 0 0	0 0 0	0 0 0	OAERONUT	12/63		MAF*
060 26236565	631467&1	169633-2-202552&3	305827&2	500.	2495.2	0.HAF*	
523900&4	299729&5	799999&1	060 967642-0	321365&2	2495.	5000.3	0.HAF*

TABLE A-1 (continued)

2	5	1	72	0	0	0	0	0	0	0	OAFRONUT	U-2045	3/63	111	HAFB2*
74200065	52360565	18886562	595324-3	20540366	51772362	1000.	3520.2	100.	HAFB2*	-					
74200065	78681165	21004662-753793-6	-25692755	59247162	3520.	5000.3	100.	HAFB2*	-						
1	6	1	72	0	0	0	0	0	0	0	CAERONUT	U-2045	3/63	111	HAFC*
44700065	34846265	15860262-236443-3	-47211067	37929662	1000.	4160.2	100.	HAFC*	-						
44700065	55675665	14604962	740357-6	33672465	42938562	4160.	5000.3	100.	HAFC*	-					
4	17	1	72	0	0	0	0	0	0	0	CAFRONUT	12/63			HAFCL4*
23687966	27492366-45418262	840852-1	85958767	20695663	500.	705.2	0.	HAFCL4*	-						
22637966	10826966	39433962-773536-3	-16736667	14025963	705.	5000.3	0.	HAFCL4*	-						
4	9	1	72	0	0	0	0	0	0	0	CAERONUT	U-2045	3/63	111	HAFF4*
46140066	10711866	22602362	103650-1-62533065	11148163	100C.	1201.2	100.	HAFF4*	-						
46140066	11044666	36200162-254286-7	-12600963	12030263	1201.	5000.3	100.	HAFF4*	-						
1	7	1	72	0	0	0	0	0	0	0	CAERONUT	U-2045	3/63	111	HAFN*
88240065	35356765	15175362-181568-3	-33015747	39199762	1000.	3580.2	100.	HAFN*	-						
88240065	53257165	14274662-753941-6	-25697215	44200262	3580.	5000.3	100.	HAFN*	-						
2	8	1	72	0	0	0	0	0	0	0	CAERONUT	U-2045	3/63	111	HAFO2*
26610066	54446165	22188162-960937-5	-3443.257	57731662	1000.	3170.2	100.	HAFO2*	-						
26610066	73445065	21800062	000-0	0	0	0	0	0	0	0	63725152	3170.	5000.3	100.	HAFO2*
1	1	1	3	0	0	0	0	0	0	0	JANAF	09/62			HLI*
21665965	44915665	10745462	404759-2-776	966	35803962	500.	960.2	0.	HLI*	-					
15096065	36178065	14000062	060-815415-2	39928567	960.	2000.3	0.	HLI*	-						
1	1	1	3	1	8	0	0	0	0	0	OJANAF	03/63			HLIO*
11583966	64018465	14024152	616787-2-47612866	56871462	500.	744.2	0.	HLIO*	-						
11326266	56035965	20739962	060	329082-1	59457262	744.	3500.3	0.	HLIO*	-					
2	1	4	8	1	72	0	0	0	0	0	OJANAF	06/63			H2O4W*
28020066	10547366	34932962	311318-2-99613666	11219063	500.	1500.2	0.	H2O4W*	-						
28020066	10660466	35758162	334075-2-36208367	11266663	150C.	3000.2	0.	H2O4W*	-						
2	1	1	22	0	0	0	0	0	0	0	OJANAF	06/63			H2T1*
34500065	47599865	15328662	217900-2-12865367	42229262	500.	1200.2	0.	H2T1*	-						
34500065	44631365	19325962-319517-3	-27252267	40975062	1200.	2000.2	0.	H2T1*	-						
1	3	0	0	0	0	0	0	0	0	0	OJANAF	09/62			LI*
38410065	36948265	45742361	554063-2-30638365	32301262	300.	454.2	0.	LI*	-						
56899963	18591465	67970061-122344-4	10227966	24261862	454.	4000.3	0.	LI*	-						
2	3	1	8	0	0	0	0	0	0	0	OJANAF	03/64			LI20*
14310066	61285365	18554162	304605-2-86532766	55833862	500.	1843.2	0.	LI20*	-						
13212866	62361965	23999962	060	170840-0	62632562	1843.	4000.3	0.	LI20*	-					
2	3	2	8	0	0	0	0	0	0	0	OJANAF	09/63			LI202*
15119966	97872165	17154962	117912-1-33762866	83097562	500.	1200.2	0.	LI202*	-						
15119966	96807565	19216262	106627-1-13558667	82658062	1200.	2000.2	0.	LI202*	-						
2	3	3	8	1	22	0	0	0	0	0	OJANAF	03/64			LI203TI*
39929966	11932766	25306862	106211-1	56708766	11219463	500.	1820.2	0.	LI203TI*	-					
37437366	11727266	48000062	060-714628-0	12548063	1820.	4000.3	0.	LI203TI*	-						
3	3	1	7	0	0	0	0	0	0	0	OJANAF	12/60			LI3N*
47499965	76972765	29372262	309452-3-13299467	70921662	500.	1200.2	0.	LI3N*	-						
47499965	75530165	28983162-411775-4	-16378866	70274162	1200.	2000.2	0.	LI3N*	-						
1	7	1	73	0	0	0	0	0	0	0	OSCHICK	12/63			NTA*
59949965	40023465	16647662-300756-3	-12006167	43885262	500.	3363.2	0.	NTA*	-						
43950065	56230965	15000062-413841-9	-12967662	48708262	3363.	5000.3	0.	NTA*	-						
1	7	2	73	0	0	0	0	0	0	0	OSCHICK	12/63			NTA2*
64599965	63801965	16845262	421918-2-16868466	71351362	503.	3000.2	0.	NTA2*	-						
42599965	85802065	22499962	060	060	78684662	3003.	5000.3	0.	NTA2*	-					
1	7	1	22	0	0	0	0	0	0	0	OJANAF	12/60			NTI*
80500065	35399265	13951662	224921-3-23736567	35557962	500.	3201.2	100.	NTI*	-						
65242065	36455065	13405862	130614-4	77674166	40652462	3201.	5000.3	100.	NTI*	-					
1	7	1	40	0	0	0	0	0	0	0	OJANAF	12/61			NZR*
87300065	36841265	14740362	405595-3-38523867	38459162	500.	3225.2	100.	NZR*	-						

TABLE A-1 (concluded)

69489065	35700765	13684562	315953-4	33058667	43637262	3225.	5000.3	100.NZR*
1 8 1	22 0 0	0 0 0	0 0 0	0 0 0	OJANAF 12/60			OTI*
12390066	43556165	18210662-534802-4-15425267	41725362	500.	2010.2	0.	0.TI*	
10868266	39172465	145141&2	267716-5-20683766	47425662	2010.	5000.3	0.OTI*	
2 8 1	22 0 0	0 0 0	0 0 0	0 0 0	OJANAF 12/60			O2TI*
22550066	48835165	19082162-102491-4-14327067	51939562	500.	2128.2	100.	02TI*	
21232066	51334965	19003562-412635-5	11775366	59296462	2128.	5000.3	100.02TI*	
2 8 1	74 0 0	0 0 0	0 0 0	0 0 0	OJANAF 06/62			O2*
14094066	54795665	23309462-361730-4-53814367	55109062	500.	2000.2	100.	02W*	
000000-0	56907865	28701862	186655-4-26708268	55937862	2000.	5000.3	100.02W*	
2 8 1	40 0 0	0 0 0	0 0 0	0 0 0	OJANAF 06/61			O2ZR*
26150066	48794665	18212762-777714-3	68916867	52442062	500.	2950.2	100.02ZR*	
24551866	54037065	19565862	831149-4	16793767	59607362	2950.	5000.3	100.02ZR*
3 8 2	22 0 0	0 0 0	0 0 0	0 0 0	OJANAF 12/60			O3TI2*
36290066	94632065	36450062-320380-5-15072267	96211562	500.	2401.2	100.	03TI2*	
33466166	97269665	35984862-104734-5	19648566	10908663	2401.	5000.3	100.03TI2*	
3 8 1	74 0 0	0 0 0	0 0 0	0 0 0	OJANAF 3/63			O3W*
20146066	65137765	24821562-220326-4-12017866	71410262	500.	1745.2	1.	03W*	
19780166	7134965	31498062	149772-5-33102765	85129462	1745.	5000.3	1.03W*	
5 8 2	7 0 0	0 0 0	0 0 0	0 0 0	OSCHICK 09/63			05TA2*
48869966	12740866	37000062	656002-2-59200666	13405163	500.	2150.2	0.05TA2*	
45257966	16539766	55999962	060 702685-0	15163663	2150.	5000.3	0.05TA2*	
5 8 3	22 0 0	0 0 0	0 0 0	0 0 0	OAFRONUT 12/63			05TI3*
58765066	15057166	41600062	799999-2-468140-2	15427953	500.	2173.2	0.05TI3*	
53764966	19867566	59999962	060-452594-1	17660663	2173.	5000.3	0.05TI3*	
1 73	0 0 0	0 0 0	0 0 0	0 0 0	OSCHICK 03/63			TA*
060	19812065	783589-0	360388-2	10127067	25822362	500.	3270.2	0.TA*
67000064	27506965	85000061	060-23447961	28188262	3270.	5000.3	0.TA*	
1 22	0 0 0	0 0 0	0 0 0	0 0 0	OJANAF 12/60			TI*
000000-0	19389965	47161261-708316-4	83947067	24062262	500.	1950.2	100.TI*	
38780064	21613065	80019661	165771-5-73231865	26955662	1950.	5000.3	100.TI*	
1 74	0 0 0	0 0 0	0 0 0	0 0 0	OJANAF 12/61			W*
000000-0	18954565	77575261	991652-4-21732267	23157062	500.	3650.2	100.W*	
72020064	19612765	87483861-706194-5	42105667	25288262	3650.	5000.3	100.W*	
1 40	0 0 0	0 0 0	0 0 0	0 0 0	OJANAF 06/61			ZR*
000000-0	20328765	57503561-102844-3	63945767	26663562	500.	2128.2	100.ZR*	
52690064	21981965	85120861-197639-5	29170055	29768062	2128.	5000.3	100.ZR*	

TABLE A-2

OUTPUT FROM TC DATA PROGRAM  
 (a)  $\text{BeF}_2$  Gas

1 CURVE FIT COMPARISON FOR $\text{BeF}_2$		DATA FROM JANAF 12/63		CP	$\text{BEF}_2$
TEMPERATURE	( $F-H/T$ ) IN	( $F-H/T$ ) OUT			
1.000000E+03	5.000000E+01	5.000000E+01	1.366284E+01	1.366284E+01	$\text{BEF}_2$
1.100000E+03	5.083200E+01	5.083200E+01	1.386649E+01	1.386649E+01	$\text{BEF}_2$
1.200000E+03	5.163100E+01	5.163100E+01	1.402208E+01	1.402208E+01	$\text{BEF}_2$
1.300000E+03	5.239700E+01	5.239700E+01	1.414380E+01	1.414380E+01	$\text{BEF}_2$
1.400000E+03	5.313100E+01	5.313100E+01	1.424099E+01	1.424099E+01	$\text{BEF}_2$
1.500000E+03	5.383500E+01	5.383500E+01	1.431995E+01	1.431995E+01	$\text{BEF}_2$
1.600000E+03	5.451100E+01	5.451100E+01	1.438510E+01	1.438510E+01	$\text{BEF}_2$
1.700000E+03	5.516000E+01	5.516000E+01	1.443960E+01	1.443960E+01	$\text{BEF}_2$
1.800000E+03	5.578400E+01	5.578400E+01	1.448573E+01	1.448573E+01	$\text{BEF}_2$
1.900000E+03	5.638500E+01	5.638500E+01	1.452522E+01	1.452522E+01	$\text{BEF}_2$
2.000000E+03	5.696440E+01	5.696440E+01	1.455936E+01	1.455936E+01	$\text{BEF}_2$
2.100000E+03	5.752300E+01	5.752300E+01	1.458914E+01	1.458914E+01	$\text{BEF}_2$
2.200000E+03	5.806200E+01	5.806200E+01	1.461534E+01	1.461534E+01	$\text{BEF}_2$
2.300000E+03	5.858400E+01	5.858400E+01	1.463857E+01	1.463857E+01	$\text{BEF}_2$
2.400000E+03	5.908800E+01	5.908800E+01	1.465931E+01	1.465931E+01	$\text{BEF}_2$
2.500000E+03	5.957700E+01	5.957700E+01	1.467795E+01	1.467795E+01	$\text{BEF}_2$
2.600000E+03	6.005000E+01	6.005053E+01	1.469482E+01	1.469482E+01	$\text{BEF}_2$
2.700000E+03	6.051000E+01	6.050996E+01	1.471015E+01	1.471015E+01	$\text{BEF}_2$
2.800000E+03	6.095600E+01	6.095604E+01	1.472418E+01	1.472418E+01	$\text{BEF}_2$
2.900000E+03	6.938900E+01	6.938950E+01	1.473708E+01	1.473708E+01	$\text{BEF}_2$
3.000000E+03	6.981100E+01	6.981100E+01	1.474899E+01	1.474899E+01	$\text{BEF}_2$
CONSTRAINTS					
TEMPERATURE	TYPE	INPUT	CALCULATED		
3.0000000E+03	CP	1.4749000E+01	1.4748999E+01		$\text{BEF}_2$
DHF .298 DH298-3K	ALPH1 ALPH2 ALPH3	S.3000	TLO THI P RHO		
-191300+6 374160+5	147905+2	289774-4-115672+7	822830+2	500. 3000.1	0.BEF2
TEMPERATURE	( $F-H/T$ ) IN	( $F-H/T$ ) OUT	CP		
3.000000E+03	6.981100E+01	6.981100E+01	1.474899E+01	1.474899E+01	$\text{BEF}_2$
3.100000E+03	7.022100E+01	7.022116E+01	1.475059E+01	1.475059E+01	$\text{BEF}_2$
3.200000E+03	7.062000E+01	7.062056E+01	1.475397E+01	1.475397E+01	$\text{BEF}_2$
3.300000E+03	7.100900E+01	7.100973E+01	1.475892E+01	1.475892E+01	$\text{BEF}_2$
3.400000E+03	7.138900E+01	7.138917E+01	1.476527E+01	1.476527E+01	$\text{BEF}_2$
3.500000E+03	7.175900E+01	7.175933E+01	1.477285E+01	1.477285E+01	$\text{BEF}_2$
3.600000E+03	7.212000E+01	7.212065E+01	1.478152E+01	1.478152E+01	$\text{BEF}_2$
3.700000E+03	7.247300E+01	7.247354E+01	1.479118E+01	1.479118E+01	$\text{BEF}_2$
3.800000E+03	7.281800E+01	7.281838E+01	1.480172E+01	1.480172E+01	$\text{BEF}_2$
3.900000E+03	7.313600E+01	7.315553E+01	1.481305E+01	1.481305E+01	$\text{BEF}_2$
4.000000E+03	7.348500E+01	7.348531E+01	1.482510E+01	1.482510E+01	$\text{BEF}_2$
4.100000E+03	7.380800E+01	7.380805E+01	1.483778E+01	1.483778E+01	$\text{BEF}_2$
4.200000E+03	7.412400E+01	7.412403E+01	1.485105E+01	1.485105E+01	$\text{BEF}_2$
4.300000E+03	7.443400E+01	7.443355E+01	1.486485E+01	1.486485E+01	$\text{BEF}_2$
4.400000E+03	7.473700E+01	7.473685E+01	1.487913E+01	1.487913E+01	$\text{BEF}_2$
4.500000E+03	7.503400E+01	7.503419E+01	1.489385E+01	1.489385E+01	$\text{BEF}_2$
4.600000E+03	7.532600E+01	7.532579E+01	1.490898E+01	1.490898E+01	$\text{BEF}_2$
4.700000E+03	7.561200E+01	7.561188E+01	1.492447E+01	1.492447E+01	$\text{BEF}_2$
4.800000E+03	7.589300E+01	7.589267E+01	1.494030E+01	1.494030E+01	$\text{BEF}_2$
4.900000E+03	7.616800E+01	7.616835E+01	1.495644E+01	1.495644E+01	$\text{BEF}_2$
5.000000E+03	7.643900E+01	7.643911E+01	1.497287E+01	1.497287E+01	$\text{BEF}_2$
CONSTRAINTS					
TEMPERATURE	TYPE	INPUT	CALCULATED		
3.0000000E+03	CP	1.4749000E+01	1.4748999E+01		$\text{BEF}_2$
DHF .298 DH298-3K	ALPH1 ALPH2 ALPH3	S.3000	TLO THI P RHO		
-191300+6 374160+5	138154+2	209328-3 274481+7	822830+2	3000. 5000.1	0.BEF2

TABLE A-2 (concluded)

(b) BeF<sub>2</sub> Consensed phase

1 CURVE FIT COMPARISON FOR BEF <sub>2</sub> *		DATA FROM JANAF 12/63		
TEMPERATURE	(F-H/T) IN	(F-H/T) OUT	CP	
1.000000E+03	2.250300E+01	2.250437E+01	2.128969E+01	BEF2*
1.100000E+03	2.376400E+01	2.376291E+01	2.119129E+01	BEF2*
1.200000E+03	2.497400E+01	2.497248E+01	2.111611E+01	BEF2*
1.300000E+03	2.613200E+01	2.613149E+01	2.105730E+01	BEF2*
1.400000E+03	2.724100E+01	2.724075E+01	2.101035E+01	BEF2*
1.500000E+03	2.830200E+01	2.830225E+01	2.097220E+01	BEF2*
1.600000E+03	2.931700E+01	2.931852E+01	2.094073E+01	BEF2*
1.700000E+03	3.029100E+01	3.029227E+01	2.091440E+01	BEF2*
1.800000E+03	3.122500E+01	3.122621E+01	2.089212E+01	BEF2*
1.900000E+03	3.212200E+01	3.212296E+01	2.087304E+01	BEF2*
2.000000E+03	3.298500E+01	3.298499E+01	2.085655E+01	BEF2*
<b>CONSTRAINTS</b>				
TEMPERATURE	TYPE	INPUT	CALCULATED	
2.0000000E+03	F	3.2985000E+01	3.2984997E+01	BEF2*
2.0000000E+03	H	3.3853000E+04	3.3853001E+04	BEF2*
DHF.298 DH298-3K	ALPH1 ALPH2 ALPH3	S.3000	TLO THI P RHO	
-241957+6 546211+5	207446+2-139307-4	558937+6	583302+2	500. 2000.2 10.BEF2*
TEMPERATURE	(F-H/T) IN	(F-H/T) OUT	CP	
2.000000E+03	3.298500E+01	3.298500E+01	2.095623E+01	BEF2*
2.100000E+03	3.381600E+01	3.381572E+01	2.096889E+01	BEF2*
2.200000E+03	3.461600E+01	3.461633E+01	2.097989E+01	BEF2*
2.300000E+03	3.538900E+01	3.538879E+01	2.098952E+01	BEF2*
2.400000E+03	3.613500E+01	3.613492E+01	2.099801E+01	BEF2*
2.500000E+03	3.685600E+01	3.685637E+01	2.100553E+01	BEF2*
2.600000E+03	3.755500E+01	3.755464E+01	2.101222E+01	BEF2*
2.700000E+03	3.823100E+01	3.823113E+01	2.101821E+01	BEF2*
2.800000E+03	3.888700E+01	3.888711E+01	2.102360E+01	BEF2*
2.900000E+03	3.952400E+01	3.952374E+01	2.102947E+01	BEF2*
3.0000000E+03	4.014200E+01	4.014211E+01	2.103289E+01	BEF2*
<b>CONSTRAINTS</b>				
TEMPERATURE	TYPE	INPUT	CALCULATED	
2.0000000E+03	F	3.2985000E+01	3.2985000E+01	BEF2*
2.0000000E+03	H	3.3853000E+04	3.3853000E+04	BEF2*
DHF.298 DH298-3K	ALPH1 ALPH2 ALPH3	S.3000	TLO THI P RHO	
-241957+6 548613+5	210844+2-256246-5-533447+6	584292+2	2000. 5000.2 10.BEF2*	

**APPENDIX B**

**AEROTHERM CHEMICAL EQUILIBRIUM COMPUTER PROGRAM**  
**(ACE)**

## APPENDIX B

### AEROTHERM CHEMICAL EQUILIBRIUM COMPUTER PROGRAM (ACE)

The ACE computer program is a general chemical equilibrium program with a wide variety of capability. Two of its features have been utilized in the present study. Specifically, the program option which determines the chemical equilibrium composition and thermodynamic properties of reacting gas mixtures was used in the isentropic flow calculations, and the program option which calculates equilibrium mass transfer quantities for ablative materials in chemically-reactive environments was used in obtaining the steady-state ablation solutions. Reference B-1 presents detailed information on the generalized mathematical treatment in the ACE program.

For the isentropic expansion calculations, the ACE program requires as input information the following items:

- (1) Specification of the elemental mass fractions for the chemical system being considered
- (2) Specification of the stagnation conditions for the system - pressure and either temperature or enthalpy
- (3) Thermodynamic data for each molecular species which is likely to be present in the system
- (4) An array of pressures to which the system is isentropically expanded from the stagnation condition.

For the surface equilibrium calculations the chemical system is more complex. This chemical system consists of both the boundary layer edge gas and the exposed surface material. The program considers surface thermochemical reactions under the constraint of chemical equilibrium, and for mass diffusion, considers unequal diffusion coefficients between the boundary layer and the surface. The surface removal mechanisms allowed by the program are surface chemical reactions, including surface material decomposition, phase change, and reactions with the boundary layer gas; and

liquid layer removal. Liquid layer removal is treated in terms of a fail temperature, the liquid being removed mechanically if it appears as a surface species above the specified fail temperature. The liquid layer removal model is general in that the possibility of the liquid phase surface species being different from the virgin material is considered. For calculations requiring the surface equilibrium option, the following input information is needed:

- (1) Specification of the boundary-layer-edge state - pressure and either temperature or enthalpy
- (2) Specification of the elemental mass fractions for the boundary-layer-edge gas and the ablation material
- (3) Thermodynamic data for each molecular species which is likely to be present in the overall system
- (4) Specification of an array of mass-transfer rates ( $\dot{B}$ ) for the chemical erosion and/or liquid layer removal of the surface material

Output information from the ACE program includes both listed and punched card data. The total output data includes system properties (viscosity, specific heat, diffusion coefficient, Prandtl number, Schmidt number, molecular weight, isentropic exponent), thermodynamic variables (temperature, enthalpy, entropy, pressure, density), the surface species mass removal rate (if multi-phase occurs), the virgin material total ablation rate, and the mole fractions of each molecular species present in the gas phase at the surface.

The general functional relation between input and output for the ACE program may be written as:

$$\begin{array}{ccc} \text{output} & & \text{input} \\ (z_{ie}, z_{iw}, h_w, h_{iw}, B', B_i, T_w) & = & F(\dot{B}, K_{ie}, K_{ia}, P) \end{array}$$

The functional relation represents a combined solution of the species conservation equations and chemical equilibrium relations which are employed for solving the surface energy balance equation discussed in Appendix C.

REFERENCES - APPENDIX B

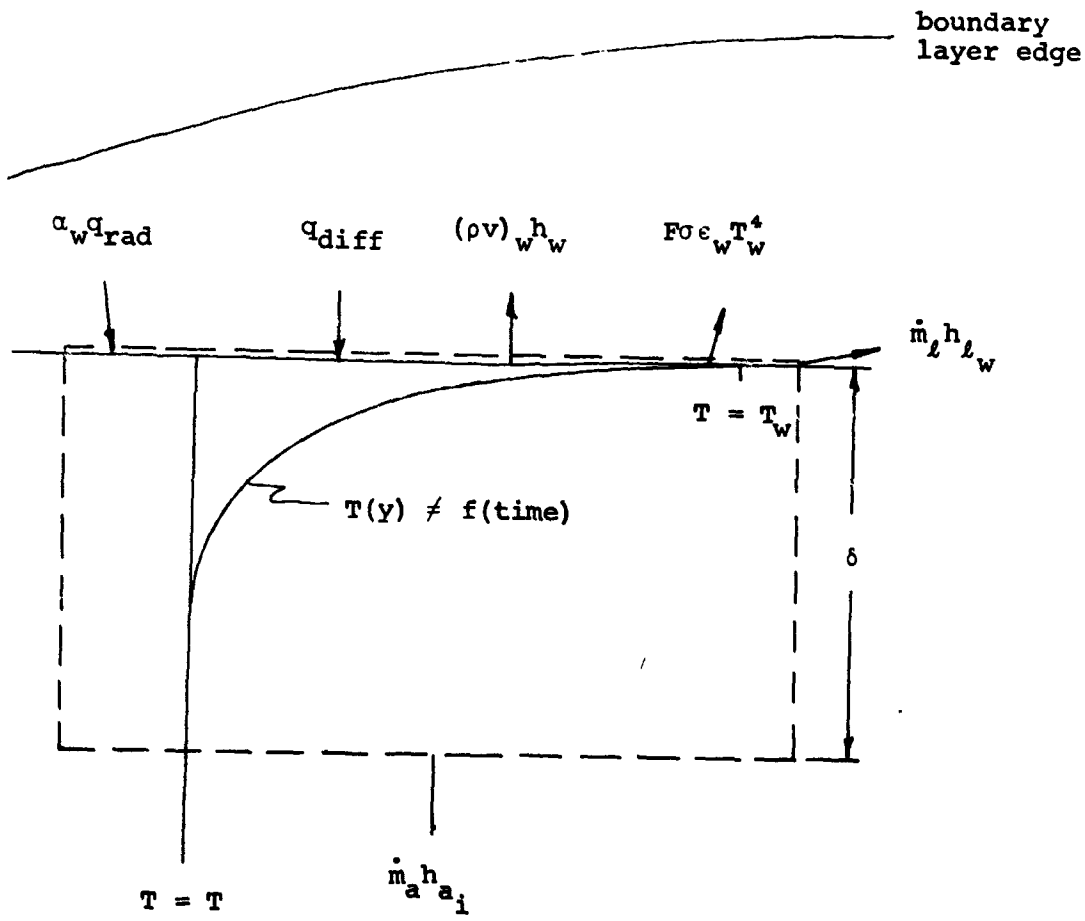
- B-1. Kendall, R.M.: A General Approach to the Thermochemical Solution of Mixed Equilibrium-Nonequilibrium, Homogeneous or Heterogenous Systems, Part V of Final Report, Contract NAS9-4599, Aerotherm Project No. 6002, March 14, 1967.

**APPENDIX C**

**STEADY STATE ABLATION ENERGY BALANCE**

APPENDIX C  
STEADY STATE ABLATION ENERGY BALANCE

The steady state energy balance equation employed in the present investigation results from performing an energy balance on a control volume which extends from the ablating surface into the material to a point where the material is at its initial temperature.



The control volume is of constant thickness ( $\delta$ ) and its position is fixed to the receding surface. As indicated in the sketch, the temperature distribution within the control volume is assumed invariant with time, so the net energy content within the control volume is constant. Since the energy change rate within the control volume is zero, an energy balance may be written which relates the energy flux terms shown in the sketch.

$$q_{\text{diff}} - (\rho v)_{w w}^h + \dot{m}_a h_{ai} - \dot{m}_l h_{lw} + \alpha_w q_{\text{rad}} - F\sigma\epsilon_w T_w^4 = 0 \quad (\text{C-1})$$

where

$q_{\text{diff}}$  represents energy to the surface as a result of thermal and chemical energy transfer through the boundary layer

$(\rho v)_{w w}^h$  represents energy transfer from the surface as a result of gas phase blowing or sucking (negative blowing) at the surface

$\dot{m}_a h_{ai}$  is the rate at which energy is transferred into the control volume by virtue of coordinate system motion associated with surface recession

$\dot{m}_l h_{lw}$  is the product of the liquid removal rate and the enthalpy of the removed liquid at the surface temperature

$\alpha_w q_{\text{rad}}$  represents the radiation energy flux absorbed by the surface

$F\sigma\epsilon_w T_w^4$  represents the radiant energy flux emitted by the surface.

The following sections describe the means employed for evaluating each of the above terms and indicate how the energy balance Equation (C-1) may be solved for the general case of arbitrary material and environment composition.

## SECTION C.1

ENERGY TRANSFER FROM THE BOUNDARY LAYER,  $q_{\text{diff}}$ 

A phenomenological model for representing energy transfer events in the multicomponent, chemically reacting boundary layer utilizing a film coefficient approach was introduced in Reference C-1. The terms appearing in the film coefficient representation of the boundary layer treatment are given further consideration in Reference C-2 where various terms are modified in such a manner that their physical meaning is more apparent and in such a manner that evaluation of the terms is more straightforward. The representation for the boundary layer energy transfer rate given in Reference C-2 is:

$$q_{\text{diff}} = \rho_e u_e C_H (H_r - H_w)_{\text{edge}} + \rho_e u_e C_M \sum_i (\tilde{z}_{i,e}^* - \tilde{z}_{i,w}^*) \Delta h_i^{T_w} \quad (\text{C-2})$$

where the first term represents energy transfer to the wall due to a "sensible" enthalpy potential and the second term represents the energy flux associated with mass diffusion and chemical reactions. The quantity,  $\rho_e u_e$ , is the boundary layer edge mass velocity, and  $C_H$  and  $C_M$  are the boundary layer Stanton numbers for heat and mass transfer respectively. For the present investigation the heat transfer coefficient is taken as  $0.5 \text{ lb}/\text{ft}^2\text{-sec}$  which is a reasonable nominal value for a 2.5-inch throat diameter and a 300 psia chamber pressure.\* This value represents the heat transfer coefficient in the absence of blowing. The blowing correction is described in the next subsection. The mass transfer coefficient ( $\rho_e u_e C_M$ ) is related to the heat transfer coefficient by the Chilton-Colburn analogy.

$$\frac{C_M}{C_H} = Le^{2/3}$$

---

\*This value was obtained by scaling results from Reference C-4 on the pressure to the 0.8 and inversely with diameter to the 0.2.

## C-4

Where the Lewis number is related to the Prandtl and Schmidt numbers

$$Le = \text{Pr}/\text{Sc}$$

Values of Pr and Sc for the six propellant systems were obtained from the ACE program as part of the output for the throat thermodynamic state calculation. The resulting values are summarized in Table C-1.

The enthalpy change in Equation (C-2),  $\Delta h_i^w$ , represents the heat of formation of gas phase molecular species  $i$  at the wall temperature (see e.g., Ref. C-3). The term  $\tilde{Z}_i^*$ , in the driving potential for mass transfer is dependent upon the gas mixture composition. Physically, it is intermediate between a mass fraction and a mole fraction for species  $i$ , and as such, it gives a more realistic weighting to higher diffusion rates of lighter species associated with their higher diffusion coefficients. An extensive discussion of this potential, and the means for its evaluation is presented in Reference C-1.

### SECTION C.2

#### BLOWING

Gas phase mass addition at the ablating surface has three effects on the net energy transfer rate to the surface: (1) the chemical composition is changed thereby modifying the driving potential for mass transfer ( $\tilde{Z}_{i_w}^* - \tilde{Z}_{i_e}^*$ ), (2) the heat transfer coefficient is reduced, and (3) energy is convected away from the surface by virtue of the mean mass motion  $(\rho v)_w$ .

The driving potential is appropriately modified since the ACE program evaluates the driving potential ( $\Delta \tilde{Z}_i^*$ ) based on the equilibrium chemical composition.

The reduction in heat transfer coefficient due to blowing is evaluated with the following correction equation for the turbulent boundary layer (Ref. C-5)

$$\frac{C_H}{C_{H_0}} = \frac{.8 \frac{(\rho v)_w}{\rho_e u_e C_{H_0}}}{\exp \left[ .8 \frac{(\rho v)_w}{\rho_e u_e C_{H_0}} \right] - 1} \quad (C-3)$$

where

$C_H$  - Stanton number with blowing

$C_{H_0}$  - Stanton number without blowing

$\rho_e u_e$  - boundary layer edge mass velocity

$(\rho v)_w$  - gas phase blowing rate normal to surface

Energy convected from the surface as a result of blowing is evaluated as the product of the blowing rate and the equilibrium enthalpy of the gas adjacent to the surface,  $(\rho v)_w h_w$ .

### SECTION C.3

#### CONVECTION OF CONDENSED PHASES

The two terms  $\dot{m}_a h_a$  and  $\dot{m}_l h_{lw}$  represent the energy convected into the control volume as a result of coordinate system motion, and energy leaving the surface in the form of liquid layer removal respectively. The quantity  $\dot{m}_a$ , is the insert material mass loss rate and  $h_a$  is the enthalpy of the insert material at the initial temperature. The quantity  $\dot{m}_l$  is the total mass removal rate of liquid material from the surface and  $h_{lw}$  is the total enthalpy of the removed liquid at the wall temperature.

**SECTION C.4**  
**RADIATION FLUXES**

The last two terms in the energy balance equation (C-1) represent radiation energy absorbed and emitted by the ablating surface respectively. If the propellant exhaust products are entirely gas phase species, radiation heat transfer interchange between the stream and the surface can be considered negligible compared to the energy transport involved in mass convection and chemical interaction between the wall and the boundary layer. However, some propellants contain condensed phase species in the exhaust products, and since radition from these particles can be appreciable an estimate of the radiant energy interchange between the wall and the particle-laden stream is included in the calculations.

The approach taken was to assume that the radiant energy flux from a particle cloud to the wall was given by

$$q_{\text{rad}} = \sigma \epsilon_p T_p^4$$

where  $\epsilon_p$  is the effective emittance of the particle cloud and  $T_p$  is the average temperature of the particles. Neglecting thermal lag effects, the temperature of the particles is equal to the static edge temperature. To estimate the effective emittance, the following equation from Reference (C-5) was used

$$\epsilon_p = 1 - (15/\pi^4)^{1/4}(Z + 1) \quad (\text{C-4})$$

where the quantity  $(15/\pi^4)^{1/4}(Z + 1)$ , termed the tetragamma function, is given as a function of Z in Reference C-5. Equation (C-4) gives the total particle-cloud emittance over all wavelengths, and assumptions leading to it are:

- (1) A representative size of  $2\mu$  for all particles
- (2) A uniform density distribution of the particles throughout the stream
- (3) A constant particle temperature throughout the stream.

With these assumptions the variable  $Z$  is defined as

$$Z = 0.57 \frac{VLT}{C_2} \quad (C-5)$$

where

$V$  = volume fraction of particles in the freestream

$L$  = effective thickness of particle cloud

$C_2$  = second Planck constant =  $8.49 \times 10^{-2}$  ft $^{-2}$ R

The volume fraction,  $V$ , was determined from the known two-phase freestream density, the known particle density, and the known mass fraction of particles in the stream resulting from the isentropic expansion calculations. The effective thickness  $L$  was taken to correspond to a nominal throat diameter of 2.5 inches. Table C-2 summarizes the calculations leading to the determination of the incident radiation term,  $q_{rad}$ .

To account for radiation from the wall to the particle-laden stream, an estimate of the wall hemispherical emittance was made. From References C-7, C-8, and C-9, it was found reasonable to assume an emittance equal to 0.9 for many refractory oxides and carbon-containing surfaces. Therefore,  $\epsilon_w = 0.9$  was assumed for all the energy balance calculations.

To evaluate the total radiation interchange between the throat and its surroundings, the following assumptions were made:

- (1) The entire nozzle wall is isothermal at the temperature  $T_w$ ; thus no net radiation interchange occurs between the unit area of interest at the throat and the remaining nozzle area.

- (2) Radiation from the throat surface to a zero temperature sink at the nozzle exit plane is negligible, since the view factor to this area is very small; this assumption is especially good for the propellant with particles, and, indeed, is mandatory because the nozzle configuration is not specified.
- (3)  $\epsilon_w = \alpha_w$ ,  $\epsilon_p = \alpha_p$ .

It follows that for the propellants containing particles, radiation heat transfer is described by

$$c_w q_{rad} - F\sigma \epsilon_w T_w^4 = \alpha_w \sigma \epsilon_p T_p^4 - \alpha_p \sigma \epsilon_w T_w^4 \quad (C-6)$$

and for the remaining propellants the radiation terms in Equation (C-1) are zero, since  $\epsilon_p = \alpha_p = 0$ .

## SECTION C.5

### ENERGY BALANCE SOLUTION

Previous sections of the Appendix identify the numerical treatment given each of the terms in the Surface energy balance equation (c-1). Substitution of the resulting expressions (Equations C-2, and C-6) into the energy balance in terms quantities readily available from the output of the ACE program, and in terms of known properties of the propellant-material combination.

$$\frac{C_H}{C_M} (H_r - H_w)_{gas, edge} + \sum_i (\tilde{z}_{ie}^* - \tilde{z}_{iw}^*) \Delta h_i^{Tw} - B' h_w \\ + \dot{B} h_{ai} - B_i h_{lw} + \frac{1}{\rho_e U_c M} \left( \alpha_w \sigma \epsilon_p T_p^4 - \alpha_p \sigma \epsilon_w T_w^4 \right) = 0 \quad (C-7)$$

The steady state energy balance is solved in two steps. The first step is performed with the ACE program (Appendix B) and requires the following input information:

1. Thermachemical data (Table A-1)
2. Boundary layer edge gas state properties and elemental composition (Tables III and IV respectively)
3. Insert material elemental composition.(Table II)
4. An array of total ablation rate parameters (usually  $0 < \dot{B} < 10$ )

With the above input information, the following output information is obtained on punched cards for each specified value of  $\dot{B}$ .

1. The surface temperature
2. The blowing rate  $B'$
3. The liquid layer removal rate,  $B_L$  (recall  $\dot{B} = B' + B_L$ )
4. The enthalpy of gases adjacent to the wall,  $h_w$
5. The enthalpy of liquid material removed at the wall temperature,  $h_{LW}$ .
6. The enthalpy of the edge gas at the wall temperature,  
 $h_w|_{\text{edge}}$ .
7. The mass transfer potential,  $\tilde{Z}_i^*$

In addition to this information the following information is also specified on punched cards for each material-propellant combination.

8. The heat transfer coefficient in the absence of blowing,  
 $\rho_e U_e C_H = 0.5 \text{ lb}/\text{ft}^2\text{-sec}$
9. The ratio of mass to heat transfer coefficients,  $C_M/C_H$ , from Table C-1
10. The incident radiation energy flux,  $q_{\text{rad}}$ , from Table C-2.
11. The surface emmittance  $\epsilon_w = \alpha_w = 0.9$

12. The boundary layer edge gas total enthalpy,  $H_e$ , from Table IV.
13. The enthalpy of the insert material at its initial temperature,  $H_{ai}$ , from Table II.
14. The insert material density,  $\rho_a$ , from Table II.

Solutions to the energy balance equation (C-7) are obtained with a small computer program, ESUM, which accepts the information, 1 through 7 above, for an array of  $\dot{B}$ , and the information, 8 through 13 above, for each material propellant combination. Output from the ESUM program consists simply of the energy imbalance for each value of  $\dot{B}$  considered. These results are machine plotted and the point at which the energy imbalance passes through zero is the solution. The value of  $\dot{B}$  and  $T_w$  at this point represent the steady state mass recession rate and is obtained within the ESUM program from the specified heat transfer coefficient, material density, ratio of heat-to-mass transfer coefficients, and the mass conservation equation.

$$\dot{S} = \dot{B} - (\rho_e u_e C_H) \frac{C_M}{C_H} \frac{1}{\rho_a} \quad (C-8)$$

## REFERENCES - APPENDIX C

- C-1 Kendall, R. M., Rindal, R. A., and Bartlett, E. P.: A Multi-component Boundary Layer Chemically Coupled to an Ablating Surface. AIAA Jour., Vol. 5, No. 6, June 1967.
- C-2 Moyer, C. B., and Rindal, R. A.: Finite Difference Solution for the In-Depth Response of Charring Materials Considering Surface Chemical and Energy Balances. Aerotherm Final Report 66-7, Part II, Contract NAS9-4599, March 14, 1967.
- C-3 JANAF Thermochemical Tables. The Dow Chemical Co., Midland, Michigan.
- C-4 Schaefer, J. W., Dahm, T. J., Rodriguez, D. R., Wool, M. R., and Clark, K. J.: Studies in Support of the NASA Large Solid Booster Program. First and Second Quarterly Progress Reports, Contract NAS7-534, Aerotherm Project 7012, July 20, 1967.
- C-5 Schaefer, J. W. and Dahm, T. J.: Studies of Nozzle Ablative Material Performance for Large Solid Boosters. NASA CR-72080, Aerotherm Rpoert No. 66-2, December 1966.
- C-6 Fontenot, John E.: Thermal Radiation from Solid Rocket Plumes at High Altitude. Technical Note, AIAA Journal, Vol. 3, No. 5, May 1965.
- C-7 Wilson, Gale R.: Hemispherical Spectral Emittance of Ablation Chars, Carbon, and Zirconia (to 3700°K). Presented at Symposium on Thermal Radiation of Solids, NASA SP-55 (Air Force ML-TDR-64-159), 1965.
- C-8 Comstock, Daniel F., Jr.: A Radiation Technique for Determining the Emittance of Refractory Oxides. Presented In Measurement of Thermal Radiation Properties of Solids, NASA SP-31, 1963.
- C-9 Moore, V. S., Stetson, A. R., Metcalfe, A. G.: Emittance Measurements of Refractory Oxide Coatings Up to 2900°K. Presented in Measurement of Thermal Radiation Properties of Solids, NASA SP-31, 1963.

TABLE C-1

MASS-TRANSFER TO HEAT-TRANSFER COEFFICIENT RATIO  
FROM THE CHILTON-COLBURN ANALOGY

No.	Propellant	Pr	Sc	$Le^{2/3}$
1	OF <sub>2</sub> -B <sub>2</sub> H <sub>6</sub>	0.43210	0.65192	0.746
2	Flox-Methane	0.40293	0.62544	0.746
3	Al-Solid	0.46035	0.68050	0.771
4	Be-Solid	0.43280	0.67914	0.741
5	Al-Hybrid	0.45486	0.64283	0.795
6	OF <sub>2</sub> -Li Hybrid	0.63803	0.70651	0.935

Note:  $\frac{C_M}{C_H} = Le^{2/3}$

TABLE C-2  
RADIANT ENERGY FLUX FROM PARTICLE-LADEN STREAM  
Part 1

Propellant	Particle	$T_p$ (°R)	$\rho_{\text{particles}}$ (lb/ft³)	$\rho_{\text{products}}$ (lb/ft³)	$K_p$	$V^*$ (ft³/ft³)
#3 Aluminum Solid	$\text{Al}_2\text{O}_3^*$	5,434	249.6	0.08005	0.2534	$8.13 \times 10^{-5}$
#4 Beryllium Solid	$\text{BeO}^*$	5,874	188.0	0.07200	0.2340	$8.96 \times 10^{-5}$
#5 Aluminum Hybrid	$\text{Al}_2\text{O}_3^*$	6,393	249.6	0.06980	0.2750	$7.69 \times 10^{-5}$

Part 2

Propellant	$Z^{****}$ ( - )	$\frac{15}{\pi^4} \downarrow'''(Z + 1)^{**}$ ( - )	$\epsilon_p$ ( - )	$q_{\text{rad}}^{***}$ (Btu/ft³ sec)
#3 Aluminum Solid	0.6175	0.170	0.830	345
#4 Beryllium Solid	0.7370	0.135	0.865	495
#5 Aluminum Hybrid	0.6890	0.150	0.850	684

$$*V = K_p (\rho_{\text{products}} / \rho_{\text{particles}})$$

\*\*  $(15/\pi^4) \downarrow'''(Z+1)$  given from Reference C-6

$$*** q_{\text{rad}} = \sigma \epsilon_p T_p^4$$

\*\*\*\* Equation C-5